Bioanalysis of Pteroyl Derivatives in Various Aspects of Human Health

By

Leon van Haandel

Submitted to the graduate degree program in the Department of Pharmaceutical Chemistry and the Graduate Faculty of the University of Kansas in partial fulfillment of the requirements for the degree of Doctor of Philosophy.

_____

J.F. Stobaugh, Ph.D.

_____

S.M. Lunte, Ph.D.

_____

T.D. Williams, Ph.D.

_____

C. Schöneich, Ph.D.

_____

T.E. Prisinzano, Ph.D.

Date Defended: 11/08/2010

The Dissertation Committee for Leon van Haandel

certifies that this is the approved version of the following dissertation:

Bioanalysis of Pteroyl Derivatives in Various Aspects of Human Health

_____

Chairperson: J.F.Stobaugh, Ph.D.

Date approved: 11/29/10

Abstract

This dissertation describes the development of bioanalytical strategies for a group of experimental and known therapeutic agents and chemically related essential substances. The array of analytes include the antifolate methotrexate, its various (in)active metabolites and related bio-conjugates, plus several forms of folic acid family, a group of essential substances not synthesized by mammalian species, but endogenously required in numerous biochemical processes. These analytes all share a common structural feature, the heterocyclic pteridine ring system. Analyte identity results from variations of the ptereridine-ring system redox state, a result of minor structural variations of the heterocyclic ring and changes in conjugation status (i.e. polyglutamated or nanoparticle conjugated).

Specific and sensitive detection of the individual species was of high interest, as the various chemical forms of these substances may constitute biomarkers for individualizing low dose MTX therapy in autoimmune diseases such as JIA, but is also required for the (pre)clinical studies of novel nano-device MTX drug delivery systems. The dissertation presents state-of-the-art bioanalytical methodology suitable for the specific determination of any specific analyte in the presence of all other analytes. The strategy for each particular analyte possesses its own unique strength and weakness, with the final strategy collectively being based on the specific structure and associated physical-chemical property of a given analyte, the biological environment, and the clinical question to be answered.

Acknowledgements

At the end of August in the summer of 2005, I arrived in Kansas for the first time to fulfill the internship requirement of my Free University masters program in the laboratories of Dr. Stobaugh at the University of Kansas (KU). At the time I opted for the internship in the United States I felt was ready for an adventure, a 9 month adventure abroad. Now 5 years later, I'm writing the acknowledgements section of my doctoral dissertation, and realize that these small innocent choices ended up as major turning points in my life. Upon my first arrival at the airport in Kansas City (KC), I did not know anyone, and to make matters worse, the two suitcases containing my only possessions at that point, did not make it to KC. Since that time I have met numerous friends, that have made my stay in the U.S. the pleasant experience that it has been. I it will be impossible to acknowledge each one of you, but I'm sure you know who you are.

First I would like to thank my advisor Dr. J. Stobaugh. As illustrated by this dissertation, the projects we have been working on in your laboratory have been challenging, but very rewarding due to their intimate relationship to "real" clinical problems. Your mentorship throughout my graduate career together with the experience obtained in your laboratory, will undoubtedly benefit me in my future career. I will certainly miss working in your laboratory. It is impossible to think about KU pharmchem and my graduate school opportunities without Dr. H. Lingeman. You have raised my initial interest in bioanalysis during my time at the Free University, and were responsible for giving me the opportunity to study abroad. I would also like to thank Dr. T. Williams, it was a pleasure working in your laboratory and with someone with as much mass spectrometry know-how as you have. Furthermore it was your willingness to think

outside of the box, that made this project work in the end. That being said, I apologize for my +128 legacy that will linger around your laboratory for the next 5 years. I would like to thank Dr. Lunte for being a reader of this dissertation, and Dr. Schöneich, and Dr. Prisinzano for serving as committee members.

I would like to thank Dr. Becker from Children's Mercy Hospital. You were the big engine behind the JIA part of the dissertation. It was, and is a pleasure working with somebody as highly motivated as you, and hopefully we can continue our research efforts in my future at CMH. The same accounts for Dr. Leeder, who generated an excellent post-doc position at CMH for me. I would like to thank Anton Heemskerk, who worked closely with me on a number of projects during his 8 month internship. Much of the data in chapter 6 would not have been generated without Anton.

Furthermore I would like to thank my good friends Justin Pennington and Ryan Funk, without them graduate school would have not been the same. Finally I would like to thank my family, including my parents, brother and grandparents. Living overseas, 1000s of miles away from home is not always easy and you are/were all missed. I would like to thank my parents in particular for all your support throughout my entire education, it would not have been possible without it, and I love you. I would like to thank my brother for visiting me twice during my stay here in the USA. We have made two memorable road trips through California and Colorado/Utah. I hope we can add some more trips to the list in the future.

Bioanalysis of Pteroyl Derivatives in Various Aspects of Human Health

Table of Contents

Appendices

List of Acronyms

5,10-METHF → 5,10-Methylenetetrahydrofolate

5,10-MTHF → 5,10-Methenyltetrahydrofolate

5-FTHF → 5-Formyltetrahydrofolate

5-MTHF → 5-Methyltetrahydrofolate

7OH-MTX → 7-hydroxymethotrexate

10-FTHF → 10-Formyltetrahydrofolate

ACN → Acetonitrle

AMP → Aminopterin

ATIC → 5-Aminoimidazole carboxamide ribotide transformylase

CE → Capillary electrophoresis

DAMP → 2,4-diamnio-6-methylpteridine

DAMPA → 4-amino-4-deoxy-N^{10}-methylpteroicacid

DHFR → Dihydrofolate reductase

DHF → 7,8-Dihydrofolate

DMF → N,N-dimethylformamide

DMPA → N,N,-dimethylpentylamine

DMHA → N,N,-dimethylhexylamine

DMHPA → N,N,-dimethylheptylamine

ESI → Electrospray ionization

FA → Folic acid

FD → Fluorescence detection

FPGS → Folylpolyglutamyl synthase

FR → Folate receptor

FWHH → Full width at half height

G5 → Generation 5

GART → Glycinamde ribonucleotide formyltransferase

GGH → Gamma glutamyl hydrolase

HLB → Hydrophilic lipophilic balance

HPLC → High performance liquid chromatography

IP → Ion-pair

I.S. → Internal standard

IV → Intra veneous

JIA → Juvenile idiopathic arthritis

kDa → Kilo dalton

LC → Liquid chromatography

LC-MS/MS → Liquid chromatography followed by tandem mass spectrometry detection

LC-PC(hv)-FD → Liquid chromatography followed by post column photochemical degradation and fluorescence detection

LD → Low dose

LLOQ → Lower limit of quantitiation

LOD → Limit of detection

M/z → Mass over charge

MeOH → Methanol

MRM → Multireaction monitoring

MS → Mass spectrometer

MTHFR → methylene tetrahydrofolate reductase

MTX → Methotrexate

MTXPGs → Methotrexate polyglutamates

NMR → Nuclear magnetic resonance

PAMAM → Polyamido amine

PCA → Perchloric acid protein precipitation

PGs → Polyglutamates

PCFT → Proton coupled folate receptor

PK → Pharmacokinetic

RA → Rheumatoid Arthritis

RBC → Red blood cell

RFC → Reduced folate carrier

SAX → Strong anion exchange

SC → Subcutaneous

SEC → Size exclusion chromatography

SPE → Solid phase extraction

SLC19A1 → see RFC

THF → 5, 6, 7, 8-Tetrahydrofolate

TOF → Time of flight (mass spectrometry)

TYMS → Thymidylate synthase

UV → Ultraviolet

WCX → Weak cation exchange

Chapter 1: Introduction to Pteroyl Derivatives in General Human Health and as Pharmaceutically Relevant Antimetabolites

Chapter 1: Introduction to pteroyl Derivatives in General Human Health and as Pharmaceutically Relevant Antimetabolites

Table of Contents

Table of Figures

1.1   Establishment of Nomenclature

This doctoral dissertation is centered around the development of bio-analytical methods for the detection of various biological and pharmaceutically relevant pteroylglutamic acid derivatives in biological matrices (figure 1). In a general sense, these molecules are composed of three different moieties (1) a pteridine ring system that is redox active, and changes oxidation state from the oxidized form to a 7,8-dihydro and a 5,6,7,8-tetrahydrofolate form (2) a para-aminobenzoic acid spacer (3) and a (γ-poly)glutamated terminal chain (figure 1).
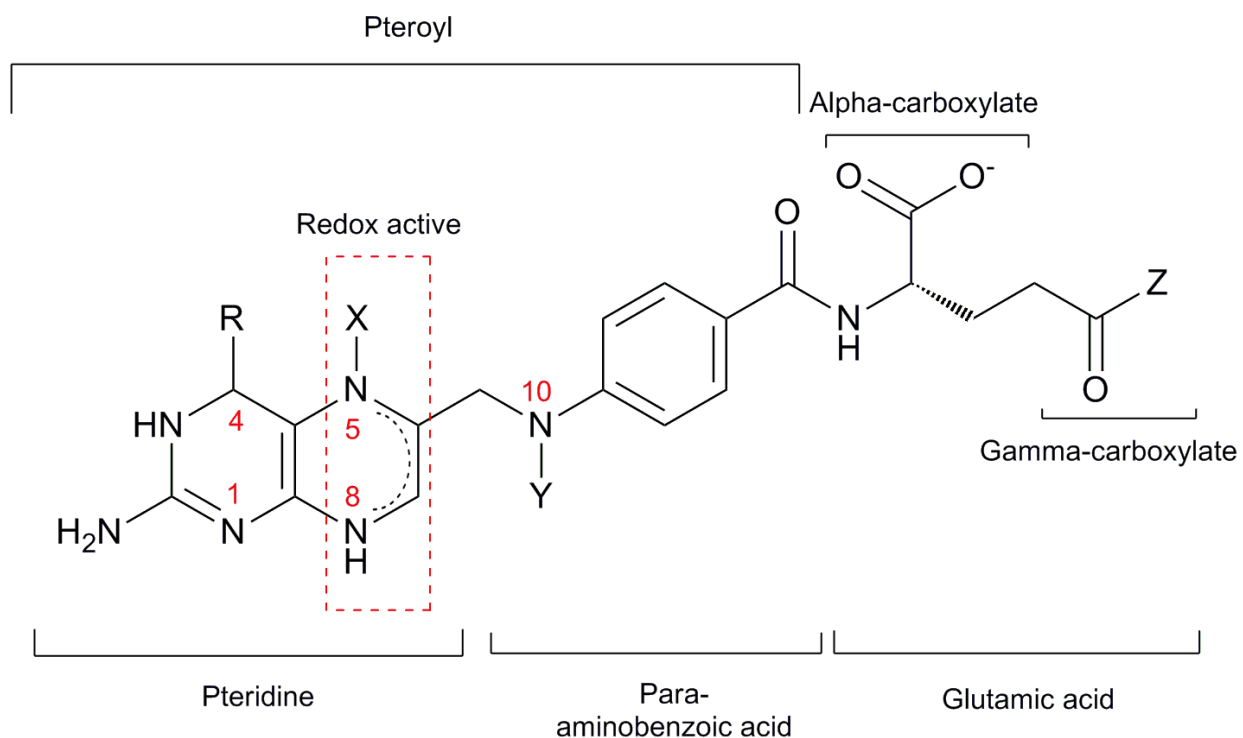
Figure 1. *Generic skeleton of biologically active pteroylglutamic acid derivatives. Common structural variations occur at the sites indicated by R, X, Y and Z.*

These entities play an important role in general human health as they are the chemical basis of the water-soluble B9 vitamins generally referred to as folate. For humans, folate is an essential vitamin necessary for normal cell growth and development and is aquired through the diet. The commonly accepted nomenclature for this vitamin is confusing because folic acid and folate are both commonly used to describe this vitamin, but in fact have different meanings. Based on established chemical nomenclature, one would believe the difference between folate and folic acid is just a proton. However, the term folic acid refers to pteroylglutamic acid which is the synthetic and most stable form of this vitamin with a fully oxidized pteridine ring system. In general the term folate is used for the naturally occurring, biologically active (polyglutamated) species, which posseses a reduced ring system with a variety of possible substitutions. A detailed description of these various folate structures can be found in section 1.3 of this dissertation. Throughout this dissertation the terms folate and folic acid (FA) will be used to refer to the natural and synthetic form respectively.

1.2   The discovery of folate

The discovery of folate has been closely related to the understanding of hematologic disorders and malignancies. In 1931, Lucy Wills reported the observation that macrocytic anemia during pregnancy was most predominant among women with vegetable, fruit and protein deficient diet[1]. She went on to discover that this anemia could be reversed through the addition of liver and yeast extracts to the diet, indicating the presence of an essential dietary component in these sources[2]. As is now well

known, such foods and extracts are a rich source of folate[3]. A decade after its first description, this component was isolated from 4 tons of spinach leaves in 1941 by Mitchell et al, and named "folic acid"[4]. This name was derived from the latin word for leaf, 'folium'. It took another 2 years to elucidate the structure of folic acid and synthesize a pure crystalline form[5]. Once the synthetic for was available, folic acid proved to be effective in reversing several types of anemia[6-7].

1.3   The various folate forms

On the molecular level, folic acid is composed of an oxidized pteridine ring, coupled to para-aminobenzoic acid and glutamic acid, leading to the name 'pteroylglutamic acid' (figure 2)[8]. Soon after its synthesis it became apparent that the naturally occurring folates were usually structurally altered analogs of FA acid in three respects: (1) Reduction within the pteridine ring to 7,8-dihydrofolate (DHF) and further reduction to 5,6,7,8-tetrahydrofolate (THF). (2) The fully reduced form, THF, is subject to variations in carbon status at the N(5) and N(10) position, e.g. 5-methyl (5-MTHF), 5-formyl-THF (5-FTHF), 10-formyl-THF (10-FTHF), 5,10-methylene-THF (5,10-METHF) and 5,10-methenyl-THF (5,10-MTHF) (figure 2), (3) Natural folates in foods and biological systems are almost exclusively in the (γ-linked) polyglutamated state (i.e. an increased number of glutamates).
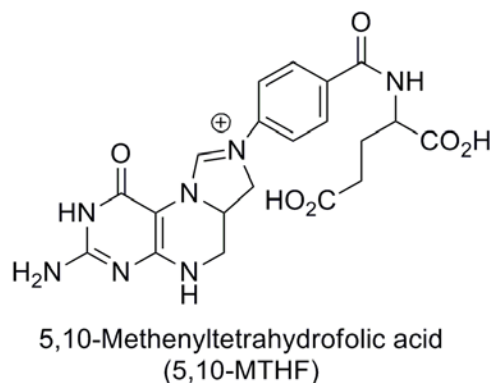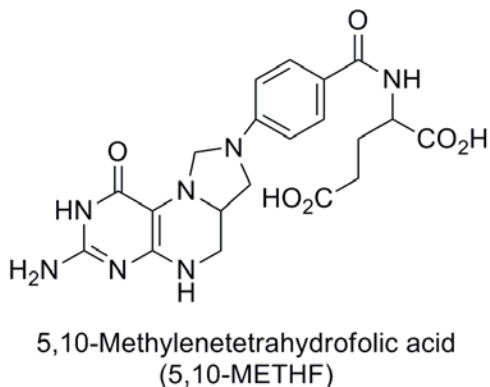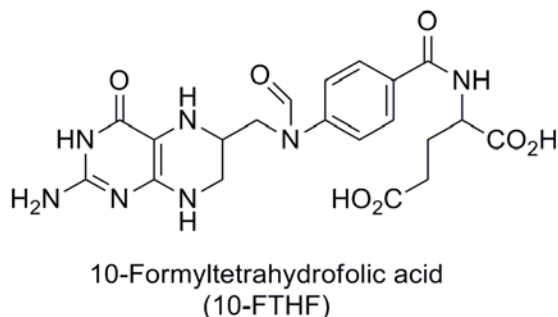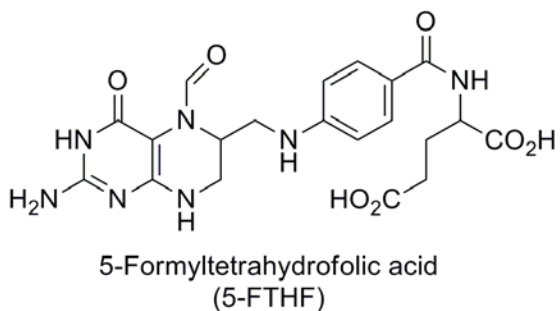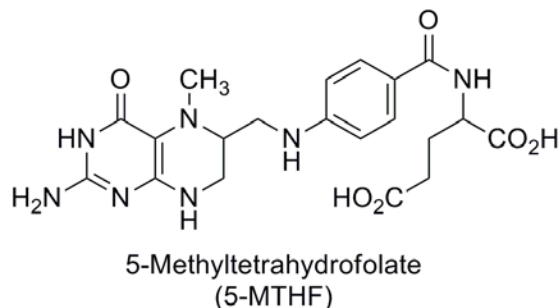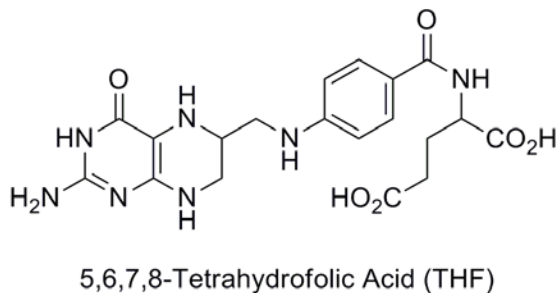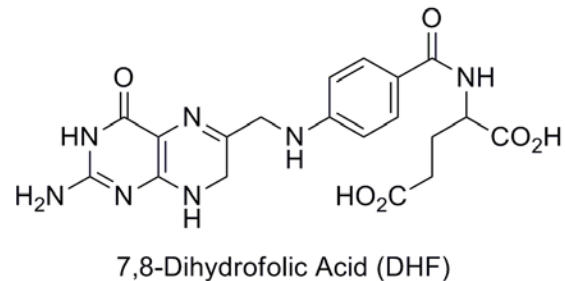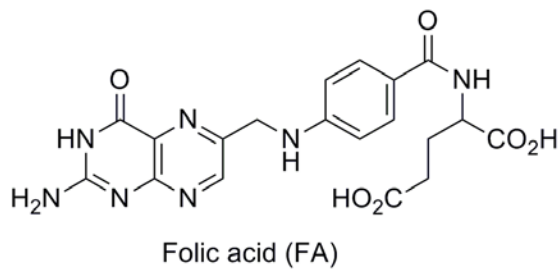
Figure 2. *Molecular structures of various folate species, the synthetic form folic acid (FA) and the naturally occurring forms of 7,8-dihydrofolate and 5,6,7,8-tetrahyrofolate (derivatives).*

1.4 Folate uptake

Folates are absorbed by the human body in the monoglutamyl form. Since dietary sources of the essential vitamin contain folates in the polyglutamated form, hydrolysis must occur in order to allow for efficient absorption. Folate hydrolysis occurs in the gut by the enzyme folyl-γ-glutamate carboxypeptidase (FGCP), a protein that is immobilized on the intestinal apical brush border. Deglutamated folate species are subsequently absorbed in the duodenum and upper part of the jejunum by the high-affinity proton-coupled folate receptor (PCFT). After absorption, the bioavailable form present in the systemic circulation is 5-MTHF. Circulating 5-MTHF is then transported into the cell by the reduced folate carrier (RFC) or the folate receptors (FR) present on the cell membrane. Following folate internalization, the polyglutamation chain is reconstructed intracellularly by the enzyme folylpolyglutamate synthase (FPGS). A schematic overview of this process is shown in figure 3.

1.5 Biological function of folates

Biological active folate species consist of the various substituted forms of intra cellular tetrahydrofolate. These molecules function as substrates and coenzymes in the acquisition, transport and enzymatic processing of one-carbon units for amino acid and nucleic acid metabolism and metabolic regulation. Nucleic acid synthesis is facilitated by the role of carbon donating folates in the synthesis of purines and thymidylate and through deoxycytosine methylation. Furthermore, 5-MTHF is required in the regeneration of methionine from homocysteine, which is employed for various cellular methylation reactions and protein synthesis.
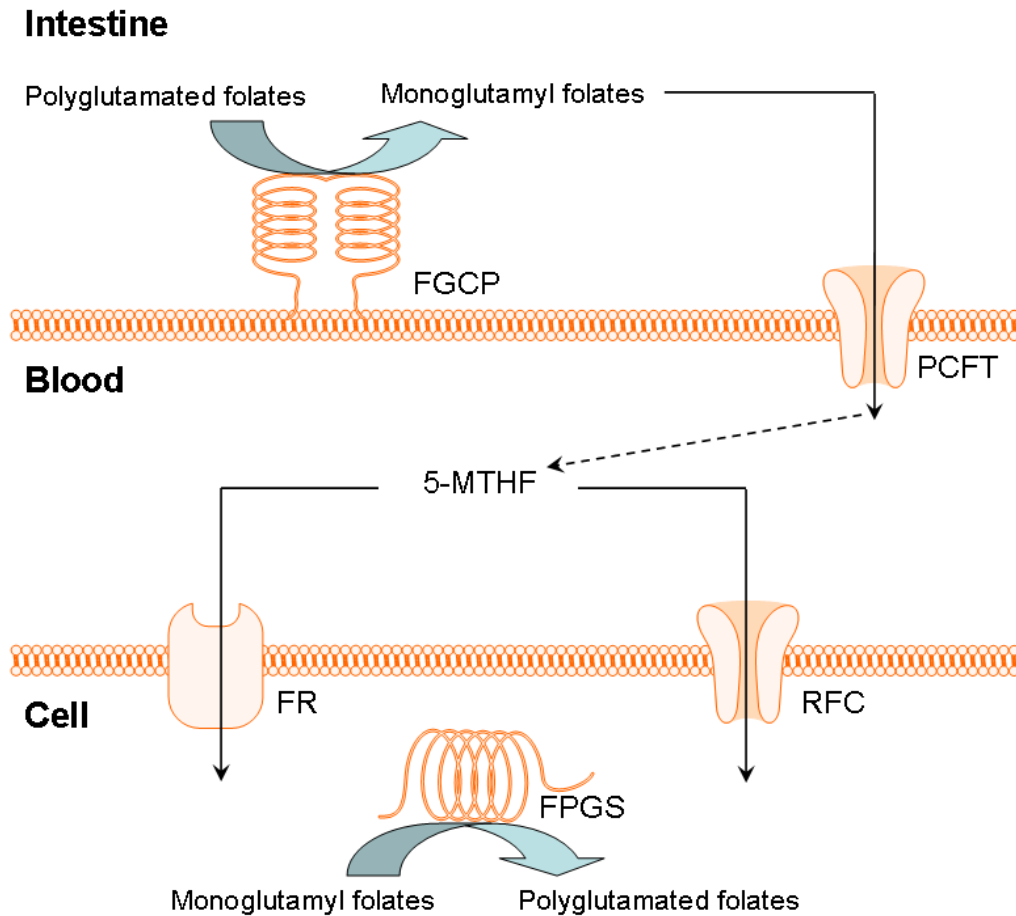
Figure 3. *Schematic overview of folate uptake and transport from the intestine. Deglutamated folates are absorbed into the systemic circulation by the PCFT. Circulation 5-MTHF is internalized intracellularly trough either the reduced folate carrier or the family of folate receptors, after which polyglutamation by FPGS occurs. Figure adapted from Blom et al.[9]*

Due to the its multitude of functions, folate plays a pivotal role in the synthesis and maintenance of DNA, RNA and proteins. A general schematic representation of the intracellular folate cycle is given in figure 4.

Folate deficiency and/or changes in folate isoform distribution have more recently been related to elevated blood homocysteine concentrations, which in turn is closely associated with various forms of vascular diseases, such as coronary heart disease and venous thrombosis[10]. Inadequate folate status during pregnancy increases the risk of neural tube defects and other birth defects[11]. Since folate species play a crucial role in the transmethylation reactions required for the biosynthesis of neurotransmitters, folate deficiency may also lead to depression[12-15]. Folate status also seems to play a role in the development of neurodegenerative disease such as in Alzheimers disease[16]. It has also been reported that an individual's folate status is related to colon, cervical and breast cancers[17-18].
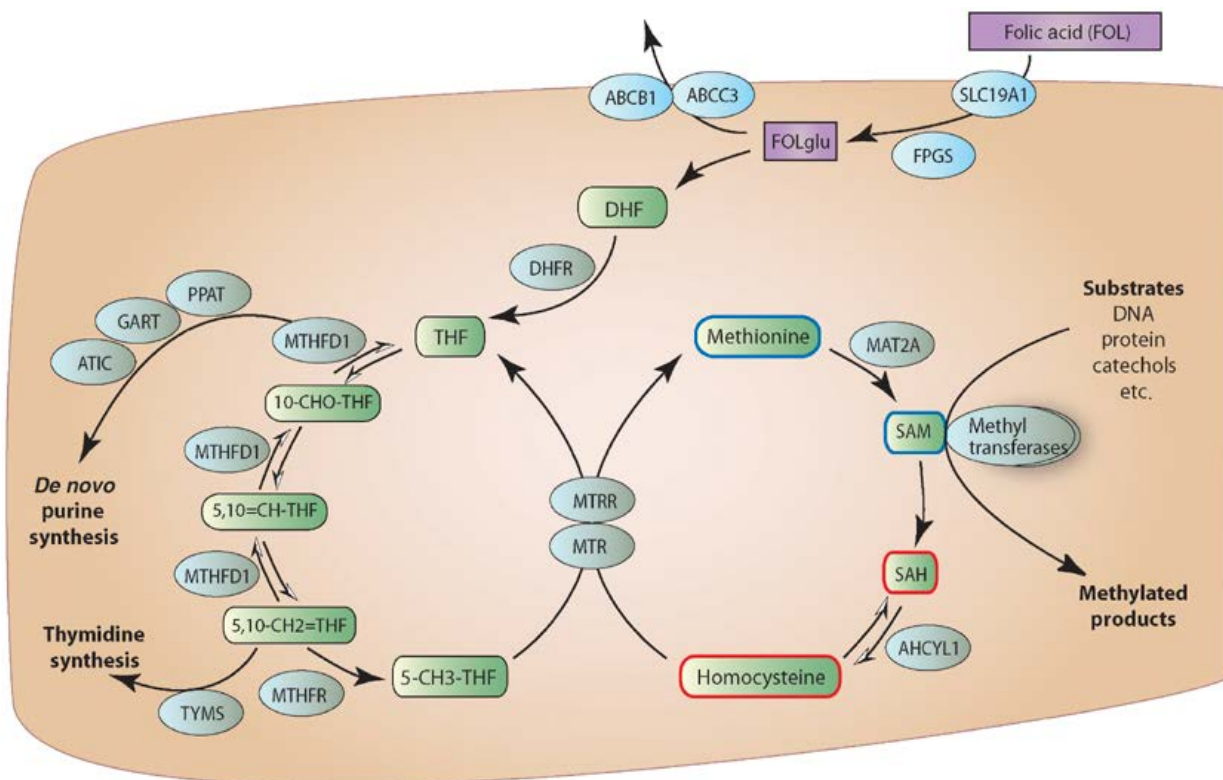
Figure 4. *Intracellular folate cycle. (figure is adapted and reproduced with permission from PharmGKB and Stanford University).*

1.6 Antifolates
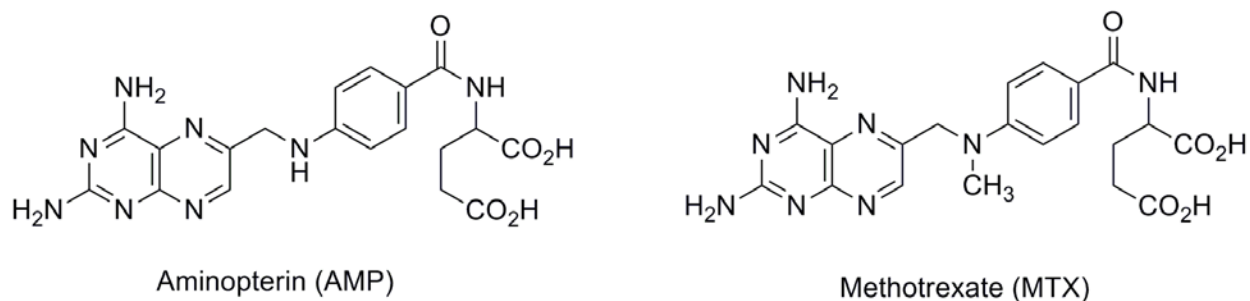
Figure 5. *Structures of two key antifolates, aminopterin (AMP) and the still widely used methotrexate (MTX).*

The first antifolates were developed as potential treatments for leukaemia. In the early 1940s the observation was made that leukemic lymphoblasts seen in the bone marrow of patients with acute lymphocytic leukaemia resembled the megaloblasts seen in pernicious anemia and was correlated with the observation of a low plasma folate status. Therefore it was postulated that acute leukaemias were the result of folate deficiency[19]. In an attempt to control the disease, patients were treated with FA, a strategy that led to the inverse of the desired effect, increasing in the number of leukemic cells within these patients. With FA identified as a proliferative factor, Heinle and Welch tried an opposite approach and demonstrated a decrease in leukemic cells in folate deficiency[20]. This observation triggered the development of folate anti-metabolites/antagonists. The first antifolate was developed in 1947 and is currently known as aminopterin[21] (AMP) (figure 5). A year later this compound was shown to cause temporarily remission in children with acute lymphocytic leukemia[22]. In the same year the less toxic analog of AMP, methotrexate (MTX) (figure 5), was introduced[23]. In

11

1956, it was demonstrated that MTX possessed a therapeutic index superior to that of AMP, and based on these results, MTX has supplanted AMP in the clinic.

MTX therapy is now widely used for the treatment of a wide spectrum of cancers and tumors, including: leukemia[24], lymphoma[25], choriocarcinoma[26], head and neck cancer[27] and osteogenic sarcoma[28-30]. More recently the therapeutic scope of MTX has expanded to the treatment of various autoimmune diseases, such as, rheumatoid arthritis[31-32], juvenile idiopathic arthritis[33-36], and psoriasis[37-38] and for the prevention of graft-versus-host disease[39-40] after transplantation.

1.7   MTX mechanism of action in cancer therapy

The mechanism of action of MTX in high doses for anticancer therapy is well understood. As described in section 1.5 of the introduction, cells rely on a supply of fully reduced folates that drive a cascade of one-carbon reactions that are required for DNA synthesis and cell proliferation. MTX has a tight, but reversible, binding to the enzyme dihydrofolate reductase (DHFR), an enzyme that is responsible for the reduction of FA to DHF, and more importantly also facilitates the reduction of DHF to THF. Interfering with this enzymatic pathway will result in a buildup of partly oxidized folate species and a depletion of the biologically active fully reduced folates, therefore inhibiting the *de novo* purine synthesis pathway and other pathways that rely on reduced folate cofactors. MTX displays a stoichiometric binding to DHFR when the ratio of inhibitor to enzyme is low, however a complete blockade of DHFR requires an excess of unbound drug[41].

1.8   Polyglutamation

An important aspect of folate homeostasis is the biological process of intracellular polyglutamation. Polyglutamation occurs by the sequential addition of glutamates to the gamma carboxylate of the terminal folate glutamate residue, resulting in a pool of folate polyglutamates (folatePGs). The intracellular, ATP dependant, process of polyglutamation is catalyzed by the enzyme folylpolyglutamate synthase (FPGS)[42]. Polyglutamation is an important biological process as it is responsible for increasing the size of the molecule, rendering it much more anionic, and as a result folate polyglutamates cannot diffuse outside the cell. The process of polyglutamation therefore allows for intracellular accumulation of folates against the extracellular space concentration gradient. Intracellular concentrations of folate are typically in the micro-molar (µM) range, as opposed to the lower nano-molar (nM) range in plasma. The second important feature of polyglutamation is bioactivation, as polyglutamated folates have an increased cofactor affinity[43]. The intracellular enzyme gamma glutamyl hydrolase (GGH) is involved in the deglutamation of folatePGs. Since polyglutamation and deconjugation both are gamma-glutamate specific, the cell has the ability to tailor glutamate chain length without affecting other biomolecules such as peptides and proteins.

MTX is a relatively poor substrate for FPGS but does compete with the other intracellular folates for polyglutamation. The polyglutamated forms of MTX are either equipotent or only marginally more potent DHFR inhibitors compared to native MTX. A decrease in MTX polyglutamation has been identified as an important source of clinical resistance to MTX. This indicates that MTX polyglutamation serves an important MTX

13

retention/accumulation mechanism rather increasing its DHFR blocking capabilities. The polyglutamated forms of MTX however are much more potent inhibitors of enzymes in the *de novo* purine synthesis pathway and pyrimidine synthesis pathway (figure 3). The K_i of the pentaglutamyl form of MTX was found to be 250 times higher for thymidylate synthase (TYMS), 2500 times higher for 5-aminoimidazole carboxamide ribotide transformylase (ATIC), and 30 times higher for glycinamide ribonucleotide formyl transferase (GART) (figure 6)[44]. High-dose MTX in chemotherapy mechanistically works due to competitive blockade of DHFR. This is demonstrated by the effectiveness of leucovorin in reversing MTXs cytotoxic effect by repletion of the intracellular reduced folate pool.

1.9   The development of novel antifolate drugs

Attempts to further improve the spectrum of therapeutic activity and the effectiveness of MTX, as well as the observations of intrinsic and acquired resistance to MTX, has led to the search for novel antifolate entities and novel drug delivery strategies for the classic agent. The rationale behind the development of novel antifolates for the treatment of cancers has been extensively reviewed[45-46]. Briefly these new agents include the development of novel DHFR blockers with altered pharmacological features, targeting of different enzyme(s) in the folate pathway, modifications to improve affinity for FPGS to increase intracellular half-life, and finally "non-classical" lipophilic antifolates have been introduced that do not require transport or polyglutamation. Virtually all of these approaches are currently the topic of continuing investigations.

Figure 6. *Cellular folate pathway with both folic acid and MTX represented. Red lines represent known inhibition of target enzymes with MTX. (figure reproduced with permission from PharmGKB and Stanford University).*

1.10   Use of MTX in drug delivery systems for cancer treatment

Site specific delivery of chemotherapy drugs is currently receiving renewed attention. Delivery of a drug to a specific tissue or cell type can be achieved by conjugating a chemotherapeutic agent to a base material that targets specific receptors. In principle the controlled delivery of chemotherapy agents allows for smaller doses of drug to be effective against cancer and minimizes collateral damage to the surrounding healthy cells and tissues.   MTX is an ideal candidate for such a strategy for aforementioned reasons.

A promising experimental therapeutic for the improvement of the efficacy of MTX and the reduction of its side effects is a chemically elaborated generation 5 polyamidoamine nanoparticle (G5-PAMAM) (Avidimer Therapeutics, Ann Arbor, MI). Surface modifications of the nanoparticle include the incorporation of MTX and FA as the API and targeting vector respectively (G5-MTX-FA) (figure 7). As stated before, FA is an essential component for cell growth and is required in extreme amounts to support the rapid cellular division of cancer cells. Not surprisingly, an important characteristic of many cancer cells is the over expression of the folic acid receptor on the cell surface. Therefore conjugation of FA to a carrier system provides not only targeting, but also a potential internalization mechanism for these nanoparticle conjugated MTX over the free MTX. The efficacy of the G5-MTX-FA conjugate compared to free MTX has been demonstrated in several *in-vitro* [47] and *in-vivo* [48] studies. Mouse studies also demonstrated that MTX toxicity was significantly reduced when delivered as G5-MTX-FA as compared to the free drug, as indicated by the disappearance of typical high dose MTX side effects such as hair and weight loss[49].
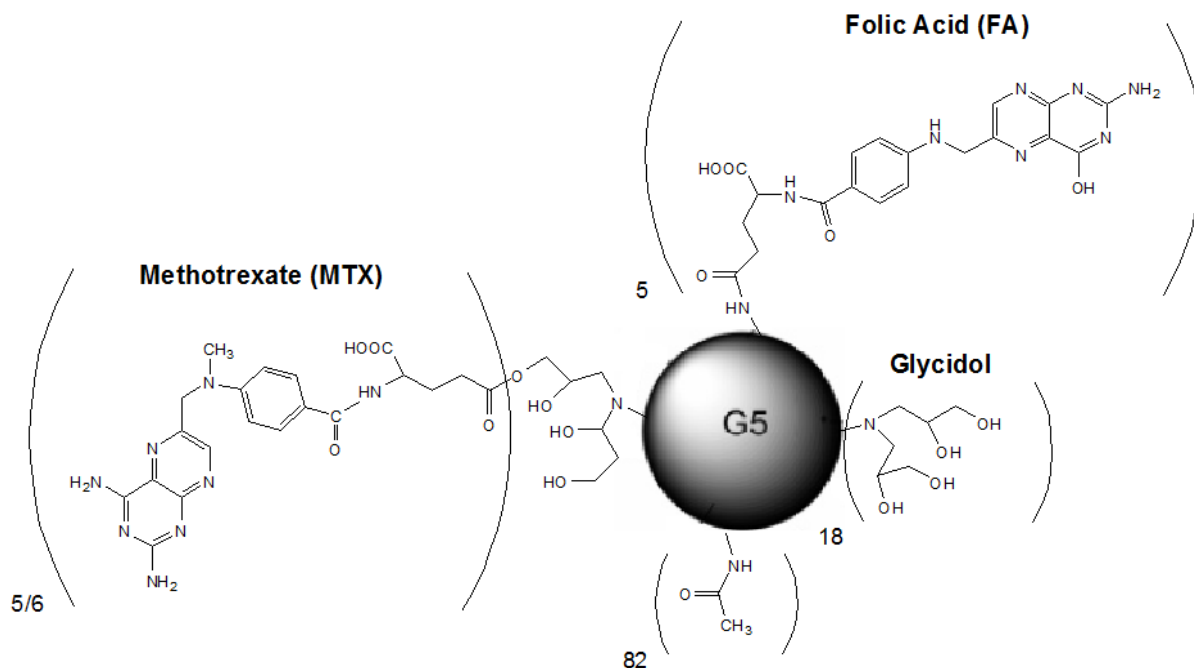
Figure 7. *Chemical structure of G5-MTX-FA. The G5 PAMAM core is illustrated by the sphere (not scale).*

Although promising, these high molecular weight nanoparticles are challenging to characterize due to their polydispersity which is a result of the multistep synthetic procedure used for their preparation. The inherent polydispersity, macromolecular size, and the use of structurally related pteridins (i.e. MTX and FA) of these nanoparticles generates a significant bioanalytical challenge for preclinical and clinical investigations. Chapter 2 and 3 of this dissertation review the history of these G5-MTX-FA nanoparticles and present bioanalytical methodology with high sensitivity and selectivity that is needed to support appropriate preclinical and/or clinical investigations of these experimental therapeutic agents.

1.11   Use of low dose MTX for the treatment of JIA

JIA is one of the most common chronic diseases of childhood, affecting an estimated 300,000 children in the U.S. alone, and is an important cause of morbidity and disability in children[50]. Low dose (LD)-MTX intervention, although the most commonly used second-line therapeutic agent used to treat JIA worldwide, has shown considerable inter-individual variability in both clinical response and adverse reactions, regardless of age or disease. Thus far, no predictive variables have been identified for outcomes in patients taking this medication, which is used alone and as an "anchor drug" for many rheumatic conditions.

In contrast to the high dose use of MTX in cancer therapy, the mechanism of action of LD-MTX in the therapy of JIA is still not clearly understood. It is not due to DHFR inhibition alone since the therapeutic effects of MTX cannot be reversed with leucovorin. Although the mechanism is unclear, it is believed that the low dose mechanism of action is attributed to inhibition of several additional number of enzymes, including TYMS, GART and ATIC by intracellular MTX polyglutamates. MTX polyglutamates have a partially increased affinity for ATIC, with the pentaglutamate demonstrating a potency increase of 2500 times of that of free MTX. Inhibition of ATIC leads to a cascade of biological events resulting in release of adenosine, which is a potent endogenous anti-inflammatory mediator. In other words, whereas the goal of high-dose MTX in cancer therapy is selective cell apoptosis, in LD-MTX the therapeutic aim is to perterb the various biochemical pathways of the cell to enhance the excretion of adenosine while minimizing cell damage and toxic effects.

The development of sensitive bioanalytical methodology for the detection of active MTX metabolites could provide an entry to the much needed objective of quantitative individualization of MTX therapy in JIA. Plasma MTX concentrations do not correlate to LD-MTX efficacy and/or toxicity in autoimmune diseases and therefore interest has shifted towards to detection of polyglutmated forms of MTX in human red blood cells (RBCs)[51]. In adult arthritis an individual's RBC MTX polyglutamation status has been correlated to MTX effectiveness as well as toxicity[52-53]. However, more recent studies have failed to reproduce these results[54-55]. The measurement of RBC MTX polyglutamation status and its predictive value towards individualization of MTX therapy has not been investigated in JIA.

In chapter 4 of this dissertation the performance of current methodology for RBC MTXPG determination is investigated. Based on the results obtained by this study, a novel bioanalytical method was developed which is suitable for the specific and sensitive measurement of MTXPG polyglutamation status in JIA. This method was applied to the analysis of a clinical cohort involving 100 JIA patients on weekly low dose MTX therapy in a collaborative effort with our colleagues at Children's Mercy Hospital (KC, MO). The clinical relevance and its potential for guiding MTX therapy in JIA is discussed in appendix 1 and 2.

Since the measurement of RBC MTXPGs appears to be a useful biomarker for individualization of MTX therapy in juveniles, analytical methodology suitable for clinical use is required. Chapter 5 and 6 of this dissertation present analytical methodology suitable for RBC MTXPG measurement in a clinical setting.

1.12   The measurement of folates

Since the polyglutamated forms of MTX are competitive inhibitors of various enzymes in the folate cycle, enzyme inhibition is a result of intracellular folate/MTX (polyglutamation) ratio. As folate is an essential nutrient (i.e. humans lack the ability to synthesize folate), an individuals folate status is the result of multiple factors including diet. The discrepancy currently noted in the literature about the usefulness of the measurement of MTXPG status in RA and JIA therapy, might be the result of the failure to recognize the MTX/folate antagonistic balance[55]. One must note that bioanalytical methodology for measured of folate isoforms and polyglutamation chain length has not been described in human tissues or cells[56]. The detection of both isoform and polyglutamation status is challenging from a specificity and sensitivity standpoint. Chapter 7 of this dissertation presents bioanalytical methodology for the detection of the folate isoform and polyglutamation chain length in the RBCs of JIA patients. The presented analytical methodology described was utilized for the determination of folate isoform and polyglutamation status of samples obtained from approximately 200 JIA patients, in a collaborative effort with our colleagues at Children's Mercy Hospital (KC, MO).

Approximately 100 patients were on MTX therapy and the other half of the cohort was comprised of JIA patients not on MTX therapy. The establishment of a MTX and non-MTX group in the patient cohort allows the establishment of a baseline folate status and reveals how MTX perturbation alters the intracellular folate cycle. Additionally the measurement of the intracellular folate distribution (i.e. isoform and polyglutamation) in combination with the measurement of MTXPGs gives us insight in the folate/antifolate species present within the cell that compete for similar enzymatic targets. As these

bioanalytical assays will lead to an increased understanding of the intracellular folate/MTX balance within the cell, it might be possible to describe a "folate signature" of MTX responders, or optimize (increase efficacy and reduce toxicity) MTX therapy based on quantitative values. This information is invaluable in guiding MTX therapy in JIA as alternative therapies are limited.

1.13   Overall goal of the dissertation

As can be concluded from the introduction, MTX is a versatile drug with a long history of clinical use. The more recent applications of MTX are its use for drug delivery, and the utilization of low dose MTX therapy for the treatment of autoimmune diseases. Classical plasma measurements of free MTX has been proven useful for the guidance of free MTX therapy for the treatment of cancers, but has limited value for these more recent applications. Therefore novel sensitive bioanalytical methods are needed to support the development of novel entities involving MTX and its metabolites, and for optimizing and individualizing MTX usage in low dosage regimes.

From a bioanalytical perspective, the challenges involving the detection of novel MTX nanoparticle conjugates, MTX metabolites (polyglutamates) and the detection of folates are intimately related. This family of entities (folate or antifolate) all share a common pteridine moiety, where changes in compound identity are the result of a minor number of substitutions on the pteridine ring system. A similar argument can be made for the other end of the molecule, where MTX or folate glutamyl conjugation plays an important role (e.g. to a nanoparticle or a γ-glutamyl-polypeptide).

This dissertation presents novel bioanalytical methods for the detection of (anti)folate species for these more recent MTX application areas. The relevance of the bioanalytical methods described in this dissertation is illustrated by direct clinical applications. The reader of this dissertation however, is encouraged to utilize the presented methods creatively as they are easy adaptable and could be applied to modern clinical investigations of antifolate therapy. An example of such an adaption is given in Chapter 6, where a derivatization reaction initially developed for nanoparticle conjugated MTX determination in plasma was utilized for the determination of total MTXPG pool in human RBCs. Many techniques presented in this dissertation might also be relevant for the bioanalytical chemist working with clinicians in the optimization of MTX therapy in fields as psoriasis, adulthood arthritis, inflammatory bowel disease and cancer treatment.

1.14 References

[1] L. Wills, Treatment of "pernicious anaemia of pregnancy" and "tropical anaemia". *Br Med J.* **1931**, *1*, 1059.

[2] L. Wills, Treatment of "pernicious anaemia of pregnancy" and "tropical anaemia" with special reference to yeast extract as a curative agent. 1931. *Nutrition.* **1991**, *7*, 323.

[3] S. Babu, S. G. Srikantia, Availability of folates from some foods. *Am J Clin Nutr.* **1976**, *29*, 376.

[4] H. K. Mitchell, E. E. Snell, R. J. Williams, Journal of the American Chemical Society, Vol. 63, 1941: The concentration of "folic acid" by Herschel K. Mitchell, Esmond E. Snell, and Roger J. Williams. *Nutr Rev.* **1988**, *46*, 324.

[5] R. B. Angier, J. H. Boothe, B. L. Hutchings, J. H. Mowat, J. Semb, E. L. R. Stokstad, Y. Subbarow, C. W. Waller, D. B. Cosulich, M. J. Fahrenbach, M. E. Hultquist, E. Kuh, E. H. Northey, D. R. Seeger, J. P. Sickels, J. M. Smith, JR., Synthesis of a compound identical with the l. casei factor isolated from liver. *Science.* **1945**, *102*, 227.

[6] F. M. HANES, Diagnostic Criteria and Resistance To Therapy in the Sprue Syndrome. *The American Journal of the Medical Sciences.* **1942**, *204*, 436.

[7] L. S. Davidson, R. H. Girdwood, E. M. Innes, Folic acid in the treatment of the sprue syndrome. *Lancet.* **1947**, *1*, 511.

[8] A. V. Hoffbrand, D. G. Weir, The history of folic acid. *Br J Haematol.* **2001**, *113*, 579.

[9] H. J. Blom, Y. Smulders, Overview of homocysteine and folate metabolism. With special references to cardiovascular disease and neural tube defects. *J Inherit Metab Dis.* **2010**.

[10] G. Ntaios, C. Savopoulos, D. Grekas, A. Hatzitolios, The controversial role of B-vitamins in cardiovascular risk: An update. *Arch Cardiovasc Dis.* **2009**, *102*, 847.

[11] L. D. Botto, C. A. Moore, M. J. Khoury, J. D. Erickson, Neural-tube defects. *N Engl J Med.* **1999**, *341*, 1509.

[12] R. Green, J. W. Miller, Folate deficiency beyond megaloblastic anemia: hyperhomocysteinemia and other manifestations of dysfunctional folate status. *Semin Hematol.* **1999**, *36*, 47.

[13]   R. Fraguas, Jr., G. I. Papakostas, D. Mischoulon, T. Bottiglieri, J. Alpert, M. Fava, Anger attacks in major depressive disorder and serum levels of homocysteine. *Biol Psychiatry.* **2006**, *60*, 270.

[14]   M. S. Morris, M. Fava, P. F. Jacques, J. Selhub, I. H. Rosenberg, Depression and folate status in the US Population. *Psychother Psychosom.* **2003**, *72*, 80.

[15]   M. Fava, J. S. Borus, J. E. Alpert, A. A. Nierenberg, J. F. Rosenbaum, T. Bottiglieri, Folate, vitamin B12, and homocysteine in major depressive disorder. *Am J Psychiatry.* **1997**, *154*, 426.

[16]   D. A. Snowdon, C. L. Tully, C. D. Smith, K. P. Riley, W. R. Markesbery, Serum folate and the severity of atrophy of the neocortex in Alzheimer disease: findings from the Nun study. *Am J Clin Nutr.* **2000**, *71*, 993.

[17]   B. M. Ryan, D. G. Weir, Relevance of folate metabolism in the pathogenesis of colorectal cancer. *J Lab Clin Med.* **2001**, *138*, 164.

[18]   Y. I. Kim, Folate and carcinogenesis: evidence, mechanisms, and implications. *J Nutr Biochem.* **1999**, *10*, 66.

[19]   J. R. Bertino, Karnofsky memorial lecture. Ode to methotrexate. *J Clin Oncol.* **1993**, *11*, 5.

[20]   R. W. Heinle, A. D. Welch, Experiments with pteroylglutamic acid and pteroylglutamic acid deficiency in human leukemia. *J Clin Invest.* **1948**, *27*, 539.

[21]   D. R. Seeger, J. M. Smith, M. E. Hultquist, ANTAGONIST FOR PTEROYLGLUTAMIC ACID. *Journal of the American Chemical Society.* **1947**, *69*, 2567.

[22]   S. Farber, L. K. Diamond, Temporary remissions in acute leukemia in children produced by folic acid antagonist, 4-aminopteroyl-glutamic acid. *N Engl J Med.* **1948**, *238*, 787.

[23]   T. H. Jukes, A. L. Franklin, E. L. R. Stokstad, Pteroylglutamaic acid antagonists. *Annals of the New York Academy of Sciences.* **1950**, *52*, 1336.

[24]   N. L. Seibel, Treatment of Acute Lymphoblastic Leukemia in Children and Adolescents: Peaks and Pitfalls. *Hematology.* **2008**, *2008*, 374.

[25]   J. J. Zhu, E. R. Gerstner, D. A. Engler, M. M. Mrugala, W. Nugent, K. Nierenberg, F. H. Hochberg, R. A. Betensky, T. T. Batchelor, High-dose methotrexate for elderly patients with primary CNS lymphoma. *Neuro Oncol.* **2009**, *11*, 211.

[26] J. P. Yarris, A. J. Hunter, Roy Hertz, M.D. (1909-2002): the cure of choriocarcinoma and its impact on the development of chemotherapy for cancer. *Gynecol Oncol.* **2003**, *89*, 193.

[27] P. M. Specenier, J. B. Vermorken, Current concepts for the management of head and neck cancer: chemotherapy. *Oral Oncol.* **2009**, *45*, 409.

[28] J. Ritter, S. S. Bielack, Osteosarcoma. *Ann Oncol.* **2010**, *21 Suppl 7*, vii320.

[29] Y. Fujita, T. Nakamura, T. Aomori, H. Nishiba, H. Shinozaki, T. Yanagawa, K. Takagishi, H. Watanabe, Y. Okada, K. Nakamura, R. Horiuchi, K. Yamamoto, Pharmacokinetic individualization of high-dose methotrexate chemotherapy for the treatment of localized osteosarcoma. *J Chemother.* **2010**, *22*, 186.

[30] N. Jaffe, Osteosarcoma: review of the past, impact on the future. The American experience. *Cancer Treat Res.* **2009**, *152*, 239.

[31] A. J. Kinder, A. B. Hassell, J. Brand, A. Brownfield, M. Grove, M. F. Shadforth, The treatment of inflammatory arthritis with methotrexate in clinical practice: treatment duration and incidence of adverse drug reactions. *Rheumatology.* **2005**, *44*, 61.

[32] S. L. Whittle, R. A. Hughes, Folate supplementation and methotrexate treatment in rheumatoid arthritis: a review. *Rheumatology (Oxford).* **2004**, *43*, 267.

[33] H. Truckenbrodt, R. Hafner, Methotrexate therapy in juvenile rheumatoid arthritis: a retrospective study. *Arthritis Rheum.* **1986**, *29*, 801.

[34] C. A. Wallace, The use of methotrexate in childhood rheumatic diseases. *Arthritis Rheum.* **1998**, *41*, 381.

[35] A. Cespedes-Cruz, R. Gutierrez-Suarez, A. Pistorio, A. Ravelli, A. Loy, K. J. Murray, V. Gerloni, N. Wulffraat, S. Oliveira, J. Walsh, I. C. Penades, M. G. Alpigiani, P. Lahdenne, C. Saad-Magalhaes, E. Cortis, L. Lepore, Y. Kimura, C. Wouters, A. Martini, N. Ruperto, Methotrexate improves the health-related quality of life of children with juvenile idiopathic arthritis. *Ann Rheum Dis.* **2008**, *67*, 309.

[36] A. V. Ramanan, P. Whitworth, E. M. Baildam, Use of methotrexate in juvenile idiopathic arthritis. *Arch Dis Child.* **2003**, *88*, 197.

[37] R. E. Kalb, B. Strober, G. Weinstein, M. Lebwohl, Methotrexate and psoriasis: 2009 National Psoriasis Foundation Consensus Conference. *J Am Acad Dermatol.* **2009**, *60*, 824.

[38] M. J. Boffa, R. J. Chalmers, Methotrexate for psoriasis. *Clin Exp Dermatol.* **1996**, *21*, 399.

[39] S. Vigouroux, R. Tabrizi, C. Melot, J. Coiffard, X. Lafarge, G. Marit, K. Bouabdallah, A. Pigneux, T. Leguay, M. S. Dilhuydy, A. Schmitt, J. M. Boiron, N. Milpied, Methotrexate reduces the incidence of severe acute graft versus host disease without increasing the risk of relapse after reduced-intensity allogeneic stem cell transplantation from unrelated donors. *Biol Blood Marrow Transplant.* **2010**.

[40] L. Giaccone, P. Martin, P. Carpenter, C. Moravec, H. Hooper, V. A. Funke, R. Storb, M. E. Flowers, Safety and potential efficacy of low-dose methotrexate for treatment of chronic graft-versus-host disease. *Bone Marrow Transplant.* **2005**, *36*, 337.

[41] J. C. White, S. Loftfield, I. D. Goldman, The Mechanism of Action of Methotrexate III. Requirement of Free Intracellular Methotrexate for Maximal Suppression of [14C]Formate Incorporation into Nucleic Acids and Protein. *Molecular Pharmacology.* **1975**, *11*, 287.

[42] A. Gangjee, N. P. Dubash, Y. Zeng, J. J. McGuire, Recent advances in the chemistry and biology of folypoly-gamma-glutamate synthetase substrates and inhibitors. *Curr Med Chem Anticancer Agents.* **2002**, *2*, 331.

[43] R. G. Matthews, C. Ghose, J. M. Green, K. D. Matthews, R. B. Dunlap, Folylpolyglutamates as substrates and inhibitors of folate-dependent enzymes. *Advances in enzyme regulation.* **1987**, *26*, 157.

[44] B. A. Chabner, C. J. Allegra, G. A. Curt, N. J. Clendeninn, J. Baram, S. Koizumi, J. C. Drake, J. Jolivet, Polyglutamation of methotrexate. Is methotrexate a prodrug? , *J Clin Invest.* **1985**, *76*, 907.

[45] J. Walling, From methotrexate to pemetrexed and beyond. A review of the pharmacodynamic and clinical properties of antifolates. *Investigational New Drugs.* **2006**, *24*, 37.

[46] K. Robien, Folate During Antifolate Chemotherapy: What We Know... and Do Not Know. *Nutrition in Clinical Practice.* **2005**, *20*, 411.

[47] T. P. Thomas, I. J. Majoros, A. Kotlyar, J. F. Kukowska-Latallo, A. Bielinska, A. Myc, J. R. Baker, Targeting and Inhibition of Cell Growth by an Engineered Dendritic Nanodevice. *Journal of Medicinal Chemistry.* **2005**, *48*, 3729.

[48] J. F. Kukowska-Latallo, K. A. Candido, Z. Cao, S. S. Nigavekar, I. J. Majoros, T. P. Thomas, L. P. Balogh, M. K. Khan, J. R. Baker, Jr., Nanoparticle Targeting of Anticancer Drug Improves Therapeutic Response in Animal Model of Human Epithelial Cancer. *Cancer Res.* **2005**, *65*, 5317.

[49] I. J. Majoros, C. R. Williams, A. Becker, J. R. Baker, Jr., Methotrexate delivery via folate targeted dendrimer-based nanotherapeutic platform. *Wiley Interdiscip Rev Nanomed Nanobiotechnol.* **2009**, *1*, 502.

[50] M. L. Becker, J. S. Leeder, Developmental pharmacogenetics in pediatric rheumatology: utilizing a new paradigm to effectively treat patients with juvenile idiopathic arthritis with methotrexate. *Hum Genomics Proteomics.* **2010**, *2010*, 257120.

[51] P. Angelis-Stoforidis, F. J. Vajda, N. Christophidis, Methotrexate polyglutamate levels in circulating erythrocytes and polymorphs correlate with clinical efficacy in rheumatoid arthritis. *Clin Exp Rheumatol.* **1999**, *17*, 313.

[52] T. Dervieux, D. Furst, D. O. Lein, R. Capps, K. Smith, J. Caldwell, J. Kremer, Pharmacogenetic and metabolite measurements are associated with clinical status in patients with rheumatoid arthritis treated with methotrexate: results of a multicentred cross sectional observational study. *Ann Rheum Dis.* **2005**, *64*, 1180.

[53] T. Dervieux, D. Orentas Lein, J. Marcelletti, K. Pischel, K. Smith, M. Walsh, R. Richerson, HPLC Determination of Erythrocyte Methotrexate Polyglutamates after Low-Dose Methotrexate Therapy in Patients with Rheumatoid Arthritis. *Clin Chem.* **2003**, *49*, 1632.

[54] L. K. Stamp, J. L. O'Donnell, P. T. Chapman, M. Zhang, J. James, C. Frampton, M. L. Barclay, Methotrexate polyglutamate concentrations are not associated with disease control in rheumatoid arthritis patients receiving long-term methotrexate therapy. *Arthritis & Rheumatism.* **2010**, *62*, 359.

[55] M. Danila, L. Hughes, E. Brown, S. Morgan, J. Baggott, D. Arnett, S. Bridges, Measurement of Erythrocyte Methotrexate Polyglutamate Levels: Ready for Clinical Use in Rheumatoid Arthritis? , *Current Rheumatology Reports.* **2010**, *12*, 342.

[56] E. P. Quinlivan, A. D. Hanson, J. F. Gregory, The analysis of folate and its metabolic precursors in biological samples. *Anal Biochem.* **2006**, *348*, 163.

Chapter 2: Bioanalytical Method Development for a Generation 5 Polyamidoamine Folic Acid Methotrexate Conjugated Nanoparticle

Chapter 2: Bioanalytical Method Development for a Generation 5 Polyamidoamine Folic Acid Methotrexate Conjugated Nanoparticle

Table of Contents

List of Figures

List of Tables

2.1 Introduction

The following chapter deals with the bioanalytical method development of an experimental anticancer agent based on a chemically elaborated nanoparticle carrier. First the chemical structure and the physical chemical properties of the nanoparticle are described. Subsequently a (clinical relevant) metabolic pathway is proposed and analytical targets were selected based on this scheme. The remainder of the chapter presents analytical method development, validation, and application of the method to obtain preliminary pharmacokinetic data.

2.1.1 Poly(amidoamine) dedritic nanocarriers

Poly(amidoamine) (PAMAM) dendrimers are hyper-branched, spherical molecules with a well defined structure as a result of their stepwise repetitive synthetic route[1]. They are constructed around an ethylenediamine core unit, elaborated by repetitive alternating alkylation and amidation steps[2]. Each repetitive synthetic iteration results in the next dendrimer generation, which has increased size, molecular weight and (terminal) surface functional groups[3]. PAMAM dendrimers, the first commercial available dendrimers, are currently being touted as drug delivery platforms[4] as a result of their relatively monodisperse yet multivalent structure[5-6]. The internal cavities of PAMAM dendrimers are relatively hydrophobic and as a result have been utilized for encapsulation of poorly water soluble drugs[7], while the ionizable amines of the surface can undergo non-covalent electrostatic interactions with an acidic drug[8]. These drug-dendrimer interactions provide an apparent enhancement of drug solubility[9], improved

31

bioavailability[10] and favorable release profiles. Taking advantage of their surface functional groups structural features to potentially achieve tissue specific targeting, these dendrimers have been conjugated with numerous molecules to created a chemically based drug delivery nanodevice (a number of conjugates are summarized by Cheng et al.)[5].

2.1.2 G5-MTX-FA

G5-MTX-FA (Avidimer Therapeutics, Ann Arbor, MI) is a chemically elaborated generation 5 (G5) PAMAM dendrimer (figure 8). The present research focuses on the development of plasma assay methodology suitable to support preclinical evaluation of G5-MTX-FA as a targeted chemotherapeutic drug delivery device[11]. The nanodevice is a bi-functional G5-PAMAM dendrimer conjugate where the surface primary amine
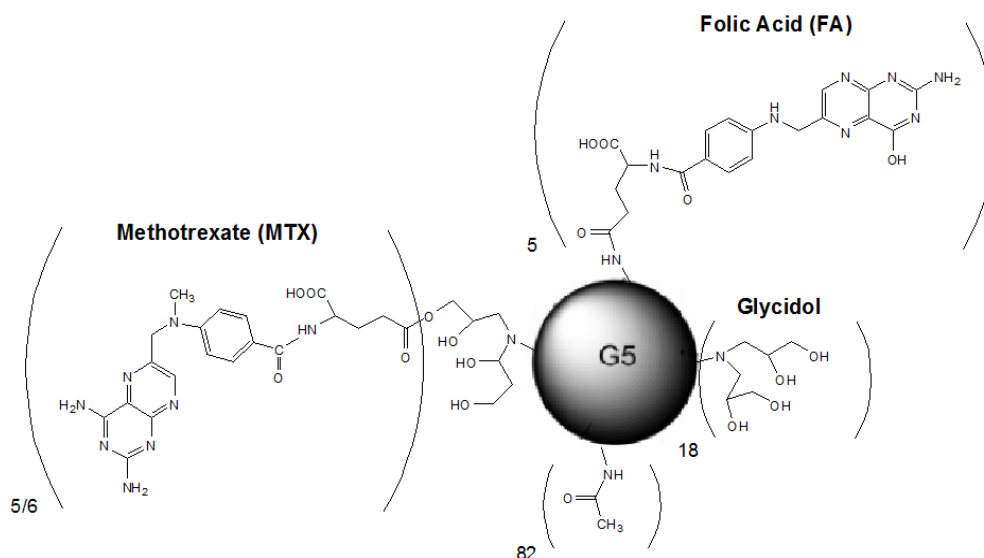
Figure 8. *Chemical structure of G5-MTX-FA. The G5 PAMAM core is illustrated by the sphere (not scale).*

groups have been largely blocked via acetylation[12] in order to reduce non-specific interactions and increase solubility[13]. Folic acid (FA) moieties are covalently bonded to the dendrimer surface in order to target the nanodevice towards over expressed folate receptors that are present on the cell surface of various forms of cancer cells[14]. Following receptor binding, the nanodevice appears to be internalized by folic acid receptor mediated endocytosis[15]. The therapeutically active agent methotrexate (MTX), also covalently attached to the dendrimer surface, is thus delivered to the cell. A detailed description of the synthesis procedure for this nanodevice is described elsewhere[16]. The efficacy of the G5-MTX-FA conjugate over free methotrexate has been demonstrated in several *in-vitro*[17] and *in-vivo*[18] studies.

Based on this biological scenario, the obvious therapeutic goal is the clinical development of this potential site specific delivery system whereby the therapeutic agent MTX is effective at a lower overall dosage that maximizes effectiveness and minimizes side effects. Hence bioanalytical methodology of high sensitivity and selectivity is needed to support appropriate preclinical and/or clinical investigations.

2.1.3 Proposed metabolic pathway of G5-MTX-FA

Since MTX is conjugated through a potentially labile ester bond, G5-MTX-FA may release MTX *in-vivo*. The free MTX will then be subject to known metabolic pathways[19-21] (figure 9). The major plasma metabolite, 7-hydroxymethotrexate (7OH-MTX), is known to exhibit approximately1/100 the bioactivity of MTX. Other known metabolites include various polyglutamates (PGs) and 4-amino-4-deoxy-N^{10}-methylpteroic acid (DAMPA). Intracellular metabolism of MTX produces the various MTXPGs, which limit

the extrusion of MTX by active transport[22]. DAMPA, an inactive metabolite, appears to result mainly from oral administration of MTX where the drug substance undergoes extracellular metabolism by intestinal bacterial flora[23]. When one considers all of these aspects, it is clear that one needs to develop plasma assay methodology for bound MTX (i.e., dendrimer associated), free MTX, and the major metabolite 7OH-MTX. In contrast it is unnecessary to assay the MTXPG family of metabolites, since they are essentially trapped in an intracellular pool, nor DAMPA since G5-MTX-FA is intended only for vascular administration thus circumventing its formation.
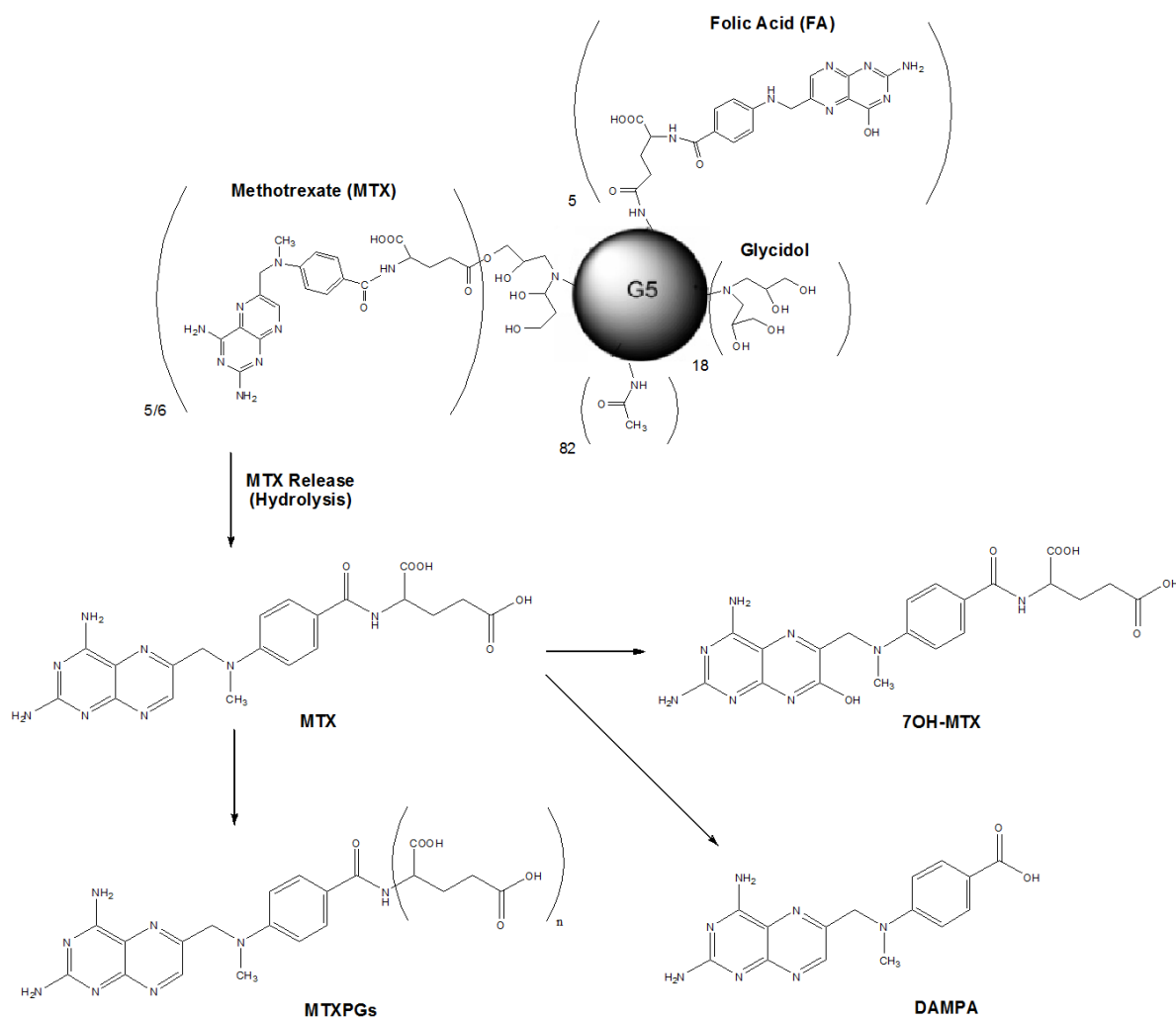
Figure 9. *Proposed metabolic degradation scheme for G5-MTX-FA.*

34

2.1.4 Reflection on analytical methodology

As an analytical strategy for plasma determination of G5-MTX-FA is devised, one must be aware that a number of structural deviations are introduced at different stages of its multistep synthesis procedure. For example, in building the G5 PAMAM dendrimer core, various skeletal defects (i.e. missing arms, molecular loops, dimers and/or traces of trailing generations) result, and further, additional variability is introduced during the process of functionalizing the dendrimer surface[24].

In the past, a variety of complementary analytical strategies have been utilized in order to characterize the degree of heterogeneity of such nanoparticles. Spectroscopic techniques include, but are not limited to: various types of NMR[12, 24-26], mass spectrometric methods (chemical ionization, fast atom bombardment, laser desorption, electrospray ionization and matrix assisted laser desorption/time of flight (MALDI-TOF)[24, 27]) and low angle laser light scattering[1]. A number of separation methods including size exclusion chromatography (SEC)[1, 12, 24], capillary electrophoresis (CE) [24, 28] and polyacrylamide gel electrophoresis[24] have been applied to PAMAM dendrimers. Reversed-phase liquid chromatography has been used to separate different generations of dendrimers[29] and in one report was able to partially resolve dendrimers of the same generation possessing surface modifications with minor variations[30].

With regard to bioanalysis of G5-MTX-FA, such results are not particularly useful as one would expect broad or perhaps multiple unresolved peaks. Review of these various techniques immediately reveals that separation performance declines with increasing dendrimer size and/or (partial) surface elaboration, leading one to conclude that they are not suitable for bioanalysis of G5-MTX-FA in a biological matrix.

35

2.1.5 Analytical method requirements

From an analytical perspective, due to imperfections in the synthetic preparation, G5-MTX-FA is a heterogeneous large molecule therapeutic; however, subsequent to dosing, this situation can potentially become even more complex, since there is the potential for step-wise release of MTX through ester cleavage. Such a scenario would result in an altered nanodevice still possessing therapeutic potential but of lower MTX titer. Therefore any bioanalytical methodology should be capable of specific determination of total dendrimer associated MTX. In the present report, the issues of macromolecular chromatographic inefficiency and analyte heterogeneity (G5-MTX-FA MTX titer) are addressed via a sample preparation step wherein the selective release of a highly fluorescent MTX reporter molecule (2,4-diamino-6-methylpteridine) is achieved. Assay of the reporter allows for selective and sensitive (low nM) determination by liquic chromatography with fluorescence detection (LC-FD) of G5-MTX-FA associated MTX. The remaining analytes of interest, free MTX and the metabolite 7OH-MTX, were determined by LC separation followed by online post column photochemical reaction with fluorescence detection. The developed methodology was used to obtain plasma pharmacokinetic profiles of G5-MTX-FA administered to rats by intravenous bolus and subcutaneous injections.

2.2 Experimental

2.2.1 Materials

HPLC grade N,N-dimethylformamide (DMF), Folic acid (FA), 30% solution of hydrogen peroxide (H_2O_2), methotrexate (MTX), potassium permanganate ($KMnO_4$), sodium dithionite ($Na_2O_4S_2$), sodium hydroxide (NaOH) and tris hydrochloride were obtained from Sigma-Aldrich. (St. Louis, MO). Potassium phosphate monobasic (KH_2PO_4), Potassium phosphate dibasic (K_2HPO_4), Ammonium acetate and HPLC grade solvents acetonitrile (ACN) and methanol (MeOH) were obtained from Fisher Scientific (Fair Lawn, NJ). 7-Hydroxymethotrexate (7OH-MTX) was purchased from Synfine Research (Ontario, Canada). G5-MTX-FA was obtained from Avidimer Therapeutics. Blank heparin stabilized rat plasma (Sprague Dawley) was obtained from Bioreclamation, Inc (Westbury, NY).

2.2.2 Instrumentation and Apparatus

G5-MTX-FA System: This system consisted of two Shimadzu LC6A solvent delivery modules that were operated through a Shimadzu SCL-6B system controller. Sample introduction occured by a Shimadzu SIL-6B autosampler equipped with a 50 µL injection loop. A Phenomenex Luna C18(2), 5 µm, 100 Å, 250 x 2.0 mm analytical column was guarded by a Supelcosil LC-8, 5 µm, 2 x 2.1 mm guard column and maintained at 30°C by a Shimadzu CTO-6A column oven. Detection occurred by a Shimadzu RT-10Axl fluorescence detector with excitation and emission wavelengths of 367 nm and 463 nm, respectively. The data was collected using TurboChrom V4.1. The

mobile phase used with this chromatograph consisted of solvent A: 15 mM tris-HCl adjusted to pH 6.8 by a 10% NaOH solution and solvent B: consisting of MeOH. The system was operated at a flow rate of 0.2 mL/min with 75% A and 25% B.

Post column photo oxidation system: Solvent was delivered by a Shimadzu LC6A binary pumping system that was operated through a Shimadzu SIL-6B system controller. The sample was introduced by a Shimadzu SIL-6B autosampler equipped with a 100 µL injection loop. The separation was conducted on a Phenomenex Intertsil C18 (150 x 4.6 mm) column with 5 µm particles with a 100 Å pore size that was protected by a Supelcosil LC-8, 5 µm, 2 x 4.0 mm guard column. Two meters of transparent Teflon tubing (0.012" id x 0.030" od), one meter in the center braided, was used as reactor coil and connected to the outlet of the column (total reactor coil volume 0.14 mL). An in-house fabricated online photochemical reactor was constructed using a GE Germicidal 9W lamp as a light source inside of the photochemical reactor (figure 10). Detection occurred by a Jasco FP-920 Intelligent Fluorescence Detector (excitation: 360nm and emission: 417nm) and data was collected by TurboChrom V4.1. The mobile phase used with this chromatograph consisted of solvent A: 975 mL 10 mM potassium phosphate buffer pH 6.2, 25 mL DMF and 1.5 mL 30% solution of H_2O_2 and solvent B: consisting of 200 mL ACN, 800 mL H_2O and 1.5 mL 30% solution of H_2O_2. The system was operated at a flow rate of 1.0 mL/min with 60% A and 40% B. A schematic of the instrument configuration is shown in figure 10.
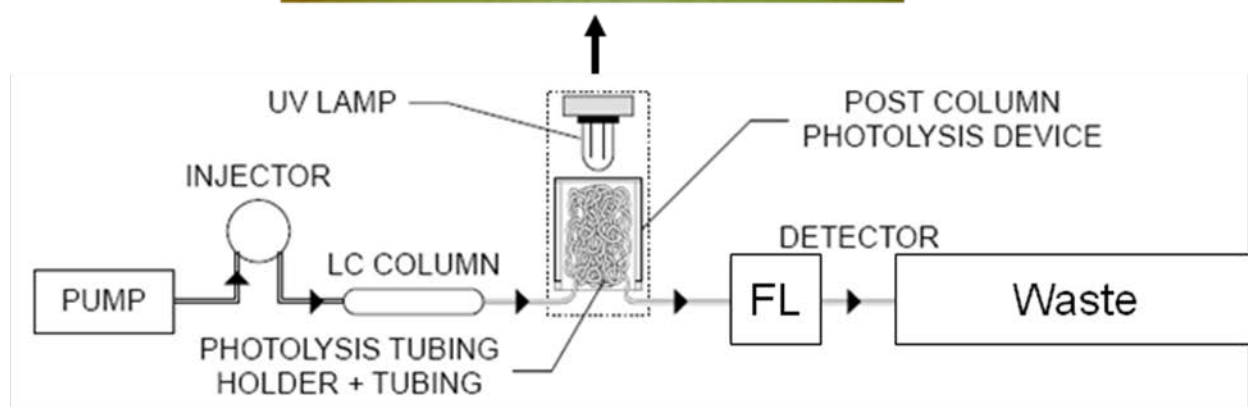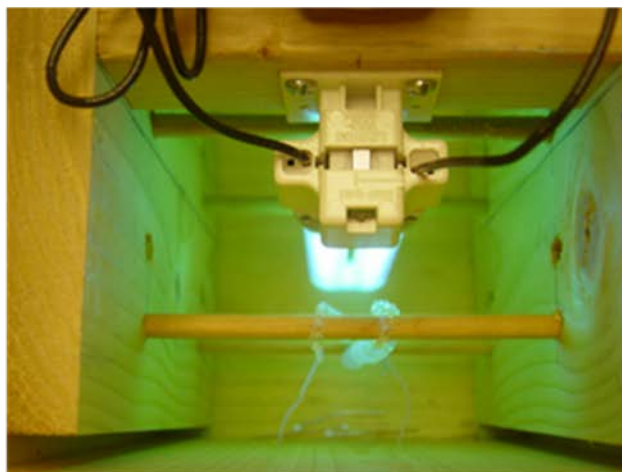
Figure 10. *Schematic of the post column photo-oxidation HPLC system*

2.2.3 Preparation of stock solutions, samples and calibration

Stock solutions of MTX and 7OH-MTX were prepared according to an earlier method presented by Steinborner et al[31]. MTX was dissolved in 95% MeOH and 5% formic acid. 7-OHMTX was dissolved in 50% DMSO, 50% H_2O. G5-MTX-FA is freely soluble and was dissolved in H_2O. The stock solutions were diluted with water to the desired concentration and spiked into a 100 μL blank plasma matrix to yield calibration standards. The linearity and reproducibility of the G5-MTX-FA methodology was assessed by the analysis of calibrants (n=6) spiked with 0, 2, 4, 20 , 40, 100, 200, 300 and 400 μg/mL. Samples spiked with similar concentrations were used to determine

intra-day (six replicate) and inter-day (18 replicates analysis conducted over 3 separate runs) precision and accuracy. The linearity and reproducibility of the free MTX and 7-OHMTX methodology was assessed by the analysis of calibrants (n=6) spiked with 0.075:0.010, 0.15:0.02, 0.75:0.1, 1.5:0.2, 3.7:0.5, 7.6:1.0. 11.4:1.5, 15.3:2.0 µM MTX:7-OHMTX. Samples spiked with similar concentrations were used to determine intra-day (six replicates) precision and accuracy.

2.2.4 Reduction reaction of G5-MTX-FA

An aliquot of 100 µL of (spiked/sampled) plasma was diluted with a 1.0 M ammonium acetate solution to 800 µL in a plastic vial. Once all samples and calibrants were prepared they were placed in an in-house manufactured sample holder (details provided in supplemental section) that has the ability to lock the caps. Subsequently 200 µL of a freshly prepared 50 mM $Na_2O_4S_2$ solution was added and the vials were closed and secured by the holder. The entire holder was then vortexed for 10 seconds and placed into a water bath of boiling water. After 15 minutes the holder was removed from the water bath and stored in a refrigerator for 30 minutes. The cooled samples were removed from the holder and placed into a centrifuge for 5 minutes at 10,000 rpm to spin down denatured and precipitated plasma proteins. The supernatant was transferred into 1.0 ml autosampler vials and 50 µL was injected into the G5-MTX-FA LC-FD HPLC system.

2.2.5 Sample preparation for MTX and 7OH-MTX analyses

The first step for analysis of the free analyte fraction was protein precipitation achieved by adding 30 µL of 10% perchloric acid to 100 µL spiked or sampled plasma. The vial then was closed and vortexed for 10 seconds, and the precipitated proteins were spun down for 5 minutes at 1.000g. The deproteinized sample was diluted by addition of 900 µL of 100 mM ammonium bicarbonate solution (pH 8.0). Aliquots (950 µL) of the diluted samples were subjected to Solid Phase Extraction (SPE), as described below. The recovered analytes were heated in 40 °C water and evaporated to dryness under a gentle stream of nitrogen. The residue was reconstituted in 200 µL of 100 mM ammonium bicarbonate (pH 8.0). The solution was transferred into a 1.0 mL autosampler vial with 350 µL insert and 100 µL was injected onto the post column photo-oxidation HPLC system.

2.2.6 Solid Phase Extraction (SPE)

A 100 mg, 1.0 ml Varian Bond Elute Strong Anion Exchange (SAX) SPE device was activated with 1.0 ml of MeOH. The column was equilibrated with 1.0 ml of 100 mM ammonium bicarbonate solution (pH 8.0). Then 950 µL of sample was applied. Interferences were washed from the column with 1.0 ml of 100 mM ammonium bicarbonate solution. The retained analytes were eluted by 1.0 ml of a soltution consisting of 95% MeOH and 5% formic acid. During extraction the SPE cartridges were mounted in a Waters vacuum manifold and the vacuum was adjusted to maintain a flowrate of approximately 0.5 ml/min through the cartridge.

2.2.7 Rat pharmacokinetic studies

Animal studies were performed externally by Bolder BioPATH (Bolder, CO), including obtaining the appropriate ethical permission. A total of twelve female Lewis rats (Charles river, Wilmington, MA) were subjected to treatment in the study. Six animals were treated with 65 mg/kg G5-MTX-FA by intravenous injection, and six animals were dosed in the subcutaneous tissue in the back of the neck. The drug concentration in the saline vehicle was 13 mg/mL. Blood samples were drawn at trough, 1 hr and 4 hr for three animals and at 0.5 hr, 2 hr and 8 hr for the remaining three animals of the group. Blood was collected in heparinized tubes and subsequently spun down to obtain the plasma fraction, which was snap frozen and shipped on dry ice. The received samples were stored at -70 °C for a month, and thawed before analysis.

2.3   Results and Discussion

2.3.1 Analytical strategy for G5-MTX-FA MTX titer determination

As noted in the introduction, G5-MTX-FA is a G5 PAMAM dendrimer core that has been chemically elaborated to result in a nanodevice whose surface primary amine groups have undergone several differing covalent modifications including acetylation, conjugation of glycidol, and attachment of folic acid (via an amide linkage) and methotrexate (via an ester linkage) (figure 8, 9). Purely on a statistical basis, one would expect a relative degree of heterogeneity in the preparation of such an nanodevice, including the loading of the purported therapeutic agent MTX. For example, a typical loading of MTX could be described as an average of 5.5 equivalents per dendrimer, but in actuality be constituted from a range of various dendrimer loadings. Similarly, the same arguments can be made for all of the G5-PAMAM core modifications. Since MTX is attached via an ester linkage, a site that is potentially susceptible to biochemical mediated hydrolysis, there is the possibility for the *in vivo* creation of additional heterogeneity with respect to dendrimer bound MTX, all with respect to a therapeutic agent of whose molecular weight is approximately 40,000 Daltons. For the therapeutic evaluation of G5-MTX-FA, one will be concerned with all the dendrimer associated MTX species, i.e. the total G5-MTX-FA MTX titer irrespective of molecular species, as well as any released MTX. Also as noted earlier, the chromatographic efficiency for a macromolecule, in this case approximately 40,000 Daltons, as compared to a typical small molecule, is significantly compromised.
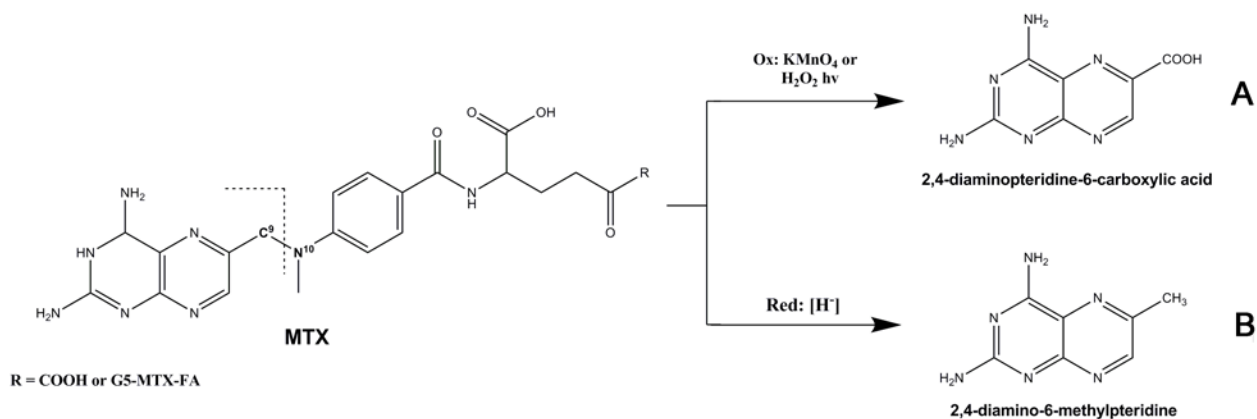
Figure 11. *Two routes of generating fluorescent pteridines involving cleavage of the C9-N10 bond. A) Oxidative cleavage mediated by KMnO$_4$ B) Reductive cleavage with Na$_2$O$_4$S$_2$.*

In reviewing various derivatization reactions typical for methotrexate, one notes that the C^9-N^{10} bond is labile to oxidation [32-38] and reduction [39] reactions, in either case resulting in the formation of 2,4 diaminopterin derivatives, each of which are known to be highly fluorescent (figure 11). The utilization of such reactions in a sample preparation step creates a small molecule "reporter" that would exhibit excellent chromatographic properties and be highly detectable. Furthermore in the case of G5-MTX-FA, if this approach was quantitative, it would result in an amplification of analyte concentration on a molar basis since there is expected to be approximately 5-equivalents of MTX to each dendrimer equivalent. One must also note the similar reactions are applicable to bound FA, and depending on the overall sample preparation operations, it could represent an unwanted interference. While these reactions have been applied to MTX determinations [19], application to dendrimer bound MTX (or FA) is unknown. However, if successful, this strategy would effectively transform a large molecule analyte to a small molecule analyte, a highly attractive possibility.

2.3.2 Initial Evaluation of the Reporter Approach

As noted above, in order to achieve MTX analysis by HPLC with fluorescence detection, MTX is commonly degraded by the oxidative pathway (figure 11A). This transformation has been performed by pre-column addition of $KMnO_4$ [32-34], but also can be performed post column with the use of H_2O_2 and photochemical initiation of the reaction[35-38]. Post-column degradation of dendrimer associated MTX is not a viable option since the degradation products of FA and MTX have similar excitation and emission profiles, resulting in a FA-MTX total response rather than a specific response for G5-MTX-FA associated MTX. The application of pre-column oxidation to G5-MTX-FA by $KMnO_4$, while being an effective derivatization method for unconjugated MTX (figure 12A), resulted in a complex mixture of fluorescent products that could not be resolved by reversed phase LC (figure 12B). Far less known and applied is reduction of MTX by $Na_2O_4S_2$ to form 2,4-diamino-6-methylpteridine (DAMP) (figure 11B). The yield of the reductive reaction has been reported to be 70% [39]. The application of this method to aqueous solutions of MTX is shown in (figure 12c), yielding a single peak. Reduction of G5-MTX-FA followed by subsequent analysis by LC-FL yielded two distinct peaks (figure 12D) that could be assigned as fluorescent methylpterines resulting from reduction of G5-MTX-FA associated FA and MTX, indicating successful release. Importantly, in contrast to the oxidative release result (figure 12B), the reductive approach (figure 12F) was devoid of the numerous chromatographic interferences observed by the oxidative method.
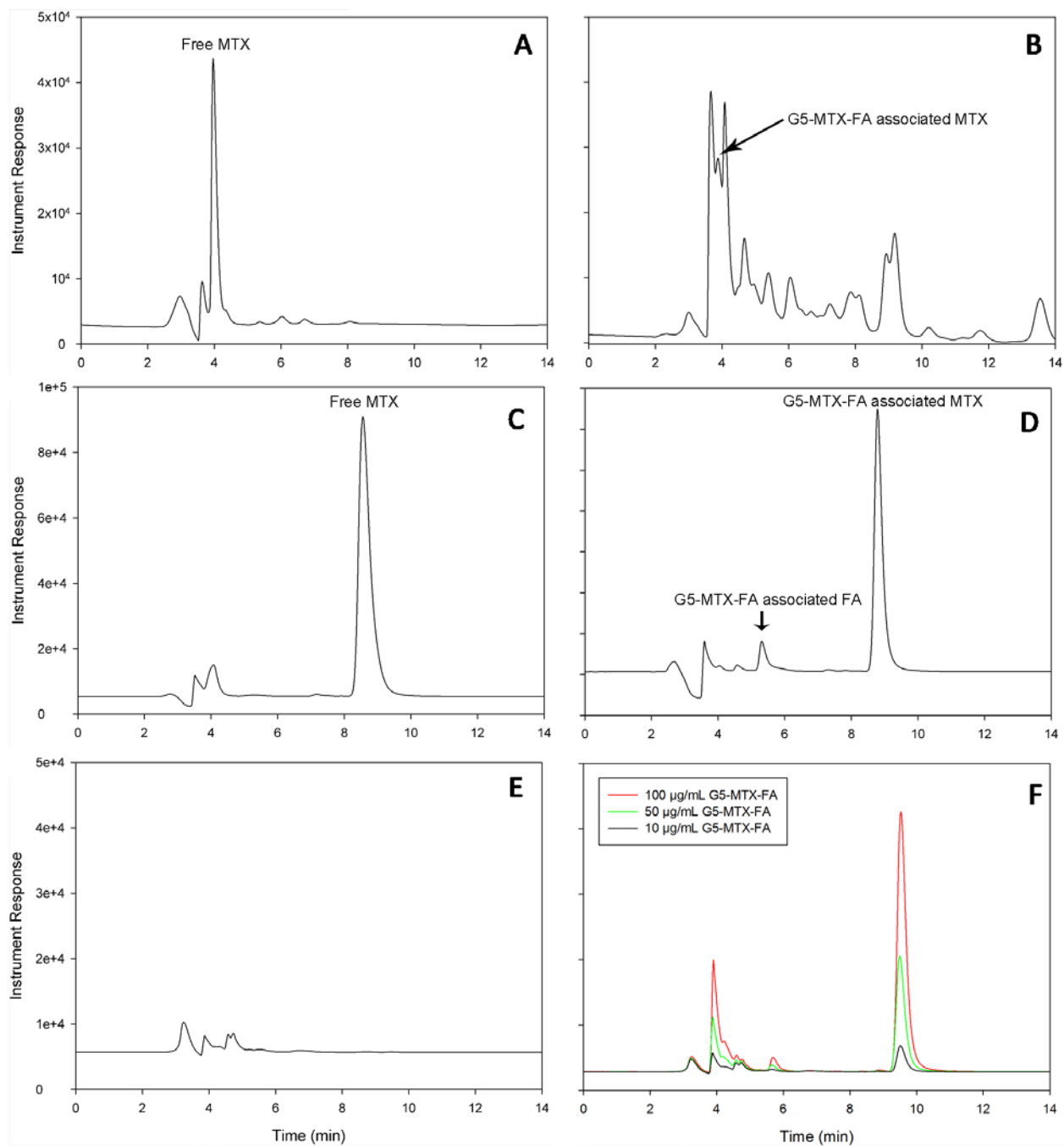
Figure 12. *A) Chromatogram of free MTX degraded by the oxidative pathway B) Chromatogram of G5-MTX-FA subjected to the oxidative procedure C) Chromatogram of free MTX degraded by the reductive pathway D) Chromatogram of G5-MTX-FA subjected to the reductive procedure E) Chromatogram of blank rat plasma subjected to the reductive procedure F) Chromatogram of low concentrations of G5-MTX-FA subjected to the reductive procedure in rat plasma.*

2.3.3 Rat plasma determination of G5-MTX-FA

For plasma analysis, the original MTX reductive method reported the use of perchloric acid to achieve deproteinization prior to reduction. This approach was found to be incompatible with the G5-MTX-FA apparently due to quantitative co-precipitation with plasma proteins. Alternatively the $Na_2O_4S_2$ mediated reduction of G5-MTX-FA in the plasma was evaluated. Reduction of a blank plasma sample at 100 °C led to the denaturation and precipitation of plasma proteins to the extent allowing for direct injection of the supernatant into the LC system without untoward consequences. The result obtained for blank rat plasma is illustrated by chromatogram of figure 12e, where it is may be noted that minimal biological noise was generated from the various plasma constituents. Subsequently, a G5-MTX-FA spiked rat plasma sample was treated in this fashion and, as illustrated in figure 12F, resulted in the successful release of the reporter DAMP from the nanodevice. In order to validate the bioanalytical assay, eight-point calibration runs involving six replicates were performed on three consecutive days (table 1).

Table 1. G5-MTX-FA intra- and inter-day precision and accuracy in a rat plasma matrix.

	Intra-run (n=6)			Inter-run (n=18)		
Nominal Concentration (µg/mL)	Mean observed concentration (µg/mL)	Precision (RSD %)	Mean Accuracy of target value (%)	Mean observed concentration (µg/mL)	Precision (RSD %)	Mean Accuracy of target value (%)
400	391.1	4.9	97.8	403.1	9.0	100.8
300	307.4	4.1	102.5	300.9	6.1	100.3
200	202.6	6.5	101.3	200.4	6.8	100.2
100	108.5	5.9	108.5	104.4	10.2	104.4
40	39.8	5.5	99.5	38.7	6.7	96.6
20	19.3	6.9	96.7	19.2	8.1	96.2
4	3.9	6.9	97.6	3.8	8.5	95.3
2	2.0	4.0	101.5	2.0	6.1	101.4

It was found that the procedure was linear over an G5-MTX-FA concentration range of 2-400 µg/mL utilizing only 100 µL of plasma. Since G5-MTX-FA has an estimated molecular weight of 37 kDa, one could also express the results on a molar scale, ranging in a dynamic range from ~50 to 10,000 nM, covering the anticipated *in-vivo* concentration range of this experimental therapeutic. Inter-day and intra-day precision and accuracy were found to be well within the commonly accepted guidelines for a bioanalytical assay.

2.3.4 Dog plasma determination of G5-MTX-FA

In-vivo toxicology studies of G5-MTX-FA were also conducted in Beagle dogs, along with the various rat studies. In order to support these studies, the suitability of the rat plasma method presented in section 2.3.3 was explored for the analysis of dog plasma samples. G5-MTX-FA spiked dog plasma gave similar chromatograms compared to G5-MTX-FA enriched rat plasma, indicating that the method could be directly transferred between these matrices. In order to assess the reproducibility and accuracy of the method in dog plasma, a similar validation experiment was performed as reported in section 2.3.3 (table 2). As demonstrated by table 1 and 2, the performance (precision and accuracy) of the reductive method for the analysis of G5-MTX-FA is similar in both, dog and rat plasma respectively. Inter- and intra-run accuracy and precision are well within the FDA guidelines of Crystal City defining that accuracy and precision should be within <15% in the calibration range, and <20% at the detection limit. Limits of detection were set 2ug/mL, however the precision of 8.7% at this value suggest limit of detection could be challenged further.

48

Table 2. Intra- and inter-day precision and accuracy in a Beagle plasma matrix.

Nominal Concentration (µg/mL)	Intra-run (n=6)			Inter-run (n=18)		
	Mean observed concentration (µg/mL)	Precision (RSD %)	Mean Accuracy of target value (%)	Mean observed concentration (µg/mL)	Precision (RSD %)	Mean Accuracy of target value (%)
400	393.9	5.0	98.5	396.2	6.5	99.1
300	309.6	4.1	103.2	302.9	5.4	101.0
200	204.1	6.6	102.1	205.4	6.6	102.7
100	109.3	5.0	109.3	107.1	7.8	107.1
40	40.1	5.6	100.3	38.0	6.3	95.1
20	19.5	6.9	97.4	19.0	7.8	94.8
4	3.9	7.0	98.3	3.4	10.3	86.0
2	2.0	4.0	102.3	1.9	8.7	92.5

2.3.5 Determination of free MTX and 7OH-MTX

Determination of *in-vivo* released MTX and the metabolite 7-OHMTX was accomplished by established methodology that involved liquid chromatography (LC) fractionation followed by post-column photochemistry ((PC(*hv*)) with fluorescence detection (FD)[35-38]. This approach allows for the separation and specific quantitation of MTX and various metabolites including 7O-HMTX and if necessary DAMPA. Since G5-MTX-FA would only be dosed via intravenous injection, DAMPA was not an analytical target of the present effort. However, using the LC-PC(*hv*)-FD approach, the resulting methodology is such that DAMPA is not an interference with respect to MTX and 7OH-MTX, and if required could be used for DAMPA determination.

Separation of MTX and 7OH-MTX was conducted on a end-capped reversed phase C18 column. The selectivity factor of this column for the separation of MTX and 7OH-MTX is not optimal, and as a result MTX and 7OH-MTX were only partially resolved, or lengthy analysis times are required in order to facilitate separation (figure

13A). It has been shown that the resolution between both compounds can be improved on a C18 column through the addition of dimethylformamide (DMF) to the mobile phase[36]. Using relatively small percentages of DMF as a mobile phase additive, typically 2.5% by volume, allowed for high separation selectivity with respect to the resolution of MTX and 7OH-MTX and an overall separation time of 10 minutes (figure 13B, C, D).
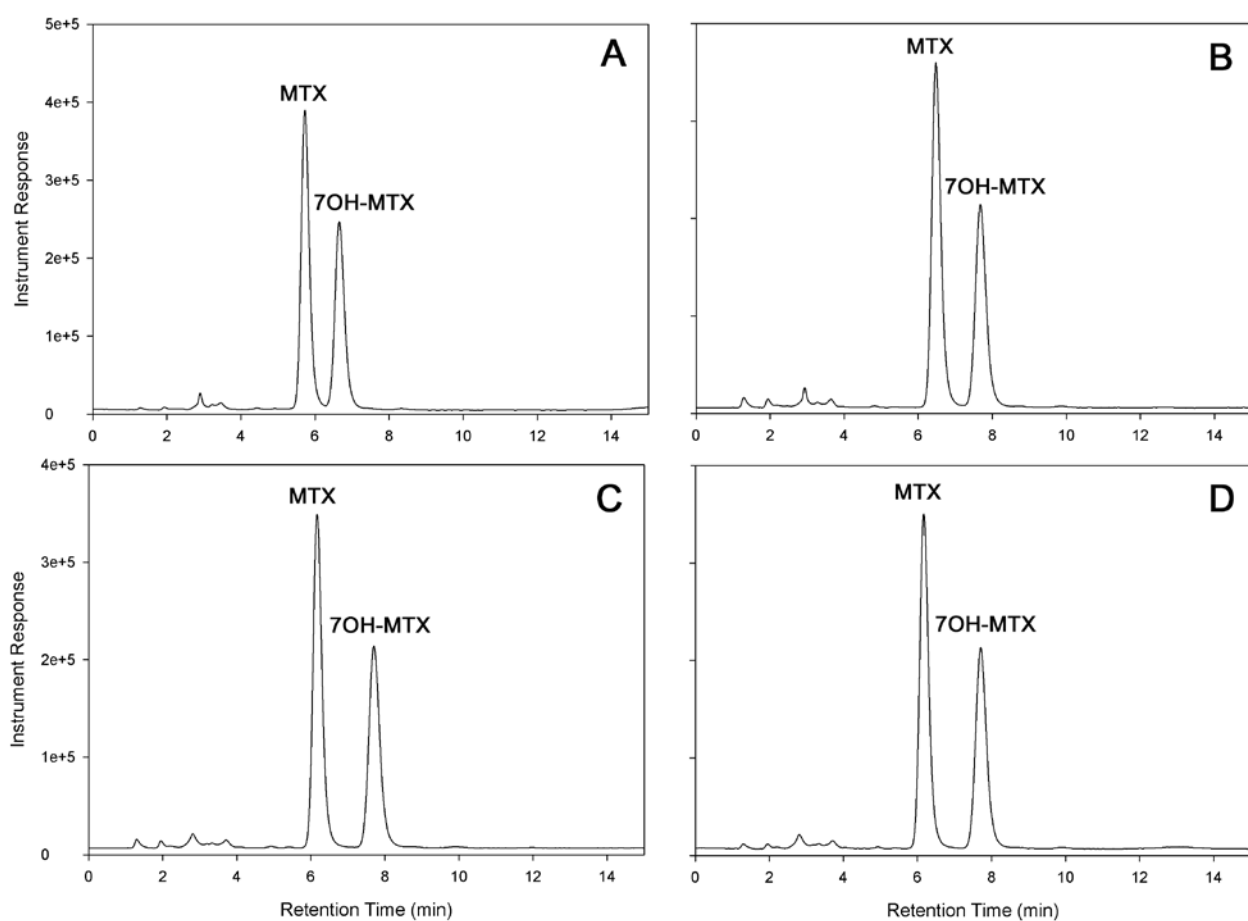
Figure 13. *Separation of MTX and 7OH-MTX with A) no DMF in the mobile phase B) 1% DMF in the mobile phase C) 2.5% DMF in the mobile phase D) 5% DMF in the mobile phase.*

Sensitive detection of both MTX and 7OH-MTX was achieved by optimization of the post column PTFE reaction coil length. Longer columns would allow for more sensitive detection of MTX, but lead to over oxidation of 7OH-MTX resulting in diminished detection sensitivity (figure 14). A compromise was made between both signals by using a reactor coil with a length of 1 meter, resulting in an exposure/residence time of the analytes in the photo reactor of about 4 seconds at a flow rate of 1.0 mL/min. This residence time maximizes the detection sensitivity of the MTX metabolite 7OH-MTX which is generally a present in lower concentrations that MTX itself in plasma, therefore maximizing the detection potential for this low abundance metabolite.
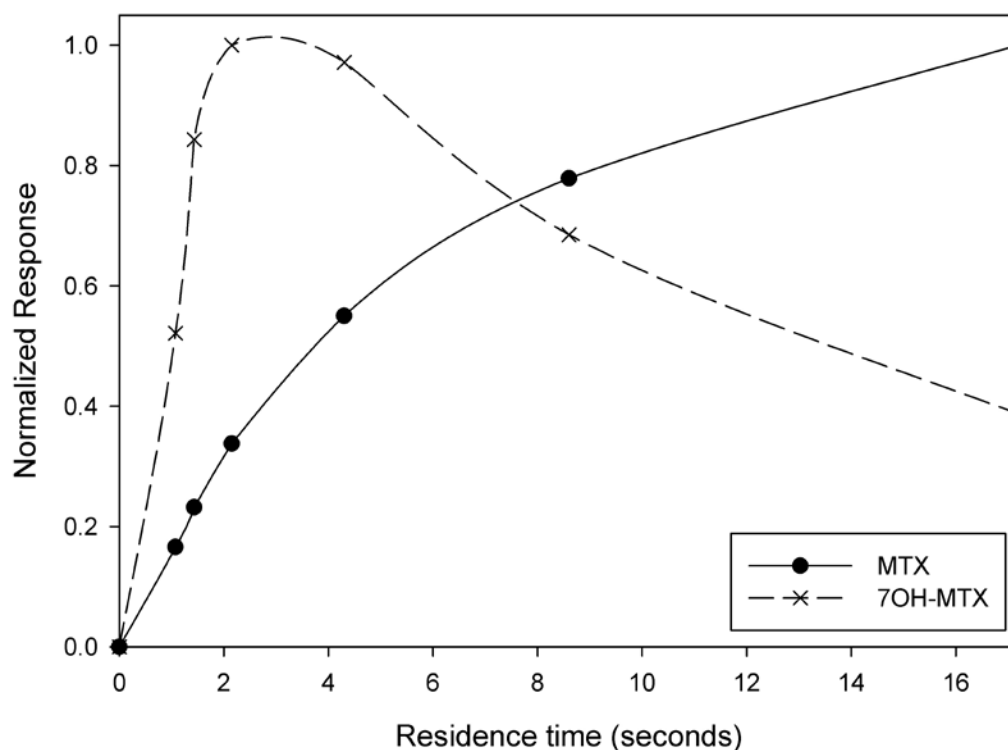
Figure 14. *Optimization of the fluorescence signal for MTX and 7OH-MTX by varying the reactor coil length and therefore reaction/residence time.*

2.3.5.1 Determination of free MTX and 7OH-MTX out of rat plasma
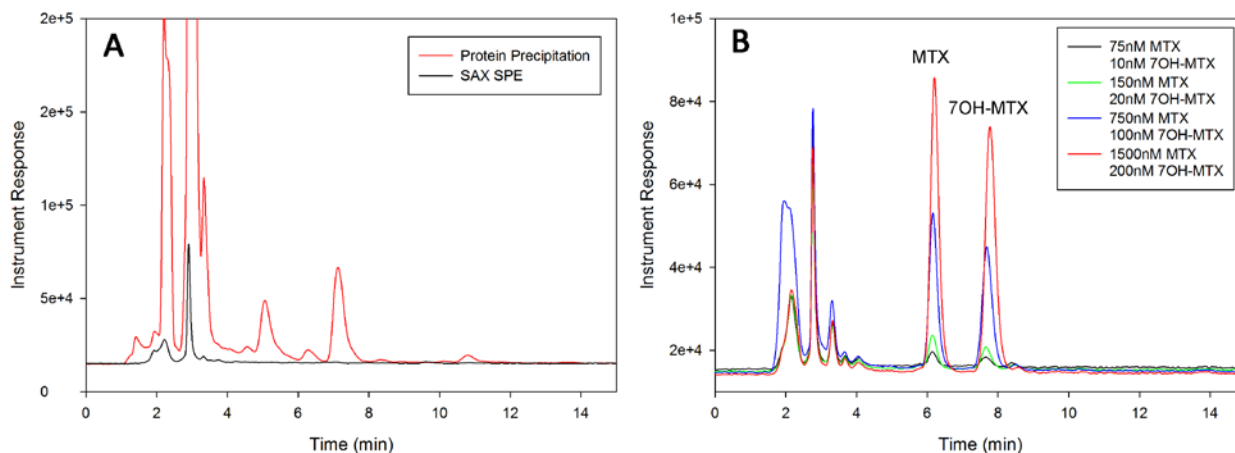
Figure 15. *A) Rat plasma interference removal by performing a SAX SPE extraction. B) rat plasma enriched with MTX and 7OH-MTX at various concentrations.*

Sample preparation consisted of two straightforward steps. The analytes were first isolated in the supernatant obtained subsequent to perchloric acid mediated protein precipitation. In a second step the analytes were subjected to an SPE extraction, using a strong anion exchange (SAX) cartridge in order to reduce biological background (figure 15A). The SPE step provided an interference free chromatographic window which was utilized for the isocratic separation of MTX and 7OH-MTX (figure 15B).

Table 3. Intraday validation of free MTX in rat plasma

Nominal MTX Concentration (µM)	Mean observed concentration (µM) (n=6)	Precision (RSD %)	Mean Accuracy of target value (%)
15.3	15.2	2.0	99.3
11.4	11.1	5.6	97.0
7.6	7.8	7.3	102.9
3.7	4.3	5.3	116.2
1.5	1.4	11.3	96.6
0.75	0.67	3.8	89.0
0.15	0.14	6.1	94.4
0.075	0.080	14.5	107.0

Table 4. Intraday validation of free 7OH-MTX in rat plasma

Nominal 7OH-MTX Concentration (µM)	Mean observed concentration (µM) (n=6)	Precision (RSD %)	Mean Accuracy of target value (%)
2	2.0	3.4	101.10
1.5	1.4	5.8	96.14
1	1.1	7.6	105.04
0.5	0.59	5.5	118.94
0.2	0.18	9.4	91.49
0.1	0.09	5.7	92.05
0.02	0.020	4.9	99.62
0.01	0.009	19.9	85.65

Assay specificity with regard to G5-MTX-FA associated MTX was investigated by the analysis of various spiked controls (concentrations as high as 0.1 mg/mL). G5-MTX-FA was not observed in any of the LC-PC(*hv*)-FD chromatograms, thus demonstrating the assay is specific for MTX and 7OH-MTX regardless of G5-MTX-FA concentrations. A limited validation (8 points calibration with 6 replications for each concentration) was performed since this methodology has been largely described in the literature (table 3 and 4). The limit of quantitation for MTX and 7OH-MTX was determined to be 50 nM and 10 nM, respectively.

2.3.5.2 Determination of free MTX and 7OH-MTX out of Beagle plasma

As stated before *in-vivo* toxicology studies of G5-MTX-FA were also conducted in Beagle dogs. It was found that the free analyte method could be directly transferred from rat plasma to dog plasma without any alterations to the chromatographic system or sample preparation procedure. The method was validated according to a similar protocol

as in 2.3.5.1, running 6 replicates at 8 different concentrations (table 5 and 6). As illustrated by table 2 and 3 intra-day accuracy and precision are well within FDA guidelines for a bioanalytical assay, where deviations up to 20% are acceptable.

Table 5. Intraday validation of free MTX in Beagle plasma

Nominal MTX Concentration (µM)	Mean observed concentration (µM) (n=6)	Precision (RSD %)	Mean Accuracy of target value (%)
15.3	14.5	3.6	94.5
11.4	11.5	3.8	100.7
7.6	8.1	0.7	106.1
3.7	3.8	3.5	102.0
1.5	1.3	4.1	89.8
0.75	0.66	3.2	87.5
0.15	0.13	5.4	83.3
0.075	0.064	7.4	85.2

Table 6. Intraday validation of free 7OH-MTX in Beagle plasma

Nominal 7OH-MTX Concentration (µM)	Mean observed concentration (µM) (n=6)	Precision (RSD %)	Mean Accuracy of target value (%)
2	1.9	3.3	95.2
1.5	1.6	4.3	107.1
1	1.2	2.4	119.1
0.5	0.57	3.9	114.8
0.2	0.22	4.3	108.6
0.1	0.11	3.1	111.3
0.02	0.019	3.2	95.4
0.01	0.009	14.9	92.0

2.3.6 G5-MTX-FA Sample Preparation Issues

Pre-column reduction for detection of G5-MTX-FA associated MTX is compromised by any (released) free MTX within the sample that will form the same fluorescent product upon degradation. In order to achieve specific detection of G5-MTX-FA associated MTX, attempts were made to separate the nanodevice from free MTX. A variety of SPE sorbents including C18, SAX, WCX and PLEXA® were explored in order to either retain the dendrimer conjugate with free MTX eluting in the void volume, or vice versa. The recovery of G5-MTX-FA after SPE extraction was found to be low, non-linear and highly irreproducible, with lower regions of the calibration curve affected more severely. Similar behavior of G5-MTX-FA was observed utilizing SEC and ultra-filtration materials. Significant analyte loss at low µM concentrations due to adsorption could be observed upon exposure of a standard solution of G5-MTX-FA to a glass surface. Previous work has reported that amine-terminated PAMAM dendrimers adsorb tenaciously to polar surfaces making chromatography on this class of compounds difficult[29]. In the present investigation, adsorption of a surface deactivated G5-MTX-FA dendrimer conjugate was observed, suggesting that the G5 PAMAM core may become partially exposed and available for interactions, perhaps due to an initial absorption and subsequent rearrangement of the three dimensional structure.

2.3.7 Successful Sample Pretreatment of G5-MTX-FA

Significant loss of G5-MTX-FA was encountered in all of the various sample preparation steps examined. Reflecting upon this situation, these results are could be due to the numerous polar interaction sites of the macromolecule (numerous amide

moieties reside along each of the dendrimer arms), thus once a given untoward interaction occurs, a second and following interactions likely would occur, essentially providing a cascade of events leading to unwanted binding and loss of the macromolecule analyte. However, as previously noted, reductive cleavage to provide a small molecule reporter was a highly successful approach to quantitation of G5-MTX-FA. If one subjected an untreated plasma sample to the reduction reaction, perhaps there would be a reproducible release of the reporter, which would remain in solution and not be subject to the various G5-MTX-FA loss processes previously observed. However, the consequence is that the total measured MTX concentration consists of G5-MTX-FA associated MTX and free MTX. Since free MTX can be determined accurately and independently of G5-MTX-FA associated MTX, one could perform both determinations and subtract the free MTX value from the apparent total to obtain G5-MTX-FA associated MTX. As this strategy was devised, the *in-vivo* MTX release behavior of G5-MTX-FA was not clear, but three scenarios could be expected. Category 1, none to very little (<1%) MTX is released from G5-MTX-FA. In this scenario free MTX could be determined accurately and the total MTX value obtained by the reductive method closely reflects G5-MTX-FA associated MTX with minimal correction required. Category 2, MTX release is significant but not the major product and total G5-MTX-FA requires correction. Category 3, there is a significant release of MTX from the nanodevice, with free MTX serving to dominate the total value as compared to G5-MTX-FA associated MTX.

Table 7. Method specificity and mathematical correction.

MTX (μM)*	Spiked Free MTX (μM)	Total MTX in sample (μM)	Total MTX Measured by reduction (μM)	Free MTX measured (μM)	Calculated G5 MTX content (μM)	Mean Accuracy of G5-MTX value (%)
23.0	3.9	26.9	25.9	3.9	22.0	95.6
17.3	0.8	18.0	17.0	0.9	16.1	93.5
11.5	1.6	13.1	13.2	1.6	11.7	101.5
5.8	15.6	21.4	22.6	15.5	7.1	123.6
2.3	7.8	10.1	9.5	7.7	1.8	79.9
1.2	11.7	12.9	12.6	11.9	0.8	65.4

*Concentrations of G5 associated MTX are based on the assumption that on spiked G5-average 5.48 MTX molecules are attached.

In order to analyze the feasibility of this approach, a number of cases with significant MTX release were simulated. Various samples were spiked with G5-MTX-FA and free MTX, divided into two separate aliquots, and analyzed by the reductive (total MTX obtained) and the LC-PC(*hv*)-FD method respectively (table 7). Analysis of the first 3 cases in table 4 (falling in category 2) show that free MTX content was determined accurately and independently of G5-MTX-FA concentration. Subtraction of the free MTX content from the measured MTX total by the reductive method yielded the expected (known) G5-MTX-FA concentration, proving that subtraction is a viable method for category 2 cases. The last 3 cases could be assigned as category 3, having high free MTX content. Free MTX could again be determined accurately independently of G5-MTX-FA content, however subtraction of free MTX content from the obtained MTX total did not result in accurate G5-MTX-FA associated MTX values. High standard deviations are however expected in this type of scenario, since a relatively large number (and its associated absolute standard deviation) is subtracted from a nearly equal number (with its standard deviation), resulting in a relatively small difference. A result observed for this

mathematical correction is a extremely large relative standard deviation, and thus imprecision associated with the G5-MTX-FA determination. As these results became available, information emerged indicating that category 1 describes the *in-vivo* fate of G5-MTX-FA for rats (see the results provided in the application section), thus no further method development efforts were required.

2.3.8 Stability

Stability data is shown in table 8. The stability of G5-MTX-FA was studied at intermediate to high concentrations, so significant amounts of released MTX would be detectable. The derivatized product DAMP was found to be stable in the autosampler at room temperature for 24 hr illustrated by the small R.S.D. for repetitive analysis over this time course. All of the samples were analyzed within 24 hr this window. G5-MTX-FA spiked plasma samples were stable over three consecutive freeze-thaw cycles, and no free MTX due to ester cleavage could be detected. Prior work has described the stability of the MTX ester linkage to the nanodevice at pH 2.25 for 59 days at room temperature in highly aqueous media[30]. The percentage of released MTX was found to be less than 1 percent, suggesting that the ester linkage not particularly labile. In order to demonstrate that the ester linkage is not hydrolyzed by esterases during sample processing, G5-MTX-FA spiked plasma samples were incubated at room temperature for 4 hours (exceeding standard processing time), and subsequently analyzed. Free MTX could not be detected, indicating that esterlinkage is stable in rat plasma during sample processing and handling. Samples from a pharmacokinetic study were stored for

58

a month before analysis occurred. G5-MTX-FA was found to be stable at -70 °C over this time frame (table 8).

Table 8. Stability of G5-MTX-FA under various conditions (n=5)

Storage condition	G5-MTX-FA related MTX concentration (μg/mL)		R.S.D. (%)	Free MTX	Free 7OH-MTX
	nominal	measured		measured	measured
Stability in autosampler	50	51.9	0.8	ND	ND
	100	103.4	0.8	ND	ND
	200	188.1	0.5	ND	ND
Freeze-thaw stability	50	47.5	10.1	ND	ND
	100	102.9	3.9	ND	ND
	200	198.9	4.0	ND	ND
Incubation at 25 °C (4h)	50	46.1	1.9	ND	ND
	100	100.9	0.7	ND	ND
	200	182.6	2.5	ND	ND
Stability at -20 °C (1 month)	50	54.6	4.5	ND	ND
	100	104.2	7.7	ND	ND
	200	207.7	3.0	ND	ND

2.3.4 Reporter Chemistry for Determination of G5-MTX-FA Titer

As noted in the introduction, characterization of the degree of surface modification of dendrimer conjugates is an analytical challenge. In order to determine an average MTX or FA titer of the G5-PAMAM derivatives, researchers have applied UV spectroscopy, gel permeation chromatography or have taken advantage of MTXs or FAs aromatic hydrogens on the *para*-aminobenzoic acid residue that appears downfield in a proton NMR spectrum[16]. The effectiveness of both strategies diminishes with increasing size, complexity and intermolecular interaction of dendrimer conjugates.

The reductive release method demonstrated in the previous paragraph provides a potential complimentary strategy for determination of MTX titer. Assuming the yield of

reductive cleavage of the C^9-N^{10} bridge in free MTX and G5 conjugated MTX is similar, the G5-MTX titer can be determined by running individual calibration curves. The difference in slope between individual calibration curves of free MTX and G5 conjugated MTX reveals the number of MTX molecules associated with G5 (equation 1).

(Eq. 1) MTX loading = G5-MTX-FA related MTX slope / MTX std slope.

Although not within the scope of method development, a similar argument could be made for determination of the FA loading of the nanodevice (equation 2).

(Eq. 2) FA loading = G5-MTX-FA related FA slope / FA std slope.

Various lots of G5-MTX-FA were supplied by Avidimer Therapeutics for valuation of MTX and FA titer (table 9). The MTX titer varied between 4.84 and 10.16 MTX molecules per nanoparticle. Lot 0505-001 of G5-MTX-FA was used for the analytical method development and was found to bear on average 5.15 molecules of MTX per G5 PAMAM core unit, by the reductive method (table 9). Information provided by the supplier indicated approximately 5-6 MTX molecules per G5 PAMAM core unit could be expected, which is in substantial agreement with the present findings.

Table 9. G5-MTX-FA related MTX FA titer determination

lot	std	[G5-MTX-FA] uM	MTX area	MTX - statistics	MTX titer	FA area	FA - statistics	FA titer
123-34	1	0.086	1411591	r^2: 0.998		69465	r^2: 0.993	
	2	0.171	3698321			228743		
	3	0.342	6844653		6.22[1]	334365		0.49[2]
	4	0.685	13581518	slope: 21571743		712390	slope: 953099	
	5	1.37	29421989			1217554		
0505-001	1	0.081	1480690	r^2: 0.999		42701	r^2: 0.998	
	2	0.162	3197696			94691		
	3	0.324	5768268		5.15[1]	174527		0.32[2]
	4	0.6487	11721408	slope: 17831219		386135	slope: 637559	
	5	1.297	23257656			816670		
0147-135	1	0.086	1718343	r^2: 0.998		40306	r^2: 0.998	
	2	0.172	4093268			142838		
	3	0.346	7560776		4.84[1]	287852		0.41[2]
	4	0.691	16051808	slope: 16741453		548374	slope: 792169	
	5	1.382	31118674			1085550		
06-02-0001	1	0.089	1568317	r^2: 0.993		82331	r^2: 0.998	
	2	0.179	3781184			170311		
	3	0.357	8095449		5.90[1]	371968		0.49[2]
	4	0.714	14435970	slope: 20428177		706376	slope: 948106	
	5	1.428	-			1355976		
0083-112	1	0.085	2681269	r^2: 0.999		38670	r^2: 0.997	
	2	0.169	5271335			97636		
	3	0.338	11856236		10.16[1]	204302		0.32[2]
	4	0.676	23316396	slope: 35184146		379370	slope: 618420	
	5	1.352	47191623			831796		

[1] MTX standard curve statistics: r^2: 0.999, slope: 3462379

[2] FA standard curve statistics: r^2: 0.986, slope: 1942248

G5-MTX-FA was found to bear on average 0.5 FA molecules per core unit, which was substantially different from the information supplied by the provider of G5-MTX-FA, which had indicated an average of 5 FA molecules covalently attached to the nanocarrier core. The nature of this discrepancy at this point is not understood, however the difference might be indicative of side reactions during coupling of FA or the introduction of structural modifications to the FA pteridine core in subsequent synthetic steps (reaction with glycidol and the addition of MTX). Detecting these minor FA modifications is challenging with the spectroscopic techniques described earlier in this introduction of this chapter. However, (slighty) structurally altered FA will behave differently upon reduction, possibly have different emission and excitation wavelengths, and will be separated by reversed phase chromatography, and thus (minor) variations chemical variations will lead to a diminished FA titer using this method.

In order to investigate the effect of side reactions, the FA titer was determined on several isolated intermediates during the G5-MTX-FA synthesis procedure. The first step in the synthetic procedure is partial acylation of the PAMAM dendrimer core, followed by carbodiimide coupling of FA. Analysis of the FA coupled intermediate revealed by the reductive procedure indicated that 0.82 FA molecules were attached per dendrimer core unit, again significantly less than the suggested 5 FA molecules/dendrimer core unit (figure 16), but higher than the 0.32 FA/G5-MTX-FA measured on the final product.
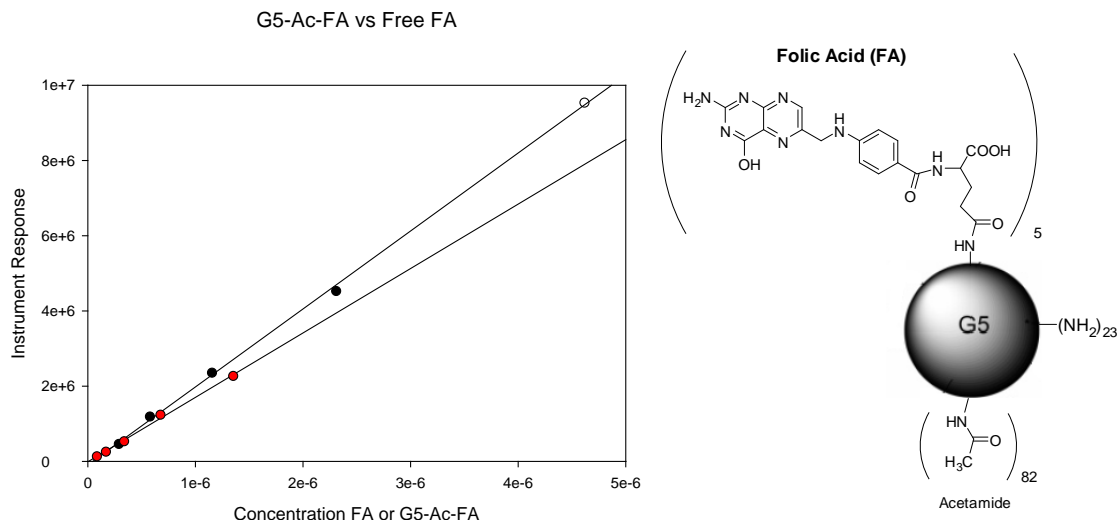
Figure 16. *FA-titer determination (a) on a G5-MTX-FA intermediate (b) that has been partially acylated, followed by conjugation with FA. The FA-titer was determined at 0.82 FA/core unit.*

The next step in the synthetic procedure aims for derivitization of the remaining primairy amines on the surface of the PAMAM nanoparticle with glycidol (figure 17). Subjection of this 2nd intermediate to the reductive procedure reveals that there are 0.30 FA molecules associated with the nanoparticle, indicating a further loss of roughly 2/3 of the FA molecules during this procedure. As suggested earlier in this paragraph, due to the high specificity of this method, a lower FA titer can also be observed due to covalent modifications on FA. Since characterization of G5-MTX-FA was not within the research scope, further studies to investigate the discrepancies between the various analysis methods were not conducted. However, it is important to note that the targeting vector of the nanodevice (FA) might have a covalently altered structure and largely presents itself in this fashion to the over expressed folate receptors on the cancer cell surface, rather than glutamyl linked native FA.
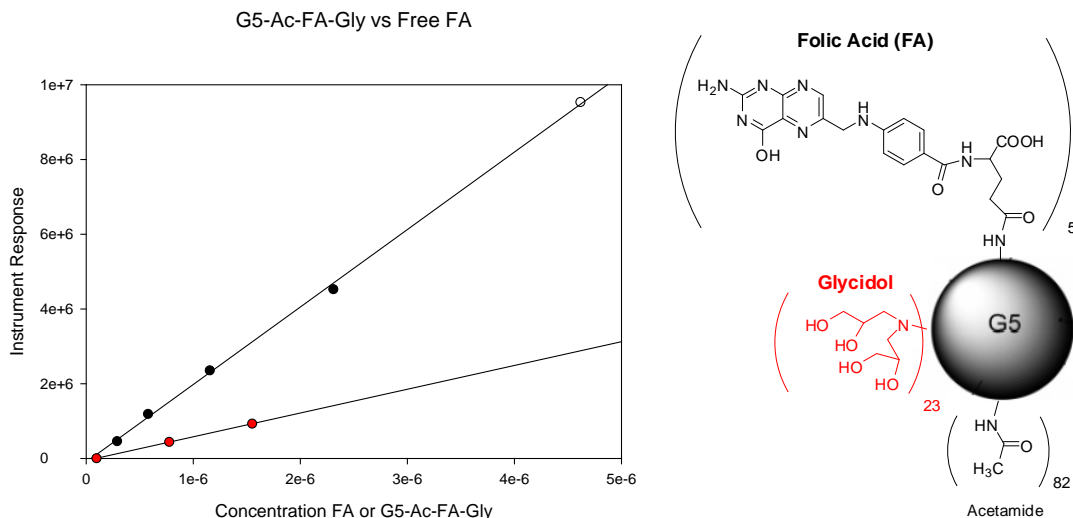
Figure 17. *FA-titer determination (a) on a G5-MTX-FA intermediate that has been subjected to reaction with glycidol (b) The FA-titer was determined at 0.30 FA/core unit.*

2.3.5 Application of the method

The plasma reduction approach described above was utilized for analysis of plasma samples obtained form a toxicology study in rats. The rats were given doses of 50, 200, 400 and 800mg/kg G5-MTX-FA by intavenous injection (IV). The early time point samples had to be diluted 1:10 prior to analysis (i.e after reduction) in order to reduce concentration and prevent detector over-ranging. G5-MTX-FA could be determined in all of the resulting plasma samples (Figure 18A). Free analytes, MTX and 7OH-MTX, only could be detected in rats dosed at 800mg/kg. The MTX concentrations observed were low and quickly dropped below the limits of detection for the free analyte assay (Figure 18B). The plasma profile of MTX suggests, that at a given time point, the circulating free MTX mass accounts for ~0.06% of the total MTX mass. In prior work, stability of the MTX ester bond linkage to the nanodevice had been tested at pH 2.25 for

59 days at room temperature in highly aqueous media [30]. The percentage of released MTX was found to be less than 1 percent, suggesting that the ester linkage not particularly enzyme labile. In the present investigation, it appears that the ester bond is also stable *in-vivo* in the presence esterases and other endogenous compounds, however future work is needed to ascertain the hydrolysis rate constant in biological matrices. The presently described analytical methodology would allow for such a study, but is beyond the scope of the present work.

Preliminary pharmacokinetic profiles of G5-MTX-FA in rats at dosages clinically more relevant were also obtained. Three animals received G5-MTX-FA at a dose of 65 mg/kg by IV injection (Figure 18C), and three animals were treated with a similar dose by subcutaneous injection (SC) (Figure 18D). After IV injection, G5-MTX-FA appears to undergo a rapid distribution phase (Figure 18A, C) followed by rapid clearance from plasma, which is consistent with earlier reports [18]. G5-MTX-FA plasma concentrations observed, when administered in the SC tissue, were typically much lower compared to the IV samples. The maximal G5-MTX-FA plasma concentration was observed 8 hours after administration (Figure 18D). For accurate pharmacokinetic modeling, an increased number of data points is required, especially with regard to the elimination phase. However, the sensitivity of the present analytical methodology was found adequate for the plasma analysis of G5-MTX-FA in rats and would support such a study.
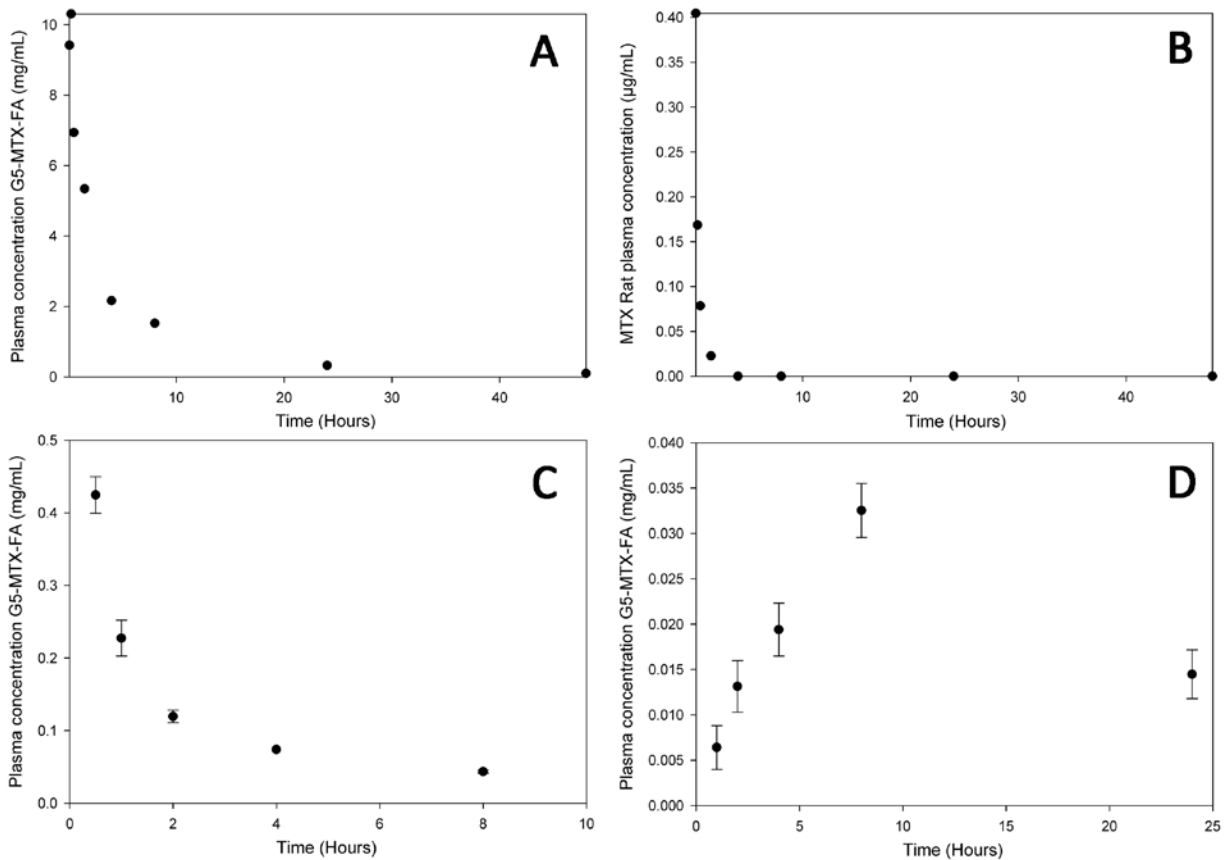
Figure 18. *A) G5-MTX-FA plasma PK profile of a 800mg/kg IV dosed rat. B) PK profile of G5-MTX-FA released MTX, same animal as shown in (A). C) G5-MTX-FA plasma PK profile of 65mg/kg IV dosed rats (n=3). D) G5-MTX-FA plasma PK profile of 65mg/kg SC dosed rats (n=3).*

2.4 Conclusion

A bioanalytical assay is presented for the analysis of G5-MTX-FA associated MTX, released MTX and the major metabolite 7OH-MTX in plasma samples. Due to difficulties associated with various sample preparation approaches, a strategy was developed wherein the sample was divided into two aliquots with each being analyzed with differing but complementary methodology. The result was that one aliquot, without any other sample preparation steps, could be subjected to a reductive reaction to release a highly fluorescent reporter molecule. The second sample aliquot was used to determine any released MTX and the major metabolite 7OH-MTX after subjecting the sample to an appropriate SPE procedure followed by LC-PCR(hv)-FD. The analysis strategy for G5-MTX-FA associated MTX could not distinguish between conjugated and free MTX. However, it was demonstrated that the amount of MTX released in plasma by the nanodevice is insignificant, and as a result the presented strategy is specific for G5-MTX-FA associated MTX. Free MTX and 7OH-MTX could be determined specifically, irrespective of the nanodevice concentration. The presented methodology was successfully used to establish a preliminary plasma pharmacokinetic profile of G5-MTX-FA in rats. Finally, the reductive release method allows for the determination of glutamyl conjugated MTX titer of functionalized PAMAM polymers.

2.5 References

[1]   D. A. Tomalia, A. M. Naylor, W. A. G. III, Starburst Dendrimers: Molecular-Level Control of Size, Shape, Surface Chemistry, Topology, and Flexibility from Atoms to Macroscopic Matter. *Angewandte Chemie International Edition in English.* **1990**, *29*, 138.

[2]   A. K. Patri, I. J. Majoros, J. R. Baker, Dendritic polymer macromolecular carriers for drug delivery. *Current Opinion in Chemical Biology.* **2002**, *6*, 466.

[3]   R. Esfand, D. A. Tomalia, Poly(amidoamine) (PAMAM) dendrimers: from biomimicry to drug delivery and biomedical applications. *Drug Discovery Today.* **2001**, *6*, 427.

[4]   A. T. Florence, Dendrimers: a versatile targeting platform. *Advanced Drug Delivery Reviews.* **2005**, *57*, 2.

[5]   Y. Cheng, T. Xu, The effect of dendrimers on the pharmacodynamic and pharmacokinetic behaviors of non-covalently or covalently attached drugs. *European Journal of Medicinal Chemistry.* **2008**, *43*, 2291.

[6]   Y. Cheng, Z. Xu, M. Ma, T. Xu, Dendrimers as drug carriers: Applications in different routes of drug administration. *Journal of Pharmaceutical Sciences.* **2008**, *97*, 123.

[7]   J. F. G. A. Jansen, E. M. M. de Brabander-van den Berg, E. W. Meijer, Encapsulation of Guest Molecules into a Dendritic Box. *Science.* **1994**, *266*, 1226.

[8]   O. M. Milhem, C. Myles, N. B. McKeown, D. Attwood, A. D'Emanuele, Polyamidoamine Starburst® dendrimers as solubility enhancers. *International Journal of Pharmaceutics.* **2000**, *197*, 239.

[9]   C. Yiyun, X. Tongwen, F. Rongqiang, Polyamidoamine dendrimers used as solubility enhancers of ketoprofen. *European Journal of Medicinal Chemistry.* **2005**, *40*, 1390.

[10]   A. S. Chauhan, S. Sridevi, K. B. Chalasani, A. K. Jain, S. K. Jain, N. K. Jain, P. V. Diwan, Dendrimer-mediated transdermal delivery: enhanced bioavailability of indomethacin. *Journal of Controlled Release.* **2003**, *90*, 335.

[11]   A. K. Patri, J. F. Kukowska-Latallo, J. J. R. Baker, Targeted drug delivery with dendrimers: Comparison of the release kinetics of covalently conjugated drug and non-covalent drug inclusion complex. *Advanced Drug Delivery Reviews.* **2005**, *57*, 2203.

[12]   I. J. Majoros, B. Keszler, S. Woehler, T. Bull, J. R. Baker, Acetylation of Poly(amidoamine) Dendrimers. *Macromolecules.* **2003**, *36*, 5526.

[13]   J. R. Baker, A. Quintana, L. Piehler, M. Banazak-Holl, D. Tomalia, E. Raczka, The Synthesis and Testing of Anti-Cancer Therapeutic Nanodevices. *Biomedical Microdevices.* **2001**, *3*, 61.

[14]   S. Hong, P. R. Leroueil, I. J. Majoros, B. G. Orr, J. R. Baker Jr, M. M. Banaszak Holl, The Binding Avidity of a Nanoparticle-Based Multivalent Targeted Drug Delivery Platform. *Chemistry & Biology.* **2007**, *14*, 107.

[15]   A. Quintana, E. Raczka, L. Piehler, I. Lee, A. Myc, I. Majoros, A. Patri, T. Thomas, J. Mulé, J. Baker, Design and Function of a Dendrimer-Based Therapeutic Nanodevice Targeted to Tumor Cells Through the Folate Receptor. *Pharmaceutical Research.* **2002**, *19*, 1310.

[16]   I. J. Majoros, T. P. Thomas, C. B. Mehta, J. R. Baker, Poly(amidoamine) Dendrimer-Based Multifunctional Engineered Nanodevice for Cancer Therapy. *Journal of Medicinal Chemistry.* **2005**, *48*, 5892.

[17]   T. P. Thomas, I. J. Majoros, A. Kotlyar, J. F. Kukowska-Latallo, A. Bielinska, A. Myc, J. R. Baker, Targeting and Inhibition of Cell Growth by an Engineered Dendritic Nanodevice. *Journal of Medicinal Chemistry.* **2005**, *48*, 3729.

[18]   J. F. Kukowska-Latallo, K. A. Candido, Z. Cao, S. S. Nigavekar, I. J. Majoros, T. P. Thomas, L. P. Balogh, M. K. Khan, J. R. Baker, Jr., Nanoparticle Targeting of Anticancer Drug Improves Therapeutic Response in Animal Model of Human Epithelial Cancer. *Cancer Res.* **2005**, *65*, 5317.

[19]   F. M. Rubino, Separation methods for methotrexate, its structural analogues and metabolites. *Journal of Chromatography B: Biomedical Sciences and Applications.* **2001**, *764*, 217.

[20]   F. Albertioni, B. Pettersson, O. Beck, C. Rask, P. Seideman, C. Peterson, Simultaneous quantitation of methotrexate and its two main metabolites in biological fluids by a novel solid-phase extraction procedure using high-performance liquid chromatography. *Journal of Chromatography B: Biomedical Sciences and Applications.* **1995**, *665*, 163.

[21]   C.-Y. Kuo, H.-L. Wu, H.-S. Kou, S.-S. Chiou, D.-C. Wu, S.-M. Wu, Simultaneous determination of methotrexate and its eight metabolites in human whole blood by capillary zone electrophoresis. *Journal of Chromatography A.* **2003**, *1014*, 93.

[22]   B. A. Chabner, C. J. Allegra, G. A. Curt, N. J. Clendeninn, J. Baram, S. Koizumi, J. C. Drake, J. Jolivet, Polyglutamation of methotrexate. Is methotrexate a prodrug? , *J Clin Invest.* **1985**, *76*, 907.

[23] L. Genestier, R. Paillot, L. Quemeneur, K. Izeradjene, J.-P. Revillard, Mechanisms of action of methotrexate. *Immunopharmacology.* **2000**, *47*, 247.

[24] X. Shi, W. Lesniak, M. T. Islam, M. C. MuÑiz, L. P. Balogh, J. R. Baker Jr, Comprehensive characterization of surface-functionalized poly(amidoamine) dendrimers with acetamide, hydroxyl, and carboxyl groups. *Colloids and Surfaces A: Physicochemical and Engineering Aspects.* **2006**, *272*, 139.

[25] A. D. Meltzer, D. A. Tirrell, A. A. Jones, P. T. Inglefield, Chain dynamics in poly(amidoamine) dendrimers: a study of proton NMR relaxation parameters. *Macromolecules.* **2002**, *25*, 4549.

[26] A. D. Meltzer, D. A. Tirrell, A. A. Jones, P. T. Inglefield, D. M. Hedstrand, D. A. Tomalia, Chain dynamics in poly(amidoamine) dendrimers: a study of carbon-13 NMR relaxation parameters. *Macromolecules.* **2002**, *25*, 4541.

[27] J. Peterson, V. Allikmaa, J. Subbi, T. Pehk, M. Lopp, Structural deviations in poly(amidoamine) dendrimers: a MALDI-TOF MS analysis. *European Polymer Journal.* **2003**, *39*, 33.

[28] X. Shi, I. J. Majoros, A. K. Patri, X. Bi, M. T. Islam, A. Desai, T. R. Ganser, J. R. Baker, Jr., Molecular heterogeneity analysis of poly(amidoamine) dendrimer-based mono- and multifunctional nanodevices by capillary electrophoresis. *Analyst.* **2006**, *131*, 374.

[29] M. T. Islam, X. Shi, L. Balogh, J. R. Baker, HPLC Separation of Different Generations of Poly(amidoamine) Dendrimers Modified with Various Terminal Groups. *Analytical Chemistry.* **2005**, *77*, 2063.

[30] M. T. Islam, I. J. Majoros, J. J. R. Baker, HPLC analysis of PAMAM dendrimer based multifunctional devices. *Journal of Chromatography B.* **2005**, *822*, 21.

[31] S. Steinborner, J. Henion, Liquid−Liquid Extraction in the 96-Well Plate Format with SRM LC/MS Quantitative Determination of Methotrexate and Its Major Metabolite in Human Plasma. *Analytical Chemistry.* **1999**, *71*, 2340.

[32] T. Suzuki, H. Hashimoto, N. Ichinose, Microanalysis of methotrexate by high-performance liquid chromatography using a fluorescence detector. *Fresenius' Journal of Analytical Chemistry.* **1995**, *351*, 806.

[33] M. C. Roach, P. Gozel, R. N. Zare, Determination of methotrexate and its major metabolite, 7-hydroxymethotrexate, using capillary zone electrophoresis and laser-induced fluorescence detection. *Journal of Chromatography B: Biomedical Sciences and Applications.* **1988**, *426*, 129.

[34] J. Arly Nelson, B. A. Harris, W. J. Decker, D. Farquhar, Analysis of Methotrexate in Human Plasma by High-Pressure Liquid Chromatography with Fluorescence Detection. *Cancer Res.* **1977**, *37*, 3970.

[35] J. Salamoun, J. Frantisek, Determination of methotrexate and its metabolites 7-hydroxymethotrexate and 2,4-diamino-N10-methylpteroic acid in biological fluids by liquid chromatography with fluorimetric detection. *Journal of Chromatography B: Biomedical Sciences and Applications.* **1986**, *378*, 173.

[36] J. Salamoun, M. Smrz, F. Kiss, A. Salamounová, Column liquid chromatography of methotrexate and its metabolites using a post-column photochemical reactor and fluorescence detection. *Journal of Chromatography: Biomedical Applications.* **1987**, *419*, 213.

[37] A. Mandl, W. Lindner, Improved detection of leucovorin in mixed folates and antifolates by reversed-phase liquid chromatography and on-line post-column UV irridiation. *Chromatographia.* **1996**, *43*, 327.

[38] Z. Yu, D. Westerlund, K.-S. Boos, Determination of methotrexate and its metabolite 7-hydroxymethotrexate by direct injection of human plasma into a column-switching liquid chromatographic system using post-column photochemical reaction with fluorimetric detection. *Journal of Chromatography B: Biomedical Sciences and Applications.* **1997**, *689*, 379.

[39] W. M. Deen, P. F. Levy, J. Wei, R. D. Partridge, Assay for methotrexate in nanomolar concentrations with simultaneous detection of citrovorum factor and vincristine. *Analytical Biochemistry.* **1981**, *114*, 355.

Chapter 3: Detection of G5-MTX-FA in Urine

Chapter 3: Detection of G5-MTX-FA in Urine

Table of Contents

List of Figures

List of Tables

3.1   Introduction

It has been shown that half life plays an important role in the effectiveness of dendritic nanoparticles[1-2]. The decline in blood concentration after nanoparticle administration results from elimination by the body. The elimination rate constant is predominantly a function of hepatic and renal clearance. The size of the dendritic nanoparticle plays an important role in its susceptibility towards renal clearance. There have been several recent reports that indicate that once the molecular weight of a spherical nanoparticle approaches 30,000 to 40,000 dalton, the renal excretion rate and the volume of distribution of the entity reduces significantly, resulting in longer circulation times and an increased half-life[3-4]. Based on size, it has been stated that the hydrodynamic radius of dendritic particles should at least approach that of a renal pore (~5 nm) to avoid elimination due to glomerular filtration[5]. The diameter of a generation 5 PAMAM nanoparticle is about 5.3 nm, and the diameter of G5-MTX-FA will be slightly increased due to the additional surface modifications, placing it near the renal clearance cut-off values presented for these type of entities. The preliminary pharmacokinetic data presented in the previous chapter (Chapter 2, figure 18) revealed a relatively short half-life of G5-MTX-FA, suggesting this nanoparticle is a candidate for renal clearance. Knowledge of the fraction of the drug excreted into urine is an important parameter in understanding how the human body handles the drug and provides useful information about the influence of renal disease. Accurate modeling of the fraction of the experimental therapeutic excreted into urine requires an analytical method for detection of the drug and its metabolites with a similar rationale presented in chapter 2.

The previous chapter described the reaction and chromatographic conditions for the detection of nanoparticle associated MTX and free MTX in plasma matrices. Initially it was believed that the method could be transferred with minor modifications (i.e. chromatographic conditions) towards urine analysis. However, it became apparent that besides a number of alterations to the chromatographic and sample preparation, the derivatization procedure did not proceed to desirable extent in urine. This chapter deals with the optimization of the derivatization reaction, sample preparation and chromatography of G5-MTX-FA in urine.

3.2   Experimental

3.2.1 Materials

HPLC grade N,N-dimethylformamide (DMF), folic acid (FA), 30% solution of hydrogen Peroxide (H_2O_2), methotrexate (MTX), potassium permanganate ($KMnO_4$), sodium dithionite ($Na_2O_4S_2$), sodium hydroxide (NaOH) and TRIS-hydrochloride were obtained from Sigma-Aldrich. (St. Louis, MO). potassium phosphate monobasic (KH_2PO_4), potassium phosphate dibasic (K_2HPO_4), ammonium acetate and HPLC grade solvents acetonitrile (ACN) and methanol (MeOH) were obtained from Fisher Scientific (Fair Lawn, NJ). 7-hydroxymethotrexate (7OH-MTX) was purchased from Synfine Research (Ontario, Canada). G5-MTX-FA was obtained from Avidimer Therapeutics (Ann Arbor, MI). Blank heparin stabilized rat plasma (Sprague Dawley) , blank heparin stabilized dog plasma (Beagle) and blank unfiltered urine was obtained from Bioreclamation, Inc (Westbury, NY).

3.2.2 Instrumentation and Apparatus

G5-MTX-FA System: This system consisted of two Shimadzu LC6A solvent delivery modules that were operated through a Shimadzu SCL-6B system controller. Sample introduction occured by a Shimadzu SIL-6B autosampler equipped with a 50 µL injection loop. A Phenomenex Luna C18(2), 5 µm, 100 Å, 250 x 2.0 mm analytical column was guarded by a Supelcosil LC-8, 5 µm, 2 x 2.1 mm guard column and maintained at 30°C by a Shimadzu CTO-6A column oven. Detection occurred by a Shimadzu RT-10Axl fluorescence detector with excitation and emission wavelengths of 367 nm and 463 nm, respectively. The data was collected using TurboChrom V4.1. The mobile phase used with this chromatograph consisted of solvent A: 15 mM tris-HCl adjusted to pH 6.8 by a 10% NaOH solution and solvent B: consisting of MeOH. The system was operated at a flow rate of 0.2 mL/min with 75% A and 25% B, unless stated otherwise.

Post column photo oxidation system: Solvent was delivered by a Shimadzu LC6A binary pumping system that was operated through a Shimadzu SIL-6B system controller. The sample was introduced by a Shimadzu SIL-6B autosampler equipped with a 100 µL injection loop. The separation was conducted on a Phenomenex Intertsil C18 (150 x 4.6 mm) column with 5 µm particles with a 100 Å pore size that was protected by a Supelcosil LC-8, 5 µm, 2 x 4.0 mm guard column. Two meters of transparent Teflon tubing (0.012" id x 0.030" od), one meter in the center braided, was used as reactor coil and connected to the outlet of the column (total reactor coil volume 0.14 mL). An in-house fabricated online photochemical reactor was constructed using a GE Germicidal 9W lamp as a light source inside of the photochemical reactor. Detection occurred by a

Jasco FP-920 Intelligent Fluorescence Detector (excitation: 360nm and emission: 417nm) and data was collected by TurboChrom V4.1. The mobile phase used with this chromatograph consisted of solvent A: 975 mL 10 mM potassium phosphate buffer pH 6.2, 25 mL DMF and 1.5 mL 30% solution of H_2O_2 and solvent B: consisting of 200 mL ACN, 800 mL H_2O and 1.5 mL 30% solution of H_2O_2. The system was operated at a flow rate of 1.0 mL/min with 60% A and 40% B, or as stated otherwise.

3.2.3 Reduction reaction of G5-MTX-FA

An aliquot of 100 µL of (spiked/sampled) urine was diluted with a 1.0 M ammonium acetate solution to 800 µL in a (1.5 mL) plastic vial. If plasma was added to the vial as well, the 100 µL urine samples was diluted 1:1 with rat plasma, prior to further dilution by the ammonium acetate solution. Once all samples and calibrants were prepared they were placed in an in-house manufactured sample holder (details provided in supplemental section) that has the ability to lock the caps. Subsequently 200 µL of a freshly prepared 50 mM $Na_2O_4S_2$ solution was added and the vials were closed and secured by the holder. The entire holder was then vortexed for 10 seconds and placed into a boiling water bath. After 15 minutes the holder was removed from the water bath and stored in a refrigerator for 30 minutes. The cooled samples were removed from the holder and placed into a centrifuge for 5 minutes at 10,000 rpm (1,000 g) to spin down denatured and precipitated plasma proteins. The supernatant was transferred into 1.0 ml autosampler vials and 50 µL was injected into the G5-MTX-FA LC-FI HPLC system.

3.2.4 Preparation of Stock Solutions, samples and calibration

Stock solutions of MTX and 7OH-MTX were prepared according to an earlier method presented by Steinborner et al. MTX was dissolved in 95% MeOH and 5% Formic acid. 7-OHMTX was dissolved in 50% DMSO, 50% H_2O. G5-MTX-FA is freely soluble and was dissolved in H_2O. The stock solutions were diluted with water to the desired concentration and spiked into a 100 µL blank plasma matrix to yield calibration standards. The linearity and reproducibility of the G5-MTX-FA methodology was assessed by the analysis of calibrants (n=6) spiked with 25, 50, 125, 250, 375 and 500 µg/mL for rat urine analysis, and concentrations of 13, 25, 63, 125, 188 and 250 µg/mL were used in combination with dog urine. Samples spiked with similar concentrations were used to determine intra-day (six replicate) and inter-day (18 replicates analysis conducted over 3 separate runs) precision and accuracy. The linearity and reproducibility of the free MTX and 7OH-MTX methodology was assessed by the analysis of calibrants (n=6). MTX and 7OH-MTX were spiked in as a mixture and concentrations are given in table 3 and 4. Samples spiked with similar concentrations were used to determine intra-day (six replicates) precision and accuracy.

3.2.5 Sample preparation for MTX and 7OH-MTX analyses

Spiked urine sample (volume 100 µL) were diluted by addition of 900 µL of 100 mM ammonium bicarbonate solution (pH 8.0). Aliquots (950 µL) of the diluted samples were subjected to Solid Phase Extraction (SPE). The recovered analytes were heated in 40 °C water and evaporated to dryness under a gentle stream of nitrogen. The residue was reconstituted in 200 µL of 100 mM ammonium bicarbonate (pH 8.0). The solution

was transferred into a 1.0 mL autosampler vial with a 350 μL liner and 100 μL was injected onto the post column photo-oxidation HPLC system.

3.2.6 Solid Phase Extraction (SPE)

A 500 mg, 1.0 ml Varian Bond Elute Strong Anion Exchange (SAX) SPE device was activated with 1.0 ml of MeOH. The column was equilibrated with 1.0 ml of 100 mM ammonium bicarbonate solution (pH 8.0). To the equilibrated column, 950 μL of sample was applied. Interferences were washed from the column with 1.0 ml of 100 mM ammonium bicarbonate solution. The retained analytes were eluted by 1.0 ml consisting of 95% MeOH and 5% formic acid. During extraction the SPE cartridges were mounted in a Waters vacuum manifold and the vacuum was adjusted to maintain a flowrate of approximately 0.5 ml/min through the cartridge.

3.3 Results and Discussion

3.3.1 Chromatographic Method Development

Initial rat urine method development involving the detection of G5-FA-MTX associated MTX was started by evaluating the methods performance towards the urine matrix, utilizing the previously established plasma analysis protocol (chapter 2). The pilot experiments demonstrated a more complex biological background in urine as opposed to plasma, including co-elution of the analytes derivatization product (DAMP) with an unidentified endogenous compound (figure 19A). The two compounds were resolved by reduction of the modifier strength at the consequence of increased analysis time and reduction of analytical throughput (figure 19B, C). Separate batches of rat urine

demonstrated variable interference patterns (figure 19C, D), with one batch demonstrating a interferent (1) requiring the previously discussed increase in chromatographic analysis time. However this interferent did not appear in any of the other samples (figure 19D). Peak purity was checked by analysis of various blank urine matrices and no co-eluting/interfering compounds were detected in the elution window of DAMP using the LC-FL system.

The interference pattern of dog urine was substantially different compared to rat urine, requiring an additional chromatographic method (figure 20A). Dog urine contained a co-eluting compound with the analyte being retained for about 20 minutes, a separation time that provided an adequate separation in rat urine analysis. The co-elution of these compounds is indicative of a poor selectivity factor between the compounds using a C18 stationary phase and methanol as the organic modifier. The interferent and analyte could be baseline separated in a lengthy chromatographic procedure requiring an analysis time of about 50 minutes and an isocratic separation with 5% MeOH (Figure 20, B, C). The resulting procedure suffered from a lack of sample throughput and broad peaks that reduced the limit of detection. A substantial improvement selectivity factor was achieved when the organic modifier was changed from MeOH to tetrahydrofuran (THF). The increased selectivity factor resulted in a fast isocratic separation of DAMP from endogenous interferences within 15 minutes (figure 20, D). It is important to note that the elution order of the interferent and reduction product has reversed, something that proved to be favorable for trace analysis, where small amounts of DAMP would otherwise have to be detected on the shoulder of a dominant peak resulting from the interferent.
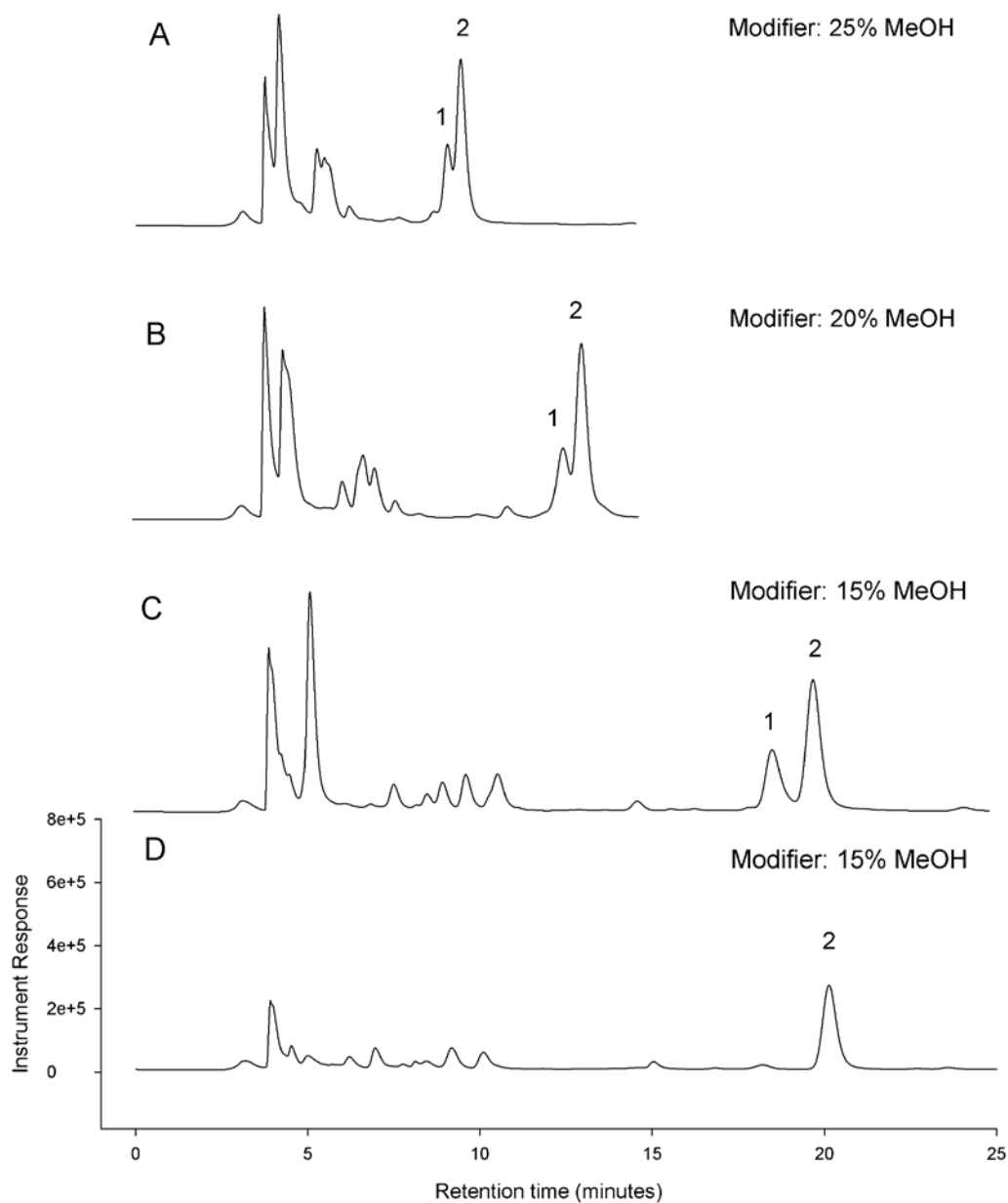
Figure 19. *HPLC-FL chromatograms of G5-MTX-FA spiked rat urine (derivatized). (1) endogenous interferent, (2) G5-MTX-FA reporter (DAMP). (A) Chromatogram obtained at 25% B, 1 and 2 co-elute. (B) Chromatogram obtained at 20% B, 1 and 2 co-elute. (C) Chromatogram obtained at 15% B, 1 and 2 are separated. (D) Chromatogram of G5-MTX-FA spiked in a different batch of rat urine where the major endogenous interferent (1) is not present.*

82
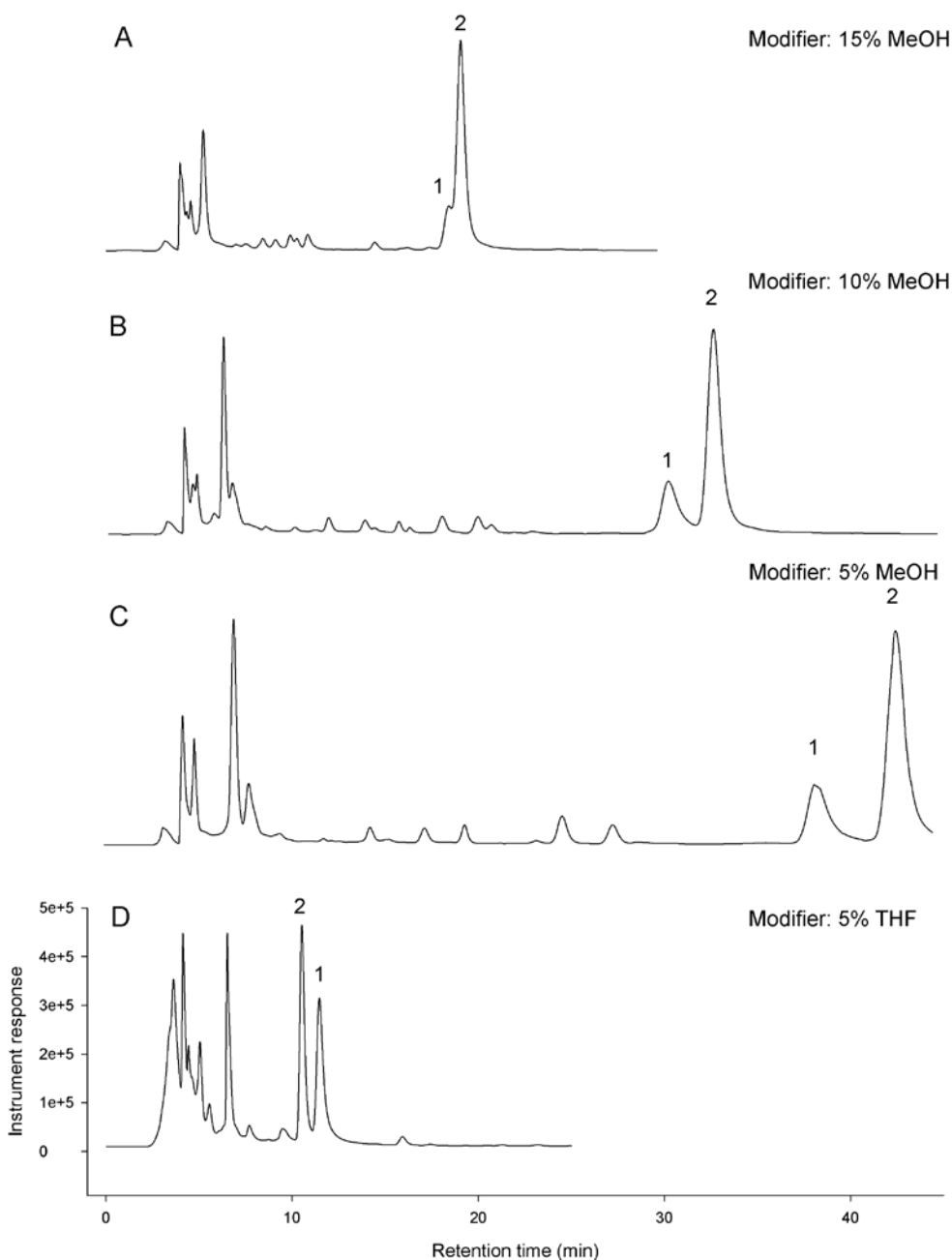
Figure 20. *HPLC-FL chromatograms of G5-MTX-FA spiked dog urine (derivatized). (1) endogenous interferent, (2) G5-MTX-FA reporter (DAMP). (A) Chromatogram obtained at 15% B, 1 and 2 co-elute. (B) Chromatogram obtained at 10% B, 1 and 2 co-elute. (C) Chromatogram obtained at 5% B, 1 and 2 are separated. (D) Chromatogram obtained with THF instead of MeOH as modifier, note that the elution order of the peaks 1 and 2 is inverted.*

3.3.2 Matrice Influence on the Derivatization Procedure

Once the chromatographic variables were established, the G5-MTX-FA associated MTX analysis procedure in rat urine was validated. Surprisingly, the derivatization reaction that proved to be useful for the plasma analysis did not perform adequately in the urine matrix, both from a sensitivity and reproducibility (within and between days) perspective (figure 21, red trace). Analysis of the regression line slope indicates a relative yield for the G5-MTX-FA reduction reaction of 5.1% in rat urine when compared against a similar protocol utilizing rat plasma (figure 21, black trace). One might argue that a loss of 20 fold in sensitivity of the analytical method is (at least partly) compensated for by the fact that compounds that are primarily eliminated through the renal clearance pathway accumulate into urine, reducing the need for optimal limits of detection. However, additionally the derivatization reaction also proved to be irreproducible, demonstrating relative standard deviations up to 47% in the linear range, vastly exceeding acceptable error tolerances for bioanalytical method development. The low yield of the reaction in rat urine as opposed to rat plasma suggests that there is a reaction mediating factor present in plasma, and/or an effective reaction quenching component in urine.

Early in the plasma method development process it was observed that the relative derivatization yield in the plasma matrice was 2.5 (figure 21, blue trace) times higher when compared to a similar procedure utilizing water opposed to plasma, supporting the hypothesis of the presence of a reaction mediating/catalyzing compound. This increase in apparent yield of reaction was not further investigated at the time, however the importance of a consistet matrix throughout preparation of standards and

84

samples was pointed in the previous chapter. Despite the favorable properties of the plasma matrix on the reaction, it is also clear that the urine matrix reduces the extent of the derivatization reaction to an addition degree, demonstrated by a significant lower yield of the derivatization reaction in urine compared to water (figure 21).

Based on an extensive screening of sample preparation stratagies, chapter 2 concludes that derivatization has to occur directly within the biological matrix to yield reproducible results, before exposure to any sample clean-up procedures. Within these borders the key to a successful analysis strategy for urine analysis would be optimizing the urine derivatization reaction so it behaves comparable to the plasma derivatization reaction, rather than including an extensive clean-up procedure. Improving the derivatization procedure requires an extensive knowledge of the various chemical pathways, so the reaction could be directed to yield the desired products. The following section will present a plausible reaction mechanism based on data that has appeared in the literature.
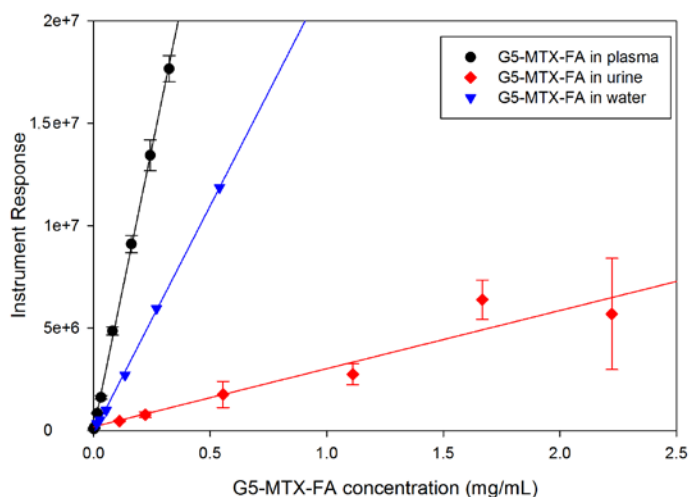
Figure 21. *Individual G5-MTX-FA calibration curves in various matrices. rat plasma (black line), rat urine (red line), water (blue line).*

3.3. 4 Mechanism of Reduction
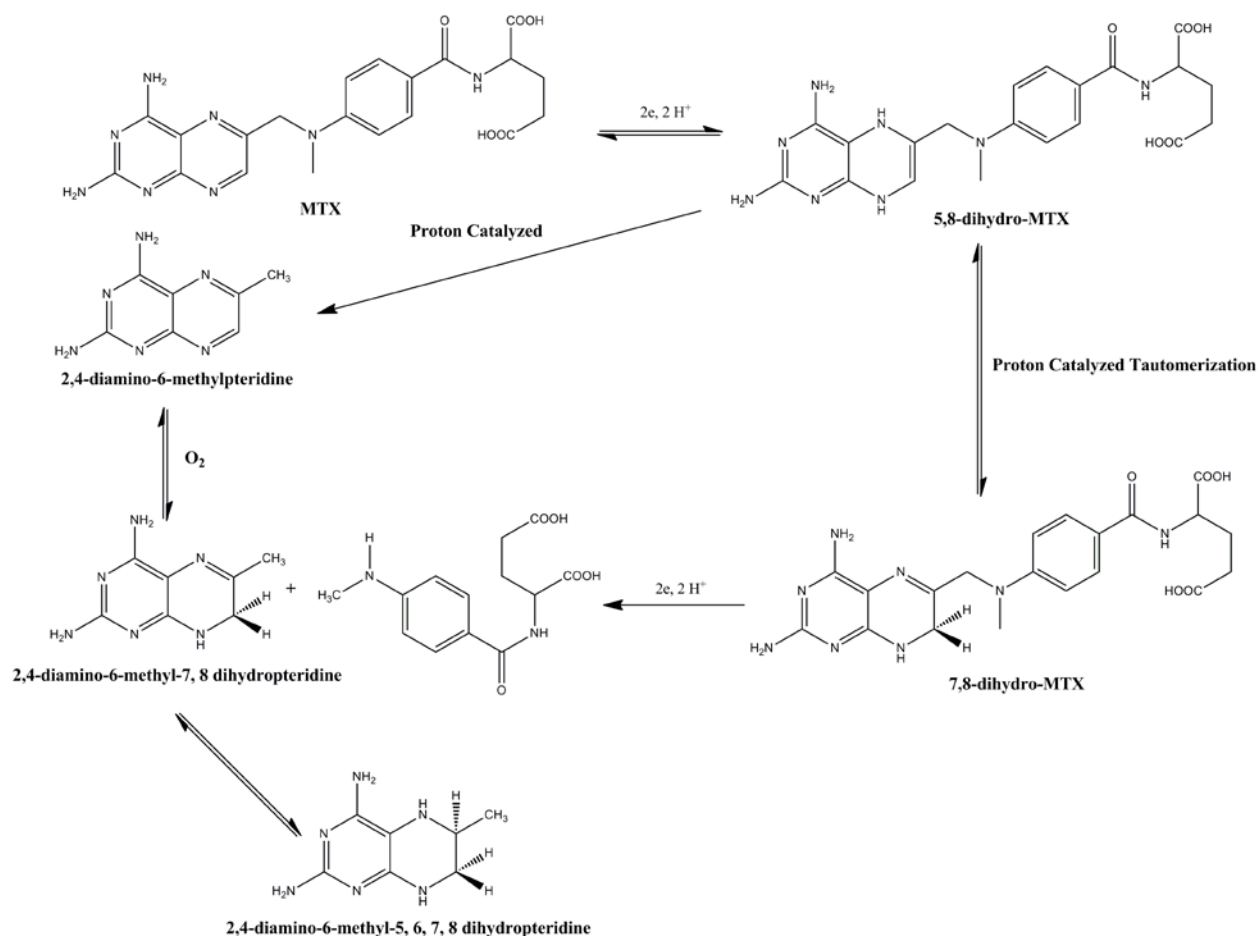
Figure 22. *Hypothesized derivatization scheme of G5-MTX-FA associated MTX in the presence of dithionite (only the MTX related reactions are shown).*

The reduction of MTX to 2,4-diamino-6-methylpteridine (DAMP) is a multistep chemical cascade, involving multiple electron transfer steps. A reaction scheme has been proposed by R.C Gurira et al., based on results obtained by various analytical techniques and electrochemical reduction (figure 22). Whilst making the assumption that G5-MTX-FA behaves similar to free MTX under reductive conditions, these observations

would also hold for the derivatization procedure of the nanoparticle. In an initial reduction step, MTX undergoes a 2 electron, 2 proton reduction to 5, 8-dihydro-MTX. Depending on the pH of the solution 5,8-dihydro-MTX tautomerizes to the more stable 7,8-dihydro-MTX or a proton catalyzed cleavage of the C(9)-N(10) bond to yield DAMP. 7,8-dihydro-MTX can undergo a reductive cleavage of the C(9)-N(10) bond, to yield 2,4-diamine-6-methyl-7,8 dihydropteride (7,8-dihydroDAMP), which upon subsequent (auto)oxidation step gives raise to the desired fluorescent reporter DAMP. At this time it is unclear which kinetic pathway is dominating in the G5-MTX-FA derivatization procedure at pH 6.0 with excess dithionite, but independent of the kinetic pathway DAMP is generated. R.C Gurira et al also report that at pH 3-9 MTX and DAMP have similar reduction potentials. Considering the fact that the derivatization procedure utilizes a large molar excess of dithionite, it should be expected that any DAMP formed by the protoncatalyzed cleavage of the C(9)-N(10) bridge of 5,8-dihydro-MTX will be rapidly reduced to 7,8-dihydroDAMP until the dithionite is depleted, and then auto-oxidation to DAMP will occur. An additional reduction of 7,8-dihydroDAMP is possible to 2,4-diamino-6-methyl-5,6,7,8-tetrahydropteridine, however this reduction has a potential of - 1.31 V at pH 6 and therefore does not occur with dithionite as reducing agent (- 0.66 V at pH 7). To conclude, it appears that the sodium dithionite mediated reduction of MTX follows the following pathway, MTX → 7,8-dihydro-MTX → DAMP → 7,8-dihydroDAMP → DAMP.

3.3.5 Adapting the Urine Derivatization Reaction

As mentioned before 7,8-dihydroDAMP is a highly unstable compound which is susceptible for auto-oxidation to DAMP. From a detection point of view this is a desirable process, and it appears that there is a component in plasma that facilitates this auto-oxidation. Whilst the compound(s) in plasma responsible for this behavior are unknown, it was hypothesized that various metals in plasma are responsible for this redox behavior. These metals are present in both, a free, and protein bound form where they are released upon denaturation of the protein in the incorporated boiling stage, possibly providing a constant oxidation factor in the procedure. In an attempt to address this auto-oxidation factor in plasma, various concentrations (0, 0.1, 1, 10 mM) of Fe^{3+} were added to the aqueous buffer solution before the derivatization procedure was started. The presence of Fe^{3+} greatly influenced the apparent yield of reaction, reaching a maximal effect at 1 mM (figure 23).
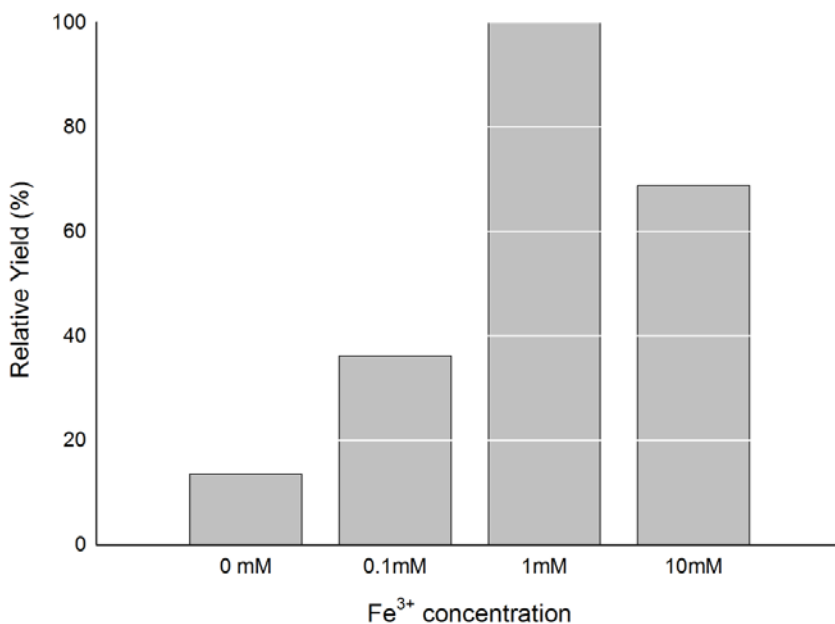
Figure 23. *Effect of Fe^{3+} concentration on reaction yield (fluorescence response)*

It is tempting to believe that Fe^{3+} aids in the re-oxidation of 7,8-dihydroDAMP to DAMP. If this were true, the addition of Fe^{3+} post reduction should yield similar results. An experiment was conducted where 1 mM of Fe^{3+} was added prior and post reaction (figure 24 A). Independent of the stage of Fe^{3+} addition a similar increase in formation of DAMP was observed compared to a reference derivatization reaction in buffer. It was also observed that the overall yield was about 70% of that obtained when derivatizing in a plasma matrix. In order to investigate if the addition of Fe^{3+} was beneficial for G5-MTX-FA urine analysis, a comparable experiment was performed using a rat urine matrix. The presence of Fe^{3+} during the derivatization reaction had similar beneficial effects as reported before. However, the addition of Fe^{3+} post derivatization did not demonstrate any increase in apparent reaction yield (figure 24 B).
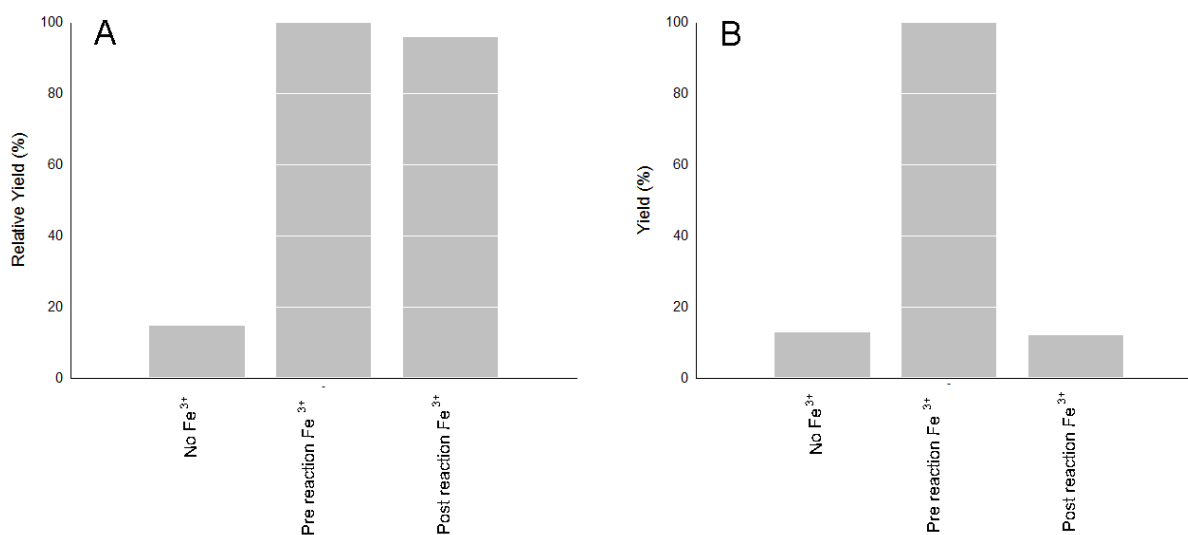
Figure 24. *The influence of the stage of Fe^{3+} addition, aqueous reference, reduction in the presence of 1 mM Fe^{3+}, and an reduction followed by the addition of 1 mM Fe^{3+}. (A) aqueous matrix (B) rat urine matrix.*

Elucidating the reaction mechanism was beyond the scope of this work. However on a speculative basis it seems plausible that due to the addition of Fe^{3+} post reaction, competing nucleophiles present in the urine matrix have a time window to scavenge the unstable/partly reduced 7,8-dihydroDAMP. Since urine contains large quantities of organic molecules with reactive sulfur and nitrogen functional groups, nucleophilic addition reactions are a possibility, trapping and depleting 7,8-dihydroDAMP levels before reoxidation to DAMP could occur upon the addition of Fe^{3+}. With the discovery that the presence of an oxidation factor/mediator during reduction was important in the derivatization procedure, a validation experiment was performed, using Fe^{3+} during the reduction of G5-MTX-FA in rat urine. It was found that sensitivity of the method had increased, but the precision of the method was still poor when compared to validation result of similar measurements out of plasma (figure 25).
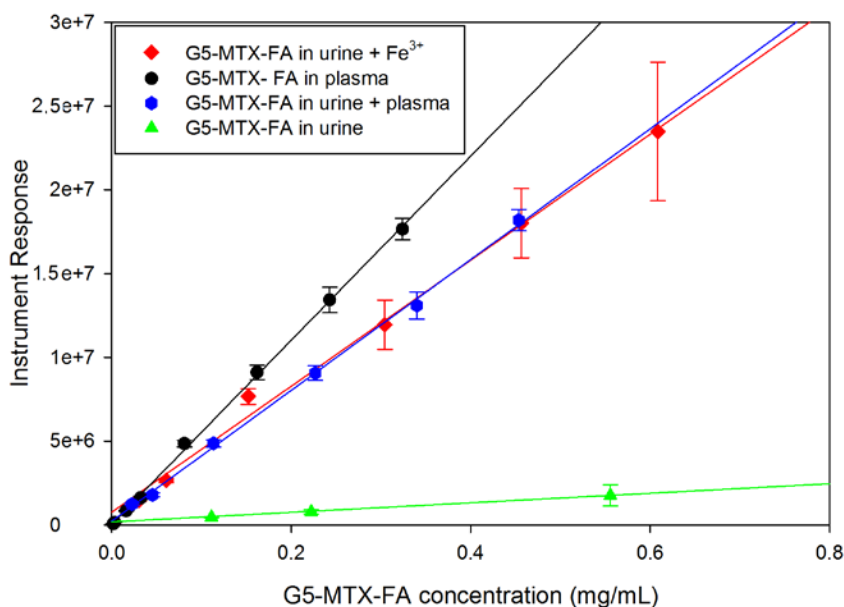
Figure 25. *Comparison between the various matrix compositions and instrument response. G5-MTX-FA in plasma (black line), G5-MTX-FA in urine + Fe^{3+} (red line), G5-MTX-FA in urine + plasma (blue line), G5-MTX-FA in urine (green line).*

90

Since the reduction of MTX to DAMP occurs in a reproducible fashion, and plasma being identified as an important component of the derivatization reaction, it was tempting to believe that the addition of an aliquot of plasma to a urine sample would lead to precise and reproducible MTX derivatization. The addition of plasma to urine however, adds numerous endogenous interferences to the already complex biological sample. However it was expected, based on the observation that since the derivatization reaction of MTX in plasma resulted in relatively clean LC-FL chromatograms, the addition of rat plasma would not further complicate the chromatogram. Chromatograms of G5-MTX-FA derivatized in a plasma/urine matrix are presented in figure 26. As illustrated by figure 26 A and C, the addition of plasma to the urine matrix did not result in more complex chromatograms, demonstrating the feasibility of plasma enrichment of the urine sample, to mediate the derivatization reaction.

In order to investigate if the addition of plasma to the urine matrix would yield the desired increase in robustness of the method, a single day calibration involving the analysis of urine samples containing 6 different concentrations in 5 replicates was performed (figure 25, blue line). The experiment indicated that precision and reproducibility of G5-MTX-FA reduction in a combined urine plasma matrix was greatly improved when compared to derivatization in Fe^{3+} enriched urine (figure 25, red line). The yield of the plasma mediated urine derivatization reactions is overall about 70% of that compared to reduction plasma, indicating that competing kinetic pathwats, trapping reduced forms of MTX derivatives during their transformation pathway to DAMP are still partially active.
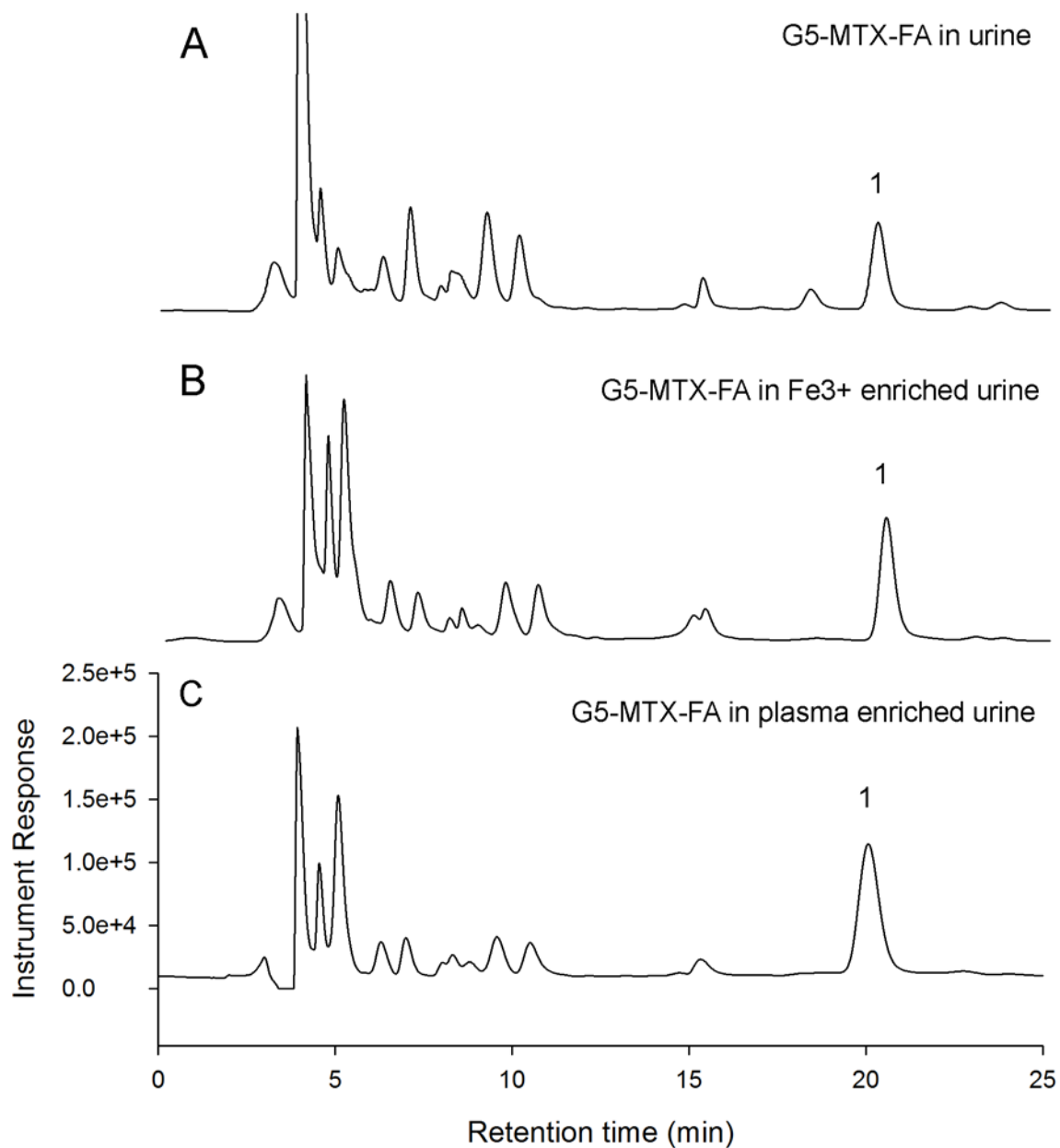
Figure 26. *HPLC-FD chromatograms of derivatized G5-MTX-FA in various urine matrix compositions. (A) Blank rat urine spiked with G5-MTX-FA. (B) 1 mM Fe^{3+} enriched rat urine spiked with G5-MTX-FA (C) G5-MTX-FA spiked in blank rat urine that was combined with an aliquot of rat plasma.*

3.3.6 Validation of the G5-MTX-FA Associated MTX Analytical Procedure

As it appeared that the procedure was repeatable when rat plasma was used as an oxidative mediator, an extensive validation procedure was started utilizing rat and dog urine as model systems. The linear range, precision and accuracy of the method were assessed by analyzing 6 different G5-MTX-FA concentrations in 6 replicates. The reproducibility of the method was addressed by repeating the experiment for three consecutive days. Intra- and inter-run validation data involving the rat urine matrix is demonstrated in table 10. The precision of the method was in general < 10% except for the most concentrated value, where the inter-run precision was 19.7%. The accuracy of the method was also acceptable with values in general deviating <10% from the target value. At the low end of the calibration curve some larger deviations are seen, however not exceeding 15%. A typical intra-day calibration plot can be described by the equation: $y = 3.903 * 10^7x + 2.259 * 10^5$, where (y) is the instrument response and (x) is the concentration of G5-MTX-FA in rat urine in mg/mL). The lowest intra-day correlation coefficient obtained was $R^2 = 0.9985$, spanning a 500 fold change in concentration range (0.025 – 0.500 mg/mL). The limit of quantification for G5-MTX-FA associated MTX was around 0.025mg per mL of rat urine.

Intra- and inter-run validation data in dog urine is summarized in table 11. The precision of the method was in general < 10% except for the most dilute value, where the inter-run precision was 31.6%.The accuracy of the method was also acceptable with values deviating in general <10% from the target value. The limit of quantification for G5-MTX-FA associated MTX was around 0.025mg per mL of dog urine. A typical intra-day calibration plot can be described by the equation: $y = 7.907* 10^7x - 1.645 * 10^5$, where

93

(y) is the instrument response and (x) is the concentration of G5-MTX-FA in dog urine in mg/mL). The lowest intra-day correlation coefficient obtained was R² = 0.9992.

Table 10. Rat Urine validation, intra- and inter-day precision and accuracy results

Nominal G5-MTX-FA Concentration (mg/mL)	Intra-run (n=6)			Inter-run (n=18)		
	Mean observed concentration (mg/mL)	Mean Accuracy of target value (%)	Precision (RSD %)	Mean observed concentration (mg/mL)	Mean Accuracy of target value (%)	Precision (RSD %)
0.025	0.029	114.7	6.4	0.024	94.1	6.7
0.050	0.044	88.4	7.2	0.046	91.9	7.3
0.125	0.131	105.0	4.7	0.132	105.9	7.3
0.250	0.250	99.9	4.9	0.250	100.0	7.0
0.375	0.364	97.0	6.3	0.373	99.4	10.4
0.500	0.508	101.5	3.6	0.500	100.1	19.7

Table 11. Dog Urine validation, intra- and inter-day precision and accuracy results

Nominal G5-MTX-FA Concentration (mg/mL)	Intra-run (n=6)			Inter-run (n=18)		
	Mean observed concentration (mg/mL)	Mean Accuracy of target value (%)	Precision (RSD %)	Mean observed concentration (mg/mL)	Mean Accuracy of target value (%)	Precision (RSD %)
0.013	0.013	99.1	2.9	0.013	99.8	31.6
0.025	0.022	101.8	5.1	0.025	93.1	9.6
0.063	0.065	99.0	4.4	0.063	103.8	5.9
0.125	0.124	104.7	6.4	0.125	99.6	5.9
0.188	0.191	89.0	5.6	0.188	100.7	7.1
0.250	0.248	100.5	11.2	0.250	99.5	6.6

3.7 Free MTX and 7OH-MTX Analysis in Rat and Dog Urine
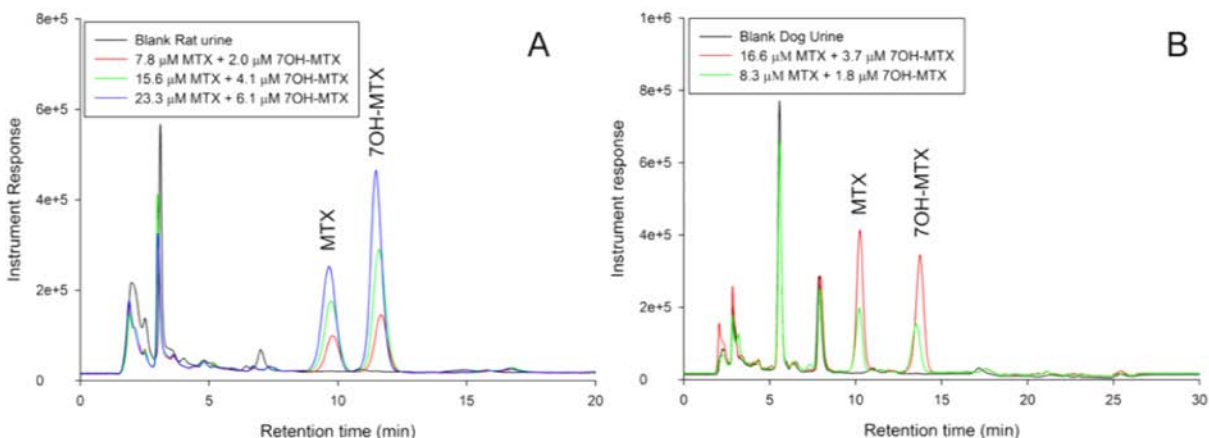
Figure 27. *Chromatograms of MTX and 7OH-MTX in rat urine extracts (A) and dog urine SPE extracts (B).*

As demonstrated in chapter 2, minor amounts of MTX are hydrolysed from the G5-MTX-FA nanoparticle *in vivo*. Liberated MTX will be a candidate for hepatic metabolism, transforming MTX in 7OH-MTX. Both of these entities are largely excreted into urine. A detection strategy for free MTX and 7OH-MTX in plasma has been presented in the previous chapter and involved reversed phase separation combined with post column photo chemical derivatization and fluorescence detection. Sample preparation occurred by strong anion exchange (SAX) solid phase extraction (SPE), followed by an evaporation and reconstitution step in order to obtain an RP-HPLC compatible sample. In the process of obataining an analysis strategy for free MTX and 7OH-MTX the plasma method was evaluated towards a dog and rat urine matix. The high ionic strength in the urine matrix led to break through of the 100 mg SAX SPE cartridge, leading to low recoveries (10-20%) and irreproducible results. The analyte breakthrough was eliminated by increasing the bed volume of the SAX SPE cartridge to

500 mg. The use of these 500 mg cartridges resulted in recoveries >90% for both analytes and reproducible results. Furthermore the application of these cartridges led to relatively "clean" chromatograms where the analytes could be separated within 15 minutes (figure 27 A and B). There were some hydrophobic interferences observed that had long retention times. In order to prevent the carryover of these more hydrophobic entities in a subsequent analysis, a step gradient was incorporated at the end of each run in order to clean the column.

Since the detection of free MTX and 7OH-MTX has been largely described in the literature, a limited intra-day validation was performed, demonstrating the viability of the presented method. The Intra-day precision and accuracy of the free analyte assay was determined by analyzing 6 replicates of standards spiked with six different MTX and 7OH-MTX concentrations in both rat (table 12, 13) and dog urine (table 14, 15). The intra-day precision did not exceed 11.6% and in was in general well below 10%, both for dog and rat urine. The accuracy of assay in rat urine did not exceed 20% deviation at the limit of detection (1.6 µM), and was well within the limits for a bioanlytical assay over the remaining part of the linear range. Similar observations were made in the analysis of MTX and 7OH-MTX in dog urine.

Table 12. Intra-day validation of free MTX in rat urine

Nominal Concentration (μM)	Mean observed concentration (μM) (n=6)	Precision (RSD %)	Mean Accuracy of target value (%)
31.1	30.6	3.6	98.2
23.3	23.7	1.8	101.7
15.6	16.1	6.1	103.7
7.8	7.9	7.2	101.0
3.1	2.9	4.8	94.2
1.6	1.3	9.2	81.1

Table 13. Intra-day validation of free 7OH-MTX in rat urine

Nominal Concentration (μM)	Mean observed concentration (μM) (n=6)	Precision (RSD %)	Mean Accuracy of target value (%)
5.9	5.8	4.8	98.0
4.4	4.5	1.7	103.0
2.9	3.0	5.6	101.7
1.5	1.5	8.1	99.2
0.59	0.57	2.8	96.9
0.29	0.26	11.6	88.8

Table 14. Intraday validation of free MTX in dog urine

Nominal Concentration (µM)	Mean observed concentration (µM) (n=6)	Precision (RSD %)	Mean Accuracy of target value (%)
36.6	35.9	7.9	98.0
27.4	28.6	3.9	104.0
18.3	17.3	10.0	94.3
9.2	9.3	6.5	101.9
3.7	4.0	10.4	108.3
1.8	1.7	12.2	91.1

Table 15. Intraday validation of free 7OH-MTX in dog urine

Nominal Concentration (µM)	Mean observed concentration (µM) (n=6)	Precision (RSD %)	Mean Accuracy of target value (%)
8.2	8.2	9.8	100.4
6.1	6.3	6.6	103.8
4.1	3.6	8.6	89.3
2.0	2.0	3.5	99.7
0.82	0.90	3.2	110.5
0.42	0.50	11.0	123.0

3.4   Conclusion

The analysis and characterization of G5-MTX-FA imposes an analytical challenge. The detection of this entity in biological matrices is even further complicated by the presence of a large number of endogenous compounds. Attempts at isolating G5-MTX-FA from a sample matrix by common sample preparation techniques such as SPE extraction have failed to give reproducible results and linear responses. The sodium dithionite mediated reduction of G5-MTX-FA associated MTX to DAMP gives rise to a highly detectable small molecule entity that does not demonstrate any of the negative physical chemical properties complicating intact G5-MTX-FA analysis. Interestingly, the matrix plays an important role in the chemical degradation pathway of G5-MTX-FA conjugated MTX to DAMP. The highest and most reproducible derivatization yields are obtained when there is a plasma component within the derivatization matrix, possibly aiding in the re-oxidation of 7,8 –dihydroDAMP to DAMP. This observation proved to be useful for the analysis of G5-MTX-FA associated MTX in dog and rat urine. Precision, accuracy and sensitivity of the urine assay were significantly improved when the derivatization occurred in the presence of an aliquot of rat plasma. Chromatographic analysis of dog and rat urine samples was complicated by a larger number of endogenous interferents. Both dog and rat urine needed matrix individualized chromatographic procedures. A co-eluting compound in dog urine could not be separated in an acceptable time frame using MeOH as the modifier, however a separation could be accomplished when the selectivity factor of the assay was adapted by using THF as the organic modifier.

Detection of free MTX and 7OH-MTX was relatively straight forward, utilizing SAX SPE, followed by HPLC separation and post column photochemical degradation and fluorescence detection. It was observed that the bed volume of the SPE cartridge needed to be increased when dealing with samples with an increased ionic strength. Whereas an SAX SPE cartridge with an 100mg bed volume was adequate for plasma analysis, the bed volume needed to be increased to 500mg per SPE cartridge in order to prevent the analyte from breaking through during urine analysis. The same isocratic chromatographic separation could be performed independent of the matrix composition, however the detection of free analytes out of urine required the addition of a step gradient at the end of each analysis in order to eliminate hydrophobic contaminants from the chromatographic media.

In the animal studies discussed in chapter 2 urine was not collected. Due to this absence of urine samples, the methods presented have not been applied to animal urine samples in order to detect G5-MTX-FA associated MTX and related analytes in urine. The renal clearance rate of G5-MTX-FA has therefore not been determent yet, and animals studies need to be performed in order to adequately answer this question.

3.5   References

[1]   Y. Matsumura, H. Maeda, A New Concept for Macromolecular Therapeutics in Cancer Chemotherapy: Mechanism of Tumoritropic Accumulation of Proteins and the Antitumor Agent Smancs. *Cancer Research.* **1986**, *46,* 6387.

[2]   R. Duncan, Polymer conjugates for tumour targeting and intracytoplasmic delivery. The EPR effect as a common gateway? , *Pharm Sci Technolo Today.* **1999**, *2*, 441.

[3]   E. R. Gillies, E. Dy, J. M. J. Fréchet, F. C. Szoka, Biological Evaluation of Polyester Dendrimer: Poly(ethylene oxide) "Bow-Tie" Hybrids with Tunable Molecular Weight and Architecture. *Molecular Pharmaceutics.* **2005**, *2*, 129.

[4]   L. M. Kaminskas, B. J. Boyd, P. Karellas, G. Y. Krippner, R. Lessene, B. Kelly, C. J. H. Porter, The Impact of Molecular Weight and PEG Chain Length on the Systemic Pharmacokinetics of PEGylated Poly l-Lysine Dendrimers. *Molecular Pharmaceutics.* **2008**, *5*, 449.

[5]   J. Drobník, F. Rypáček, in *Polymers in Medicine, Vol. 57*, Springer Berlin / Heidelberg, **1984**, pp. 1.

Chapter 4: A Novel HPLC Mass Spectrometry Method for Improved Selective and Sensitive Measurement of Methotrexate Polyglutamation Status in Human Red Blood Cells.

Chapter 4: A Novel HPLC Mass Spectrometry Method for Improved Selective and Sensitive Measurement of Methotrexate Polyglutamation Status in Human Red Blood Cells.

Table of Contents

List of Figures

List of Tables

4.1 Introduction

In adult populations, methotrexate (MTX) is one of the most commonly prescribed drugs for the treatment of rheumatoid arthritis (RA)[1-2]. In contrast to non-steroidal anti-inflammatory drugs used to relieve the symptoms of RA, MTX is categorized as a disease modifying anti-rheumatic drug, i.e. an agent that reduces disease activity and slows the progression of joint damage. MTX also forms the therapeutic cornerstone for pediatric patients suffering from Juvenile Idiopathic Arthritis (JIA)[3]. The efficacy, safety and relatively low toxicity of weekly low dose MTX therapy in children with JIA has been shown in a number of clinical trials[4-6].

Despite the fact that MTX is one of the best tolerated disease modifying drugs, there is a large inter-patient variability in clinical response and toxicity that is poorly understood in both RA and JIA. The MTX dose that provides an acceptable level of disease control varies greatly, and studies have been published indicating the presence and absence of a dose-response relationship. Measurement of MTX plasma concentrations in low dose MTX therapy is of little value since there is a lack of correlation between serum concentrations and disease activity, mainly because MTX is largely cleared from plasma within 24 hours by glomerular filtration and tubular secretion or is stored intracellularly as MTX polyglutamates (MTXPGs)[7-8] (figure 28).

MTX is transported into cells by the reduced folate carrier where it is converted by folylpolyglutamate synthase to MTXPGs by sequential addition of glutamic acid residues at the γ position of the terminal glutamate residue[9]. Polyglutamation results in an overall increase in net negative charge, providing a cellular retention mechanism.
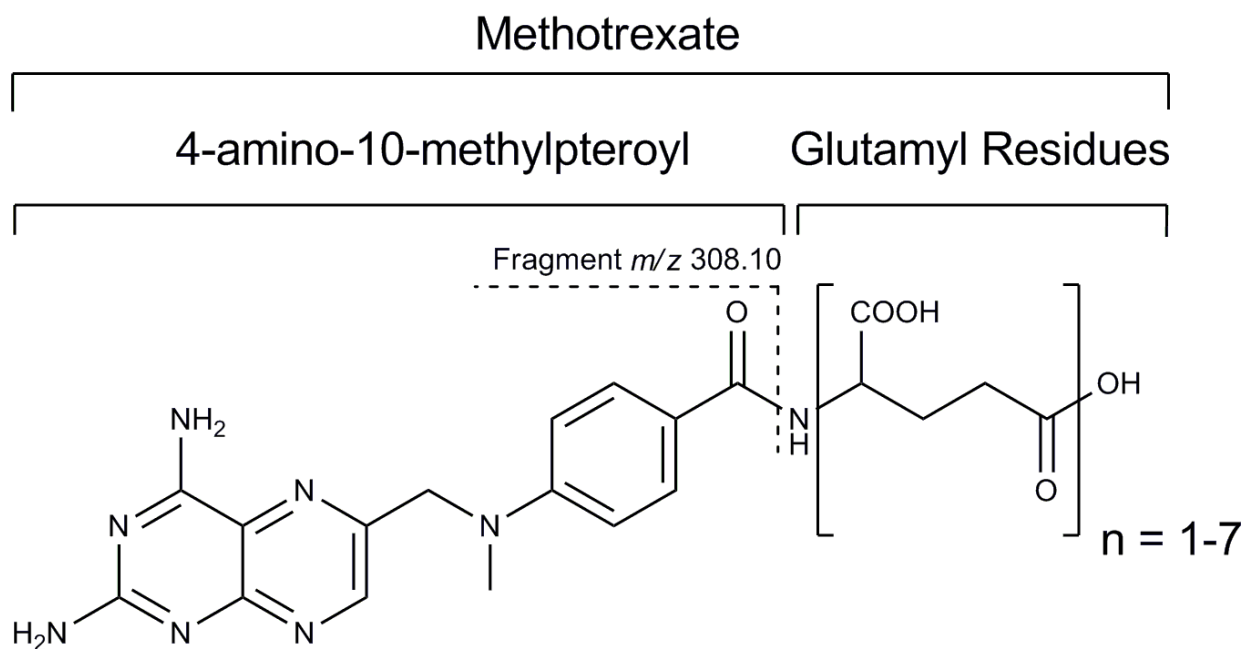
Figure 28. *Structure of methotrexate and its polyglutamates. The common m/z 308.10 fragment obtained by collision induced dissociation is illustrated by the dotted line.*

A number of studies have indicated that MTXPGs are the bioactive form of MTX, with pharmacological action related to MTXPGs concentration and population distribution[9-11]. The anti-inflammatory action of MTX results from inhibition of enzymatic pathways involved in *de novo* purine synthesis, leading to increased concentrations of adenosine, which has the ability to serve as an anti-inflammatory agent[12]. Since intra-cellular MTXPGs appear to form the therapeutically active bioavailable pool, these substances obviously constitute an interesting analytical target to monitor and potentially utilize as a basis for optimization of MTX therapy.

With MTX historically being used in high dose as an anti-cancer agent, analytical methods were focused on the detection of MTX[13] and MTXPGs[14] in plasma and urine,

mainly by chromatographic methods, rather than intracellular levels of MTXPGs. Current methodology for the determination of MTXPGs in human red blood Cells (RBCs) can be categorized into methods that detect the sum of MTXPGs, and methods that are able to determine cellular levels of individual MTXPGs, typically $MTXPG_{1-5}$. Chromatographic methods for total MTXPG are based on an pre-chromatographic enzymatic de-glutamation step that converts the MTXPGs back to MTX. Total MTX is then determined by LC separation (isocratic[15] or gradient elution[16]) and a subsequent post-column photochemical[17-18] (PCR($h\nu$)) or electrochemical[19] reaction to form a product(s) amenable to fluorescent detection (FD). Other reported strategies involve the use of radiochemical-ligand binding[20], enzymatic[21] and fluorescence polarization immunoassays[22]. Individual MTXPGs have been measured by coupling a fractionation step to earlier reported assays[23-24], leading to complicated labor intensive assays. The specificity of these non-chromatographic detection methods has been questioned due to discrepancies observed for results obtained by LC based methods[25]. In 2003, Dervieux *et al*. reported a strategy utilizing reversed-phase liquid chromatography post-column photochemical reaction (LC-PCR($h\nu$)–FD) for detection of $MTXPG_{1-7}$ in a single run[16]. Surprisingly to date, mass spectrometry detection (MS) of (intra-cellular) MTXPG levels has received little attention. Recently Chen *et al*. reported an LC tandem mass spectrometry assay (LC-MS/MS) for the measurement of $MTXPG_{1-5}$ in Caco-2 cells, leading to improved selectivity and lower detection limits[26]. However, no reports of LC-MS/MS based methods for the detection of MTXPGs in RBCs have appeared in literature.

Presently our laboratory is collaborating with colleagues at Children's Mercy Hospitals and Clinics (Kansas City, MO) to investigate the MTXPG state in combination with genomic assesment of children undergoing therapy for JIA. In the present work we evaluated the performance of an LC-PCR($h\nu$)-FD, which was found to be problematic. As a result we have subsequently developed LC-MS/MS based methodology that is highly sensitive and specific for the detection of MTXPGs and appears to be superior to all previously reported methods.

4.2   Experimental

4.2.1   Materials

LC grade solvents acetonitrile (ACN) and methanol (MeOH) were obtained from Fisher Scientific (Fair Lawn, NJ, USA). Ammonium bicarbonate, N, N-Dimethylhexylamine (DMHA) and methotrexate were purchased from Sigma-Aldrich (St Louis, MO, USA). Methotrexate polyglutamation standards 4-amino-10-methylpteroyldiglutamic acid ($MTXGlu_2$), 4-amino-10-methylpteroyltriglutamic acid ($MTXGlu_3$), 4-amino-10-methylpteroyltetraglutamic acid ($MTXGlu_4$), 4-amino-10-methylpteroylpentaglutamic acid ($MTXGlu_5$), 4-amino-10-methylpteroylhexaglutamic acid ($MTXGlu_6$), 4-amino-10-methylpteroylheptaglutamic acid ($MTXGlu_7$) were purchased as the ammonium salts from Schircks Laboratories (Jona, Switzerland). Oasis HLB solid phase extraction (SPE) cartridges (30mg) were obtained from Waters (Milford, MA, USA).

4.2.2   Preparation of erythrocyte (RBC) lysates

Blood samples (~5 ml) obtained from patients were centrifuged at low speed (2000 rpm) in a Beckman tabletop centrifuge to pellet the RBCs. After recovery of the plasma, the RBCs were suspended in an equal volume of sterile normal saline, mixed by gentle inversion and subjected to a second low speed centrifugation. The supernatant was discarded and the wash procedure was repeated a second time. After discarding the supernatant, the packed RBCs were divided into four aliquots and stored at -70°C until use.

4.2.3 LC-PCR(*hν*)-FD

The LC-PCR(*hν*)-FD system consisted of two Shimadzu LC6A solvent delivery modules that were operated through a Shimadzu SIL-6B system controller. The sample was introduced by a Shimadzu SIL-6B autosampler equipped with a 100 µL injection loop. The separation was conducted on a Phenomenex Intertsil C18 (150 x 4.6 mm) column with 5 µm particles with a 100 Å pore size, that was protected by a Supelcosil LC-8, 5 µm, 2 x 4.0 mm guard column. The column was coupled to an in-house manufactured online photochemical reactor. Two meters of transparent Teflon tubing (0.012" id x 0.030" od) with 1 meter in the center braided was used as reactor coil. A GE Germicidal 9W lamp, GBX9/UVC lamp was used as light source inside of the photochemical reactor. Detection was accomplished using a Jasco FP-920 Intelligent Fluorescence Detector (excitation: 274nm and emission: 470nm) with the data recorded by TurboChrom V4.1. The mobile phase used with this chromatographic system consisted of solvent A: 10 mM Sodium Phosphate buffer pH 6.2 with 1.5 mL/L 30% H_2O_2 and solvent B: 20% ACN with 1.5 mL/L 30% H_2O_2. The system was operated at a flowrate of 1.0 mL/min with a gradient elution program of 10% B to 55% B in 15 minutes, followed by an isocratic hold for 5 minutes. The column was allowed to re-equilibrate for 10 minutes at the initial conditions. Sample preparation was conducted according to the procedure described by Dervieux et al[16].

4.2.4 Sample preparation for LC-MS/MS analysis

Packed RBCs obtained from patients were thawed prior to sample workup and analysis. A 200 µL aliquot was transferred into a plastic vial and subsequently 210 µL of

water was added to ensure complete lysis of the red blood cells. The vial was closed and vortexed for 10 seconds yielding a suspension. Protein precipitation was performed by addition of 40 µL of 70% perchloric acid, immediately followed by vortex mixing for 20 seconds or until complete precipitation had visually occurred. The precipitated suspension was centrifuged for 5 minutes at 13,000 RPM, resulting in a clear solution with an aggregate at the bottom of the vial. The solution was diluted by the addition of 550 µL of water and subjected to SPE. The SPE procedure consisted of 5 steps. First the cartridge was activated with 2 mL of MeOH. Second, the cartridge was equilibrated with 2 mL of a 0.1% aqueous formic acid solution. Third, 950 µL of sample was applied to the cartridge. Fourth, the cartridge was washed with 2 mL of the equilibration buffer. Fifth, analytes were eluted with 4 mL of a MeOH:3% NH_4OH (9:1) solution. The flow through the cartridge was adjusted to approximately 1.0 mL per minute during all steps. The eluent was evaporated to dryness under a gentle stream of nitrogen, while heating at 40° C in a waterbath. Analytes were redissolved in 300 µL of mobile phase A, vortexed for 20 seconds and transferred to an auto-sampler vial with 250 µL liner.

4.2.5 Preparation of standards

Methotrexate (polyglutamation) standards were dissolved in 100 mM NH_4HCO_3 buffer. Individual standards were combined and diluted to generate stock solutions containing each of the standards at a concentration of 1 µM, 100 nM and 10 nM. Stock solutions were stored at -80 °C and prepared on weekly basis. In order to validate the method, six-point calibration plots were constructed by analyzing methotrexate (polyglutamation) standards with concentrations of: 0, 2.5, 5, 10, 50, 100 nM. These

standards were prepared by spiking the appropriate volume of stock solution in 200 µL of blank RBCs obtained from healthy individual RBC donors. A seven-point calibration (0, 0.5, 1, 5, 10, 50, 100 nM) was performed for the analysis of patient samples. The calibration standards were treated the same as patient samples, with the exception that the volume of water used to lyse the cells was lowered by the volume of stock solution used to spike the calibration standard.

4.2.6 Liquid chromatography with MS detection

Solvent was delivered either by a Waters Associates Alliance 2695 Chromatographic System, or a Waters Acquity UPLC. Separation occurred on a 50 x 1.00 mm Phenomenex Synergy Hydro-RP LC column, packed with 4 µm, 80 Å particles. The column was guarded by a Supelcosil LC-8, 5 µm, 2 x 2.1 mm cartridge in the appropriate Supelcosil holder. The mobile phase consisted of (A) 10 mM NH_4HCO_3 buffer with 5 mM DMHA adjusted to pH 7.5 with HCO_2H, (B) consisted out of ACN with 5mM DMHA. The total flow rate was set to 200 µL/min. The solvent program for elution consisted of an isocratic hold at 90% A for 1 minute, followed by a linear gradient to 70% A in 9 minutes and was held for 2 minutes. The column was re-equilibrated for 8 minutes at 90% A. The injection volume using a Waters Associates Alliance 2695 Chromatographic System was 100 µL. Needle wash solution for this chromatograph consisted out of a basic solution of 50% 0.1 M NH_4OH: 50% MeOH. A Waters Acquity UPLC was equipped with a 20 µL loop and 100 µL sample syringe. Strong needle wash consisted out of 70% MeOH: 30% H_2O, weak needle was consisted out of 5% MeOH: 95% H_2O.

4.2.7 Mass Spectrometry

Instrumentation was a Micromass Quattro Ultima "triple" quadrupole mass spectrometer (Manchester UK) equipped with an electrospray ionization source. The instrument was operated in positive ion mode. Source parameters, including the cone voltage for each analyte were optimized by maximizing the area under the curve of multiple LC runs of the standard mixture at various programs. The probe capillary was optimized at 3.0kV, and the desolvation and source temperatures were set to 400 °C and 125 °C, respectively. The cone voltage was optimized by maximizing the area under the curve for each individual analyte by repetitive IP-LC runs varying the cone voltage. The cone gas flow rate was optimized at 80L/hr, the desolvation and nebulizer gas flow rate was adjusted for maximum signal of analyte. Argon was used for collision induced dissociation (CID) and the cell vacuum was set at 2.4 x 10^{-3} mbar. Q1 and Q3 were set to transmit ions with a resolution of 0.8 u FWHH. Multiple Reaction Monitoring (MRM) parameters (table 16) including precursor ions, product ions and collision energy were optimized by direct infusion of the individual analytes dissolved in 80% A and 20% B at 10 µM, closely resembling chromatographic conditions.

Table 16. MRM parameters used for the LC/MS/MS analysis of MTXPGs.

Analyte	Precursor ion (m/z)	Product ion (m/z)	Cone Voltage (V)	Collision energy (V)
MTXGlu$_1$	455.2	308.10	20	20
MTXGlu$_2$	584.3	308.10	20	26
MTXGlu$_3$	713.3	308.10	20	33
MTXGlu$_4$	842.3	308.10	20	40
MTXGlu$_5$	971.3	308.10	20	48
MTXGlu$_6$	1100.4	308.10	20	56
MTXGlu$_7$	1229.4	308.10	20	64

4.3   Results and Discussion

4.3.1 Performance of the LC-PCR(hν)-FD Method

Dervieux et al. presented the use of LC-PCR($h\nu$)-FD for the detection of MTXPGs in 2003[16]. To date, this is still the only published chromatographic method for the detection of individual MTXPG species. The authors claimed the method to be sensitive and to exhibit the required selectivity with minimal biological interferences. However, the authors do note that the method lacks the ability to robustly separate and quantify long-chain MTXPGs. When the published methodology was implemented in-house in order to analyze RBCs obtained from JIA patients on MTX therapy, the results of Figure 29 were observed. Improvements over the Dervieux method were achieved by utilizing a Phenomenex Intertsil C18 column instead of the reported Waters Terra MS C18 column with similar dimensions. A baseline separation with improved chromatographic efficiency and peak symmetry (note the similar time frame for the separation with narrower peaks, i.e. improved efficiency) of a 50 nM spiked MTXPG$_{1-7}$ mixture in water is demonstrated in Figure 29A).

114
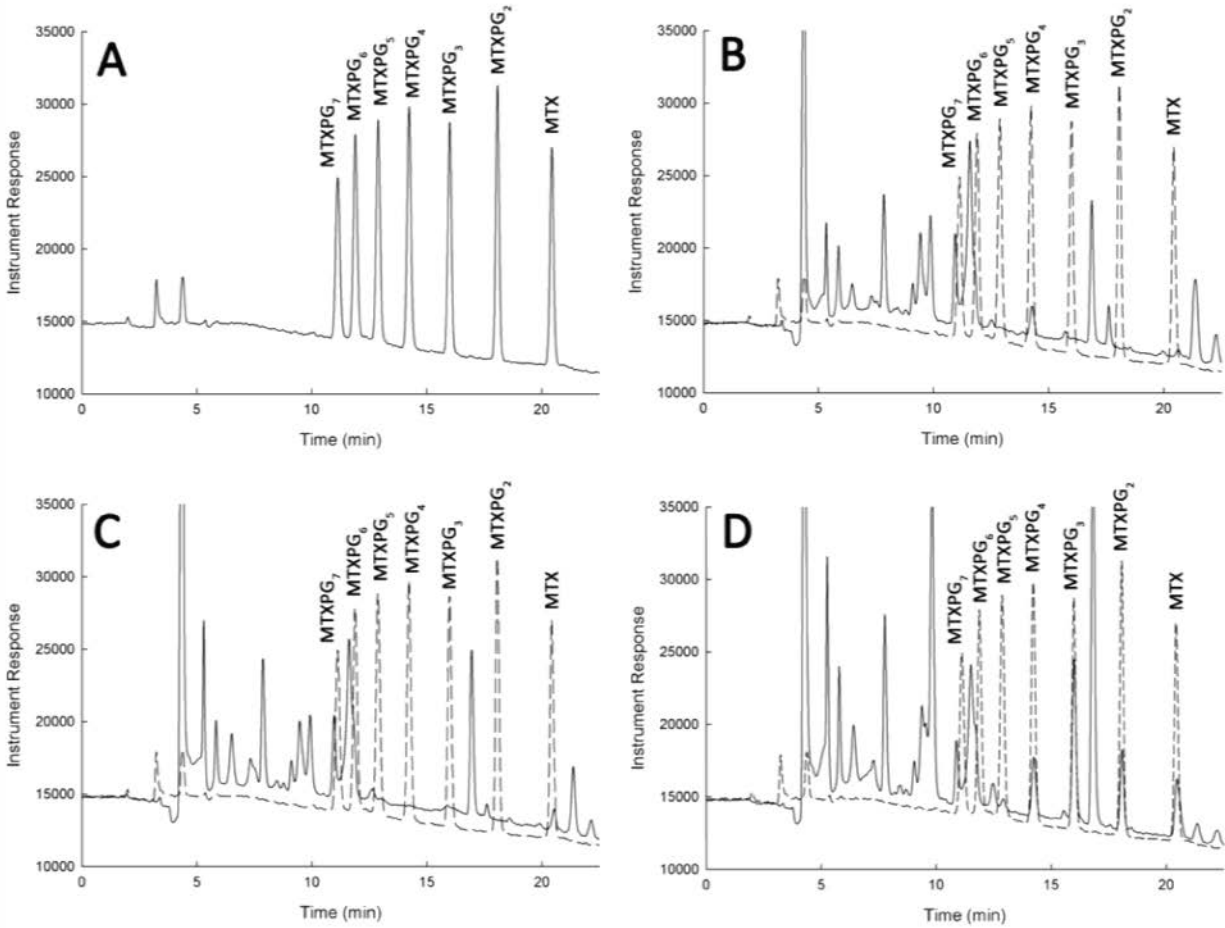
Figure 29. *Chromatograms of calibrators in water, blank RBCs and a patient. A) Chromatogram of MTXPG standards spiked at a final concentration of 50nM/each in water. This chromatogram is presented in B, C and D as the dotted line for reference purpose. B) Example chromatogram of a RBC blank from an individual donor with an endogenous interferent in the elution window of MTXPG$_4$. C) Example chromatogram of a RBC blank from an individual donor with an endogenous interferent in the elution window of MTX. D) Example chromatogram of RBCs from a patient on low dose (7.5mg) MTX.*

However, even with improved chromatographic performance, blank RBCs collected from eight healthy individuals showed a variety of endogenous interferences with variable retention times. The chromatograms of two of these individuals are shown in Figure 29B and 29C. Figure 29B shows a chromatogram of a blank RBC lysate from a healthy donor containing a significant interference that would, based on its retention time, falsely identify and quantitate as $MTXPG_4$. This individual also has another peak eluting near the $MTXPG_2$ standard that could be misinterpreted as $MTXPG_2$ and thus lead to over estimation. Another chromatogram of a healthy RBC donor is shown in Figure 29C, demonstrating a contaminant that would be falsely identified as MTX by this method. A chromatogram of a patient on weekly low dose (7.5 mg) MTX therapy is presented in Figure 29D. By comparing Figures 29B, 29C and 29D, it is obvious that these interfering peaks can significantly influence measured concentrations of individual MTXPGs, leading to a gross over estimation of $MTXPG_{total}$ and skew the MTXPG "fingerprint" within the RBC. Despite the fact that the original work reported quantitation of MTXPGs in individual patients on MTX therapy, it appeared blank RBCs were obtained from a blood bank and pooled before preparation of the RBC calibration standards. The use of pooled RBCs could have led to an average blank RBC picture, disguising individual analyte variations due to dilution.

The nature of these interferences is unknown at this point, but likely to be folate related since a number of folates share the same chromatographic behavior and fluorescent spectroscopic properties as MTX under these conditions[27-28]. MTX as a folate antagonist has been shown to interfere with the folate cycle by blocking key enzymes, which could lead to a buildup of oxidized folate (polyglutamated) species[10-11]. In a worst case scenario, this could lead to false identification and over estimation of

MTXPGs in patients on MTX therapy, as compared to situation presently demonstrated by the individual RBC blanks (figure 29B and 29C). These observations dictated the need for development of a more specific and sensitive method for the present research. The approach taken was based on LC separation followed by tandem mass spectrometry detection.

4.3.2 Chromatographic conditions for mass spectrometry

The chromatographic performance of several supports (Waters Atlantis T3, Altech Alltima and Phenomenex Synergy) was screened for the separation of MTXPGs in the reversed phase mode. The Phenomenex Synergy Hydro RP column provided the highest selectivity factor together with symmetrical peaks for the MTXPGs, especially for $MTPG_{5-7}$, analytes that were poorly resolved by the other columns, likely due to unfavorable secondary retention mechanisms. In order to separate MTXPGs a pH > 5.0 (resulting in proportionally higher anionic character for longer PGs) was required, resulting in elution inversely proportional to polyglutamation number. The highly anionic character of the MTXPGs in this pH range led to poor retention, leading to organic concentrations at the low limit (i.e. a 0.5%-3% B gradient was used). The highly aqueous elution conditions were found to suppress overall ionization efficiency, with the most severe effects observed for the longer polyglutamates.

Garratt et al. presented the use of DMHA as volatile ion-pair reagent in reversed-phase ion-pair (IP) chromatography mass spectrometry for the analysis of a broad spectrum of folate polyglutamates[29]. In the present case, a similar concentration of DMHA (5 mM) led to improved retention and successful separation of $MTXPG_{1-7}$ within

117

10 minutes. The elution order of MTXPGs was observed to be directly proportional to the number of glutamate residues. The pH of the mobile phase was buffered at 7.5, the pH limit at which the column was reported to be stable and thus maximizing ionization of the glutamate carboxylates.

4.3.3 LC-MS/MS conditions

MTXPG standards were screened in positive and negative ion ESI mode, in the presence and absence of DMHA. In contrast to folate polyglutamates being reported to have an overall more favorable signal-to-noise ratio in negative ion mode, MTXPGs were found to ionize more efficient in positive ion mode. In the absence of DMHA (in reversed phase LC-mode), it was found that longer polyglutamates formed increasingly higher multiple charged species (i.e. doubly and triply charged), that were more susceptible to formation of unfavorable sodium clusters (Figure 30A, 30B and 30C). The use of DMHA as the ion-pairing reagent, led to the nearly exclusive formation of the singly charged species, $[M+H]^+$. MTX was susceptible to the formation of a $[M+DMHA+H]^+$ cluster (Figure 30D), an effect that was significantly reduced in longer MTXPGs (Figure 30E and 30F). Interestingly the observed instrument response between the singly charged species of the individual MTXPGs was found to be virtually identical, with MTX being slightly lower due to formation of the $[M+DMHA+H]^+$ cluster. It was found that a low cone voltage was optimal for all MTXPGs (table 16).
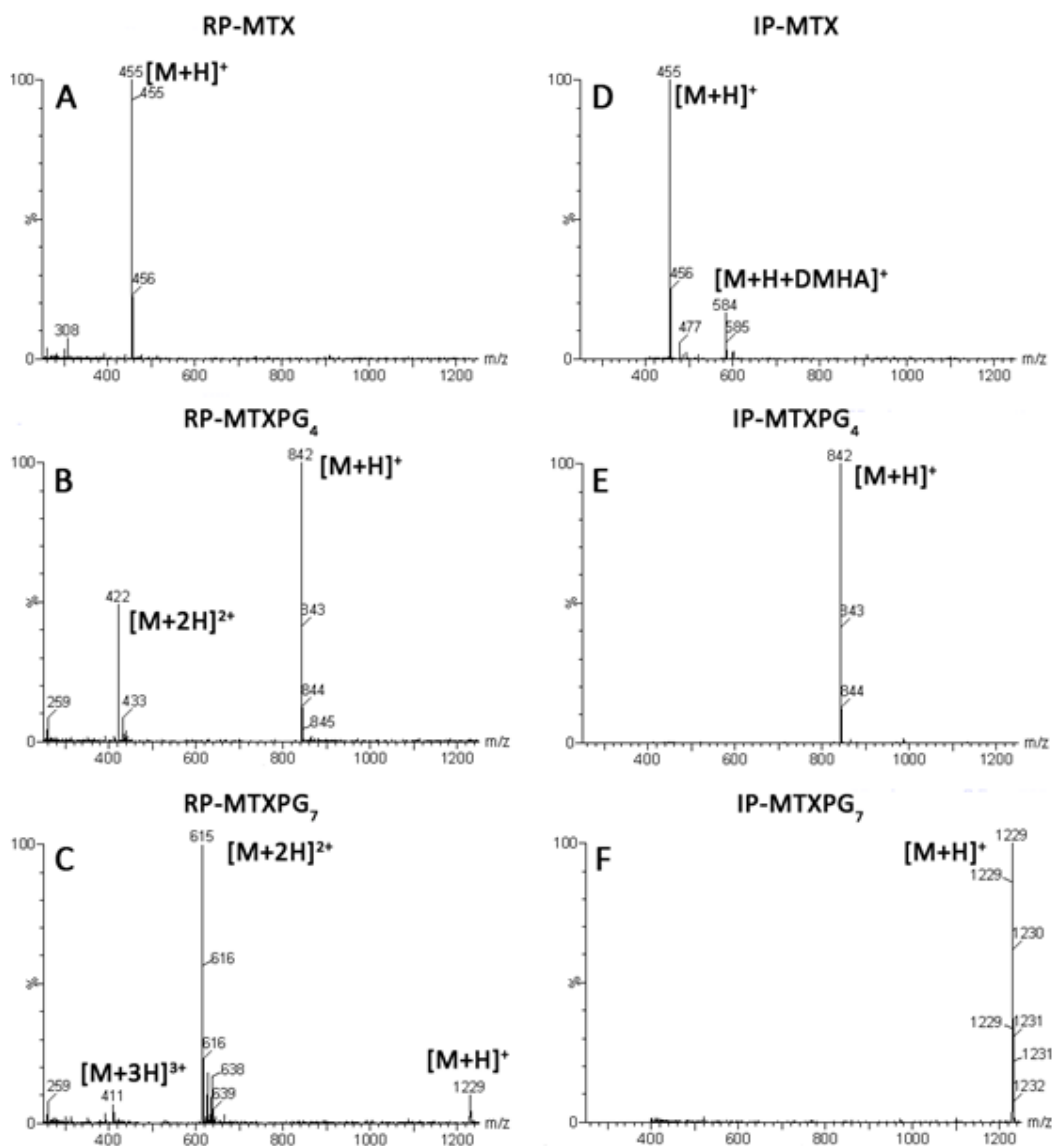
Figure 30. *Ionization characteristics comparison of MTXPGs in reversed phase chromatography (left) and ion-pair chromatography (right). A) MTX under reversed phase conditions forms a singly charged ion. B) MTXPG₄ forms a singly and doubly charged ion under reversed phase conditions. C) MTXPG₇ forms under reversed phase conditions the singly charged ions, doubly charged ions that form sodium adducts, and triply charged ions. D) MTX forms mainly the singly charged species and a DMHA adduct in IP-mode. E) MTXPG₄ forms an exclusively singly charged molecule in IP-mode. F) MTXPG₇ forms an exclusively singly charged molecule in IP-mode.*

Collision induced dissociation of MTX and the polyglutamates yielded a consistant pattern of product ions (figure 31) including an abundant product ion at *m/z* 308.10, corresponding to the 4-amino-10methylpteroyl fragment (figure 28). This *m/z* 308.10 fragment was selected as product ion for all of the MTXPGs in multi reaction monitoring (MRM). The collision energy was optimized for the product ion by infusion of the individual analytes (table 16) and was found to proportionally increase with glutamation number.
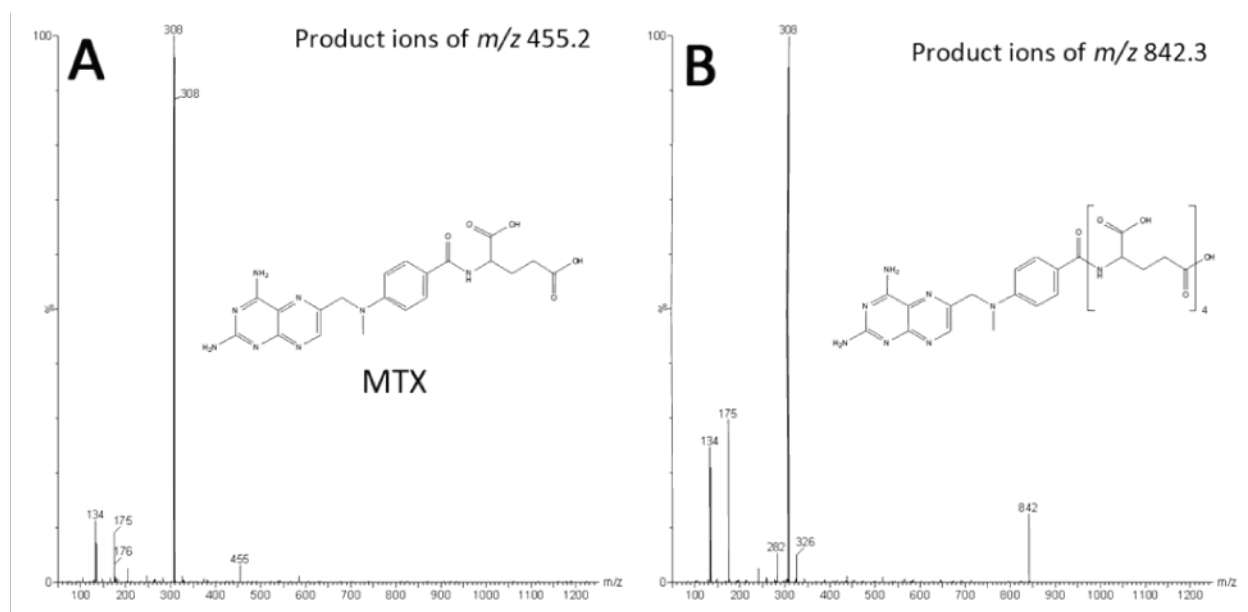
Figure 31. *Product ion spectra of MTX (A) and MTXPG4 (B).*

4.3.4 Sample preparation from erythrocytes

The most commonly used sample preparation for the LC analysis of MTXPGs out of RBCs involves addition of an aliquot of water to assist in lysis of RBCs, followed by a perchloric acid protein precipitation step and direct injection of the supernatant. This procedure results in diluted samples of high ionic strength that are incompatible with LC/MS. In an effort to desalt, clean-up and pre-concentrate MTXPGs from RBCs the performance of silica based reversed phase C18 and strong anion-exchange (SAX) solid-phase extraction phases were investigated. It was found that higher order PGs were not retained by the C18 cartridge, whereas their recovery was incomplete and inconsistent from the SAX cartridge. Reproducible recovery and strong retention of all MTXPGs was obtained by the use of a Oasis HLB SPE cartridge (30 mg), that has a polymeric stationary phase. Clean extracts were eluted and evaporated to dryness and reconstituted in a small volume, effectively reducing dilution of the samples prior to analysis.

Ideally, the use of an isotopically labeled internal standard is preferred in this multistep sample preparation procedure. However, d3-MTX is extremely costly to purchase or synthesize[30], and isotopically labeled MTXPGs are not commercially available. As an alternative internal standard, the anti-folate aminopterin (AMP) is used[26]. It was found that AMP is poorly retained under LC-IP conditions, suffering from matrix effects, and as a result was found unsuitable as internal standard. With a suitable internal standard not being readily available, the method was performed with external calibration.

Table 17. Intra- and inter-day precision, accuracy and analyte recovery results

Analyte	Nominal RBC Concentration (nM)	Intra-run (n=5)			Inter-run (n=20)		
		Precision (RSD %)	Mean observed concentration (nmol/L)	Mean Accuracy of target value (%)	Precision (RSD %)	Mean observed concentration (nmol/L)	Mean Accuracy of target value (%)
MTXPG$_1$	2.5	12.6	2.5	100.0	19.2	2.2	88.6
	5	11.3	4.8	96.8	16.3	5.4	107.2
	10	17.1	10.7	106.6	15.4	10.8	107.8
	50	15.2	50.8	101.6	10.3	51.0	102.0
	100	11.9	98.7	98.7	11.8	101.1	101.1
MTXPG$_2$	2.5	11.9	2.6	102.4	19.1	2.3	93.0
	5	8.4	5.0	99.2	11.4	5.0	100.1
	10	10.7	9.4	94.2	10.6	10.6	106.3
	50	7.9	52.3	104.5	12.5	51.2	102.4
	100	9.1	98.3	98.3	9.6	99.0	99.0
MTXPG$_3$	2.5	19.3	2.4	95.2	23.7	2.5	99.6
	5	8.8	5.1	101.6	12.9	5.0	99.1
	10	9.5	11.0	109.8	11.9	10.5	105.4
	50	14.9	50.0	100.0	10.2	50.1	100.2
	100	9.0	98.8	98.8	10.2	99.4	99.4
MTXPG$_4$	2.5	14.2	2.56	102.4	14.5	2.4	94.8
	5	3.0	5.04	100.8	11.6	5.2	103.4
	10	4.0	9.28	92.8	12.0	10.5	105.0
	50	4.6	52.18	104.4	11.9	51.3	102.6
	100	6.8	98.5	98.5	9.0	98.1	98.1
MTXPG$_5$	2.5	20.0	2.4	95.2	16.9	2.3	93.0
	5	8.1	5.1	102.4	10.4	5.1	102.9
	10	11.4	9.5	94.8	11.4	10.6	106.4
	50	7.7	53.2	106.5	12.0	51.2	102.4
	100	7.2	97.2	97.2	8.5	98.1	98.1
MTXPG$_6$	2.5	15.4	1.9	76.8	20.7	2.2	89.0
	5	13.8	5.1	101.0	14.5	5.2	103.1
	10	12.2	10.1	100.8	10.8	10.8	107.9
	50	6.8	52.2	104.3	10.9	50.8	101.7
	100	5.8	97.1	97.1	8.9	98.1	98.1
MTXPG$_7$	2.5	20.6	2.6	102.4	15.5	2.4	95.6
	5	6.9	4.9	97.2	9.7	5.1	102.4
	10	3.2	9.5	95.2	9.2	10.4	104.4
	50	7.6	54.2	108.5	10.5	51.1	102.3
	100	6.6	96.3	96.3	7.2	98.4	98.4

4.3.5 Method performance

Simultaneous MRM analysis of blank RBCs from different individual donors, demonstrated that endogenous compounds contributed minimal background noise (Figure 32A). Standards spiked at low concentration (5 nM) in RBCs eluted free of interferences (Figure 32B). Initially the method was developed and validated on a Waters Acquity UPLC platform equipped with a 20 µL sample loop. Table 17 summarizes the intra- and inter-day precision and accuracy of the analytical assay at MTXPG concentrations spiked at 2.5 nM, 5 nM, 10 nM, 50 nM and 100 nM in 200 µL of RBCs respectively. Mean extraction recoveries for the total procedure (protein precipitation + SPE and evaporation with reconstitution) were 31.2% for $MTXPG_1$, 33.4% for $MTXPG_2$, 39.6% for $MTXPG_3$, 44.2% for $MTXPG_4$, 43.0% for $MTXPG_5$, 50.6% for $MTXPG_6$ and 47.8% for $MTXPG_7$. Low, but reproducible recoveries were mainly attributed to the protein precipitation step, that has reported recoveries of around 60%[16]. The intra-run precision was within an RSD of 3.0 and 20.0% and the inter-run precision was between 7.2 and 23.7% (table 17). Lower Limits of quantitation (LLOQ) were determined as the lowest concentration that resulted in a RSD ≤ 20% for intra-day precision. As a result the LLOQs were found to be about 2.5 nM for all of the individual MTXPGs using a 20 µL loop volume in combination with a Waters Acquity LC platform. At the LLOQ the signal to noise ratio was between 15:1 and 25:1 depending on the analyte. The Limit of detection (LOD) was derived from the LLOQ according to the equation LOD = (0.33*LLOQ). LODs were 0.8 nM for all of the individual MTXPGs. Regression analysis of various calibrants spiked with MTXPG concentrations ranging

123

from 2.5 to 100 nM, spanning the anticipated concentration range in patients, revealed a linear relationship between instrument response and analyte concentration (table 18).

Finally, in order to further improve sensitivity the method was transferred from a Waters Acquity to a Waters 2695 platform that would allow for 100 µL injection volumes (over 20 µL) effectively yielding a factor of five increase in sample loading. It was found that an 100 µL injection volume could be successfully focused on the head of chromatography column leading to an increase in sensitivity of a factor five without the loss of separation efficiency (Figure 32B and 32C), note that the detected mass is 100 fmol in both cases), resulting in LLOQs of 0.5 nM for individual MTXPGs. LOD for each MTXPG were determined to be 0.2 nM. However, it was found that the use of the 2695 platform was prone to carryover, and as a result extensive needle cleaning steps and the use of blank wash injections had to be included in order to eliminate carryover.

Table 18. Inter-day variation in calibration lines for MTXPG standards

Analyte	Slope ± SD	R^2 ± SD
MTXPG$_1$	1.012 ± 0.060	0.9993 ± 0.0007
MTXPG$_2$	0.991 ± 0.020	0.9993 ± 0.0005
MTXPG$_3$	0.999 ± 0.010	0.9993 ± 0.0007
MTXPG$_4$	0.982 ± 0.013	0.9992 ± 0.0005
MTXPG$_5$	0.982 ± 0.013	0.9992 ± 0.0005
MTXPG$_6$	0.981 ± 0.010	0.9991 ± 0.0010
MTXPG$_7$	0.986 ± 0.012	0.9986 ± 0.0019
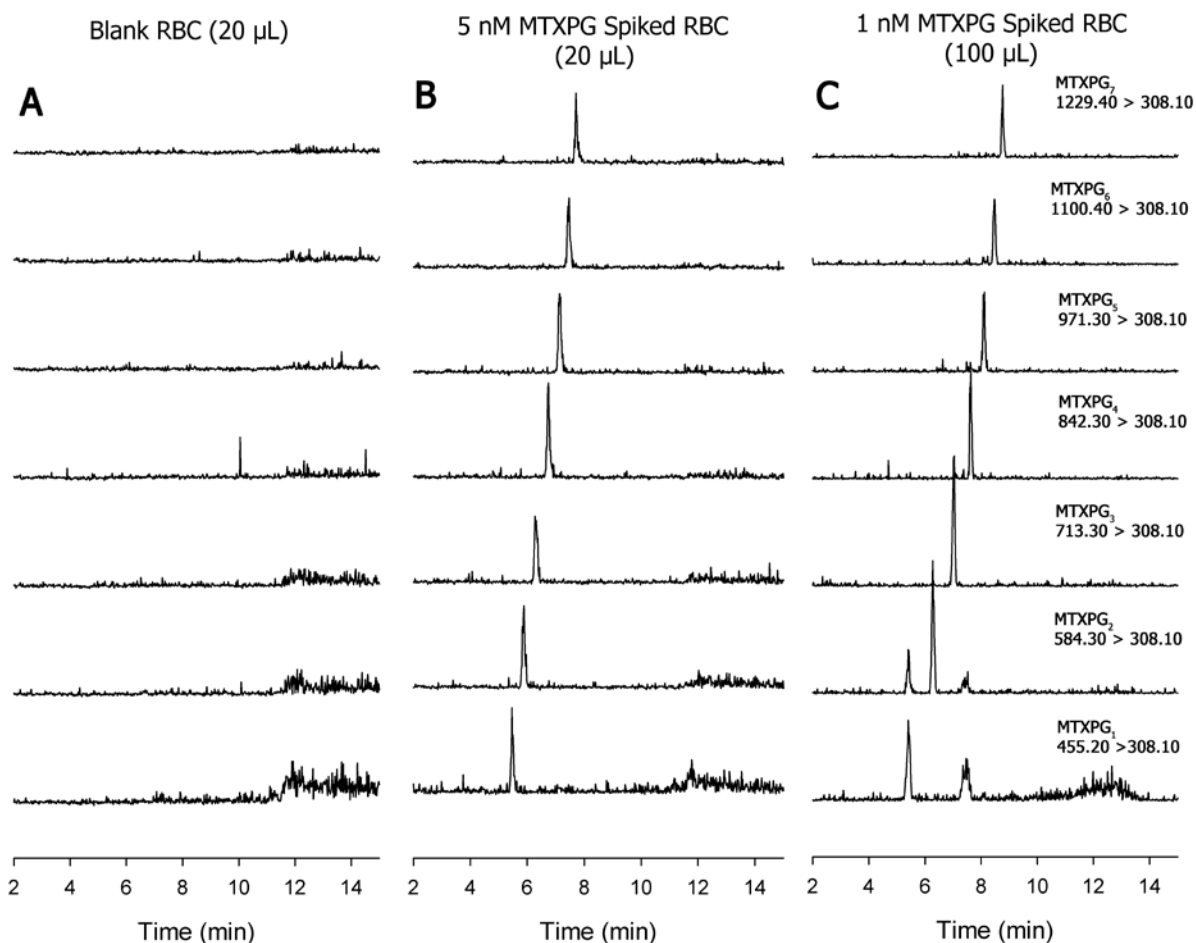
Figure 32. *A) Representative Blank RBC standard for different lots of RBCs. B) Low concentration (5nM) calibrant in the RBC analyzed by the Waters Acquity platform (20 µL injection, injected mass 100 fmol). C) Low concentration (1 nM) calibrant in the RBC analyzed by the Waters 2695 Alliance platform (100 µL injection, injected mass 100 fmol).*

Using large volume injections, an unidentified endogenous compound was observed that exhibits the same m/z as MTX and forms a 308.10 fragment, resulting in a peak in the MTX channel (Figure 32C). This molecule was separated from MTX and as a result

125

does not interfere with the analysis. The presence of such a compound has been reported in LC-MS/MS analysis of MTXPGs in Caco-2 cells as well[26]. Since the mono-isotopic mass of DMHA is equal to that of a glutamyl residue (129 Da), the formation of DMHA clusters led to the appearance of a lower $MTXPG_n$ in the MRM channel of a $MTXPG_{n+1}$. The intensity of this DMHA adduct is most abundant for MTX and significantly lower for the other MTXPGs (Figure 30 and 32C). DMHA clusters were found to not affect quantitative analysis since all PGs are baseline separated and clusters formed from lower laying MTXPG are easily identified since they have identical retention times. The use of N,N-dimethylpentylamine or N,N-dimethylheptylamine as ion-pairing reagents will be explored in the future in an effort to circumvent this issue.

4.3.6 Clinical application of the method

The LC-MS/MS methodology was used to analyze the MTXPG distribution in RBC samples from 100 JIA patients on MTX therapy, in an effort to develop correlations to genomic variations (the object of a separate investigation) and potentially serve as the basis for the rational development of individualized therapeutic regimens. The Waters 2695 platform was calibrated between 0.5 nM and 100 nM for each MTXPG. A typical patient chromatogram and resulting RBC MTXPG concentrations obtained by this method are shown in figure 33A and 33B. $MTXPG_3$ was determined to be the major species in most of the samples, which is consistent with a prior publication[31]. The improved sensitivity of the LC-MS/MS method led to the observation and low nano molar detection and quantitation (<1 nM) of long chain $MTXPG_{6-7}$ in a high number of samples. These MTXPGs were not observed in patient RBCs by earlier methods consistent with

126

reported 2 nM detection limits. Since no standards are available for MTXPG$_8$ nor higher polyglutamates, samples with high levels of MTXPG$_{total}$ were tentatively reanalyzed for the presence of MTXPG$_{8-12}$ using the common product ion and extrapolated collision energies. Despite various efforts, MTXPG$_{8-12}$ were not detected in any patient RBC samples. The detection and quantitation of long chain MTXPGs$_{5-7}$ at low concentration is of particular clinical interest since these species are associated with increased potency over short chain MTXPGs. The sensitivity of this newly developed method would also allow for pharmacokinetics analysis of long chain MTXPGs. In a study by Dalrymple *et al.*, using LC-PCR(*hv*)-FD, the elimination half-life of MTXPG$_{4-5}$ could not be accurately determined due to a lack of sensitivity for these species[32].

	Concentration (nM)
MTX	14.7
MTXPG$_2$	10.4
MTXPG$_3$	64.5
MTXPG$_4$	42.6
MTXPG$_5$	20.3
MTXPG$_6$	0.6
MTXPG$_7$	< LLOQ (0.2nM)
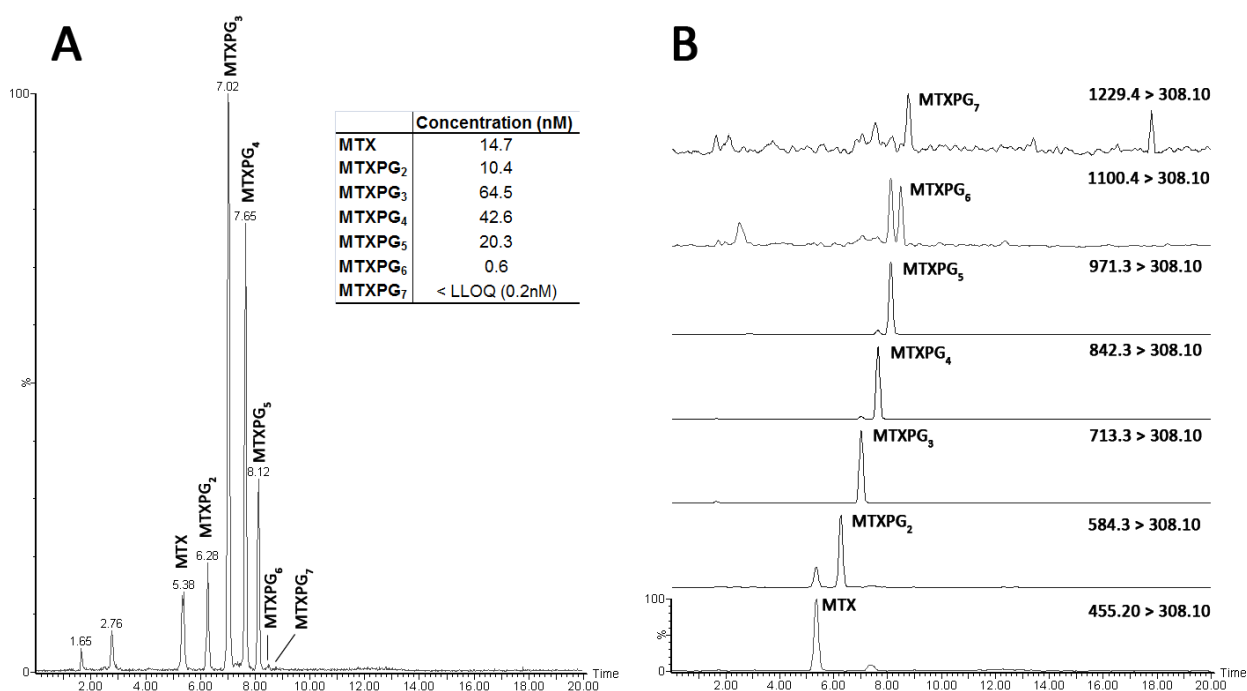
Figure 33. *A) Typical total ion current LC/MS/MS chromatogram obtained from RBCs of a patient on MTX therapy. B) Individual MRM channels used to construct (A) for the seven MTXPGs.*

127

4.3.7 Post analysis clean-up from ion pair agent

DMHA cluster ions in the mass spectrometer $[DMHA+H]^+$, $[DMHA+CH_3CN+H]^+$, and $[DMHA+HCl+H]^+$, persist well after the DMHA solvent reservoirs are removed from the chromatograph. A significant reservoir is the chromatograph itself, requiring 100's of mLs of organic solvent with 1% FA to purge (using the wet prime function on the 2695) the system. Attention to washing the large stainless steel fritted filters in the solvent bottles speeds up removal of DMHA derived ions from the chromatograph. ESI source contamination is quickly reduced by flowing about 50 mL of clean solvent (e.g. not through the chromatograph), reducing the $[DMHA+H]^+$ ion to about 2-3 times the most abundant ion in the typical low *m/z* ESI "solvent blast". Complete removal of this background ion requires source block and first hexapole cleaning on the Quattro Ultima source.

4.3.8 Patient data

The method presented in this chapter was used for MTXPG profiling of more than 100 JIA patients on low dose MTX. The MTX polyglutamation distribution is given in table 19. Data analysis was performed by our collaborators at Children's Mercy Hospitals (Kansas City, MO) and results are published (appendix 1 and 2). Appendix 1 also describes the patients demographics of this study. To summarize our findings, the route of MTX administration was a determining factor upon MTX polyglutamation distribution (appendix 1). The MTXPG chain length increased when patients received MTX in the subcutaneous tissue, as opposed to oral dosage. We have also demonstrated that longer MTXPGs are associated with liver toxicity, one of the common

adverse effects in MTX treatment in RA and JIA (appendix 2). A full discussion of all the results is beyond the scope of this dissertation, but readers are encouraged to review appendix 1 and 2.

4.4   Conclusions

The measurement of MTXPGs in RBCs is challenging due to the presence of endogenous interferences, low concentrations within RBCs and poor chromatographic behavior of longer polyglutamates, typically MTXPG$_{5-7}$. The use of an improved sample preparation strategy for clean up and sample pre-concentration followed by an innovative chromatographic procedure with tandem mass spectrometry detection led to the robust separation and detection of MTXPG$_{1-7}$ within 10 minutes in patient RBC samples. The use of DMHA as an ion-pairing agent was beneficial in both, chromatographic separation and mass spectrometry detection. Triple quadrupole mass spectrometers have become widely available and are currently routinely applied in clinical settings for therapeutic drug monitoring, thus allowing for widespread adaption of the described methodology. The new analytical approach should enhance knowledge of MTX metabolomics by providing a quantitative MTXPG "fingerprint" in patient RBCs. Such information has the potential to aid in individually optimized MTX dosing. This could result in reduction of side effects and provide valuable information in regard to interpretation of MTX pharmacogenomical data, a field that is currently receiving increased attention.

Table 19. JIA patient MTXPG profile

Patient	MTXPG concentration (nM)						
	MTXPG1	MTXPG2	MTXPG3	MTXPG4	MTXPG5	MTXPG6	MTXPG7
1	28.4	14.5	50.1	21.9	6.7	0	0
2	17	12.7	26.1	4.7	1	0.4	0
3	27.8	12.9	36.2	8.9	1.5	0	0
4	11.6	6.3	10.6	2.3	0.7	0.1	0
5	33.4	17.3	35.5	10.6	2.2	0.4	0
6	17.1	15.2	23.6	3.5	0.7	0.3	0
7	20.4	19.5	80.4	32.6	9	0.3	0.4
8	11.7	6.4	4	0.9	0.5	0	0
9	3	8.2	9.7	1.5	0.4	0.1	0
10	21.7	18.3	50.8	19	4.7	0.3	0
11	16.1	11.2	14.8	2.4	0.5	0.1	0
12	17.7	18.1	76.7	32.7	9.6	0.4	0.2
13	5.9	8.5	24.1	10	3.1	0.1	0
14	3.8	3	29.1	22.2	11.8	0.2	0
15	76	13.4	38.9	13.2	3.8	0.2	0
16	2.6	6	19.1	8.3	2.1	0.1	0
17	42.4	18.4	64.5	28.7	8.3	0.3	0
18	24.8	13.6	47	22.7	8.7	0.2	0
19	15.3	16.6	21.8	2.8	0.6	0.1	0
20	4	7.5	41.4	21.7	6.3	0.1	0
21	0.1	0.6	7.6	3.7	1.4	0.1	0
22	15	13.4	22.2	4	0.8	0	0
23	13.7	11.2	40.7	13.8	3.1	0.1	0
24	14.4	11.3	18.5	2.2	0.5	0	0
25	1.3	2	6.3	2.1	0.4	0	0
26	25.8	25	37.1	6.6	1.1	0	0
27	9.6	10	20.8	4.8	0.8	0	0
28	24.1	18.8	60.7	19.9	4.7	0.2	0
29	3.7	7.1	44.3	25.2	8.8	0.1	0
30	22.3	12.9	46	16.6	4.4	0.6	0
31	11.3	9.8	47.2	29	10.8	0.4	0
32	0.4	0.7	11.5	5.9	2	0.1	0
33	27.9	15.9	77.4	42.4	14.8	0.4	0
34	6.3	4.4	13.6	8.1	3.4	0.1	0
35	15.2	11.1	48.4	32.6	15.6	0.4	0
36	12.2	14.6	35.9	12.8	3.4	0.3	0
37	20.4	11.5	6.3	0.4	0.3	0	0
38	11.5	6.7	27.6	14.6	5	0.3	0
39	46.1	20	51.5	16.7	4.7	0.3	0
40	19.5	13.4	40	19.8	6.7	0	0

Table 19. continued

Patient	MTXPG1	MTXPG2	MTXPG3	MTXPG4	MTXPG5	MTXPG6	MTXPG7
			MTXPG concentration (nM)				
40	19.5	13.4	40	19.8	6.7	0	0
41	6.5	12.5	27.9	7.7	1.8	0.1	0.2
42	10.8	12.8	36.8	9	1.8	0.1	0
43	30.5	16	44.8	18	4.3	0.5	0
44	32.3	3.7	3	0.3	0.7	0.1	0
45	49.8	28.3	79.5	39.8	12.4	0.5	0
46	1.1	0.6	12.2	7.9	3.1	0.2	0
47	4.9	8.9	36	22.8	12.6	1	0
48	6.2	7.1	61.2	39.1	15	0.3	0
49	11.6	10.1	48.1	23	6.6	0.2	0
50	23.5	12.4	25.9	9.1	2.7	0.3	0.3
51	17.5	15.9	18.6	2.2	0.5	0.2	0.1
52	14.8	9.1	32.2	10.5	2.3	0.2	0
53	4.2	8.6	31.1	20.3	10.6	0.1	0
54	7.8	6.9	26.8	7.9	1.6	0.2	0.1
55	3.8	5.6	19	5.4	1.5	0.2	0
56	28	18.6	42.1	12.6	2.6	0.2	0.2
57	24.7	13.6	47.6	19.1	5.9	0.2	0
58	21	17.6	17.8	3.6	0.6	0	0.1
59	22.4	20.8	53.1	14.6	3	0.2	0.1
60	14.7	10.4	64.5	42.6	20.3	0.6	0.1
61	24.7	15.6	27.5	10.3	3	0.1	0.4
63	23.2	16.3	20.8	2.3	0.5	0	0
64	18	8.4	27.4	8.6	2.1	0.2	0
65	25	18.5	13.7	1.1	0.2	0.1	0
66	19.1	14.1	24.5	3.9	0.6	0.1	0
67	2.8	5.8	19.2	7.1	1.8	0	0
68	3.1	6.3	19.3	8	2.2	0.1	0.1
69	44.2	11.7	29.9	7.9	1.5	0.1	0
70	5.9	5.4	8.4	1.6	0.1	0.1	0
71	18.2	13.3	33.8	8.7	1.4	0.1	0
72	17.2	11.5	62.9	32.3	9.8	0.2	0
73	0.7	0.8	0.7	0.9	0.9	0.8	0
74	15.5	20.2	83.2	41.6	13.7	0.4	0
75	13.1	16.8	45.9	19.3	5.7	0.2	0
76	13.9	12.5	43.7	16.2	4.2	0.3	0
77	15.5	8.5	32.5	15	5.2	0	0
78	16.3	6.7	4.9	0.5	0.2	0	0
79	18.9	15.4	34.4	7.6	1.1	0.1	0
80	24.5	18.4	52.8	23.3	6.6	0.4	0
81	19.7	9	2.2	0	0	0	0
82							
83	9	13.1	50.7	21.8	7.9	0.3	0
84	12.7	15.4	73.1	31.3	9.3	0.2	0.1
85	17.6	12.9	67.6	38.7	17.2	0.5	0.1
86	0.1	4.9	15.7	3.5	1	0.1	0
87	13.1	10.1	9.2	1	0.2	0	0.1

Table 19. JIA patient MTXPG profile

Patient	MTXPG concentration (nM)						
	MTXPG1	MTXPG2	MTXPG3	MTXPG4	MTXPG5	MTXPG6	MTXPG7
88	15.1	9.3	56.2	8.3	0	0	0
89	7.6	12.6	89.7	26	6.3	0.3	0
90	18	15.7	103.1	52.8	23.8	0.5	0
91	9.7	8.4	21.2	3.5	0.7	0	0
92	5.4	4.3	27.3	12.3	4.5	0	0
93	6	6.6	11.7	1.6	0.3	0	0
94	12.7	19.4	114.1	40.8	13.6		
95	19.6	14.6	42.9	7.6	1.3	0.2	0
96	28.2	19.2	63.3	12.4	2.3	0.2	0
97	17.9	11.2	87.1	61.6	39.8	0.7	0.2
98	23.1	9.5	26.2	5.9	1.2		
99	21.5	13.1	84.9	38.5	14.2	0.3	0
100	19.4	18	60	19.4	4.9	0.2	0
101	40.8	19	48	7.3	1.1	0	0

4.5   References

[1]   L. Stamp, R. Roberts, M. Kennedy, M. Barclay, J. O'Donnell, P. Chapman, The use of low dose methotrexate in rheumatoid arthritis--are we entering a new era of therapeutic drug monitoring and pharmacogenomics? , *Biomedecine & Pharmacotherapy.* **2006**, *60*, 678.

[2]   J. Swierkot, J. Szechinski, Methotrexate in rheumatoid arthritis. *Pharmacol Rep.* **2006**, *58*, 473.

[3]   A. V. Ramanan, P. Whitworth, E. M. Baildam, Use of methotrexate in juvenile idiopathic arthritis. *Arch Dis Child.* **2003**, *88*, 197.

[4]   H. Truckenbrodt, R. Hafner, Methotrexate therapy in juvenile rheumatoid arthritis: a retrospective study. *Arthritis Rheum.* **1986**, *29*, 801.

[5]   C. A. Wallace, The use of methotrexate in childhood rheumatic diseases. *Arthritis Rheum.* **1998**, *41*, 381.

[6]   A. Cespedes-Cruz, R. Gutierrez-Suarez, A. Pistorio, A. Ravelli, A. Loy, K. J. Murray, V. Gerloni, N. Wulffraat, S. Oliveira, J. Walsh, I. C. Penades, M. G. Alpigiani, P. Lahdenne, C. Saad-Magalhaes, E. Cortis, L. Lepore, Y. Kimura, C. Wouters, A. Martini, N. Ruperto, Methotrexate improves the health-related quality of life of children with juvenile idiopathic arthritis. *Ann Rheum Dis.* **2008**, *67*, 309.

[7]   J. L. Hillson, D. E. Furst, Pharmacology and pharmacokinetics of methotrexate in rheumatic disease: Practical Issues in Treatment and Design. *Rheumatic Disease Clinics of North America.* **1997**, *23*, 757.

[8]   M. Tishler, D. Caspi, E. Graff, R. Segal, H. Peretz, M. Yaron, Synovial and serum levels of methotrexate during methotrexate therapy of rheumatoid arthritis. *Br J Rheumatol.* **1989**, *28*, 422.

[9]   B. A. Chabner, C. J. Allegra, G. A. Curt, N. J. Clendeninn, J. Baram, S. Koizumi, J. C. Drake, J. Jolivet, Polyglutamation of methotrexate. Is methotrexate a prodrug? , *J Clin Invest.* **1985**, *76*, 907.

[10]   C. J. Allegra, J. C. Drake, J. Jolivet, B. A. Chabner, Inhibition of phosphoribosylaminoimidazolecarboxamide transformylase by methotrexate and dihydrofolic acid polyglutamates. *Proc Natl Acad Sci U S A.* **1985**, *82*, 4881.

[11]   J. E. Baggott, W. H. Vaughn, B. B. Hudson, Inhibition of 5-aminoimidazole-4-carboxamide ribotide transformylase, adenosine deaminase and 5'-adenylate deaminase by polyglutamates of methotrexate and oxidized folates and by 5-aminoimidazole-4-carboxamide riboside and ribotide. *Biochem J.* **1986**, *236*, 193.

[12]   L. Genestier, R. Paillot, L. Quemeneur, K. Izeradjene, J. P. Revillard, Mechanisms of action of methotrexate. *Immunopharmacology.* **2000**, *47*, 247.

[13]   F. M. Rubino, Separation methods for methotrexate, its structural analogues and metabolites. *Journal of Chromatography B: Biomedical Sciences and Applications.* **2001**, *764*, 217.

[14]   C.-Y. Kuo, H.-L. Wu, H.-S. Kou, S.-S. Chiou, D.-C. Wu, S.-M. Wu, Simultaneous determination of methotrexate and its eight metabolites in human whole blood by capillary zone electrophoresis. *Journal of Chromatography A.* **2003**, *1014*, 93.

[15]   M. Hroch, J. Tukova, P. Dolezalova, J. Chladek, An improved high-performance liquid chromatography method for quantification of methotrexate polyglutamates in red blood cells of children with juvenile idiopathic arthritis. *Biopharm Drug Dispos.* **2009**, *30*, 138.

[16]   T. Dervieux, D. Orentas Lein, J. Marcelletti, K. Pischel, K. Smith, M. Walsh, R. Richerson, HPLC determination of erythrocyte methotrexate polyglutamates after low-dose methotrexate therapy in patients with rheumatoid arthritis. *Clin Chem.* **2003**, *49*, 1632.

[17]   J. Salamoun, J. Frantisek, Determination of methotrexate and its metabolites 7-hydroxymethotrexate and 2,4-diamino-N10-methylpteroic acid in biological fluids by liquid chromatography with fluorimetric detection. *J Chromatogr.* **1986**, *378*, 173.

[18]   J. Salamoun, M. Smrz, F. Kiss, A. Salamounova, Column liquid chromatography of methotrexate and its metabolites using a post-column photochemical reactor and fluorescence detection. *J Chromatogr.* **1987**, *419*, 213.

[19]   H. Li, W. Luo, Q. Zeng, Z. Lin, H. Luo, Y. Zhang, Method for the determination of blood methotrexate by high performance liquid chromatography with online post-column electrochemical oxidation and fluorescence detection. *J Chromatogr B Analyt Technol Biomed Life Sci.* **2007**, *845*, 164.

[20]   B. A. Kamen, P. L. Takach, R. Vatev, J. Douglas Caston, A rapid, radiochemical-ligand binding assay for methotrexate. *Analytical Biochemistry.* **1976**, *70*, 54.

[21]   H. Schroder, E. M. Heinsvig, Enzymatic assay for methotrexate in erythrocytes. *Scand J Clin Lab Invest.* **1985**, *45*, 657.

[22]   H. Hayashi, C. Fujimaki, S. Tsuboi, T. Matsuyama, T. Daimon, K. Itoh, Application of fluorescence polarization immunoassay for determination of methotrexate-polyglutamates in rheumatoid arthritis patients. *Tohoku J Exp Med.* **2008**, *215*, 95.

[23] G. R. Krakower, P. A. Nylen, B. A. Kamen, Separation and identification of subpicomole amounts of methotrexate polyglutamates in animal and human biopsy material. *Analytical Biochemistry.* **1982**, *122*, 412.

[24] H. Schroder, K. Fogh, T. Herlin, In vivo decline of methotrexate and methotrexate polyglutamates in age-fractionated erythrocytes. *Cancer Chemother Pharmacol.* **1988**, *21*, 150.

[25] S. Eksborg, F. Albertioni, C. Rask, O. Beck, C. Palm, H. Schroeder, C. Peterson, Methotrexate plasma pharmacokinetics: importance of assay method. *Cancer Lett.* **1996**, *108*, 163.

[26] G. Chen, J. P. Fawcett, M. Mikov, I. G. Tucker, Simultaneous determination of methotrexate and its polyglutamate metabolites in Caco-2 cells by liquid chromatography-tandem mass spectrometry. *Journal of Pharmaceutical and Biomedical Analysis.* **2009**, *50*, 262.

[27] J. F. Gregory, 3rd, D. B. Sartain, B. P. Day, Fluorometric determination of folacin in biological materials using high performance liquid chromatography. *J Nutr.* **1984**, *114*, 341.

[28] E. P. Quinlivan, A. D. Hanson, J. F. Gregory, The analysis of folate and its metabolic precursors in biological samples. *Anal Biochem.* **2006**, *348*, 163.

[29] L. C. Garratt, C. A. Ortori, G. A. Tucker, F. Sablitzky, M. J. Bennett, D. A. Barrett, Comprehensive metabolic profiling of mono- and polyglutamated folates and their precursors in plant and animal tissue using liquid chromatography/negative ion electrospray ionisation tandem mass spectrometry. *Rapid Commun Mass Spectrom.* **2005**, *19*, 2390.

[30] C. S. Elmore, D. C. Dean, Y. Zhang, C. Gibson, H. Jenkins, A. N. Jones, D. G. Melillo, Synthesis of methotrexate and 7-hydroxymethotrexate. *Journal of Labelled Compounds and Radiopharmaceuticals.* **2002**, *45*, 29.

[31] T. Dervieux, D. Furst, D. O. Lein, R. Capps, K. Smith, M. Walsh, J. Kremer, Polyglutamation of methotrexate with common polymorphisms in reduced folate carrier, aminoimidazole carboxamide ribonucleotide transformylase, and thymidylate synthase are associated with methotrexate effects in rheumatoid arthritis. *Arthritis Rheum.* **2004**, *50*, 2766.

[32] J. M. Dalrymple, L. K. Stamp, J. L. O'Donnell, P. T. Chapman, M. Zhang, M. L. Barclay, Pharmacokinetics of oral methotrexate in patients with rheumatoid arthritis. *Arthritis Rheum.* **2008**, *58*, 3299.

**Chapter 5: LC/MS/MS analysis of (7OH-)Methotrexate Polyglutamates
in a Clinical Environment**

Chapter 5: LC/MS/MS analysis of (7OH-)Methotrexate Polyglutamates in a Clinical Environment

Table of Contents

List of Figures

List of Tables

5.1   Introduction

In chapter 4 a novel LC/MS/MS method for the detection of MTXPGs in human erythrocytes was presented[1]. Whilst the performance of the method was adequate for reliable analysis of a limited amount of patient RBC samples in an academic research setting, the throughput of the entire analytical procedure is too low for routine operation in a clinical environment. First, the method relied on a laborious sample preparation strategy using multiple clean-up stages. In an initial work up step the sample was exposed to perchloric acid to facilitate protein precipitation and release MTXPGs from the biological matrix. As a result the pH and ionic strength of this solution were incompatible with the RP-IP chromatographic method. Furthermore the high ionic strength of the sample was also problematic for mass spectrometric detection, and as a result a lengthy SPE desalting procedure was incorporated. A multistep sample preparation is undesirable in a clinical environment as it significantly increases the chance of error. As errors are unavoidably introduced in every operation, the total error is a reflection of the error introduced by the individual components. Additionally complicated sample preparation schemes are prone to gross error introduced by the laboratory operator. A single and simple sample preparation procedure is therefore of high interest by the clinical laboratory.

The second disadvantage of the method presented in chapter 4 is that as a result of the use of N,N-dimethylhexylamine as an ionparing agent in the mobile phase cross talk between the various SRM channels was observed. Since DMHA is isobaric with the addition of a glutamate residue, the $MTXPG_n$ + DMHA adduct will cause crosstalk in the higher order $MTXPG_{n+1}$ SRM channel. In the previous chapter it was hypothesized that the use of an IP-agent with a differentiating mass would eliminate this adverse effect.

The use of N,N-dimethylpentylamine (DMPA) and N,N-dimethylheptylamine (DMHPA) were suggested as examples of such compounds. Additionally the elimination of crosstalk would negate the need for baseline separation as the various MTXPGs could be separated in the gas phase. A shortened chromatographic procedure is of great clinical interest as it would increase throughput and reduce the occupancy of the procedure on costly equipment (e.g. mass spectrometers).

A third disadvantage of the method is that due to the lack of a suitable internal standard external calibration was performed. The use of external calibration in the analysis of samples from biological samples by LC/MS/MS is undesirable since it does not account for signal alterations (ion suppression) induced by a varying matrix composition (matrix effects). In this chapter the various aspects of the assay that need to be altered to facilitate clinical MTXPG methodology are investigated and discussed. Improvements are presented in sample preparation, chromatographic and calibration procedures.

Additionally the question was raised if the MTX metabolite, 7OH-MTX could be measured and observed in RBCs. A pair of reports by Baggott et al. demonstrate the presence of 7OH-MTX in the urine of RA patients on MTX therapy[2-3]. The urine concentration of 7OH-MTX was found to be highly variable (14 fold) over a small patient population and it was hypothesized that patients that extensively catabolize MTX to 7OH-MTX would have a less efficacious response to MTX therapy. The researchers continue and hypothesize that based on a small amount of data a phenotype exists that is able to produce large amounts of 7OH-MTX. Since the metabolite is also subject to polyglutamation by polyglutamaylsynthase, this metabolite would be competing with MTX, limiting its polyglutamation and therefore enhancing MTX excretion. Finally the

researchers hypothesize: *"The variability of MTXPGs concentrations in RBCs could be a function of MTX catabolism to 7OH-MTX; 7-OH-MTX could also displace MTX from the active site of other folate metabolizing enzymes"* (quote).

Interestingly it has been demonstrated that concentrations of 7OH-MTX in the bone marrow are about 3-10 times higher in children receiving low-dose oral MTX[4]. As the RBCs develop in the bone marrow and are metabolic inactive after erythropoiesis[5], these cells are considered to be representative of the (anti)-folate status within the bone marrow[6-7]. Therefore it is tempting to believe 7OH-MTX is present in RBCs, and if so, is there a correlation between interpatient MTXPG variability and the ability of these patients to catabolize MTX to 7OH-MTX?

The presence and detection of 7OH-MTX in its native or polyglutamated form in human erythrocytes has not been described in the literature. The detection of this class of MTX metabolites is complicated by the fact that 7OH-MTX is available on a limited commercial basis and the family of polyglutamates cannot be purchased from a commercial source. At the end of this chapter a strategy is presented for the detection of 7OH-MTXPGs in human RBCs. The focus of the assay was to answer the question: is 7OH-MTX(PGs) present in significant levels in RBCs? Rather than presenting a full quantitative assay that would require the synthesis of the various standards, this chapter presents a semi-quantitative approach. The development of a more quantitative approach would be the obvious next step if RBCs were found to be a suitable biomarker for this biotransformation.

5.2 Experimental

5.2.1 Materials

LC grade solvents acetonitrile (ACN) and methanol (MeOH) were obtained from Fisher Scientific (Fair Lawn, NJ, USA). Ammonium bicarbonate, N, N-Dimethylpentylamine (DMPA), N, N-Dimethylhexylamine (DMHA), N,N-Dimethylheptylamine (DMHPA) and methotrexate were purchased from Sigma-Aldrich (St Louis, MO, USA). Methotrexate polyglutamation standards 4-amino-10-methylpteroyldiglutamic acid ($MTXGlu_2$), 4-amino-10-methylpteroyltriglutamic acid ($MTXGlu_3$), 4-amino-10-methylpteroyltetraglutamic acid ($MTXGlu_4$), 4-amino-10-methylpteroylpentaglutamic acid ($MTXGlu_5$), 4-amino-10-methylpteroylhexaglutamic acid ($MTXGlu_6$), 4-amino-10-methylpteroylheptaglutamic acid ($MTXGlu_7$) were purchased as the ammonium salts from Schircks Laboratories (Jona, Switzerland). 7-hydroxymethotrexate (7OH-MTX) was obtained from Synfine Research (Ontario, Canada).

5.2.2 Preparation of erythrocyte (RBC) lysates

Blood samples (~5 ml) obtained from patients were centrifuged at low speed (2000 rpm) in a Beckman tabletop centrifuge to pellet the RBCs. After recovery of the plasma, the RBCs were suspended in an equal volume of sterile normal saline, mixed by gentle inversion and subjected to a second low speed centrifugation. The supernatant was discarded and the wash procedure was repeated a second time. After discarding

142

the supernatant, the packed RBCs were divided into four aliquots and stored at -70°C until use.

5.2.3 Sample preparation for LC-MS/MS analysis

Packed RBCs obtained from patients were thawed prior to sample workup and analysis. A 200 μL aliquot was transferred into a plastic vial and subsequently 200 μL of a modified "Wilson and Horne" extraction buffer was added to ensure complete lysis of the red blood cells. The buffer was a 50 mM HEPES/CHES buffer at pH 7.85. The vial was closed and vortexed for 10 seconds yielding a suspension. The closed vials were placed in the in-house fabricated sample holder (chapter 2) and "sandwiched" to lock the lids. The entire sample holder was placed in boiling water for 5 minutes and after removal from the waterbath allowed to cool for 30 minutes. The boiled vials were placed into a centrifuge and spun at 13,000 RPM for 5 minutes. The supernatant was transferred to an auto-sampler vial with 250 μL liner.

5.2.4 Preparation of standards

Methotrexate (polyglutamation) standards were dissolved in 100 mM NH_4HCO_3 buffer. Individual standards were combined and diluted to generate stock solutions containing each of the standards at a concentration of 1 μM, 100 nM and 10 nM. Stock solutions were stored at -80 °C and prepared on weekly basis. In order to validate the method six-point calibration plots were constructed by analyzing methotrexate (polyglutamation) standards with concentrations of: 0, 1, 5, 10, 50, 100 nM. These

standards were prepared by spiking the appropriate volume of stock solution in 200 μL of blank RBCs obtained from healthy individual RBC donors. A seven-point calibration (0, 0.5, 1, 5, 10, 50, 100 nM) was performed for the analysis of patient samples. The calibration standards were treated the same as patient samples, with the exception that the volume of water used to lyse the cells was lowered by the volume of stock solution used to spike the calibration standard.

5.2.5 Liquid Chromatography with MS detection

Solvent was delivered by a Waters Acquity UPLC. A Waters Acquity UPLC was equipped with a 50 μL loop and 250 μL sample syringe. Strong needle wash consisted of 70% MeOH: 30% H_2O, weak needle consisted of 5% MeOH: 95% H_2O. Separation occurred on a 50 x 1.00 mm Waters BEH C18, packed with 1.7 μm particles. The column was guarded by a Waters Vanguard pre-column, 2.1 x 5 mm. The mobile phase consisted of (A) 10 mM NH_4HCO_3 buffer with 5 mM of the desired ion-pair adjusted to pH 7.5 with HCO_2H, (B) consisted out of ACN with 5mM of the desired ion-pairing agent. The total flow rate was set to 200 μL/min. Various gradient elution profiles were used, the details are given in the text. Re-equilibration occurred by a step gradient to initial conditions followed by a equilibration time of 2 minutes.

5.2.6 Mass Spectrometry

Instrumentation was a Micromass Quattro Ultima "triple" quadrupole mass spectrometer (Manchester UK) equipped with an electrospray ionization source. The

instrument was operated in positive ion mode. Source parameters, including the cone voltage for each analyte were optimized by maximizing the area under the curve of multiple LC runs of the standard mixture at various programs. The probe capillary was optimized at 3.0kV, and the desolvation and source temperatures were set to 400 °C and 125 °C, respectively. The cone voltage was optimized by maximizing the area under the curve for each individual analyte by repetitive IP-LC runs varying the cone voltage. The cone gas flow rate was optimized at 80L/hr, the desolvation and nebulizer gas flow rate was adjusted for maximum signal of analyte. Argon was used for collision induced dissociation (CID) and the cell vacuum was set at 2.4 x 10^{-3} mbar. Q1 and Q3 were set to transmit ions with a resolution of 0.8 u FWHH. Multiple Reaction Monitoring (MRM) parameters (table 20) including precursor ions, product ions and collision energy were optimized by direct infusion of the individual analytes dissolved in 80% A and 20% B at 10 µM, closely resembling chromatographic conditions.

Table 20. MRM parameters used for the LC/MS/MS analysis of the various pteroyl based entities.
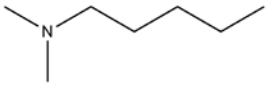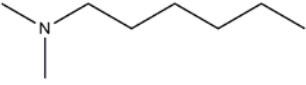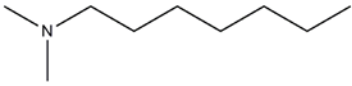
Analyte	Molecular Formula	Precursor ion (m/z)	Product ion (m/z)	Cone Voltage (V)	Collision Energy (V)	ESI mode
MTXGlu$_1$	$C_{20}H_{23}N_8O_5+$	455.2	308.1	20	20	+
MTXGlu$_2$	$C_{25}H_{31}N_9O_8+$	584.3	308.1	20	26	+
MTXGlu$_3$	$C_{30}H_{39}N_{10}O_{11}+$	713.3	308.1	20	33	+
MTXGlu$_4$	$C_{35}H_{47}N_{11}O_{14}+$	842.3	308.1	20	40	+
MTXGlu$_5$	$C_{40}H_{55}N_{12}O_{17}+$	971.3	308.1	20	48	+
MTXGlu$_6$	$C_{45}H_{63}N_{13}O_{20}+$	1100.4	308.1	20	56	+
MTXGlu$_7$	$C_{50}H_{71}N_{14}O_{23}+$	1229.4	308.1	20	64	+
7OH-MTX	$C_{20}H_{23}N_8O_6+$	471.1	324.3	15	20	+
7OH-MTX	$C_{20}H_{21}N_8O_6-$	469.1	340.1	25	24	-
7OH-MTXGlu$_2$	$C_{25}H_{29}N_8O_9-$	598.1	340.1	30	31	-
7OH-MTXGlu$_3$	$C_{30}H_{37}N_8O_{12}-$	727.2	451.1	40	32	-
7OH-MTXGlu$_4$	$C_{35}H_{45}N_8O_{15}-$	856.2	451.1	50	37	-
7OH-MTXGlu$_5$	$C_{40}H_{53}N_8O_{18}-$	985.3	451.1	55	45	-
7OH-MTXGlu$_6$	$C_{45}H_{61}N_8O_{21}-$	1114.4	451.1	60	50	-
7OH-MTXGlu$_7$	$C_{50}H_{69}N_8O_{24}-$	1243.4	451.1	70	59	-
FA	$C_{19}H_{20}N_7O_6+$	442.2	295.1	30	20	+
FAGlu$_2$	$C_{24}H_{28}N_7O_9+$	571.2	295.1	30	26	+
FAGlu$_3$	$C_{29}H_{36}N_7O_{12}+$	700.2	295.1	30	33	+
FAGlu$_4$	$C_{34}H_{44}N_7O_{15}+$	829.3	295.1	30	40	+
FAGlu$_5$	$C_{39}H_{52}N_7O_{18}+$	958.3	295.1	30	48	+
FAGlu$_6$	$C_{44}H_{60}N_7O_{21}+$	1087.4	295.1	30	56	+
FAGlu$_7$	$C_{49}H_{68}N_7O_{24}+$	1216.4	295.1	30	64	+
FA	$C_{19}H_{18}N_7O_6-$	440.2	311.1	25	24	-
FAGlu$_2$	$C_{24}H_{26}N_7O_9-$	569.2	311.1	30	31	-
FAGlu$_3$	$C_{29}H_{34}N_7O_{12}-$	689.2	422.3	40	32	-
FAGlu$_4$	$C_{34}H_{42}N_7O_{15}-$	827.3	422.3	50	37	-
FAGlu$_5$	$C_{39}H_{50}N_7O_{18}-$	956.3	422.3	55	45	-
FAGlu$_6$	$C_{44}H_{58}N_7O_{21}-$	1085.4	422.3	60	50	-
FAGlu$_7$	$C_{49}H_{66}N_7O_{24}-$	1214.4	422.3	70	59	-

5.3   Results and Discussion

5.3.1 Column selection

As described in Chapter 4, the Waters UPLC platform, including autosampler with peak needle had to be utilized to avoid carry-over of the longer chain polyglutamates. The UPLC pumps can generate up to 15,000 psi of pressure, which allows chromatographers to overcome the high backpressures associated with the use of small particles. The use of chromatographic columns packed the stationary phase dispersed in small particles is highly advantages in chromatography as it minimizes chromatographic band broadening associated with using high linear velocities. These high linear velocities are desirable in chromatography as they minimize gradient delay and allow for swift separation of the analytes. As the goal of this chapter was the development of a MTXPG LC/MS/MS assay with increased throughput tailored for clinical use, these small particle chromatography columns in combination with the UPLC demonstrate tremendous potential. In an attempt to use the UPLC to its fullest potential the method was transferred to a Waters 1.7 µm BEH C18 column. This column was selected due to its close resemblance to the previously used Phenomenex material, in an attempt to minimize change in retention/separation mechanism. The BEH columns are based on a trifunctional ligand bonding chemistry, resulting in elevated stabilities in basic media (up to pH 11). Due to the relatively high pH of the separation (pH 7.5 - 8.0) this extra stability in the basic pH range is desirable if one wishes to operate this assay on a day to day basis handling a large amount of samples and automated data handling requiring fixed retention times. The exact method transfer will be discussed in the following sections.

5.3.2 Ion-pair selection

Chemical Structure	Name and abbreviation	Mono isotopic mass	Boiling point
	N,N-dimethylpentylamine (DMPA)	115.14 Da	120 °C[1]
	N,N-dimethylhexylamine (DMHA)	129.15 Da	146-147 °C
	N,N-dimethylheptylamine (DMHPA)	143.17 Da	170 °C[1]

[1]Approximate values obtained by extrapolation, using the boilingpoints of N,N-dimethylbutylamine and N,N dimethylhexylamine

Figure 34. *Properties of the various ion-pair reagents evaluated for LC/MS/MS analysis of MTXPGs.*

As mentioned in the introduction N,N-dimethylpentylamine (DMPA) and N,N-dimethylheptylamine (DMHPA) were evaluated as alternatives to DMHA in an attempt to eliminate crosstalk between the various MTXPG channels (figure 34). DMPA varies from the previously used DMHA by a one carbon shorter alkyl-chain, resulting in a lower boiling point and less hydrophobic character. The inverse is true for DMPHA. A low boiling point of the IP-agent is generally considered to be advantageous in IP-mass spectrometry, since milli-molar concentrations in the mobile phase need to be desolvated and evaporated by the ESI-source. The lower boiling DMPA is however significantly less hydrophobic compared to DMHPA. The hydrophobicity of the IP-agent plays an important role in RP-IP chromatography, as the IP-agent has to dynamically load the hydrophobic chromatographic media. This process is driven by the equilibrium constant between the IP-agent and the hydrophobic solid support. In other words, a more hydrophobic IP-agent will be present at a higher concentration on the solid phase

and therefore introduce more chromatographic selectivity in the separation method (if mobile phase concentration is kept constant). To conclude, the ideal IP-agent from a mass spectrometric point of view would be DMPA → DMHA → DMHPA, and from a chromatographers stand point DMHPA → DMHA → DMPA (disregarding the crosstalk when DMHA is used). In order to identify the ideal IP-agent chromatograms were obtained by analyzing 100 nM aqueous mixtures of $MTPG_{1-7}$. The concentration of the IP in the mobile phase was fixed to 5 mM independent of the IP-agent used. A concentration of 5 mM DMHA was found to be optimal by Garrett and colleagues[8] for the separation of folate polyglutamates, and further optimization was not attempted. Note that this concentration is typically one to two orders of magnitude below of commonly used IP concentrations in LC-UV/FL type of assays, due to adverse effect in ESI at elevated concentrations. Isocratic separations of $MTXPG_{1-7}$ with DMPA (figure 35A), DMHA (figure 35B) and DMHPA (figure 35C) are demonstrated in figure 35. In accordance with the hypothesis, it was observed that DMPA demonstrated the lowest selectivity factor (i.e note the separation of the various analytes) and analytes were retained fairly poorly, requiring only 10% organic for an isocratic separation of all of the analytes within a time-frame of 10 minutes. DMHPA demonstrated the highest selectivity factor of the IP-agents under investigation, and yielded the sharpest and most symmetrical peaks. A gradient separation was developed for both IP-agents with an emphasis on achieving rapid separation (figure 36). A gradient separation of $MTXPG_{1-7}$ using DMPA as IP agent is show in figure 36A. The gradient consisted out of an isocratic hold of 10%B for 1 minute in order to focus the analytes on the head of the chromatography column.

Figure 35. *Isocratic separations of aqueous mixtures of MTXPGs demonstrating selectivity differences between the ion pair reagents. Each chromatogram is obtained with the IP concentration fixed at 5 mM. (A) Separation obtained with DMPA, (B) Separation obtained with DMHA, (C) Separation obtained with DMHPA.*

The isocratic hold was followed by a linear gradient with a steepness of 1.8% min^{-1} increase in B concentration. Using these settings, analytes were separated in a timeframe of 3.5 minutes following analyte introduction. A gradient program was also developed for the separation of $MTXPG_{1-7}$ with DMHPA as the IP agent (figure 36B). The initial analyte focusing step that was required using DMPA as IP agent could be circumvented by using a weak mobile phase composition (but still higher eluting strength when compared to DMPA) during injection (17.5% B), followed by a "ballistic" gradient of 8% min^{-1} increase in B concentration. The high selectivity factor observed in the assay with DMHPA as IP-reagent results in a baseline separation of aqueous $MTXPG_{1-7}$ within 2.5 minutes. Again peaks were sharper using DMHPA as the IP agent under gradient conditions. The signal to noise ratio was also more favorable for (MRM) signals obtained from a 100 nM $MTXPG_{1-7}$ mixture, probably as a result of the beneficial effects obtained by the increased organic modifier strength required for timely elution of the MTXPGs (note signal intensities in figure 36A and B). The expected negative effect using DMHPA upon MS-ionization was not observed, but could be disguised by the increase in modifier strength. Nevertheless the effect can be neglected and chromatographic advantages obtained using DMHPA outweigh other considerations.

Whilst the timeframe separation time of 2.5 minutes for the seven MTX metabolites was desirable from the throughput perspective, chromatographic peaks widths became narrow and challenged the data acquisition rate of the Ultima mass spectrometer (note the beveled peaks in figure 36). It was found that the average amounts of scans during the peak was about 5 (figure 37A), where a minimum amount of 9 datapoints through the peak is generally considered to adequate.
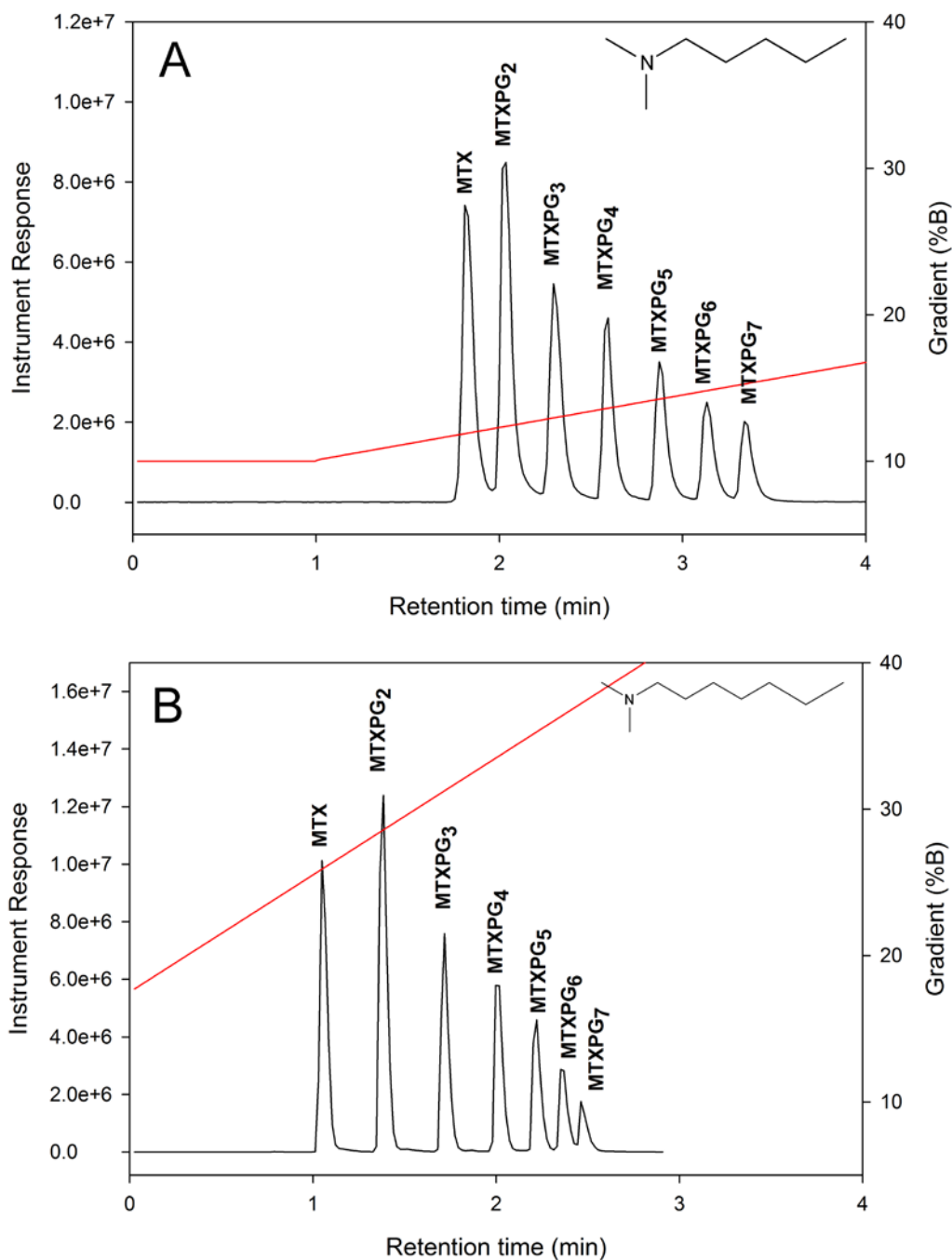
Figure 36. *Gradient profiles used to achieve a fast separation of the various MTXPGs. The gradient steepness is illustrated by the redline. (A) Gradient separation using DMPA. (B) Gradient separation using DMHPA. (note the differences in gradient steepness).*
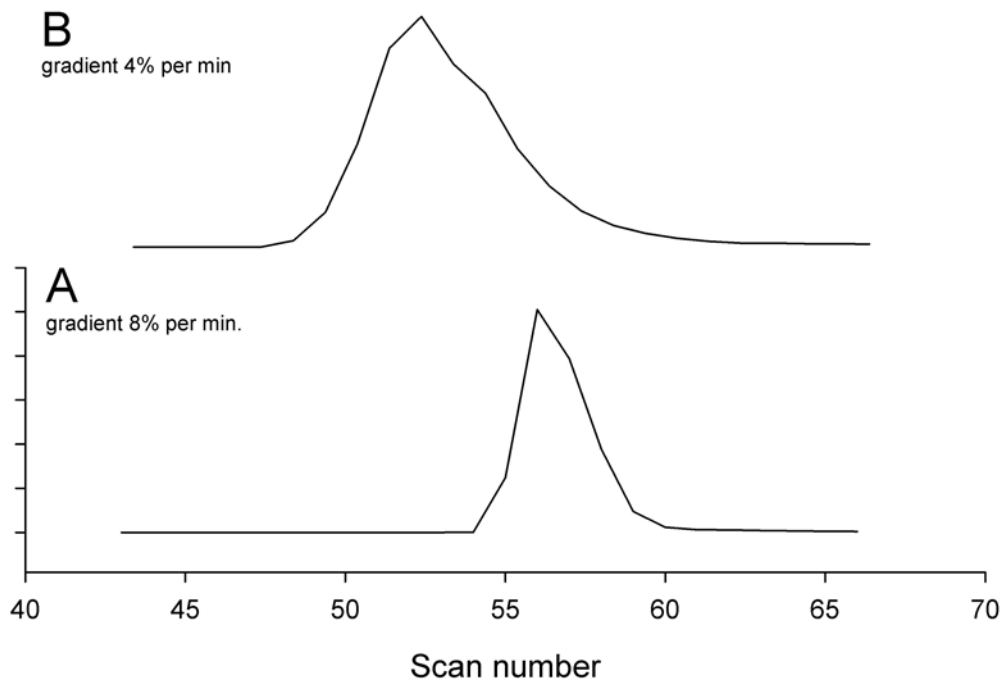
Figure 37. *Width of the MTX peak in the chromatogram based on a "scan number" axis, illustrating the number of datapoints through the chromatographic peak.*

The amount of scans through the peak could be increased by slowing the "ballistic" gradient down to a more moderate 4% change in B per min (figure 37B). The more shallow gradient doubled the amount of scans through the peak, allowing for about 10 scans through the peak. As a consequence the analysis time was increased to 4.5 minutes per sample (figure 38F). Whereas the scan rate of the Waters Ultima triple quadrupole mass spectrometer is the bottle neck for sample throughput in this procedure, the current generation of modern mass spectrometers have shorter cycle times and will be able to operate under the more demanding rapid elution conditions. As a result there is a tremendous increase in the data acquisition rate and thus these type of detectors would for the fast separations presented earlier.
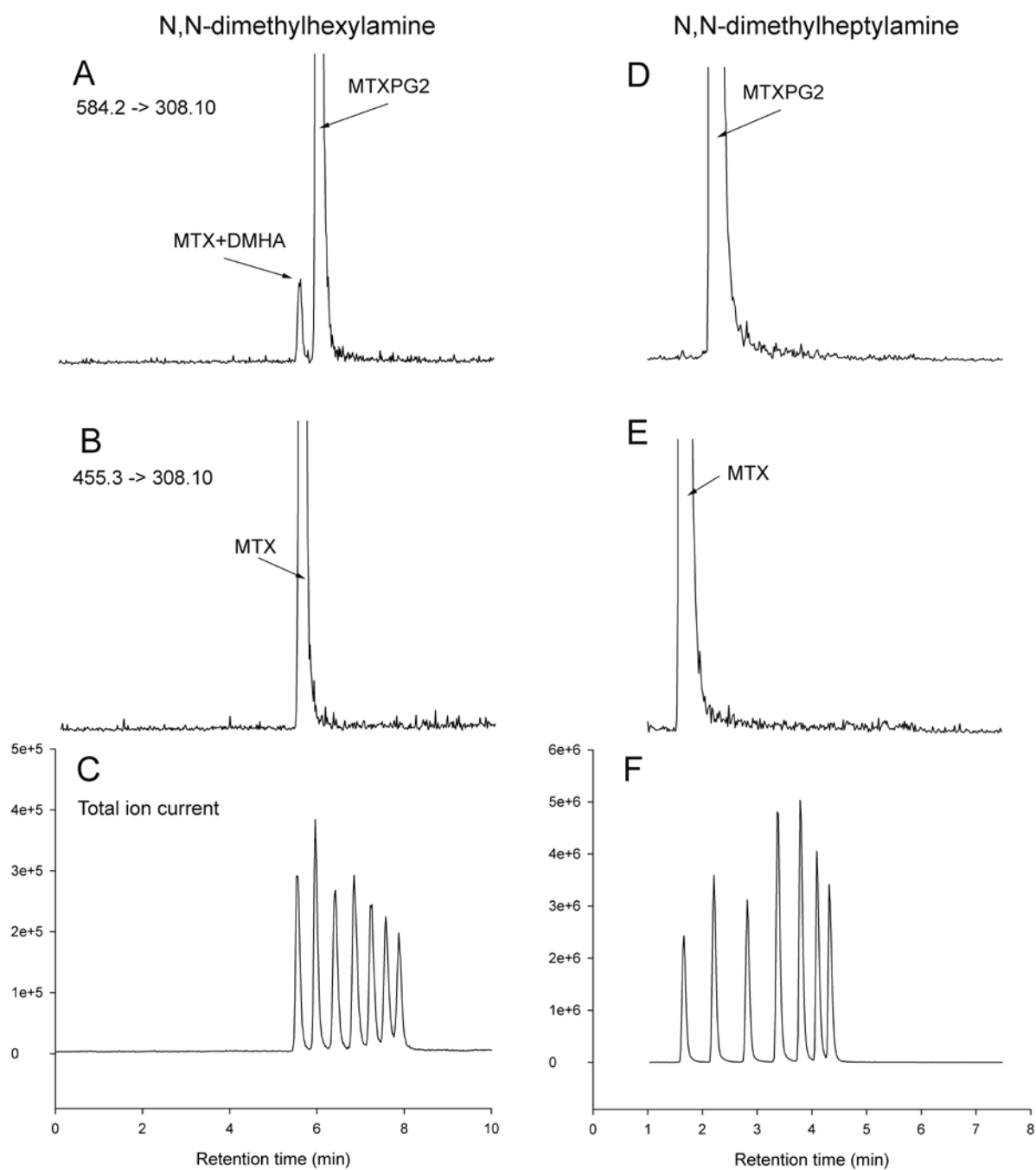
Figure 38. Illustration of crosstalk between the various SRM channels. (A) MTX DMHA adduct appears in MTXPG$_2$ MRM channel. (B) MTX channel, (C) TIC using DMHA as ion-pair reagent. (D) Using DMHPA no signal is generated by the lower MTX SRM channel. (E) MTX channel, (F) TIC using DMPHA as the ion-pair reagent.

With the establishment of DMHPA as the preferred IP-agent, the effect of adduct formation on the LC/MS/MS assay using MRM monitoring was investigated. The DMHA method demonstrated crosstalk from a $MTXPG_n$ channel (figure 38B) in the "next" $MTXPG_{n+1}$ channel (figure 38A). As hypothesized this interference due to adduct formation was not observed once DMHPA was used as the IP reagent (figure 38D, E). It can therefore be concluded that when analyzing sequential metabolites (in this case polyglutamates), the mass of the IP-agent in LC/MS/MS should not be isobaric with the molecular change of the analyte due to metabolism.

5.3.3 Sample preparation

A major drawback of the MTXPG analysis method presented in chapter 4 was the laborious procedure required to render the biological sample into a solution that could be introduced into the chromatograph. Chapter 4 describes the various strategies that had been explored in order to obtain a viable sample preparation strategy. All strategies explored as alternatives to the acid protein precipitation followed by SPE extraction were found to be ineffective. However, heat extraction, a sample preparation strategy that was applied successfully in G5-MTX-FA analysis was not explored. Additionally heat extraction has been presented in prior literature to extract various folate(polyglutamates) from a number of tissues at pH 7.85 [9-10]. The fact that MTXPGs are structural analogues of folatePGs suggests this technique could be useful for the extraction of MTXPGs in a simple step. An extraction in a single step at physiological pH would be highly desirable in this IP-LC/MS/MS analysis procedure as it would result in a mobile phase compatible sample that could be directly inject able into the HPLC system without

the need for additional sample workup. The heat extraction of folates requires a very specific buffer, consisting of ascorbic acid as the anti-oxidant, mercaptoethanol to scavange formaldehyde released by ascorbic acid, and a HEPES/CHES buffer system that fixes the pH at 7.85. In the field of folate analysis commonly referred to as the "Wilson and Horne" buffer, named after the scientists that demonstrated the effectiveness of this buffer system for the stabilization of folate extracts (more about this buffer system will be presented in chapter 7). Since MTXPGs are more (redox) stable compared to the various folates, a modified buffer was explored where ascorbic acid and mercaptoethanol were excluded from the buffer. This buffer proved to be successful for the extraction of MTXPGs from RBCs. Overall recovery based on a limit study (n=1) appears to be around 60% for the individual MTXPGs, similar to acid mediated extraction.

A full validation is presented in the next section of this chapter, demonstrating the reproducibility of this procedure.The advantage of the presented heat extraction procedure is the fact that protein bound analytes are liberated and proteins are precipitated simultaneously in one operation. After centrifugation a clear, sometimes slightly red supernatant (figure 39C, D) can be recovered and injected into the chromatograph without any deterioration in chromatographic of the analytical column for several hundreds of injections (guard columns were changed at 100 injection intervals, due to a slight increase in backpressure). The pH of the extraction solution was found to be important parameter to control, if the pH differentiated significantly from 7.85 a blackish slurry was obtained upon heat extraction (figure 39A, E). The slurry could not be separated by centrifugation and is obviously incompatible with HPLC/UPLC systems (figure 39B, F).
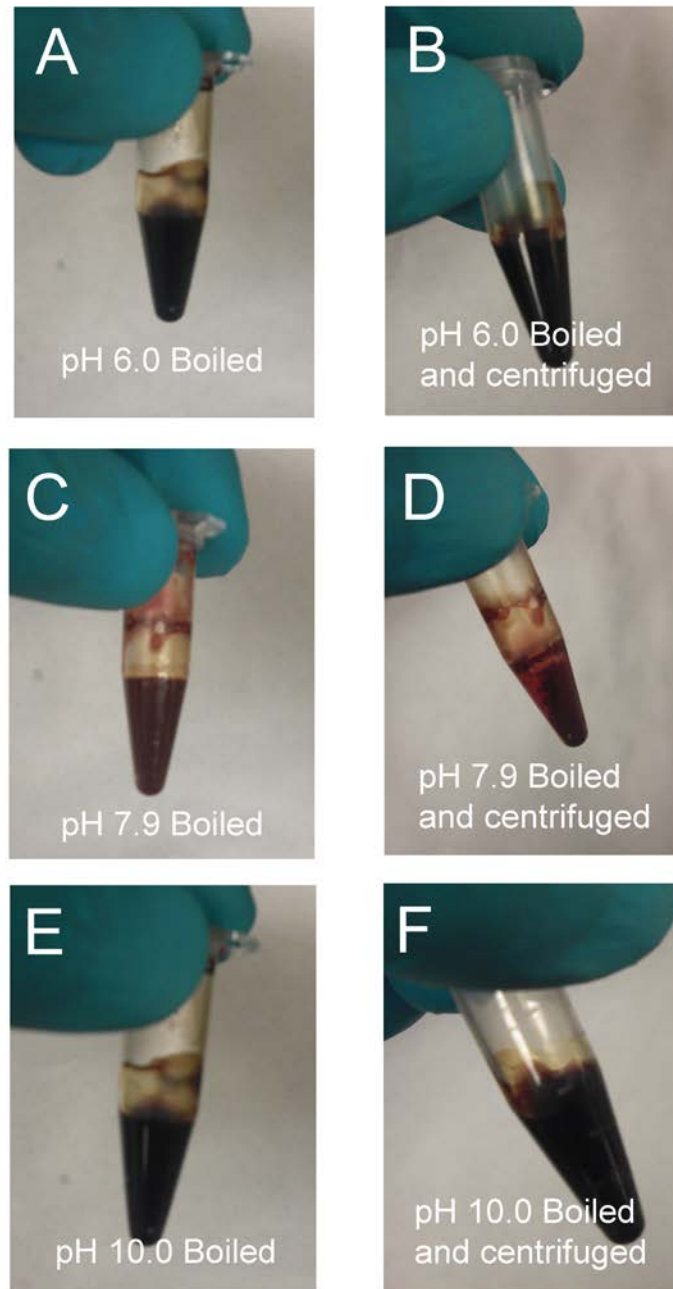
Figure 39. *The influence of the pH during sample preparation (boiling). An aliquot of 200 μL of RBCs were combined with 200 μL of buffer. (A) A solution with a pH of 6.0 was boiled, leading into a blackish sludge. (B) The sludge could not be separated by centrifugation. (C) Boiling at pH 7.85 leads to reddish "pudding". (D) Centrifugation lead to separation, with the debris at the bottom the vial. (E) Boiling at pH 10.0 lead to similar results as pH 6.0, forming a sludge. (F) Again the sludge could not be separated.*

5.3.4 Selection of internal standards

The validation results presented in chapter 4 for the MTXPG LC/MS/MS method revealed a precision that was in general between 10-15%, approaching the acceptable limits set by FDA guidelines for a bioanalytical assay[11]. It was therefore hypothesized that calibration relative to an internal standard could result in a reduction of the analysis error (i.e. improvement of the precision) and therefore would be beneficial. Furthermore the sample preparation approach presented in this chapter lacks the additional cleanup step provided by SPE extraction, making this faster and easier method more susceptible to matrix effects. The magnitude of suppression of the ion formation due to matrix effects was assessed by post column infusion of an aqueous MTXPG$_{1-7}$ solution. During the infusion a representative, (blank) boiled RBC extract was injected in the chromatographic system and the change in signal intensity was monitored throughout the gradient elution profile. Ion suppression due to endogenous components in the worked up RBC matrix will result in a reduction of the analyte signal (figure 40A) (For a review on these techniques please refer to Annesley[12].). RBC samples from different individual donors (n=5) were analyzed using this strategy. A chromatographic window (between 4-5 minutes) was identified that demonstrated significant ion-supression, affecting the analysis of MTXPG$_1$ and MTXPG$_2$. (figure 40A and B, red area) (Please note that these experiments were conducted using a significantly slowed gradient, improving resolution aiding in the visualization of the areas of interest). The longer chain MTXPGs$_{3-7}$ eluted in a chromatographic window where signal intensity was relatively stable and did not seem to be affected by matrix effects in any of the RBC samples screened (figure 40A and B, green area).
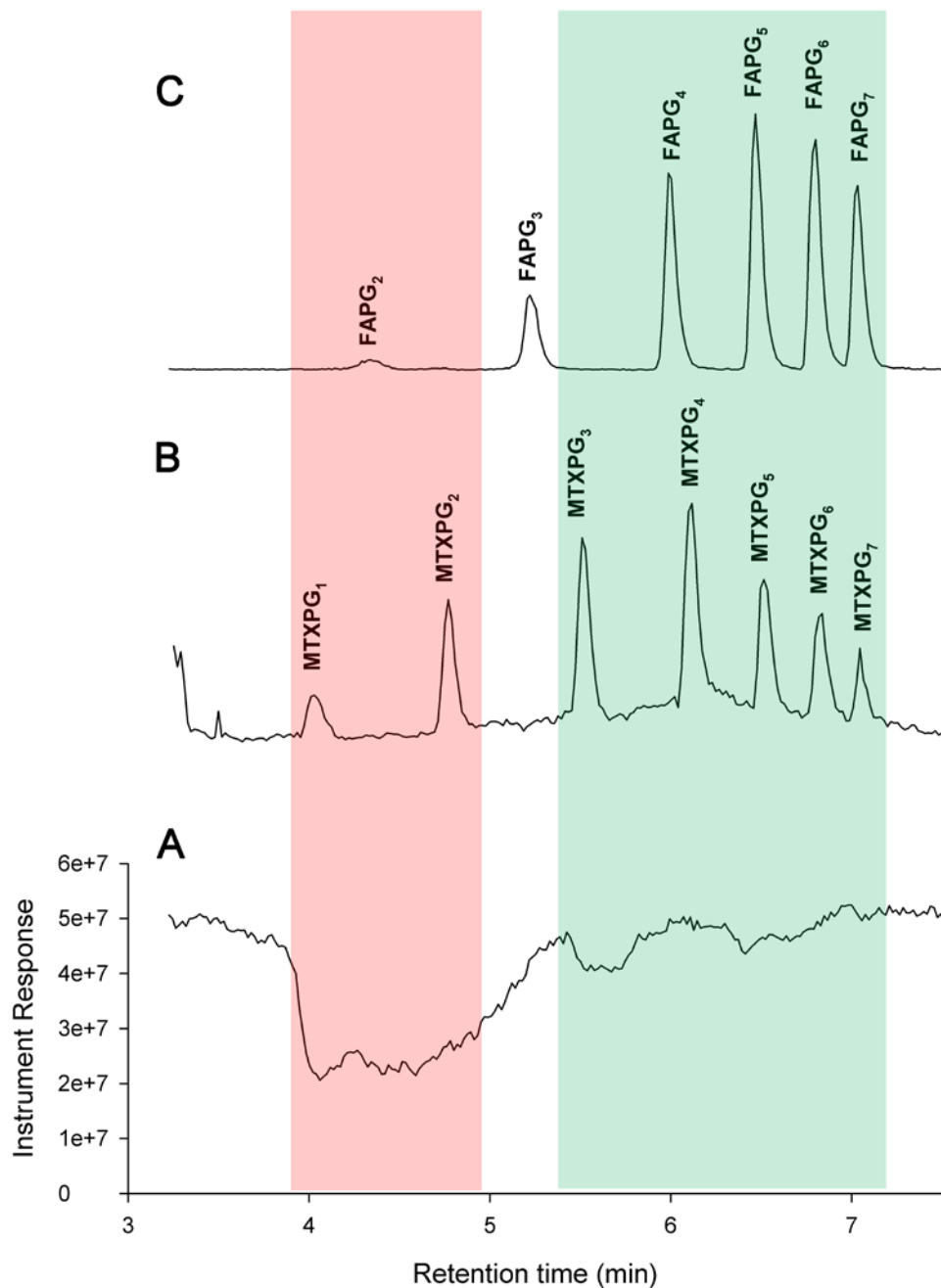
Figure 40. *The influence of matrix effects on the quantitation of MTXPGs. (A) a constant infusion of MTXPGs$_{1-7}$. Dips in the signal are indicative of suppression of ion formation. (B) MTXPGs enriched RBC extract. (C) Separation of aqueous FAPGs standards allowing for retention time comparison. The red area illustrates a part of the chromatogram where matrix effects were observed. The green part illustrates a relatively unaffected part of the chromatogram.*

As discussed earlier, the use of isotopically labeled internal standards mimicking the structure of the analytes is a hallmark in bio-analytical mass spectrometry[13]. However obtaining and synthesizing these internal standards is not always trivial, as is the case for MTXPGs. Synthesizing a deuterated (d_3) version of MTX is for instance more complicated than one would expect at a first glance[14], and the complexity increases rapidly as the polyglutamates are required as well. Based on the observed ion suppression pattern it was hypothesized that the assay would benefit from the incorporation of minimally two internal standards; one internal standard representative of the suppressed chromatographic window affecting MTX and $MTXPG_2$, and another internal standard serving the more stable signal area of the chromatogram where $MTXPG_{3-7}$ are eluting.

Since the elution window of MTX and $MTXPG_2$ is the most extensively effected, an isotopically labeled standard for these analytes would be highly desirable. As d_3-MTX is commercially available and d_3-$MTXPG_2$ is not, d_3-MTX was purchased and used as in internal standard for both MTX and $MTXPG_2$. The remaining polyglutamates ($MTXPG_{3-7}$) are in a relatively stable region of the chromatogram, justifying the use of a pseudo internal standard. Folic acid is available in its polyglutamates commercially and several reports suggest that FA in its native or polyglutamate is absent in RBCs. Assuming there is no endogenous background of FAPG(s) this series would be a good candidate to serve as a internal standard due to its related structure to MTX. As a result of the chromatographic methods selectivity towards increasing anionic character with increasing polyglutamate chainlenght, the longer chain FAPGs(4-7) eluted closely to the MTXPGs(4-7) (figure 40, B and C). Since $MTXPG_{3-7}$ are in a relatively clean area of the

160

chromatogram, (i.e. free from ion suppression) $FAPG_4$ was selected to serve as internal standard for $MTXPG_{3-7}$.

In order to check if FAPGs are present endogenously within RBC cells, RBCs from various donors (n=10) were screened for FAPGs (figure 41B, C, D). A number of RBC donors showed the presence of $FAPG_{5-7}$, in contrast to what various publications suggest (measuring deglutamated FA). The highest concentrations measured were however low and $FAPG_4$ was not detected in any samples, suggesting that this molecule was suitable for use as an internal standard. An additional safety level was however added to the method by fixing the concentration of $FAPG_4$ at a slightly elevated level (50 nM) to negate effects of unexpected low endogenous concentrations of $FAPG_4$.

Today, validation is considered essential component of the development of a clinical bio-analytical assay before it is applied to patient care[15].The newly described method, including heat extraction and fast chromatographic separation (see figure 43 for a representative chromatogram) was validated in a similar fashion as described in chapter 4. The data of the validation on four consecutive days is presented in table 21. The precision of the method was significantly increased as a result of the reduction of the number of sampling handling steps and the incorporation of internal standards. Overall the method was precise and accurate to 1 nM, with the exeption of the longer polyglutamates ($MTXPG_{5-7}$). Correlations of the individual analytes were found to approach an R^2 of 0.999, similar to earlier reported values.
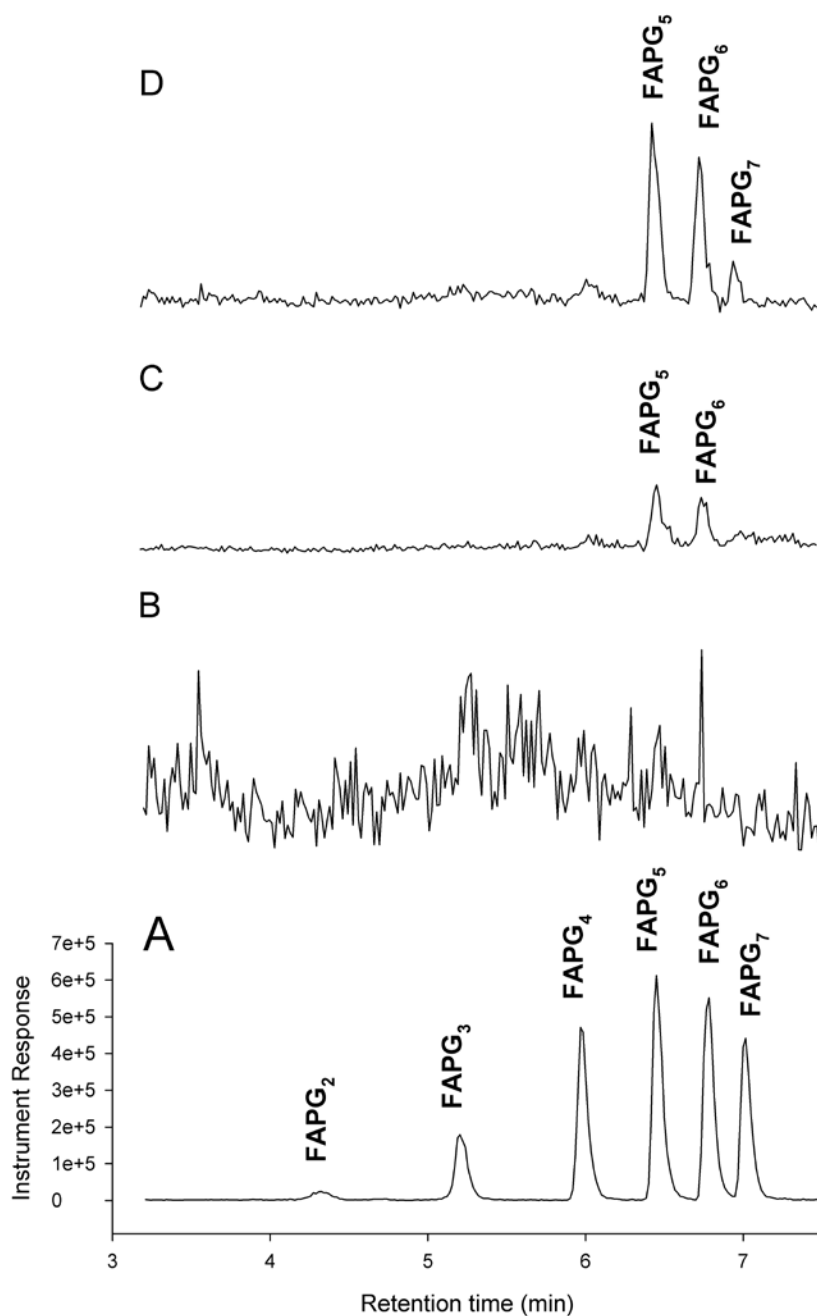
Figure 41. *Chromatograms of folic acid polyglutamates separations. (A) separation of an 50nM aqueous mixture of FAPG$_{1-7}$. (B) JIA patients on MTX therapy with no detected FA in the donated RBC sample. (C) JIA patient with FAPG$_{5-6}$ detected in concentrations <2.5 nM. (D) Chromatogram of an RBC sample from a JIA patient with FAPG$_{5-7}$ detected at concentrations <10 nM.*

Table 21. Intra- and inter-day precision and accuracy results

Analyte	Nominal RBC Concentration (nM)	Intra-run (n=5)			Inter-run (n=20)		
		Precision (RSD %)	Mean observerd concentration (nmol/L)	Mean Accuracy of target value (%)	Precision (RSD %)	Mean observerd concentration (nmol/L)	Mean Accuracy of target value (%)
MTXPG$_1$	100	7.5	100.6	100.6	5.1	100.3	100.3
	50	4.6	50.1	100.1	6.7	50.3	100.6
	10	2.7	9.4	93.5	4.9	9.5	95.5
	5	7.6	4.9	97.6	10.9	4.8	96.7
	1	10.8	1.1	106.0	18.4	1.0	102.5
MTXPG$_2$	100	2.2	101.5	101.5	5.4	101.3	101.3
	50	5.3	48.6	97.2	8.3	49.7	98.1
	10	2.6	9.8	97.5	6.4	9.7	96.9
	5	13.6	5.1	102.0	11.4	4.9	98.9
	1	11.2	1.0	98.0	14.0	1.0	101.5
MTXPG$_3$	100	4.4	98.9	98.9	5.0	100.7	100.7
	50	11.4	51.9	103.8	8.0	50.2	100.3
	10	1.9	9.1	91.3	7.8	9.2	91.9
	5	3.8	4.8	96.8	6.3	4.9	97.2
	1	11.0	1.0	104.0	14.7	1.1	106.5
MTXPG$_4$	100	1.1	98.8	98.8	5.3	100.4	100.4
	50	11.3	52.0	104.0	8.1	50.5	101.0
	10	4.5	9.0	90.3	6.9	9.2	92.5
	5	3.7	4.9	98.8	5.8	4.7	94.4
	1	11.2	1.0	102.0	14.9	1.1	108.0
MTXPG$_5$	100	1.6	98.6	98.6	5.3	100.2	100.2
	50	11.8	51.8	103.6	8.3	50.8	101.5
	10	3.3	9.5	94.8	7.5	9.2	91.9
	5	6.2	4.9	98.8	14.2	4.6	92.8
	1	30.3	1.1	108.0	31.4	1.1	113.0
MTXPG$_6$	100	2.7	99.5	99.5	7.0	99.2	99.2
	50	11.0	51.3	102.6	8.6	51.3	102.7
	10	5.0	9.1	90.5	7.6	9.5	94.9
	5	9.3	4.8	96.8	9.4	4.8	96.1
	1	8.6	1.0	104.0	32.7	1.1	107.0
MTXPG$_7$	100	2.1	97.9	97.9	8.2	96.7	96.7
	50	10.5	52.5	105.1	8.7	52.9	105.9
	10	5.0	9.8	97.8	8.7	10.1	100.6
	5	7.4	4.6	92.0	18.7	4.8	96.1
	1	22.1	1.1	108.0	60.1	1.1	105.5

5.3.5 Detection of 7OH-MTX
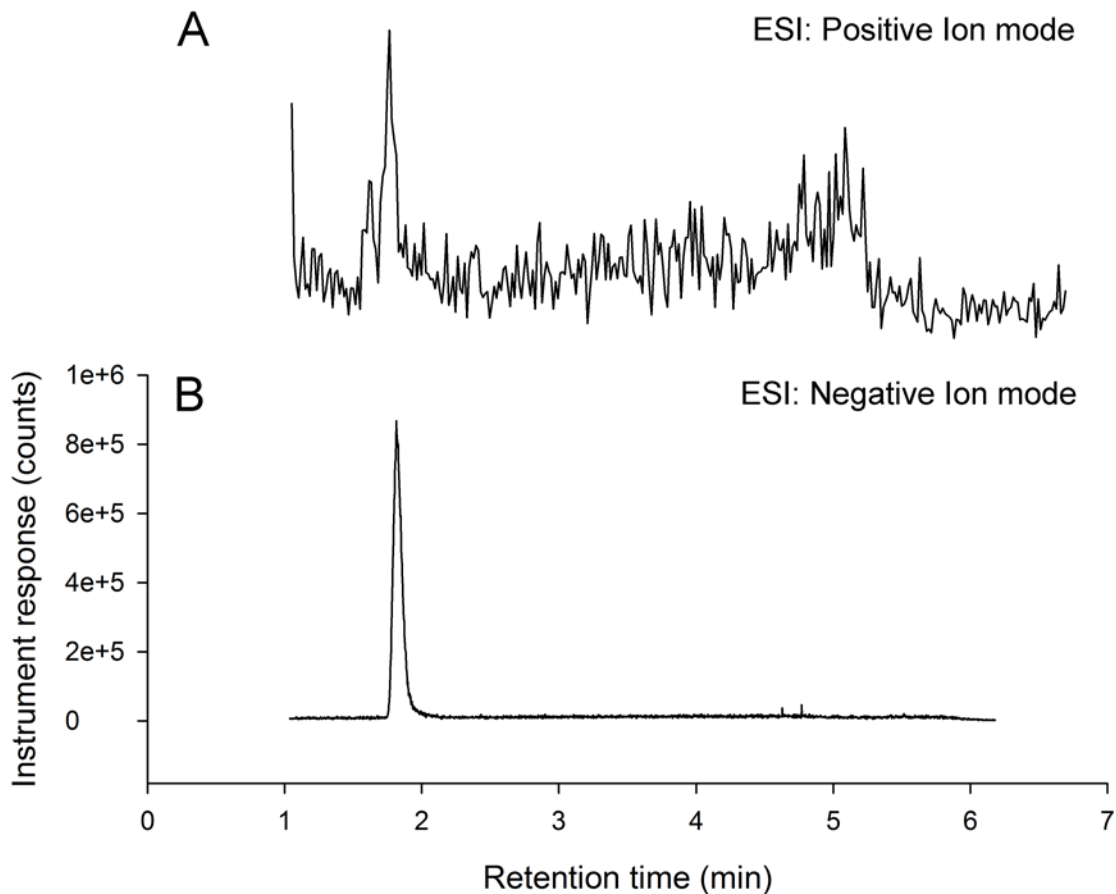
Figure 42. *An injection of a 10nM 7OH-MTX aqueous solution in both positive ion mode (A) and negative ion mode (B). Mass spectrometry setting can be found in table 1.*

As discussed in the introduction 7OH-MTX is a degradation product resulting from MTX catabolism. The measurement of these species might give provide addition insight of the MTX/folate metabolism of the individual RA patient and therefore provides a more extensive picture of all entities competing for enzymes that are responsible for folate biotransformation.

The development of an analytical strategy for 7OH-MTXPGs is complicated by the fact that polyglutamyl standards are not commercially available and synthesis is not straight forward due to the nature of the glutamyl-linkage, where individual glutamate building blocks are connected through the amino acid side chain (gamma-carboxylate). However based on the fragmentation pattern of these type of species one could tentatively scout for these entities using specific SIM detection schemes by the triple quadrupole mass spectrometer. Such a study would not allow for reliable and robust quantitation but should demonstrate the presence or absence of this group of MTX metabolites within RBCs and could be followed up by more sophisticated studies if desired.

Initial method development was initiated by investigating the ionization behavior of 7OH-MTX. Interestingly it was found that in contrast to MTXPGs, 7OH-MTX (as the parent) was ionized more efficiently in negative ion-mode. Using MRM monitoring negative ion-mode was also found to more sensitive (figure 42B) as opposed to positive mode (figure 9 A) when applied to the detection of 10 nM aqueous 7OH-MTX standards. In order to estimate the fragmentation behavior of 7OH-MTXPG in negative ion-mode, a study was conducted using folic acid polyglutamates ($FAPG_{1-7}$). Folate acid polyglutamates are commercially available and based on the assumption that 7OH-MTXPGs have similar gas phase properties as FAPGs one could extrapolate MS-SRM settings such as parent m/z, daughter m/z, cone voltage and collision energy. The results of the study are presented in table 20. The most dominant fragment was the for PG_{1-2} loss of the glutamate chain, whereas the fragmentation of higher order polyglutamates (PG_{3-7}) were forming predominantly the monoglutamate fragment. This

165

was different to what was reported by Garrett et al, who had indicated the glutamate fragment with an m/z of 127.8 was the dominant fragment[8].

Using these extrapolated settings for 7OH-MTXPGs, erythrocyte samples from JIA patients on MTX therapy were screened for the presence of 7OH-MTXPGs. Since the hypothesis was that the presence of high amounts of 7OH-MTXPGs could enhance the excretion of MTX(PGs) patient samples were selected (n=10) with low-intermediate amounts of $MTXPG_{total}$ and screened for the presence of 7OH-MTXPGs. None of the patients out of the group tested positive for the presence of 7OH-MTXPGs. As the absence of 7OH-MTX could also be the result of poor MTX absorption in general by the individual, patients with high intracellular levels of $MTXPG_{total}$ were also screened for the MTX metabolites (n=10). Again none of the patients tested positive for the presence of 7OH-MTX within donated RBC samples. An example is given in figure 43, figure 43A shows a baseline signal indicating the absence of 7OH-MTXPGs. The various MTXPGs are demonstrated in figure 43B. The fact that 7OH-MTX was not observed in any of the analyzed RBC samples suggest that this MTX metabolite is not present in RBCs. Based on the earlier reported high abundance of this metabolite in the bone marrow this is surprising. One could argue that 7OH-MTX was not observed could be due to a vast difference in fragmentation behavior in ESI- between 7OH-MTXPGs and FAPGs, and setting extrapolation fails. To appropriately address this concern one would need isolated standards of the 7OH-MTXPGs and optimize MS/MS settings by infusion of these compounds. However, the success of extrapolating MS/MS settings is proven using structurally related compounds in the final data chapter of this thesis dealing with folate analysis. Furthermore, the analytical strategy presented in the following chapter for the expedient detection of $MTXPG_{total}$ was not able to detect 7OH-MTX as well.

Based on these observations it is tempting to conclude that 7OH-MTX is not present (in significant amounts) within erythrocytes of JIA patients on weekly low dose MTX therapy.
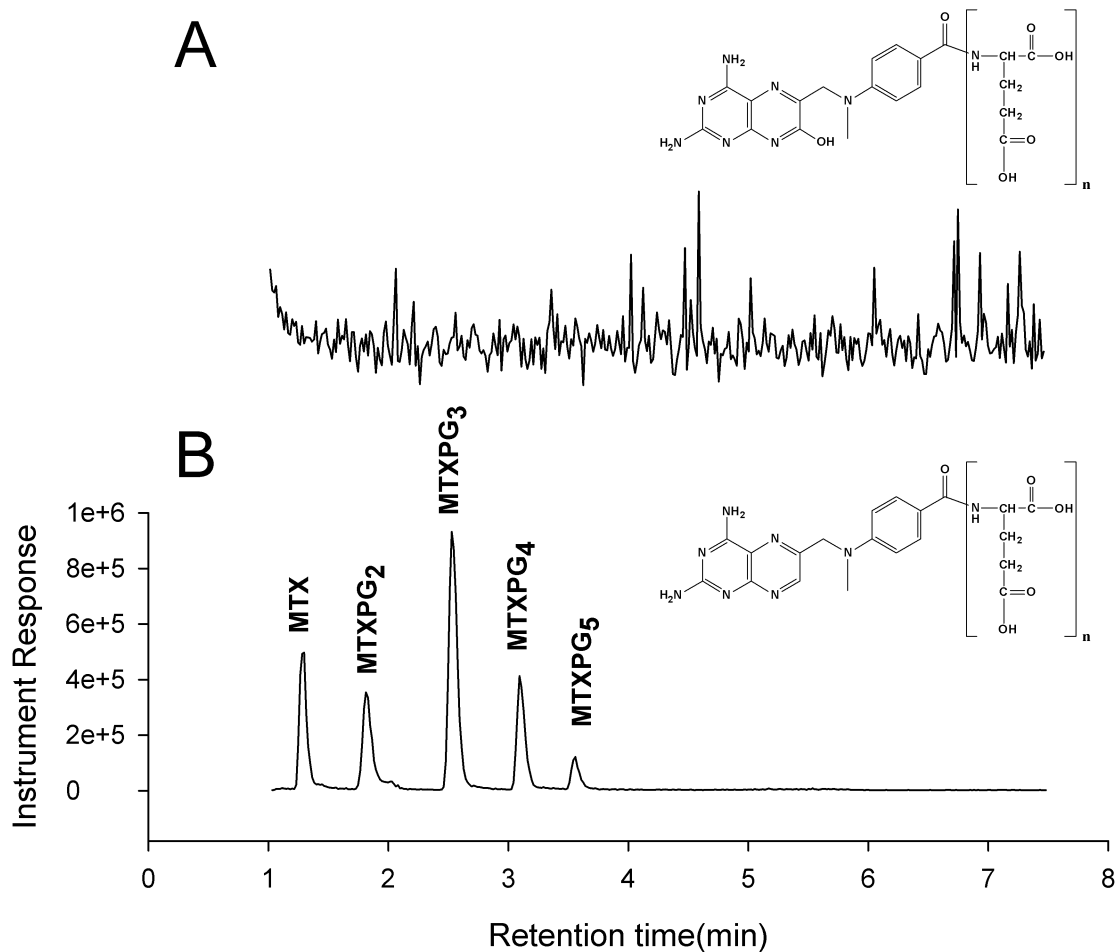
Figure 43. *Example RBC chromatograms of a JIA patient on MTX therapy. (A) Chromatogram of 7OH-MTX(PGs) (B) Chromatogram of MTXPGs*

5.4 Conclusion

The analytical methodology presented in the previous chapter (chapter 4) has been adapted for clinical use. Significant improvements were made on a number of facets of the assay. First, an improved sample preparation strategy was presented where the analytes were liberated using heat extraction. Proteins were denatured in the same step, and thus after centrifugation, a supernatant was obtained that could be introduced in the chromatograph. Second, DMHPA was found to be a more suitable ion-pairing agent when compared to DMHA and DMPA. Using DMHPA, chromatographic resolution between the analytes was increased, peak shape improved and fast gradient elution could be applied to separate the analytes within 4.5 minutes. Faster separation is chromatographically possible, but will need a mass spectrometer that clears the "ion path" faster than the Waters Ultima triple quadrupole mass spectrometer, such as the newer Xevo TQ. Third, the incorporation of d_3-MTX and $FAPG_4$ as internal standards (together with a less complicated sample preparation procedure) resulted in an improved precision, when compared to the assay that used solely external calibration.

An assay was developed for the detection of 7OH-MTX using electrospray ionization in negative ion mode. Due to the absence of polyglutamation standards the mass spectrometry settings were extrapolated based on the behavior gas phase behaver of FAPG homologues. RBC samples obtained from a number of JIA patients that displayed low, intermediate and high intracellular concentrations of MTXPGs were screened for the presence of 7OH-MTX. Interestingly, no 7OH-MTX in its native or polyglutamated form could be detected.

5.5 References

[1]   L. van Haandel, M. L. Becker, J. S. Leeder, T. D. Williams, J. F. Stobaugh, A novel high-performance liquid chromatography/mass spectrometry method for improved selective and sensitive measurement of methotrexate polyglutamation status in human red blood cells. *Rapid Communications in Mass Spectrometry.* **2009**, *23*, 3693.

[2]   J. E. Baggott, S. L. Morgan, Methotrexate catabolism to 7-hydroxymethotrexate in rheumatoid arthritis alters drug efficacy and retention and is reduced by folic acid supplementation. *Arthritis & Rheumatism.* **2009**, *60*, 2257.

[3]   J. E. Baggott, S. L. Bridges, S. L. Morgan, Evidence for two phenotypes in the metabolism of methotrexate to 7-hydroxymethotrexate in patients with rheumatoid arthritis. *Arthritis & Rheumatism.* **2005**, *52*, 356.

[4]   P. Sonneveld, F. W. Schultz, K. Nooter, K. Hahlen, Pharmacokinetics of methotrexate and 7-hydroxy-methotrexate in plasma and bone marrow of children receiving low-dose oral methotrexate. *Cancer Chemother Pharmacol.* **1986**, *18*, 111.

[5]   P. J. Bagley, J. Selhub, A common mutation in the methylenetetrahydrofolate reductase gene is associated with an accumulation of formylated tetrahydrofolates in red blood cells. *Proc Natl Acad Sci U S A.* **1998**, *95*, 13217.

[6]   Y. Lamers, R. Prinz-Langenohl, S. Bramswig, K. Pietrzik, Red blood cell folate concentrations increase more after supplementation with [6S]-5-methyltetrahydrofolate than with folic acid in women of childbearing age. *Am J Clin Nutr.* **2006**, *84*, 156.

[7]   L. B. Bailey, Folate status assessment. *J Nutr.* **1990**, *120 Suppl 11*, 1508.

[8]   L. C. Garratt, C. A. Ortori, G. A. Tucker, F. Sablitzky, M. J. Bennett, D. A. Barrett, Comprehensive metabolic profiling of mono- and polyglutamated folates and their precursors in plant and animal tissue using liquid chromatography/negative ion electrospray ionisation tandem mass spectrometry. *Rapid Commun Mass Spectrom.* **2005**, *19*, 2390.

[9]   S. D. Wilson, D. W. Horne, High-performance liquid chromatographic determination of the distribution of naturally occurring folic acid derivatives in rat liver. *Anal Biochem.* **1984**, *142*, 529.

[10]   S. D. Wilson, D. W. Horne, Evaluation of ascorbic acid in protecting labile folic acid derivatives. *Proc Natl Acad Sci U S A.* **1983**, *80*, 6500.

[11]   http://www.fda.gov

[12]   T. M. Annesley, Ion Suppression in Mass Spectrometry. *Clin Chem.* **2003**, *49*, 1041.

[13]   R. Bakhtiar, T. K. Majumdar, Tracking problems and possible solutions in the quantitative determination of small molecule drugs and metabolites in biological fluids using liquid chromatography-mass spectrometry. *Journal of Pharmacological and Toxicological Methods.* **2007**, *55*, 227.

[14]   C. S. Elmore, D. C. Dean, Y. Zhang, C. Gibson, H. Jenkins, A. N. Jones, D. G. Melillo, Synthesis of [C2H3]methotrexate and [C2H3]7-hydroxymethotrexate. *Journal of Labelled Compounds and Radiopharmaceuticals.* **2002**, *45*, 29.

[15]   M. Vogeser, C. Seger, Pitfalls Associated with the Use of Liquid Chromatography-Tandem Mass Spectrometry in the Clinical Laboratory. *Clin Chem.* **2010**, *56*, 1234.

Chapter 6: Expedient Methodology for Total Methotrexate Polyglutamation Pool Determination in Human Erythrocytes

Chapter 6: Expedient Methodology for Total Methotrexate Polyglutamation Pool Determination in Human Erythrocytes

Table of Contents

List of Figures

List of Tables

6.1 Introduction

The antifolate methotrexate (MTX) (4-amino-10-methylpteroylglutamic acid) administered in low dose, on a weekly basis, is widely used for the treatment of rheumatoid arthritis (RA) [1] and juvenile idiopathic arthritis (JIA) [2]. MTX is the first-line therapy for RA patients exhibiting inadequate disease control from treatment with non-steroidal anti-inflammatory drugs [3]. In low-dose this disease-modifying drug is generally well tolerated and considered safe, however there is a substantial percentage of patients who have poor response to MTX or develop adverse reactions [4]. This can be partly explained by a poorly understood inter-patient variation in the dose of MTX required to achieve a desirable level of disease control, making it difficult to optimize and individualize therapy. It has recently been shown that the measurement of MTX and its polyglutamate metabolites (MTXPGs) in red blood cells (RBCs), an easily accessible space thought to reflect the intra-cellular state, could be a useful tool in individualizing MTX therapy [5-8].

Whilst the exact mechanism of action of MTX in RA/JIA is poorly understood [9-10], its therapeutic effect is attributed to the various MTXPGs rather than MTX itself [11-13]. Various methods to measure intra-cellular levels of MTXPGs have appeared recently in the literature. These strategies can be categorized as methods that measure the total amount of polyglutamated MTX (i.e. as a total pool) (MTXPG$_{total}$) and methods that measure and quantify each MTXPG individually, up to the hepta-glutamate. Individual concentrations of MTXPGs in RBCs have been measured by HPLC with a post-separation photochemical (PCR(hv)) derivatization followed by fluorescence detection (FD) [6], and more recently by an ion-pair HPLC method followed by tandem mass

spectrometry (LC/MS/MS) [14]. Currently, the LC/MS/MS method is the most specific and sensitive assay for detection of MTXPGs. Whilst these methods give a detailed presentation of the intra-cellular MTX metabolome, calibration is required for each MTXPG, necessitating the use of expensive standards. Further, gradient elution separation is required to compensate for differences in chromatographic behavior of the different MTXPGs, typically resulting in a relatively long run and re-equilibration times. Clinically, the relevance of individual MTXPG concentrations or population distribution is not fully understood, and as a result the various polyglutamates are often summed to a total or alternatively, grouped as short chain (MTXPG$_{1-2}$) and long chain (MTXPG$_{3-5}$) [5-6] pools.

MTXPG$_{total}$ methods utilize the plasma enzyme ɣ-glutamyl hydrolase to deglutamate the various MTXPGs into MTX (in a similar fashion as folate polyglutamates) [15]. Typically, an aliquot of human plasma is added to a RBC lysate as a source of ɣ-glutamyl hydrolase, followed by a lengthy incubation period ranging from 6 to 14 hours at 37 °C. The amount of MTX after deglutamation (reflecting the MTXPG$_{total}$) is generally measured by HPLC- PCR(hv)-FD [6, 16]. The post column oxidative degradation used by these methods generates a fluorescent pteridine derivative by cleaving the C9-N10 bond of MTX(PGs) [17-18] (figure 44a). Hence, the only function of the elaborate deglutamation procedure is to circumvent chromatographic resolution between the various polyglutamates.

We hypothesized that a precolumn derivatization strategy leading to cleavage C9-N10 bond of MTX(PGs) would circumvent the tedious deglutamation step and as a result increase sample throughput, reduce the number of sample preparation steps and avoid the addition of blank human plasma and the ensuring incubation period. The presently

proposed analytical method would possess the attributes of being rapid and economical, an attractive alternative for the routine monitoring of total intra-cellular MTX related species in JIA and RA patients, while still providing a quantitative basis for individualization of MTX therapy.

6.2 Materials and Methods

6.2.1 Chemicals and reagents

Methotrexate (MTX) was purchased from Sigma Aldrich (St. Louis, MO, USA) and methotrexate polyglutamates (MTXPG) 2-7 were purchased from Schircks Laboratories (Jona, Switzerland). 2,4-diamino-6-methylpteridine (DAMP) was obtained from ChemDiv (San Diego, CA). HPLC grade methanol (MeOH), sodium phosphate monobasic and ammonium bicarbonate were purchased from Sigma Aldrich (St. Louis, MO, USA). Ammonium acetate and sodium phosphate dibasic were acquired from Fisher Scientific (Fairtown, NJ, USA). Sodium dithionite was purchased from Riedel – de Haën (Seelze, Germany). Demineralized water was produced by Labconco Waterpro PS (Labconco Corporation, Kansas City, MO, USA). Blank Red blood cells (RBCs) were drawn from healthy volunteers on site.

6.2.2 Chromatographic separation

Solvent was delivered by a binary pumping system containing two Shimadzu LC6A pumps. The sample was introduced by a Shimadzu SIL-6B auto injector equipped with a 50μL injection loop and a 50% water/50% ACN wash solution. Detection was accomplished by a Shimadzu RF-10Axl fluorescence detector using an excitation - emission wavelength of 367 nm and 463 nm, respectively, with a bandwith of 15nm. Chromatography was performed using a Phenomenex Inertsil ODS-3 analytical column (150 x 4.6mm) packed with 5μ 100 Å particles. The analytical column was guarded using a Supelcosil LC-8 guard column (5μ, 2 x 4.0mm). Mobile phase A consisted of 10 mM ammonium acetate in water and mobile phase B was 100% methanol. An isocratic mobile phase containing 30% B at a flow rate of 1 mlmin^{-1} was used for the separation.

6.2.3 Stock solutions and buffers

Phosphate buffers (1.0 M) of pH 5.5, 6.0, 6.5, 7.0 and 7.5 were obtained by blending a 1.0 M monobasic sodium phosphate solution with a 1.0 M dibasic sodium phosphate solution to achieve the targeted pH. MTX and MTXPGs were dissolved 0.10 M ammonium bicarbonate buffer to prepared 1.0 mM master stock solutions. The working stock solutions containing the appropriate concentrations of the analytes were created by further dilution of the master stocks solutions with water. All stock solutions were prepared daily prior to each experiment.

6.2.4 Preparation of erythrocyte (RBC) lysates

Blood samples (~5 ml) obtained from patients were centrifuged at low speed (2000 rpm) in a Beckman tabletop centrifuge to pellet the RBCs. After removal of plasma, the RBCs were suspended in an equal volume of sterile normal saline, mixed by gentle inversion and subjected to a second low speed centrifugation. The supernatant was discarded and the wash procedure was repeated a second time. After discarding the supernatant, the packed RBCs were divided into aliquots and stored at -70° C until use.

6.2.5 Derivatization protocol

A general derivatization procedure was established. An 100 μL aliquot of patient or blank RBCs was transferred to an Eppendorf reaction vial and was spiked with one of the analytes. The volume was adjusted to 200 μL using deionized water and/or aqueous

calibration solutions of MTX to obtain spiked RBCs of the appropriate concentration. The remaining mixture was subsequently homogenized via vortex mixing for 5 seconds. The pH of the homogenate was adjusted by the addition of 600 μL of pH 6.0 phosphate buffer followed by an additional 5 second vortex step. The samples were placed in an in-house constructed sample holder that was able to pressure seal the caps of the Eppendorf reaction vials. The total reaction volume was brought to 1.0 mL by addition of 200 μL of a freshly prepared solution of 10 mg/mL sodium dithionite. After sodium dithionite addition to each vial, the lids were closed and the entire holder inverted 5 times, then vortexed for 10 seconds to ensure complete mixing (this step was found to be extremely important in obtaining reproducible results). The sample holder was then placed in boiling water for 15 minutes to facilitate the reduction reaction and precipitate proteins. After the reaction period, the sample holder was refrigerated at 7° C for 30 minutes. The reaction vials were subjected to centrifugation (13,000 rpm for 5 minutes), and the resulting supernatant transferred to a 1.0 mL autosampler vials for subsequent determination.

6.2.6 Yield determination and validation

In order to determine the yield of the reduction, 100 μL of RBCs (n=5) were spiked with MTX to 1.0 μM and subjected to the derivatization procedure. The reduction yield was obtained by comparing the spiked RBC samples to an aqueous DAMP standard calibration curve (0.1, 0.5, 1.0, 1.5, 2 μM) . Method validation consisted of determination of MTX spiked RBCs at 10, 25, 50, 100, 250 and 500 nM in 5 replicates on four consecutive days.

6.3 Results and discussion

6.3.1 Selection of the Derivatization Reaction and Format

The order of operations within an overall methodology has significant analytical implications. For example, the conduct of a derivatization reaction in the pre- versus post-column format defines the nature of the data obtained. Conduct of a post-column derivatization reaction allows for separation of the various analytes of interest prior to formation of an analytical reporter product. In contrast, pre-column derivatization of a family of analytes may lead to the formation of a common product and thus loss of analytical identity. As noted previously, there are clinical situations where determination of the total concentration of all related species is sufficient and desirable, rather than determination of each individual analytical species.
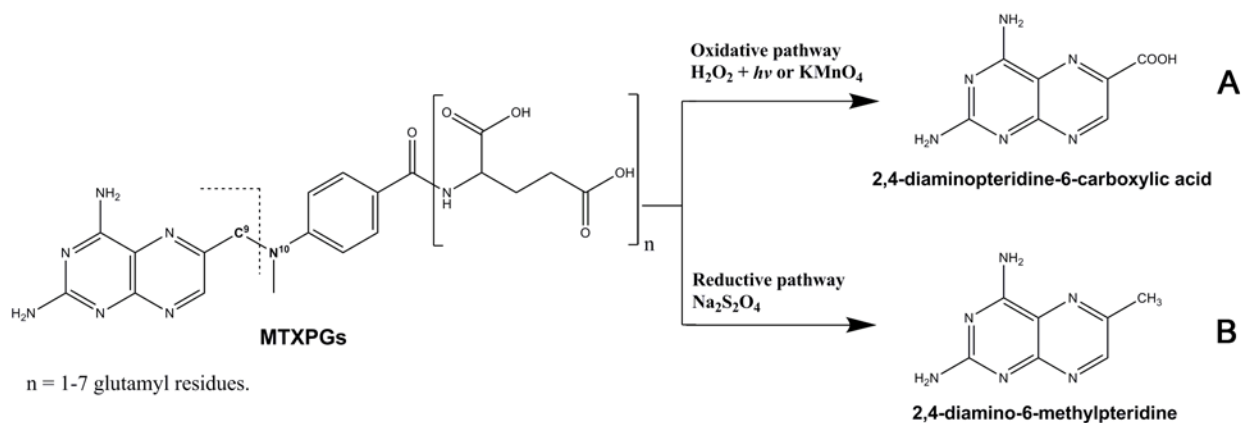
Figure 44. *The labile C9-N10 bond in MTX can be cleaved in oxidative (A) and reductive (B) environments. The resulting fluorescent derivative is either carboxylated or methylated at the C6 position, depending on the chemistry selection.*

180

Continuing with the concept of total analyte determination, as previously noted, the C9-N10 bond in methotrexate is chemically labile to oxidative [6, 16-18] and reductive [19] environments to yield fluorescent pteridine derivatives (figure 44). These different processes lead to different products, with oxidative cleavage leading to the formation of 2,4-diaminopteridine-6-carboxylic acid (DAPC) (figure 44a) while reduction cleavage leads to 2,4-diamino-6-methylpteridine (DAMP) (figure 44b). A prior publication suggests that the reductive product DAMP exhibits more favorable fluorescence properties as compared to the oxidative product DAPC, with a yield of approximately 70% being realized when the analyte is present in plasma [19].

In previous studies (Chapter 2 and 3), it was found that sodium dithionite reductive mediated reductive cleavage of the C9-N10 bond may be extended to the situation where MTX is conjugated to a macromolecular carrier via the glutamyl residue. The apparent generality of this reaction lead to the present hypothesis that sodium dithionite reductive mediated reduction could be used to measure $MTXPG_{total}$ (DAMP serves as a common reporter molecule for each MTXPG). In another consideration with respect to the choice of an oxidative versus reductive process to mediate C9-N10 cleavage, the previous investigation had also shown the reductive procedure to result in significantly less chromatographic interferences as compared to the oxidative procedure. With any bioanalytical method, simplistic and efficient sample preparation is a hallmark of a robust method. In the present case, it was observed that by conducting the reductive procedure directly in plasma (reaction for 15 minutes in boiling water), efficient protein denaturation was accomplished, and after centrifugation, the supernatant could be directly analyzed by HPLC-FL. When this procedure was investigated for the analysis of $MTXPG_{total}$ in human RBCs, the chromatograms of figure 45 were obtained. A DAMP

181

reference standard dissolved in water was used to optimize chromatographic conditions (figure 45a). Blank human RBCs showed no significant interference originating from endogenous molecules during the elution window of DAMP (figure 45a). Due to the low background a rapid isocratic separation was possible, leading to an analysis time of just 7 minutes per sample. In order to validate the hypothesis that the various MTXPGs would yield the same product (DAMP), the various individual MTXPGs were spiked in similar concentrations and derivatized in human RBCs obtained from individuals not treated with MTX. Identical chromatograms were generated regardless of the derivatized MTXPG (figure 45b).
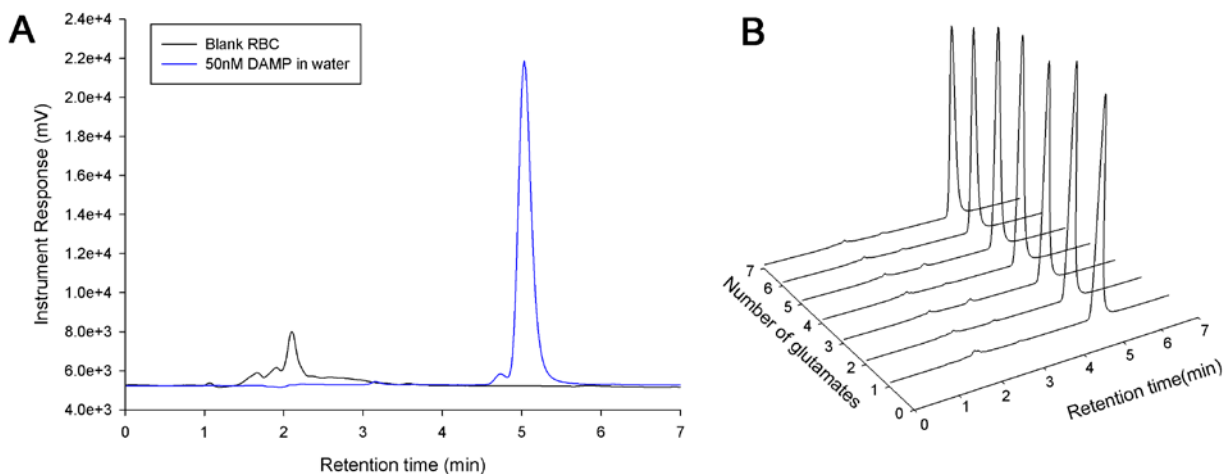
Figure 45. *(A) Illustration of a blank RBC chromatogram (black line), showing no endogenous interference during the elution of the DAMP derivatization product (blue line). (B) 7 individual chromatograms of RBC samples, each spiked with a different MTXPG standard (1-7).*

6.3.2 Yield Optimization and Comparison

Deen and coworkers stated in their plasma method that no increase in fluorescent signal was observed after 15 minutes of reaction time and/or an increase in dithionite concentrations[19]. Similar observations were made with the reaction in the RBC matrix. The influence of the pH on the reduction reaction of MTX with an RBCs matrix was investigated at pH 5.5, 6.0, 6.5, 7.0 and 7.5 (table 22). The highest fluorescence was obtained at pH values of 5.5 and 6.0. In order to maximize the buffer capacity of the phosphate buffer, a pH of 6.0 was selected. It has been shown that patients on MTX therapy show large inter-patient variability in MTXPG distributions (short-chain or long-chain MTXPGs being dominant). Since $MTXPG_{total}$ is calculated as the sum of all glutamation species from $MTXPG_1$ (parent) to $MTXPG_7$, it was essential that derivatization of the various MTXPGs proceed with similar yields in order to avoid analytical bias due to differences in the MTXPG population distribution. $MTXPG_{1-7}$ were individually (n=5) spiked at 1.0 µM in the RBC matrix and subjected to the reductive procedure (table 23). The average yield of reaction was 61.6% yield, with $MTXPG_2$ giving the highest (65.1%) and $MTXPG_7$ lowest (56.6%) yield.

Table 22. pH influence on reaction yield

pH	Relative yield	Precision (RSD %)
5.5	1.00	1.5
6.0	0.96	3.2
6.5	0.74	2.2
7.0	0.56	3.4
7.5	0.41	3.3

The MTXPG$_7$ reduction yield was significantly lower than the mean using the student t-test at the 95% convidence interval. However, this standard is very hygroscopic and had visually picked up some water during storage. Therefore it was concluded that reaction yield between the different MTXPGs was identical, with observed differences being caused by minor variations in the purities of the commercially obtained MTXPG standards. As a result, the analytical method can be calibrated with reference to MTX thus avoiding the need for specialized expensive MTXPG standards.

Table 23. Reduction Yields of various MTXPGs

	Concentration (µM)	Found (µM)	Yield (%)	RSD (%)
MTX	1.00	0.62	62	1.8
MTXPG$_2$	1.00	0.65	65	1.4
MTXPG$_3$	1.00	0.61	61	1.1
MTXPG$_4$	1.00	0.64	64	2.0
MTXPG$_5$	1.00	0.63	63	0.6
MTXPG$_6$	1.00	0.59	59	1.3
MTXPG$_7$	1.00	0.57	57	2.8

6.3.3 Matrix influence

During method development it was observed that sodium dithionite-mediated reduction to yield DAMP was matrix dependent. Unexpectedly, in aqueous solutions the reaction was less efficient (absolute yield was about 5-10%) as compared to RBC matrix (yield about 62%). As this variation was of considerable concern, further experimentation was conducted in an effort to establish the nature of this variability and to define conditions leading to reproducibility. RBCs from four separate individual donors were spiked (n=5) with an equal amount of MTX and subsequently analyzed (table 24). The various lots of RBCs did not significantly affect the derivatization yield and as a result the ability of the method to quantitate MTXPG$_{total}$ in individual RBC samples is not

compromised. Since the derivatization proceeds more efficiently in RBCs than water, it was established that it is very important to keep RBC volumes between calibrants and samples constant during the derivatization process, or in other words an identical matrix must be maintained for all samples, unknowns or standards, being subjected to sodium dithionite reduction.

Table 24. Yield of reaction in various individual RBC donors.

RBC Donor	Spiked (nM)	Found (nM)	Yield (%)	RSD (%) (n=3)
1	100	109.5	109.5	11.4
2	100	107.7	107.7	1.5
3	100	111.7	111.7	4.3
4	100	107.8	107.8	1.6

6.3.4 Method Validation

Using MTX the method was validated on four consecutive days at six different concentrations from 10-500 nM, representing a clinically relevant MTXPG$_{total}$ range reported in RBCs (table 25). The intra-run mean accuracy of the target value was between 98.1 % and 106.0 %. The intra-run precision was between 1.2 % and 8.8 %. The limit of quantification was determined to be 10 nM MTXPG$_{total}$. The limit of detection, defined as 3 times the signal to noise ratio, was 4 nM MTXPG$_{total}$. Four different calibration curves at different days revealed a linear relationship between peak area and concentration of the prepared RBC standards, with correlation coefficients r^2 > 0.999 for each day. A typical calibration curve was described by the following linear equation: y = 376.7x + 832.1, where y is peak area and x is concentration added in nMThe derivatization procedure results in a 10-fold sample dilution, however limits of quantification were within assay requirements, so no effort were made to preconcentrate the sample prior to injection.

Table 25. Intra- and inter-day precision and accuracy results

Nominal RBC MTXPG concentration (nM)	Intra-run (n=5)			Inter-run (n=20)		
	Mean observed concentration (nmol/L)	Mean Accuracy of target value (%)	Precision (RSD %)	Mean observed concentration (nmol/L)	Mean Accuracy of target value (%)	Precision (RSD %)
10	10.6	106.0	5.6	10.0	99.7	9.6
25	25.7	102.7	2.3	24.8	99.2	7.5
50	50.0	100.0	8.8	49.6	99.2	6.1
100	98.1	98.1	3.2	98.7	98.7	4.1
250	250.6	100.2	2.6	253.2	101.3	2.1
500	500.0	100.0	1.2	498.7	99.7	1.6

6.3.5 Stability

The stability of the reporter molecule (DAMP) was investigated at three different concentrations (10.0, 50.0 and 250.0 nM). After sample processing the samples were placed in the autosampler and analyzed 24 hours later (table 26). Sample deterioration was not observed, indicating that the processed samples are stable for at least 24 hours at room temperature, which is sufficient for analysis. The freeze-thaw stability was investigated in a similar manner (table 26). Recently, Hroch et al have reported sample instability when multiple freeze-thaw cycles were applied (method of detection was enzymatic deglutamation followed by HPLC-(PCR(hv)-FD) [16]. A significantly lower value (47%) was observed, especially after the third free-thaw cycle. This instability was not observed when these freeze-thaw cycled samples were analyzed by the presented methodology.

Table 26. Freeze-thaw stability and stability of the derivatization product

Storage condition	Concentration of MTXPG$_{total}$ in nM		R.S.D. (%) (n=3)
	nominal	measured	
Stability in autosampler (24h)	10	10.0	13.4
	50	50.2	6.1
	250	250.2	5.8
Freeze-thaw stability (3 cycles)	10	9.4	24.4
	50	48.3	13.3
	250	242.3	5.9

6.3.6 Patient samples analyzed by the MTXPG$_{total}$ assay and LC/MS/MS
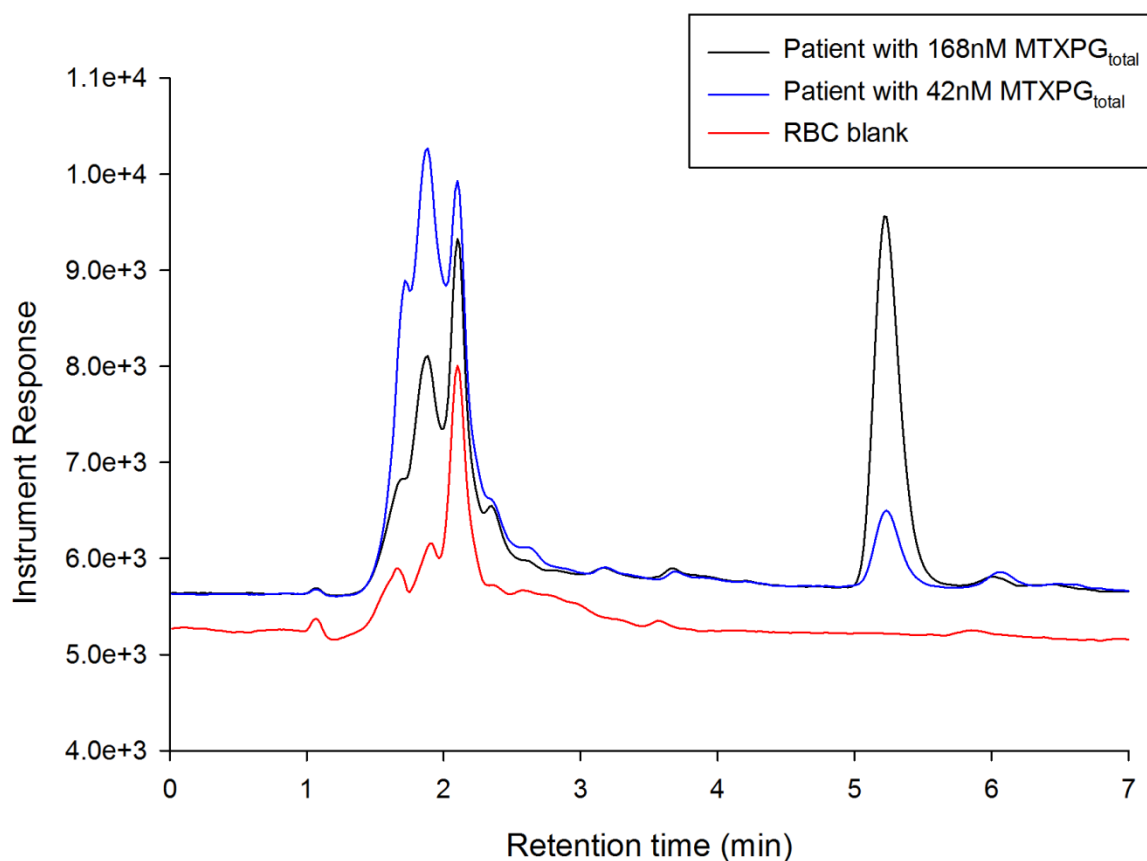
Figure 46. *Chromatograms of a patient with a relative high concentration of MTXPG$_{total}$ (black line) and a patient with lower MTXPG$_{total}$ (blue line) are demonstrated. A worked up RBC blank is included for reference purposes (red line).*

Patient samples were analyzed by the MTXPG$_{total}$ method (figure 46) and compared with our previously reported LC/MS/MS methodology (figure 47). The LC/MS/MS method was specific for each MTXPG, leading to quantification of individual MTXPGs which were added to provide MTXPG$_{total}$. Results obtained by the different methods correlated well (R^2 = 0.983) and therefore respond comparable to changes in intracellular levels of MTXPG$_{total}$ within patient RBCs. The relationship between the methods could be described by the following equation: y = 1.32x + 5.3, where y is the response in nM measured by the reductive method and x is the response in nM measured by the LC-MS/MS method.
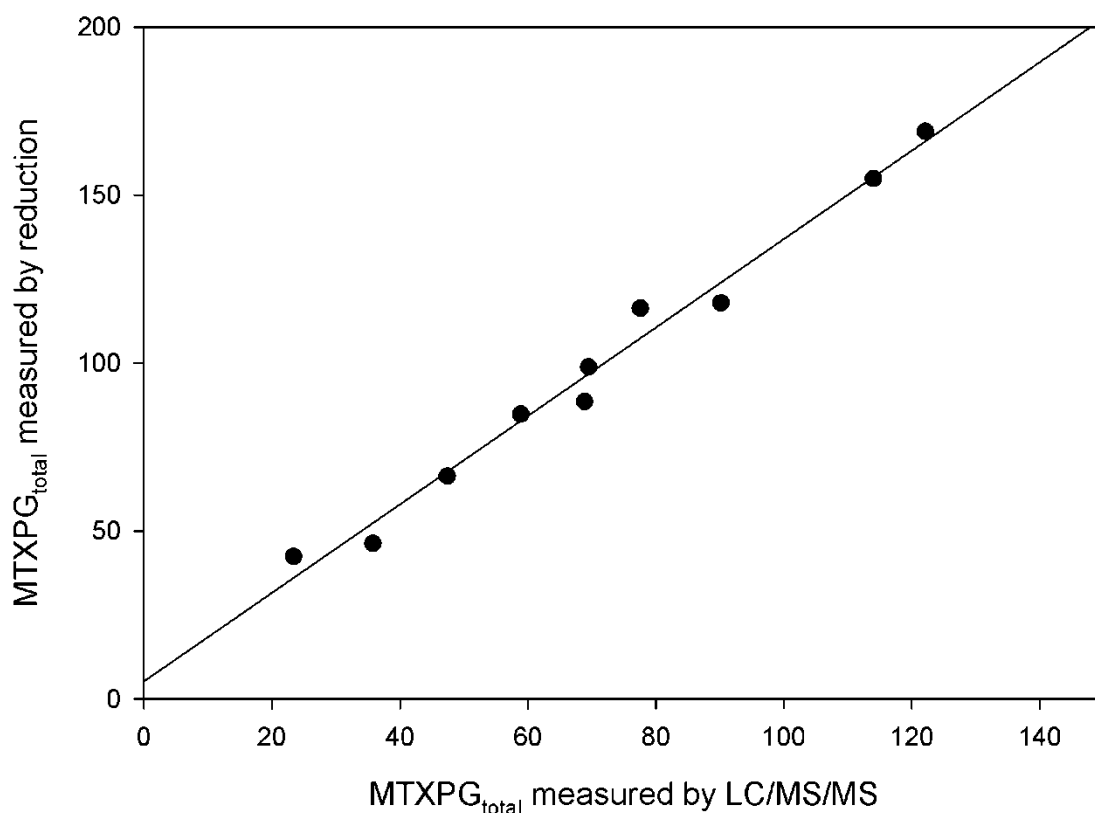
Figure 47. *Correlation between MTXPG$_{total}$ concentrations in 10 patients obtained by LC-MS/MS and the presented reductive method.*

188

Analysis of the equation reveals that the reductive procedure yields on average a 32% higher MTXPG$_{total}$ value when compared to LC/MS/MS. It has been shown that another MTX metabolite, 7OH-MTX, can accumulate to a significant extend in bone marrow and certain tissues[20]. Since red blood cells are generally considered to be a biomarker for the (anti)folate status in the bone marrow[21], it was hypothesized that these elevated levels could be due to the presence of 7OH-MTX in RBCs. In order to check the specificity of the reductive method towards 7OH-MTX, RBCs were spiked with MTX and 7OH-MTX respectively. It was found that the reductive method was less sensitive towards 7OH-MTX and more importantly was able to distinguish between the 7OH-MTX and MTX (figure 48), eliminating the possibility of measuring elevated MTXPG$_{total}$ levels due to the presence of 7OH-MTX in the patient samples. While the nature of the discrepancy between the reductive method and LC/MS/MS remains unknown, it is to be noted that interfering backgrounds have been observed when HPLC-FL was used in conjunction with the post-column photochemical derivatization. As a result, when comparing and reporting absolute MTXPG$_{total}$ concentrations the analysis strategy should be taken into account, but despite the absolute value attained, the approach provides a clear indication of MTXPG$_{total}$ that should be of clinical value.
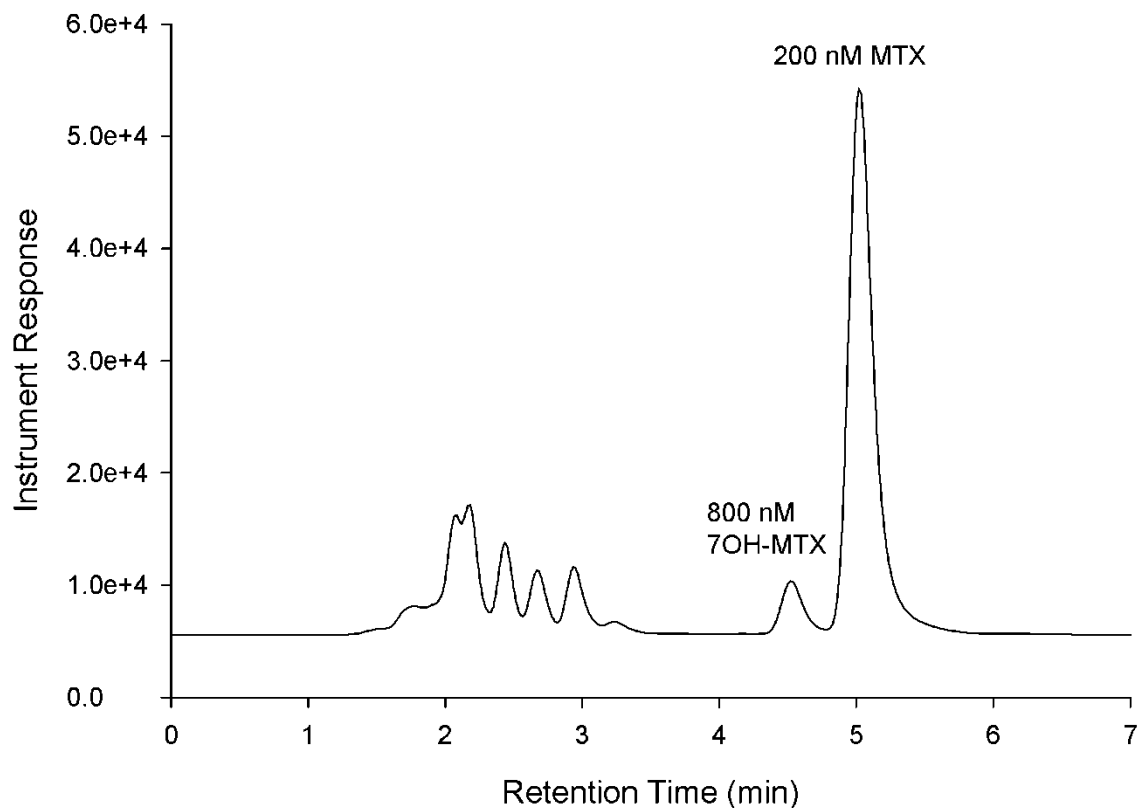
Figure 48. *Chromatogram of MTX and 7OH-MTX enriched RBCs. The reductive products DAMP and 7OH-DAMP were baseline separated.*

6.4   Conclusion

The measurement of RBC MTXPGs has potential to aid in optimization and individualization of MTX therapy in JIA and RA. Despite the clinical advantages of monitoring RBC MTXPGs this tool is currently not commonly used. Analytical methods that allow for the determination of intra-cellular MTXPGs are rather labor intensive and/or require the use of specialized equipment. Furthermore, the throughput of these methods is low and cost of analysis is high, thus making their implications in a clinical

environment challenging. In this report a method is presented for rapid analysis of MTXPG$_{total}$ status in human RBCs. The analytical procedure is a simple "one pot" pre-column reaction involving reagent addition and heating for 15 minutes. After centrifugation the supernatant is introduced into a conventional HPLC system equipped with a fluorescence detector, without the need for further workup. By performing the derivatization reaction pre-column, a time consuming (6-14h) commonly used de-glutamation procedure utilizing blank human plasma, becomes obsolete. Using the described procedure the total sample preparation time for a 50 sample run should not exceed 1-1.5 hours. The chromatographic run time per sample is 7 minutes using isocratic elution conditions. The rapid chromatographic procedure in combination with the uncomplicated sample preparation procedure should allow for same day sample determinations. Clinical results obtained by the reductive procedure correlated well with an earlier published LC/MS/MS method, however obtained absolute RBC MTXPG$_{total}$ concentrations were on average 30% higher, likely due to the enhanced selectivity accorded with the more elaborate and expensive instrumentation required for LC/MS/MS determinations.

6.5 References

[1]   L. Stamp, R. Roberts, M. Kennedy, M. Barclay, J. O'Donnell, P. Chapman, The use of low dose methotrexate in rheumatoid arthritis--are we entering a new era of therapeutic drug monitoring and pharmacogenomics? , *Biomedecine & Pharmacotherapy.* **2006**, *60*, 678.

[2]   A. V. Ramanan, P. Whitworth, E. M. Baildam, Use of methotrexate in juvenile idiopathic arthritis. *Arch Dis Child.* **2003**, *88*, 197.

[3]   Guidelines for the management of rheumatoid arthritis: 2002 Update. *Arthritis & Rheumatism.* **2002**, *46*, 328.

[4]   B. N. Cronstein, Low-dose methotrexate: a mainstay in the treatment of rheumatoid arthritis. *Pharmacol Rev.* **2005**, *57*, 163.

[5]   T. Dervieux, D. Furst, D. O. Lein, R. Capps, K. Smith, M. Walsh, J. Kremer, Polyglutamation of methotrexate with common polymorphisms in reduced folate carrier, aminoimidazole carboxamide ribonucleotide transformylase, and thymidylate synthase are associated with methotrexate effects in rheumatoid arthritis. *Arthritis Rheum.* **2004**, *50*, 2766.

[6]   T. Dervieux, D. Orentas Lein, J. Marcelletti, K. Pischel, K. Smith, M. Walsh, R. Richerson, HPLC determination of erythrocyte methotrexate polyglutamates after low-dose methotrexate therapy in patients with rheumatoid arthritis. *Clin Chem.* **2003**, *49*, 1632.

[7]   T. Dervieux, D. Furst, D. O. Lein, R. Capps, K. Smith, J. Caldwell, J. Kremer, Pharmacogenetic and metabolite measurements are associated with clinical status in patients with rheumatoid arthritis treated with methotrexate: results of a multicentred cross sectional observational study. *Ann Rheum Dis.* **2005**, *64*, 1180.

[8]   P. Angelis-Stoforidis, F. J. Vajda, N. Christophidis, Methotrexate polyglutamate levels in circulating erythrocytes and polymorphs correlate with clinical efficacy in rheumatoid arthritis. *Clin Exp Rheumatol.* **1999**, *17*, 313.

[9]   J. Swierkot, J. Szechinski, Methotrexate in rheumatoid arthritis. *Pharmacol Rep.* **2006**, *58*, 473.

[10]   J. A. Wessels, T. W. Huizinga, H. J. Guchelaar, Recent insights in the pharmacological actions of methotrexate in the treatment of rheumatoid arthritis. *Rheumatology (Oxford).* **2008**, *47*, 249.

[11] C. J. Allegra, J. C. Drake, J. Jolivet, B. A. Chabner, Inhibition of phosphoribosylaminoimidazolecarboxamide transformylase by methotrexate and dihydrofolic acid polyglutamates. *Proc Natl Acad Sci U S A.* **1985**, *82*, 4881.

[12] B. A. Chabner, C. J. Allegra, G. A. Curt, N. J. Clendeninn, J. Baram, S. Koizumi, J. C. Drake, J. Jolivet, Polyglutamation of methotrexate. Is methotrexate a prodrug? , *J Clin Invest.* **1985**, *76*, 907.

[13] J. E. Baggott, W. H. Vaughn, B. B. Hudson, Inhibition of 5-aminoimidazole-4-carboxamide ribotide transformylase, adenosine deaminase and 5'-adenylate deaminase by polyglutamates of methotrexate and oxidized folates and by 5-aminoimidazole-4-carboxamide riboside and ribotide. *Biochem J.* **1986**, *236*, 193.

[14] L. v. Haandel, M. L. Becker, J. S. Leeder, T. D. Williams, J. F. Stobaugh, A novel high-performance liquid chromatography/mass spectrometry method for improved selective and sensitive measurement of methotrexate polyglutamation status in human red blood cells. *Rapid Communications in Mass Spectrometry.* **2009**, *23*, 3693.

[15] C. Pfeiffer, J. Gregory, 3rd, Enzymatic deconjugation of erythrocyte polyglutamyl folates during preparation for folate assay: investigation with reversed-phase liquid chromatography. *Clin Chem.* **1996**, *42*, 1847.

[16] M. Hroch, J. Tukova, P. Dolezalova, J. Chladek, An improved high-performance liquid chromatography method for quantification of methotrexate polyglutamates in red blood cells of children with juvenile idiopathic arthritis. *Biopharm Drug Dispos.* **2009**, *30*, 138.

[17] J. Salamoun, J. Frantisek, Determination of methotrexate and its metabolites 7-hydroxymethotrexate and 2,4-diamino-N10-methylpteroic acid in biological fluids by liquid chromatography with fluorimetric detection. *J Chromatogr.* **1986**, *378*, 173.

[18] J. Salamoun, M. Smrz, F. Kiss, A. Salamounova, Column liquid chromatography of methotrexate and its metabolites using a post-column photochemical reactor and fluorescence detection. *J Chromatogr.* **1987**, *419*, 213.

[19] W. M. Deen, P. F. Levy, J. Wei, R. D. Partridge, Assay for methotrexate in nanomolar concentrations with simultaneous detection of citrovorum factor and vincristine. *Analytical Biochemistry.* **1981**, *114*, 355.

[20] J. E. Baggott, S. L. Morgan, Methotrexate catabolism to 7-hydroxymethotrexate in rheumatoid arthritis alters drug efficacy and retention and is reduced by folic acid supplementation. *Arthritis Rheum.* **2009**, *60*, 2257.

[21]   Y. Huang, S. Khartulyari, M. E. Morales, A. Stanislawska-Sachadyn, J. M. V. Feldt, A. S. Whitehead, I. A. Blair, Quantification of key red blood cell folates from subjects with defined MTHFR 677C>T genotypes using stable isotope dilution liquid chromatography/mass spectrometry. *Rapid Communications in Mass Spectrometry.* **2008**, *22*, 2403.

Chapter 7: The analysis of folate (polyglutamates) in various blood components by LC/MS/MS

Chapter 7: The analysis of folate (polyglutamates) in various blood components by LC/MS/MS

Table of Contents

List of Figures

List of Tables

7.1 Introduction

7.1.1 The MTX folate relationship

Following analytical method development, our group has identified patterns of MTXPGs that are associated with MTX toxicity, but not response (see chapter 4, 5, 6 for analytical method development and appendix 1 and 2 for the clinical discussion of the results). Whilst predictors of drug induced toxicity are of great clinical value, MTX therapy would further benefit from the identification of biomarkers that are indicative of drug response. During RBC MTXPG analysis it was realized an important part of the cellular milieu was not taken into account, namely the cellular folate content and polyglutamation distribution of this folate pool.

The role that folate (supplementation) plays in MTX efficacy and toxicity has been a subject of debate across disciplines. As a potent anti-folate drug, side-effects of MTX are also consistent with symptoms of folate deficiency, and baseline plasma and RBC folate concentrations have been shown to be negatively correlated with MTX toxicity scores[1]. Folate supplementation for the treatment of MTX related side-effects has been shown to be effective in diminishing MTX toxicity in vitro [2] and in vivo [1, 3], however, the effect that supplemental folic acid has upon MTX efficacy is still unclear. Although a small number of clinical studies designed to investigate folic acid supplementation in JIA have suggested no substantial effect upon drug efficacy [3-4], studies in psoriasis have shown greater improvement in skin scores in subjects on MTX monotherapy [5]. This same study also showed that the percent improvement in skin scores correlated with an increased MTXPG / Plasma folate concentration ratio, suggesting more effective folate inhibition may result in improved drug response. Recently (2010) L. Stamp et al. also

reported the lack of correlation between disease outcome and MTXPG concentrations in adult rheumatoid arthritis[6]. However, in the same study it was noted that erythrocyte folate content (measured by a standardized clinical assay) was significantly higher in patients with higher disease activity, suggesting a link between folate levels and disease activity. Interestingly (not noted by Stamp), the association between MTX and declining intra-cellular folate concentrations has been drawn in various in vitro[7-9] and in vivo[10] studies. Despite a number of encouraging clinical observations, there remains a substantial lack of clarity on the effect that cellular folate status may have upon MTX response.

As mentioned in the introduction (chapter 1) MTX(PGs) alters the activity of multiple enzymes within the folate cycle and therefore it is likely that regular intracellular folate metabolism will be distorted (figure 49). Since total folate content seems to be correlated to MTX efficacy, the next question to be answered is: how much of each folate isoforms is present (i.e. redox/methylation forms), what is its polyglutamation population distribution and how does MTX therapy affect this folate metabolism? In order to address this research question a folate control group and a group of JIA patients on MTX therapy were established. The folate control group included 100 JIA patients that were not on MTX therapy, and the MTX group consisted of the 110 patients that were analyzed earlier for MTXPGs. Whole blood samples were drawn from all patients for the purpose of comprehensive RBC folate analysis (i.e. quantitation of folate isoforms and polyglutamation distribution). The comprehensive folate analysis of RBCs is however complicated by the fact that such an analysis strategy has not appeared in the literature yet.
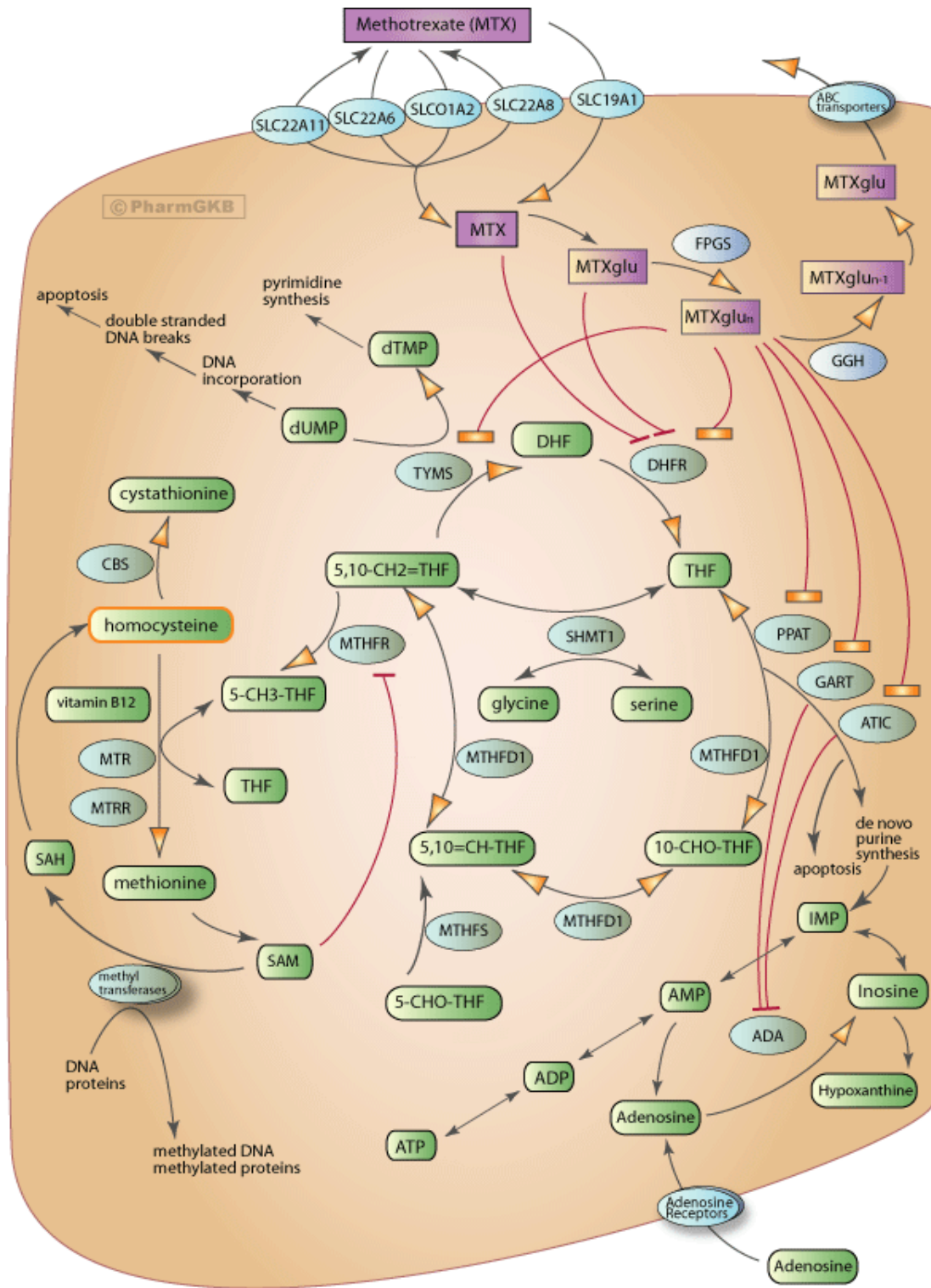
Figure 49. *Cellular folate pathway with both folic acid and MTX represented. Red lines represent known inhibition of target enzymes with MTX. (figure reproduced with permission from PharmGKB and Stanford University).*

7.1.2 RBC folate content

Until a decade ago it was believed that the only folate form present in RBCs was the polyglutamyl form of 5-MTHF[11]. More recent studies have indicated that an important exception are subjects homozygous for C677T polymorphism in the methylenetetrahydrofolate reductase (MTHFR) gene[12-13]. Individuals that display this single nucleotide polymorphism (SNPs) produce a thermolabile version of MTHFR, where an alanine residue is substituted by valine. The thermolabile variant losses about 50% of its activity, impairing the reduction of 5,10-methyleneTHF to 5-MTHF. As a consequence, subjects with the 677 TT genotype have increased amounts of non-methylTHFs (i.e. 5-FTHF, 10-FTHF, 5,10-MTHF and THF) within their RBCs, when compared to 677 CT or CC genotypes[11, 13-14]. The introduction of more sensitive and specific detectors such as LC-MS/MS has revealed that non-methylTHFs are also present in 677 CC and CT genotypes, but concentrations are typically low (i.e. <10% of total folate content)[13]. Analytical techniques for the measurement of folates in RBCs should therefore be able to discriminate between various folate isoforms and polyglutamation state.

7.1.3 Analyte selection

Folate isoforms continuously interconvert in the biological system, donating methyl groups and changing redox states, mostly by reversible but sometimes irreversible pathways (figure 49). Since the barriers for interconvertion are generally low, one has to be aware of the stability, or lack of stability of the folates of interest. Folate stability therefore directly influences analytical method development; it determines what

species could be measured and in some cases the measured folate form might be indicative of an entire subset of closely related folate isoforms. Detailed studies (using LC-MS/MS) of folate stability and interconversion have recently appeared in the literature[15]. The following section will discuss the consequences and implications of stability results presented by these papers in regard to folatepolyglutamyl analysis out of RBCs.

A chemical view of the folate cycle is demonstrated in figure 50. Folic acid (fully oxidized pterine ringsystem) is a synthetic form of folate, used for folic acid fortification in foods due to its high chemical stability. Low amounts of this folate form have been reported in RBCs, but generally this folate is not measured. Folic acid gets reduced by dihydrofolate reductase (DHFR) to dihydrofolic acid. Dihydrofolic acid (DHF) is highly unstable and has therefore not been measured human RBCs. About 50% of DHF reoxidizes to FA during folate extraction, and thus measured FA reflects the sum of the "oxidized folate forms" (FA + degraded DHF)[16]. DHF is further reduced by DHFR to tetrahydrofolate (THF), which is the entry to the biologically active folates, however no biological activity has been reported for THF itself. THF is unstable, but can be assayed for if acidic conditions are avoided. THF can be stabilized in the analytical procedure by the use of the Wilson and Horne buffer (pH 7.85, containing ascorbic acid and mercaptoethanol)[17-18]. Significant levels of THF have been reported in MTHFR 677 TT genotypes[11, 13-14, 16, 19-20]. In biological systems THF is formylated to 10-formyltetrahydrofolate (10-FTHF) and interconverts to the much more stable 5-formyltetrahydrofolate (5-FTHF)[15]. In biological systems formylated folates are utilized or further reduced to 5,10-MTHF, an interconversion that is also pH dependent. At acid pH (<1.5) the 5,10-MTHF form is exclusively formed, at basic pH values (≥ 8.5),

hydration occurs to 10-FTHF which slowly interconverts to 5-FTHF. Usually chromatographic mobile phases are acidic and therefore formylated species are measured as 5,10-MTHF. As a result of this rapidly established equilibrium, 5-FTHF, 10-FTHF and 5,10-MTHF are grouped together as "non-methylTHFs" [11-14, 16, 19-20]. In biological systems 5,10-MTHF gets reduced to 5,10-METHF, a highly unstable compound that has not been observed in RBCs[19]. Next to instability it also has been suggested that the compound is readily used within the cell, therefore no significant buildup occurs. METHF is irreversibly reduced to 5-MTHF, the dominant form of folates in RBCs. 5-MTHF is considered the most stable of the reduced folates[21].

Based on stability, detectability and biological occurrence, it was concluded that the desired analytical assay would be able to measure the polylgutamation status of the following folate isoforms: FA (representing the partly oxidized folates: FA and DHF), THF, 5-FTHF or 5,10-MTHF (representing the non methyl folates: 5-FTHF, 10-FTHF and 5,10-MTHF) and 5-MTHF.

7.1.4 Analytical methods for RBC folate measurement

Clinical methods for the determination of folate consist of the microbiological assay[22-23] and various immunoassays or competitive protein binding assays[24-25]. Although sensitive, these assays only measure total folate concentrations, and therefore do not differenciate between folate isoforms or polyglutamation distribution[11]. The presence of antifolates, including MTX, may inhibit bacterial growth and therefore lead to underestimation of folate concentrations in patients on MTX therapy[26], limiting its usefulness for a comparative folate study of JIA patients on and off MTX therapy.

Furthermore, results obtained by these methods demonstrate considerable variability [27-28]. More recently, various HPLC methods have appeared for the measurement of folates in biological matrices. The performance of these methods for folate analysis has been extensively reviewed by Quinlivian et al[26]. Briefly, these chromagraphic based assays demonstrate improved specificity when compared to the microbiological assay and immunoassay, but they often lack sensitivity. More sensitive folate measurement can be achieved by LC with fluorescence detection, however not all folates demonstrate intrinsic fluorescence and therefore this strategy does not allow for comprehensive folate determination[29].

The sensitivity of these assays can be increased by using a folate affinity precolumn and a multi-channel electrochemical detector. This strategy allows for the measurement of the various folate isoforms, and additionally polylgutamation chain length[30]. Disadvantages are that folate affinity columns are unstable (lifetime of 48 h) and binding efficiencies are based on folate isoform, an issue that is further complicated by the absence of reliable internal standards for this technique. Gas chromatography-mass spectrometry methods have for folate analysis have also been presented. These techniques require complex sample preparation schemes, where folates are treated with acid to cleave the different polyglutamated species to para-aminobenzoylglutamates[31-32].

Unfortunately, many of the discussed methods have limited utility for rigorous population studies due to complex sample pretreatment, loss of folate identity and do not compensate appropriately for folate interconversion and degradation during sample analysis. The use of stable isotope dilution LC-MS/MS eliminates many of the earlier

described problems and recently, the first HPLC mass spectrometry based methods for the detection of folates in human plasma[14, 20, 33-35], whole blood[11, 14, 16, 19, 35] and urine[35] have appeared in the literature. Folates are quantitated in the monoglutamated form using [$^{13}C_5$]-labeled internal standards, mimicking the exact structure of the folate species of interest. Erythrocyte folate is typically not directly measured as the various folates are present in the polyglutamated form and extraction is challenging. Whilst some of the aforementioned publications may suggest that erythrocyte folate is measured, these methods in fact measure whole blood folate content after deglutamation[11, 16, 19]. The folates originating from the RBCs can be calculated after correction for the plasma folate content. These strategies have demonstrated accurate quantitation of whole blood/erythrocyte folates, but as a result of the deglutamation procedure, the polyglutamation distribution is lost.

Semi-quantitative comprehensive folate measurement (including polylgutamation status) has been reported for spinach using ion-pair LC-MS/MS[36], and using hydrophilic interaction chromatography for folate profiling of bacteria[37]. Whilst these methods illustrate the ability of LC/MS/MS for the measurement of folate polyglutamates, the absence of (internal)standards renders these methods unsuitable for the reproducible, comprehensive measurement of folates present in RBCs in a large clinical cohort. A method for quantitative comprehensive RBC folate measurement has not appeared in the literature, but as illustrated by a number of recent publications, LC/MS/MS analysis clearly has the required sensitivity and specificity for the detection of the various folate isoforms, including their polyglutamation distribution. This chapter deals with analytical method development of a comprehensive folate detection strategy

in patient RBCs. The presented method has to be applicable for the analysis of large data sets and should demonstrate robustness and reproducibility to the extent that biological variations induced by MTX therapy can be accurately quantitated.
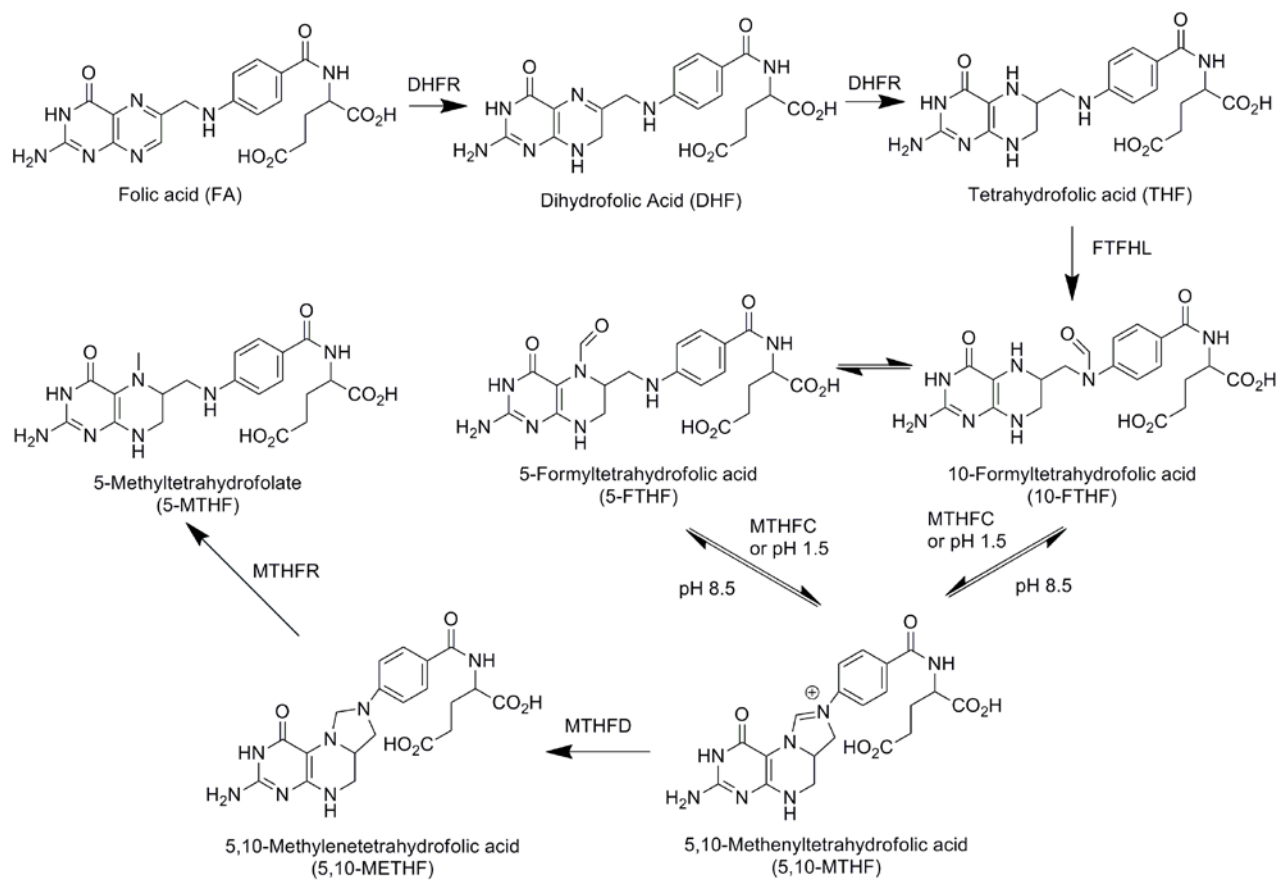
Figure 50. *The folate cycle from a chemical perspective.*

7.2 Experimental

7.2.1 Materials

LC grade solvents acetonitrile (ACN) and methanol (MeOH) were obtained from Fisher Scientific (Fair Lawn, NJ, USA). Ammonium bicarbonate, Ascorbic acid, 2-mercaptoethanol (MCE), N, N-dimethylheptylamine (DMHPA) and methotrexate (MTX) were purchased from Sigma-Aldrich (St Louis, MO, USA). Methotrexate polyglutamation standards 4-amino-10-methylpteroyldiglutamic acid (MTXPG$_2$), 4-amino-10-methylpteroyltriglutamic acid (MTXPG$_3$), 4-amino-10-methylpteroyltetraglutamic acid (MTXPG$_4$), 4-amino-10-methylpteroylpentaglutamic acid (MTXPG$_5$), 4-amino-10-methylpteroylhexaglutamic acid (MTXPG$_6$), 4-amino-10-methylpteroylheptaglutamic acid (MTXPG$_7$) were purchased as the ammonium salts from Schircks Laboratories (Jona, Switzerland). Folates obtained from this source were folicacid/pteroicacid (FA), pteroyldiglutamic acid (FAPG$_2$), pteroyltriglutamic acid (FAPG$_3$), pteroyltetraglutamic acid (FAPG$_4$), pteroylpentaglutamic acid (FAPG$_5$), pteroylhexaglutamic acid (FAPG$_6$), pteroylheptaglutamic acid (FAPG$_7$), 5-formyl-5,6,7,8-tetrahydropteroic acid (5-FTHF),), 5-formyl-5,6,7,8-tetrahydropteroyldiglutamic acid (5-FTHFPG$_2$), 5-formyl-5,6,7,8-tetrahydropteroyltriglutamicacid (5-FTHFPG$_3$), 5-formyl-5,6,7,8-tetrahydropteroyl-tetraglutamic acid (5-FTHFPG$_4$), 5-formyl-5,6,7,8-tetrahydropteroylpentaglutamic acid (5-FTHFPG$_5$), 5-formyl-5,6,7,8-tetrahydropteroylhexaglutamic acid (5-FTHFPG$_6$), 7,8-dihydrofolate (DHF), 5,6,7,8-tetrahydrofolate (THF), 5-methyltetrahydrofolate (5-MTHF), 5,10-methenyltetrahydrofolate (5,10-MTHF), 5,10-methylenetetrahydrofolate (5,10-METHF).

[$^{13}C_5$]-folicacid ([$^{13}C_5$]-FA), [$^{13}C_5$]-tetrahydrofolicacid ([$^{13}C_5$]-THF), [$^{13}C_5$]-5-methyltetrahydrofolate ([$^{13}C_5$]-5-MTHF) and [$^{13}C_5$]-5-formyltetrahydrofolate ([$^{13}C_5$]-5-FTHF) were obtained from Merck Eprova (Schaffhausen, Switzerland).

7.2.2 Preparation of erythrocyte (RBC) lysates and plasma

Blood samples (~5 ml) obtained from patients were centrifuged at low speed (2000 rpm) in a Beckman tabletop centrifuge to pellet the RBCs. After recovery of the plasma, the RBCs were suspended in an equal volume of sterile normal saline, mixed by gentle inversion and subjected to a second low speed centrifugation. The supernatant was discarded and the wash procedure was repeated a second time. After discarding the supernatant, the packed RBCs were divided into four aliquots and stored at -70°C until use.

7.2.3 Analysis of folate polyglutamation distribution

Folate polyglutamates were determined using packed RBC samples. An aliquot of 200µL of packed RBCs was diluted 1:1 with a pH 7.85 HEPES/CHES buffer containing 1% Ascorbic acid and 10 mM MCE, in order to ensure complete RBC lyses and stabilize released folates. Following lyses the RBC extracts were placed in boiling water for 5 minutes to induce protein denaturation. The denatured proteins were packed on the bottom of the vial by centrifugation, using a similar protocol as presented in chapter 5. The supernatant was transferred to an autosampler vial with a 300 µL liner and analyzed by IP-LC-MS/MS.

7.2.4 Whole blood preparation

Prior to analysis, a 5 µL internal standard solution (I.S.) containing 1000 nM of each (anti)folate isoform [$^{13}C_5$]-FA, [$^{13}C_5$]-THF, [$^{13}C_5$]-5-MTHF, [$^{13}C_5$]-5-FTHF and D_3-MTX was added to a 50 µL aliquot of whole blood, resulting in an I.S. concentration of 100 nM in whole blood. The sample was further diluted to 250 µL with a solution of 1% ascorbic acid at pH 4.0. The pH of the resulting solution was determined to be 4.7. Folates(PGs) in the solution were deglutamated by incubating the solution for 3 hours at 37 ˚C. The deglutamated lysates were further worked up by the SPE method of Huang et al[19] (unsuccessful), or by performing a protein precipitation with 40 µL of a 70% perchloric acid solution (successful). Proteins were separated by centrifugation, following the protocol presented in chapter 5. The supernatant was transferred into an autosample vial with a 300 µL liner and analyzed by LC-MS/MS.

7.2.5 Plasma analysis

Sample preparation for plasma folate LC/MS/MS analysis occurred according to Huang et al[19]. Briefly, To each plasma sample (300 µL) was added Wilson and Horne buffer (200 µL) containing 1% ascorbic acid and 10 mM 2-mercaptoethanol. After the addition of 30 µL internal standard solution (I.S. contained 100nM of each anti-folate isoform [$^{13}C_5$]-FA, [$^{13}C_5$]-THF, [$^{13}C_5$]-5-MTHF, [$^{13}C_5$]-5-FTHF and D_3-MTX) the samples were thoroughly mixed (the resulting I.S. concentration is 10nM for each analyte). Water (1 mL) containing 1% ascorbic acid and 1% methanol was added prior to purification using C18 SPE columns. Please refer to Huang et al. for SPE protocol[19].

7.2.6 Chromatographic analysis

Analysis of folate polyglutamation distribution: using the mobile phases and chromatographic system (i.e. column, guard column etc.) as described in chapter 5. An altered gradient elution profile was used. First analytes were focused on the head of the column for 2 minutes at 5% B. A linear gradient was used to 35% B in 8 minutes. A step gradient was used to return to initial conditions, and the column was allowed to re-equilibrate for 3 minutes, resulting in a total runtime of 13 minutes per injection. During the analyte focusing phase, flow from the analytical column was diverted to waste, to prevent non-volatile materials from entering the mass spectrometer. Each sample was analyzed in duplicate, first the various 5-MTHF(PGs) were measured, and in a second injection 5-FTHF(PGs) were measured. Each 25 patients (50 injections) a 50nM MTXPG$_{1-7}$ mixture was analyzed to monitor sensitivity drifts of the mass spectrometer.

Analysis of plasma and whole blood folate distribution: The chromatographic system was as described in chapter 4 and 5. Chromatography was conducted on a 50 x 2.1 mm Phenomenex kinetex column using C18 core-shell particles. Mobile phase A consisted out of water containing 5% acetic acid, and mobile phase B was a blend of 72.5% ACN, 22.5 % MeOH and 5% acetic acid. Gradient elution was used for the separation of the various mono-glutamate folates, starting with an isocratic hold for 1 minute at 1% B, followed by a linear increase to 40% B for 5 minutes. Directly after the elution gradient, a step gradient was used to return to initial conditions and the column was allowed to re-equilibrate for 2 minutes. Analysis volumes were 50 μL for both, plasma and whole blood extracts.

7.2.7 Mass Spectrometry

The instrumentation utilized was a Micromass Quattro Ultima "triple" quadrupole mass spectrometer (Manchester UK) equipped with an electrospray ionization (ESI) source. The instrument was operated in positive ion mode. Source parameters, including the cone voltage for each analyte were optimized by maximizing the area under the curve of multiple LC runs of the standard mixture at various programs. The probe capillary was optimized at 3.0 kV, and the desolvation and source temperatures were set to 400 °C and 125 °C, respectively. The cone gas flow rate was optimized at 80 L/hr, the desolvation and nebulizer gas flow rate was adjusted for maximum signal of analyte. Argon was used for collision induced dissociation (CID) and the cell vacuum was set at 2.4×10^{-3} mbar. Q1 and Q3 were set to transmit ions with a resolution of 0.8 u FWHH. Multiple Reaction Monitoring (MRM) parameters (table 27) including precursor ions, product ions and collision energy were optimized by direct infusion of the individual analytes dissolved in 80% A and 20% B at 10 µM, closely resembling chromatographic conditions.

Table 27. MRM parameters used for the LC/MS/MS analysis of the various pteroyl based entities.

Analyte	Molecular Formula	Precursor ion (m/z)	Product ion (m/z)	Cone Voltage (V)	Collision Energy (V)	ESI mode
FA	$C_{19}H_{20}N_7O_6^+$	442.2	295.1	30	20	+
FAGlu$_2$	$C_{24}H_{28}N_8O_9^+$	571.2	295.1	30	26	+
FAGlu$_3$	$C_{29}H_{36}N_9O_{12}^+$	700.2	295.1	30	33	+
FAGlu$_3$	$C_{34}H_{44}N_{10}O_{15}^+$	829.2	295.1	30	40	+
FAGlu$_5$	$C_{39}H_{52}N_{11}O_{18}^+$	958.3	295.1	30	48	+
FAGlu$_6$	$C_{44}H_{60}N_{12}O_{21}^+$	1087.4	295.1	30	56	+
FAGlu$_7$	$C_{49}H_{68}N_{13}O_{24}^+$	1216.4	295.1	30	64	+
FA	$C_{19}H_{18}N_7O_6^-$	440.2	311.1	25	24	-
FAGlu$_2$	$C_{24}H_{26}N_8O_9-$	569.2	311.1	30	31	-
FAGlu$_3$	$C_{29}H_{34}N_9O_{12}-$	689.2	422.3	40	32	-
FAGlu$_4$	$C_{34}H_{42}N_{10}O_{15}-$	827.3	422.3	50	37	-
FAGlu$_5$	$C_{39}H_{50}N_{11}O_{18}-$	956.3	422.3	55	45	-
FAGlu$_6$	$C_{44}H_{58}N_{12}O_{21}-$	1085.4	422.3	60	50	-
FAGlu$_7$	$C_{49}H_{66}N_{13}O_{24}-$	1214.4	422.3	70	59	-
5-FTHF	$C_{20}H_{24}N_7O_7^+$	470.2	327.1	30	20	+
5-FTHFGlu$_2$	$C_{25}H_{32}N_8O_{10}^+$	603.2	327.1	30	26	+
5-FTHFGlu$_3$	$C_{30}H_{40}N_9O_{13}^+$	732.3	327.1	30	33	+
5-FTHFGlu$_4$	$C_{35}H_{48}N_{10}O_{16}^+$	861.3	327.1	30	40	+
5-FTHFGlu$_5$	$C_{40}H_{56}N_{11}O_{19}^+$	990.3	327.1	30	48	+
5-FTHFGlu$_6$	$C_{45}H_{64}N_{12}O_{22}^+$	1119.4	327.1	30	56	+
5-FTHFGlu$_7$	$C_{50}H_{72}N_{13}O_{25}^+$	1248.4	327.1	30	64	+
5-FTHFGlu$_8$	$C_{55}H_{80}N_{14}O_{28}^+$	1377.5	327.1	30	70	+
5-FTHFGlu$_9$	$C_{60}H_{88}N_{15}O_{31}^+$	1506.5	327.1	30	76	+
5-FTHFGlu$_{10}$	$C_{65}H_{96}N_{16}O_{34}^+$	1635.5	327.1	30	82	+
5-FTHFGlu$_{11}$	$C_{70}H_{104}N_{17}O_{37}^+$	1764.5	327.1	30	88	+
5-FTHF	$C_{20}H_{22}N_7O_7^-$	468.2	315.0	25	20	-
5-FTHFGlu$_2$	$C_{25}H_{30}N_8O_{10}^-$	601.2	315.0	35	26	-
5-FTHFGlu$_3$	$C_{30}H_{38}N_9O_{13}^-$	730.3	454.2	40	33	-
5-FTHFGlu$_4$	$C_{35}H_{46}N_{10}O_{16}^-$	859.3	454.2	50	40	-
5-FTHFGlu$_5$	$C_{40}H_{54}N_{11}O_{19}^-$	988.4	454.2	60	48	-
5-FTHFGlu$_6$	$C_{45}H_{62}N_{12}O_{22}^-$	1117.4	454.2	70	56	-
5-FTHFGlu$_7$	$C_{50}H_{70}N_{13}O_{25}^-$	1246.5	454.2	80	64	-
5-FTHFGlu$_8$	$C_{55}H_{78}N_{14}O_{28}^-$	1375.5	454.2	90	70	-

Table 27. continued

Analyte	Molecular Formula	Precursor ion (m/z)	Product ion (m/z)	Cone Voltage (V)	Collision Energy (V)	ESI mode
5-MTHF	$C_{20}H_{26}N_7O_6^+$	460.2	313.1	30	20	+
5-MTHFGlu$_2$	$C_{25}H_{34}N_8O_9^+$	589.2	313.1	30	26	+
5-MTHFGlu$_3$	$C_{30}H_{42}N_9O_{12}^+$	718.3	313.1	30	33	+
5-MTHFGlu$_4$	$C_{35}H_{50}N_{10}O_{15}^+$	847.3	313.1	30	40	+
5-MTHFGlu$_5$	$C_{40}H_{58}N_{11}O_{18}^+$	976.4	313.1	30	48	+
5-MTHFGlu$_6$	$C_{45}H_{66}N_{12}O_{21}^+$	1105.4	313.1	30	56	+
5-MTHFGlu$_7$	$C_{50}H_{74}N_{13}O_{24}^+$	1234.4	313.1	30	64	+
5-MTHFGlu$_8$	$C_{55}H_{82}N_{14}O_{27}^+$	1363.5	313.1	30	70	+
5-MTHFGlu$_9$	$C_{60}H_{90}N_{15}O_{30}^+$	1492.5	313.1	30	76	+
5-MTHFGlu$_{10}$	$C_{65}H_{98}N_{16}O_{33}^+$	1621.5	313.1	30	82	+
5-MTHFGlu$_{11}$	$C_{70}H_{106}N_{17}O_{36}^+$	1750.6	313.1	30	88	+
THF	$C_{19}H_{24}N_7O_6^+$	444.2	299.1	30	20	+
THFGlu$_2$	$C_{24}H_{32}N_8O_9^+$	575.2	299.1	30	26	+
THFGlu$_3$	$C_{29}H_{40}N_9O_{12}^+$	704.3	299.1	30	33	+
THFGlu$_4$	$C_{34}H_{48}N_{10}O_{15}^+$	833.3	299.1	30	40	+
THFGlu$_5$	$C_{39}H_{56}N_{11}O_{18}^+$	962.4	299.1	30	48	+
THFGlu$_6$	$C_{44}H_{64}N_{12}O_{21}^+$	1091.4	299.1	30	56	+
THFGlu$_7$	$C_{49}H_{72}N_{13}O_{24}^+$	1220.4	299.1	30	64	+
THFGlu$_8$	$C_{54}H_{80}N_{14}O_{27}^+$	1349.5	299.1	30	70	+
THFGlu$_9$	$C_{59}H_{88}N_{15}O_{30}^+$	1478.5	299.1	30	76	+
THFGlu$_{10}$	$C_{64}H_{96}N_{16}O_{33}^+$	1607.5	299.1	30	82	+
THFGlu$_{11}$	$C_{69}H_{104}N_{17}O_{36}^+$	1736.6	299.1	30	88	+
DHF	$C_{19}H_{22}N_7O_6^+$	442.2	297.1	30	20	+
5,10-MTHF	$C_{20}H_{22}N_7O_6^+$	456.2	412.1	25	32	+
$^{13}C_5$-FA	$C_{19}H_{20}N_7O_6^+$	447.2	295.1	30	20	+
$^{13}C_5$-THF	$C_{19}H_{24}N_7O_6^+$	451.2	299.1	30	20	+
$^{13}C_5$-5MTHF	$C_{20}H_{26}N_7O_6^+$	465.2	313.1	30	20	+
$^{13}C_5$-5,10-MTHF	$C_{20}H_{22}N_7O_6^+$	461.2	416.1	25	32	+

7.3 Results and discussion

7.3.1 The development of a quantitative assay (rationale)

7.3.1.1 The folate standard problem

Table 28. Commercial availability of various folate standards

Folate (methylation/redox state)	Length of the glutamyl-chain							Source if available
	1	2	3	4	5	6	7	
Folic acid	X	X	X	X	X	X	X	Schircks
7,8-Dihydrofolate	X	-	-	-	-	-	-	Schircks
5,6,7,8-Tetrahydrofolate	X	-	-	-	-	-	-	Schircks
5-Methyltetrahydrofolate	X	-	-	-	-	-	-	Schircks
5-Formyltetrahydrofolate	X	X	X	X	X	X	-	Schircks
10-Formyltetrahydrofolate	O	-	-	-	-	-	-	Schircks
5,10-Methylenetetrahydrofolate	X	-	-	-	-	-	-	Schircks
5,10-Methenyltetrahydrofolate	X	-	-	-	-	-	-	Schircks
$^{13}C_5$-Folic acid	X	-	-	-	-	-	-	Merck Eprova
$^{13}C_5$-Tetrahydrofolate	X	-	-	-	-	-	-	Merck Eprova
$^{13}C_5$-5-Formyltetrahydrofolate	X	-	-	-	-	-	-	Merck Eprova
$^{13}C_5$-5-Methyltetrahydrofolate	X	-	-	-	-	-	-	Merck Eprova
$^{13}C_5$-5,10-Methenyltetrahydrofolate	O	-	-	-	-	-	-	Merck Eprova

X = commercially available and purchased, - indicates that compounds were not commercially available, O = indicates commercially available but the compound was not obtained

The development of a comprehensive folate detection strategy (i.e the detection of redox, methylation and polyglutamation state) within RBCs is complicated by the limited availability of standards. Whilst ($^{13}C_5$-labelled) folates are generally available in the various methylation and redox states as the monoglutamates, their polyglutamated forms are in general unavailable on a commercial basis (table 28). The only polyglutamated folate species that could be obtained in a sequential series were the folic acid polyglutamates (1-7) and 5-formyltetrahydrofolate polyglutamates (1-6). As discussed earlier one would expect 5-methyltetrahydrofolate as the dominant folate species within RBCs donated by individuals that were genotyped as MTHFR 677 CC

homozygotes or CT heterozygotes (accounting for 90% of the Caucasian population). Significant levels of THF and 5-formylTHF/5,10-methenylTHF (depending on pH of the analyzed solution) have been reported in individual that were classified as MTHFR 677 TT homozygotes. With the exception of 5-formylTHF, that is available up to the hexaglutamyl chain, standards of the most biologically relevant polyglutamated folates of interest for this research are commercially unavailable. The absence of these standards complicates the development of a quantitative analytical assay. First the mass spectrometer cannot be tuned for the specific compounds, and second the absence of standards eliminate the possibility to appropriately calibrate the analytical procedure.

The synthesis of the commercially unavailable folate polyglutamation standards is a complicated task, and requires the use of cell culture methodology or a partially purified folylpolyglutamase enzyme. The purification of the various folates is further complicated by the fact that different redox-forms readily can readily interconvert depending on pH and/or the presence of oxygen. Furthermore one has to realize that the measurement of folates in human erythrocytes is even further complicated by the endogenous nature of folates. Even if folate standards were available or obtained, external calibration would still be impossible since folate depleted (i.e. blank) RBCs are not available. Quantification using these standards could however occur by the standard addition method. The standard addition quantification method relies on enrichment (addition) of a number of aliquots of the sample with known amounts of calibrants. After analysis of these samples, an analyte concentration can be obtained through extrapolation. Since basically each sample is calibrated in its own matrix, standard addition is rather labor intensive and due to the fact that sample splitting has to occur a much larger sample size is required. As RBC sample size was limited (100 – 200 µL of

RBCs depending on the sample) together with the level of difficulty involving synthesis of the standards, this strategy was abandoned. While the synthesis of stable isotope enriched folate standards would eliminate the need for standard addition quantification, this solution requires a complex and costly synthetic procedure. As the implications and applications of comprehensive folate are not yet understood this strategy was not pursued either. Based on these various considerations it was concluded that analytical method development had to occur with the use of commercially available standards, despite certain limitations.

7.3.1.2 A (semi-)quantitative assay for the measurement of the folateome in RBCs

Since the goal of analytical method development was the comprehensive measurement of folates within the RBCs of JIA patients, in order to measure variations in folate (polylgutamation) status, we designed a (semi)-quantitative analysis strategy staying within the constraints that commercially available standards had to be used. Recently a number of LC-MS/MS have been presented for the quantitative "indirect" measurement of intracellular folate concentrations within RBCs. Whilst each publication presented a unique sample preparation method, the analysis strategy was common and relied on a folate deglutamation procedure using a whole blood sample of the patient (details will be presented in section 7.3.3.2. of this chapter). As a result of the deglutamation procedure utilizing whole blood, the folates are quantitated as the monoglutamate species and represent whole blood folate content, rather than RBC concentrations of the individual. Since whole blood is largely composed of a plasma and RBC components, the measured concentration is the result of the sum of the folate

contribution by each individual component. Thus if the folate plasma concentration is known besides whole blood folate concentration, RBC folate content can be calculated according to the method of Lamers et al.[38] (eq. 3).

$$RBC\ folate = \frac{(whole\ blood\ folate\ x\ 100) - (Plasma\ folate\ x\ (100 - hematocrit))}{hematocrit} \qquad \text{Eq. 3}$$

The advantage of this strategy is two-fold. 1) Deglutamation liberates the various polyglutamates and measurement of deglutamated species reduces number of folate metabolites that have to be tracked by LC-MS/MS. An additional advantage is that the redox/methylation status remains unaltered during this process, effectively converting a distribution of metabolites (i.e. polyglutamates) to a single measurable species, and thus enhancing its detectablility. 2) Stable isotope labeled monoglutamyl-folate standards of all of the folates of interest are commercially available (table 28), allowing for accurate quantification using stable isotope dilution LC-MS/MS.

There are also disadvantages to this strategy, such as the requirement for an additional assay, detecting plasma folate content. However, because of the similarities in whole blood and plasma folate measurement this development is reasonably straightforward. A more severe disadvantage of the strategy presented in the previous paragraph is loss of the polyglutamation distribution fingerprint within the RBC, an essential component of our desired assay.

It was hypothesized that this information could be obtained by the incorporation of a third assay (in addition to the folate whole blood and plasma measurements) using isolated RBCs from the patient. It is reasonable to assume that the clinical assay for the

determination of MTXPG status could be transferred (including sample preparation) into a method for the detection of the various folate polyglutamates. Since most of the polyglutamated folates are not available this assay would provide a more semi-quantitative/or relative "snapshot" of folate distribution within the RBC. A schematic overview of the total analysis strategy is presented in figure 51. The following sections will deal with the development of the individual assays; whole blood folate analysis, plasma folate analysis, and RBC polyglutamation profiling respectively.
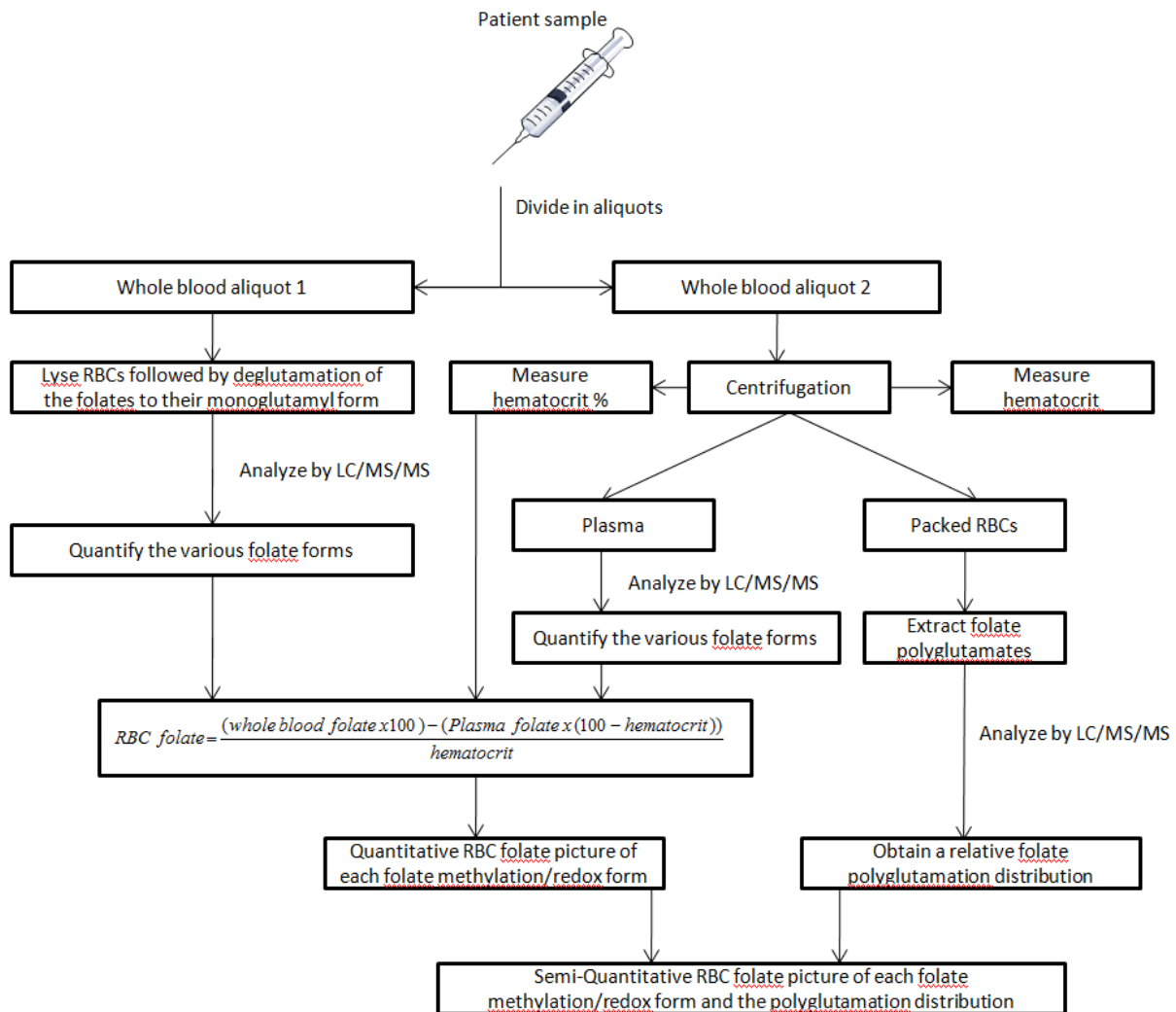
Figure 51. *Schematic overview of the proposed analytical method for comprehensive erythrocyte folate measurement.*

7.3.2 Polyglutamation profiling

7.3.2.1 Polyglutamation profiling on a relative basis using patient RBCs

As stated in the method development rationale (section 7.3.1), the measurement of the folate polyglutamation distribution is challenged by the absence of standards, and therefore quantitation is virtually impossible since calibration cannot be accomplished. However to investigate the influence of MTX therapy on the folate distribution (using RBCs) in JIA patients an absolute quantitative measurement of this distribution is not a requirement, since one is interested in the MTX induced folate polyglutamation variability. Therefore the hall-mark of the polyglutamation profiling assay became; reproducible measurement of the relative polyglutamyl distribution of the various folate methylation/redox states. The term relative polyglutamyl distribution should be interpreted as measurement of the "observed" or relative distribution by mass spectrometry, rather than measurement of the true folate polyglutamation distribution on an absolute quantitative basis, that would require standards and calibration to correct for differences in recovery and instrument related sensitivity of the individual analytes.

7.3.2.2 FolatePGs mass spectrometry settings.

Based on the successful separation of $FAPG_{1-7}$ in chapter 5 (internal standard selection for MTXPG analysis), it was hypothesized that the IP-LC/MS/MS method presented in chapter 4 and 5 could be applied in a slightly modified fashion for the measurement of the remaining folatepolyglutamates (THF, 5-MTHF, 5,10-MTHF and 5-FMTHF). Since polyglutamation standards of THF and 5-MTHF and 5,10-MTHF were

unavailable mass spectrometer settings for MRM had to be estimated. It was observed that the sequential polyglutamates of MTX, FA and 5-FTHF under positive ESI conditions all produced predominantly the singly charged $(M+H^+)$ ion. Furthermore all of these molecules yielded a charged pteroate species upon collision induced dissociation. This pteroyl residue serves as the common reporter ion for all of the explored polyglutamated species. In order to maximize the signal for the charged pteroyl fragment, it was observed that a linear increase in collision energy was necessary (figure 52A for FAPGs, figure 52B for 5-FTHFPGs, and figure 52C for MTXPGs). Furthermore the fragmentation behavior of the pteroyl chain appeared to be independent of ring redox/methylation state. Based on these observations, MRM settings for the measurement of 5-MTHFPG$_{1-12}$, THFPG$_{1-12}$, FAPG$_{8-12}$ and 5-FTHFPG$_{7-12}$ were extrapolated (table 27).
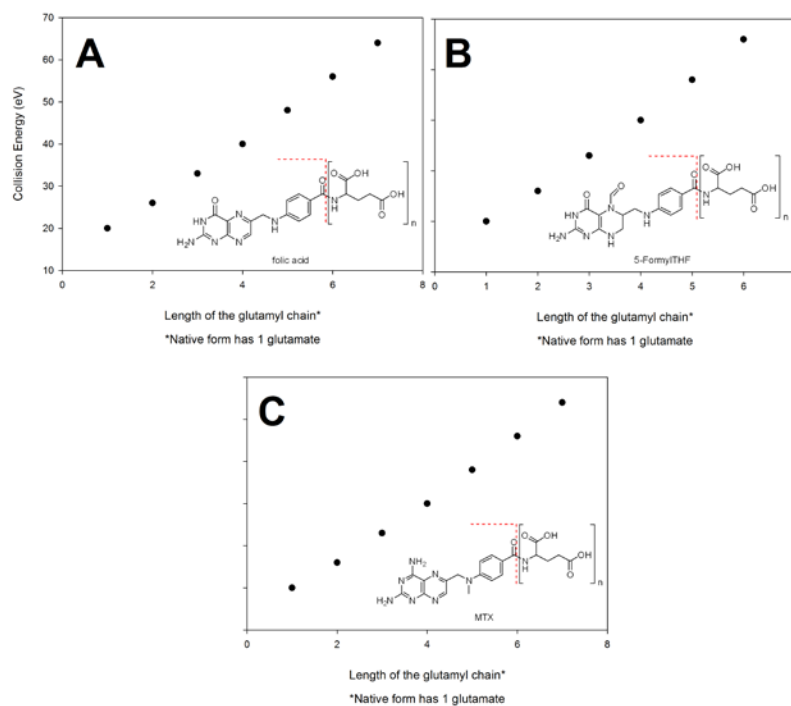
Figure 52. *Collision energy plots for optimal formation of the pteroyl residue by MS/MS.*

7.3.2.3 Folatepolyglutamate extraction from RBCs

In order to measure RBC folate distribution, folate extraction has to occur, and thus a sample preparation procedure had to be developed. As mentioned earlier in the dissertation, (anti-)folates are highly protein/tissue bound in mammalian tissues and are not readily available for analysis/extraction. Therefore it is reasonable to assume that folate extraction suffers from the same problems that were reported for MTXPG extraction in chapter 4 and 5. Furthermore, extraction of the various folates is further complicated by unique (in)stabilities associated with each folate form. For example, acid extraction that was useful for the extraction of MTXPGs, as described in chapter 4, could not be applied for folate extraction as THF demonstrates poor acid stability. As MTXPGs could be released from the RBCs by heat extraction (chapter 5) a similar strategy was explored for the extraction of folates. To stabilize the folate pool, packed RBC samples were diluted in a 1 to 1 ratio with a pH 7.85 Wilson and Horne buffer, including ascorbic acid and mercaptoethanol. The interconversion stability of various deglutamated folate forms under these conditions within the RBC matrix has been demonstrated by Smulders et al[16]. The interconversion stability of the polyglutamates of interest (i.e. 5-MTHF and THF) could not be tested but were assumed to be stable since the problematic molecular interconversions are associated with the pteroyl functionality of the polyglutamated folate molecules, as opposed to the poylglutamatyl chain length.

Another concern is deglutamation stability during sample preparation. Since the packed RBCs immediately washed following isolation, the presence of the deglutamation enzyme (pteroylpoly-ɣ-glutamylcarboxypeptidase) is highly unlikely. Furthermore the pH of the RBC lysate of 7.85 is too alkaline for optimal human

pteroylpoly-ɣ-glutamylcarboxypeptidase activity, and thus deglutamation is not expected. In order to demonstrate the absence of folate deglutamation during the sample preparation procedure, a 1:1 diluted RBC sample with extraction buffer was enriched with 100 nM of hexa-glutamyl folic acid. The hemolysate was allowed to incubate for 15 minutes, before folates were extracted by a 5 minute boiling extraction. Three replicate experiments demonstrated that deglutamation does not occur within this time frame. As the other polyglutamated folates were not available for testing, the glutamyl chain of the additional folates were assumed to be stable during sample extraction.

7.3.2.4 Chromatography and RBC folate polyglutamation analysis

As standards were unavailable, the chromatography method initially developed for the analysis of MTXPGs (chapter 5) was adapted for RBC folate extracts. RBC samples, drawn from eight healthy volunteers on site, were used for folate method development as they were readily available. Each volunteer was genotyped for MTHR polymorphism, as this appears to be the main predictor of intracellular folate redox/methylation state distribution. It was found that all of the available donors fell either in the 677 CC or 677 CT category, meaning that their folate pool was largely (> 90%) present in the methylated form (5-MTHF). These RBC samples therefore provided a solid basis for the development of the 5-MTHFPG assay. Using these RBCs, a fast separation of the 5-MTHFPG species was obtained using gradient elution, consisting of a 2 minute isocratic hold at 5% B (focusing the analytes), followed by a rapid gradient to 35% B in 8 minutes (gradient profile is illustrated in figure 53A).

The optimized chromatographic procedure was applied for polyglutamation profiling of a JIA patient on MTX therapy (figure 53B, demonstrating the total ion current). The various 5-MTHFPGs were separated within 10 minutes, and the polyglutamation length appears to be centered around 5-6 glutamyl residues (please note that this is an observed distribution). The same data is also presented in figure 54, where the individual channels are plotted as opposed to the total ion current (figure 53 B). Using the individual SIR channels, it became appearant that 5-MTHF was distributed between 3 and 10 glutamyl residues.

As mentioned before 5-FTHF(PGs), 10-FTHF(PGs) and 5,10-MTHF(PGs) readily interconvert in an pH governed equilibrium process. At acidic pH values the dehydrated form 5,10-MTHF dominates, and at alkaline pH values the formylated (hydrated) forms are exclusively formed. The sample pH is often altered during sample preparation, disturbing the equilibrium between these folate forms. Therefore these different folates are often analyzed as a group, at acidic pH (measurement of 5,10-MTHF) or alkaline pH (measurement of 5-FTHF). The analysis of the formylated (monoglutamated) form is not commonly performed as it requires the use of basic mobile phases that are in general incompatible with silica-based chromatography columns. Furthermore peak shapes in general are poor for this particular analyte.

Since the pH during RBC folatepolyglutamate extraction has to be close to 8, in order to accomplish precipitation of the proteins (chapter 5 figure 39), the equilibrium between 5-FTHF(PGs), 10-FTHF(PGs) and 5,10-MTHF(PGs) lies exclusively in favor of 5-FTHF(PGs). Additionally, the pH of the mobile phase was also fixed at 8.0, and therefore 5-FTHF was identified as the analytical reporter for this folate pool. From the analysis of the polyglutamyl-5-MTHFs it became clear that long polyglutamate chains

could be expected, and since these standards are not available, the method was optimized using RBC samples.

As the content of non-methyl folates is low in MTHFR 677 CC and 677 C>T phenotypes , which are also the phenotypes of the healthy voluntary RBC donors, these RBCs samples were found to be inadequate for 5-FTHFPG method development. Patient 46 of the folate group was identified as a 677 TT homozygote and therefore it is expected that the folate distribution in the RBC sample of this patient is shifted from the methylated- towards the non-methylated (i.e. formylated, THF, 5,10-MTHF) form, providing a basis for initial method development, as formylated species are typically the highest in this phenotype.

A chromatogram of the RBC extract from patient 46, analyzing for 5-FTHFPG species is demonstrated in figure 55. A similar polyglutamation distribution was observed for the 5-FTHFPGs when compared to the 5-MTHFPGs (figure 53B), demonstrating the ability of the chromatographic method to measure 5-FTHFPGs in addition to the 5-MTHFPGs. In general however, chromatograms for 5-FTHFPGs were much more complicated to analyze, due to the appearance of an additional peak (figure 55). The peak was well separated for 5-FTHFPG$_{4-5}$, but the resolution between the two compounds diminishes quickly when polylgutamation chain length was further increased. It was hypothesized that the additional peak indicated the presence of 10-FTHF. As the difference between 5-FTHF and 10-FTHF is the position of the formylgroup, both compounds are isobaric. Furthermore, these compounds could not be separated by collision induced dissociation in the gas phase as the formylgroup remains on the measured pteroyl-fragment. For the dominant species 5-THFPG$_{5-6}$ signal

integration was in particular compromised by the large elution volume of the 5-FTHF/10-FTHF mixture, increasing the chance of co-integration of interferents.

THF could also be measured in its polyglutamated form, in the RBC sample of a JIA patient, classified as a 677 TT phenotype (figure 56). Despite the fact that polyglutamation profiling was technically possible, the patient group was not analyzed for THFPGs, because THF could not be accurately quantitated by the whole blood assay (section 7.3.3.3).

7.3.2.5 Multiple injects for polyglutamation profiling of various folate redox/methylation states

As described in chapter 5 the scan rate of the Ultima mass spectrometer limits the amounts the amount of SIR channels that could be monitored simultaneously. Therefore, when analyzing patient samples, multiple chromatographic runs per sample were made, with each injection being specific for a class of folates (1st run detecting 5-MTHF, 2nd sample introduction detecting 5-FTHF, etc). A faster scanning instrument would be desirable in these experiments as it would allow for simultaneous determination of the various analytes in a single run, reducing the required sample volume and increasing sample throughput

7.3.2.6 Robustness of the polyglutamation assay, response factors and data interpretation

The previous section demonstrates the ability of the analysis method to measure 5-MTHFPGs, 5-FTHFPGs and THFPGs, however reproducibility has to be addressed if one wishes to compare the polyglutamation distribution of the two large patients pools (JIA patients on MTX therapy (n=100), and JIA patients without MTX treatment (n=100)). As the goal of the polyglutamation analysis method was to measure the relative distribution of the various folate polyglutamates (i.e. a polyglutamate is expressed as a fraction (%) of the total folate distribution (100%) of a certain methylation/redox state), drifts in overall sensitivity of the detector, variations in volumes due to pipetting error etc, will not affect the observed polyglutamation pattern, and in that regard the method can be considered robust. However, during method development for MTXPG analysis, it was observed that a "dirty" ion-path in the mass spectrometer led to diminishing sensitivity of the instrument, with the high molecular weight compounds affected more severely. This type of drift was not much of a concern in MTXPG analysis as timely calibration corrects for such processes. However in relative quantitation experiments, with analytes displaying a wide mass range, such a drift in sensitivity should be accounted for as this sensitivity diminishment in high molecular weight detection would result in a change in relative appearance of the folate polyglutamates (i.e. the observed distribution would shift to shorter polyglutamyl length). In order to minimize the effects of mass related sensitivity drifts of the mass spectrometer on the folate polyglutamation data set, all patient samples were sequentially analyzed after a thorough instrument cleaning (i.e. front-end, hexapoles and transfer lenses). The drift in mass related instrument sensitivity

227

was probed by the analysis of an aqueous solution (50 nM) of MTXPGs$_{1-7}$ after each batch of 25 injections. The use of MTXPG$_{1-7}$ over FAPG$_{1-7}$ was made on a stability basis, with MTXPG$_{1-7}$ demonstrating excellent aqueous stability, allowing repetitive analysis of the same solution over the 4 days time course of folate polyglutamation analysis. From the relative response of the various MTXPGs one could estimate the mass related sensitivity drifts of the mass spectrometer and correct accordingly using the concept of response factors. Chromatograms of the MTXPG mixture after 0, 100, 200 and 400 folatepolyglutamate injections are demonstrated in figure 57. It was observed that while overall sensitivity of the mass spectrometer changed a factor 1.5 (note the y-axis scale), the observed relative distribution of the various MTXPG molecules was not affected. Therefore it was believed that correction, using response factors was unnecessary and for all of the analyzed samples, polyglutamation patterns are reflective of their true relative peak areas.
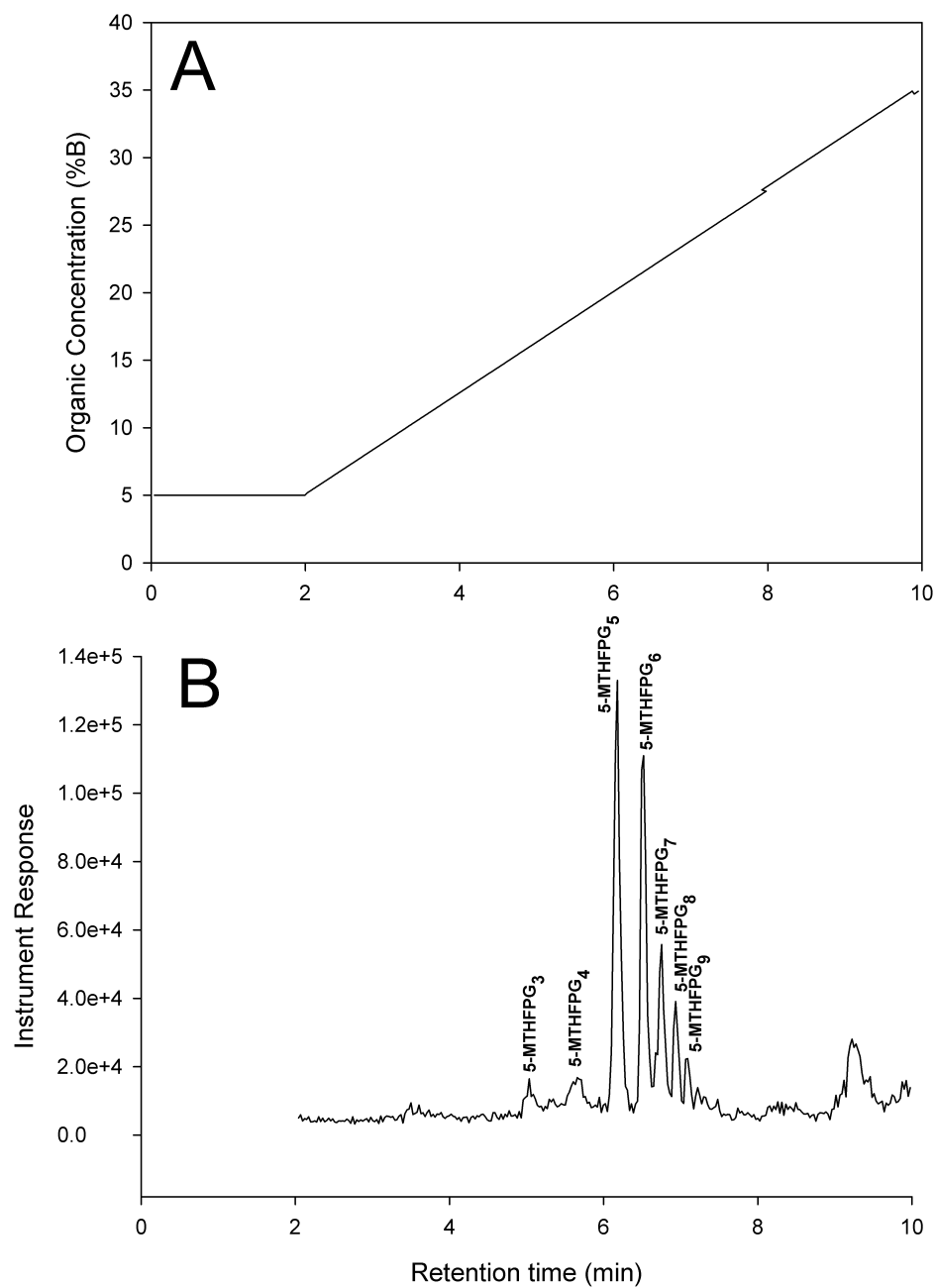
Figure 53. *Method development for the detection of 5-MTHFPGs, (A) optimal gradient for rapid separation of the various 5-MTHFPGS. (B) Total ion current chromatogram demonstrating the separation of 5-MTHFPG$_{3-10}$ in a RBC extract obtained from a donor that was a MTHFR 677 CC genotype.*
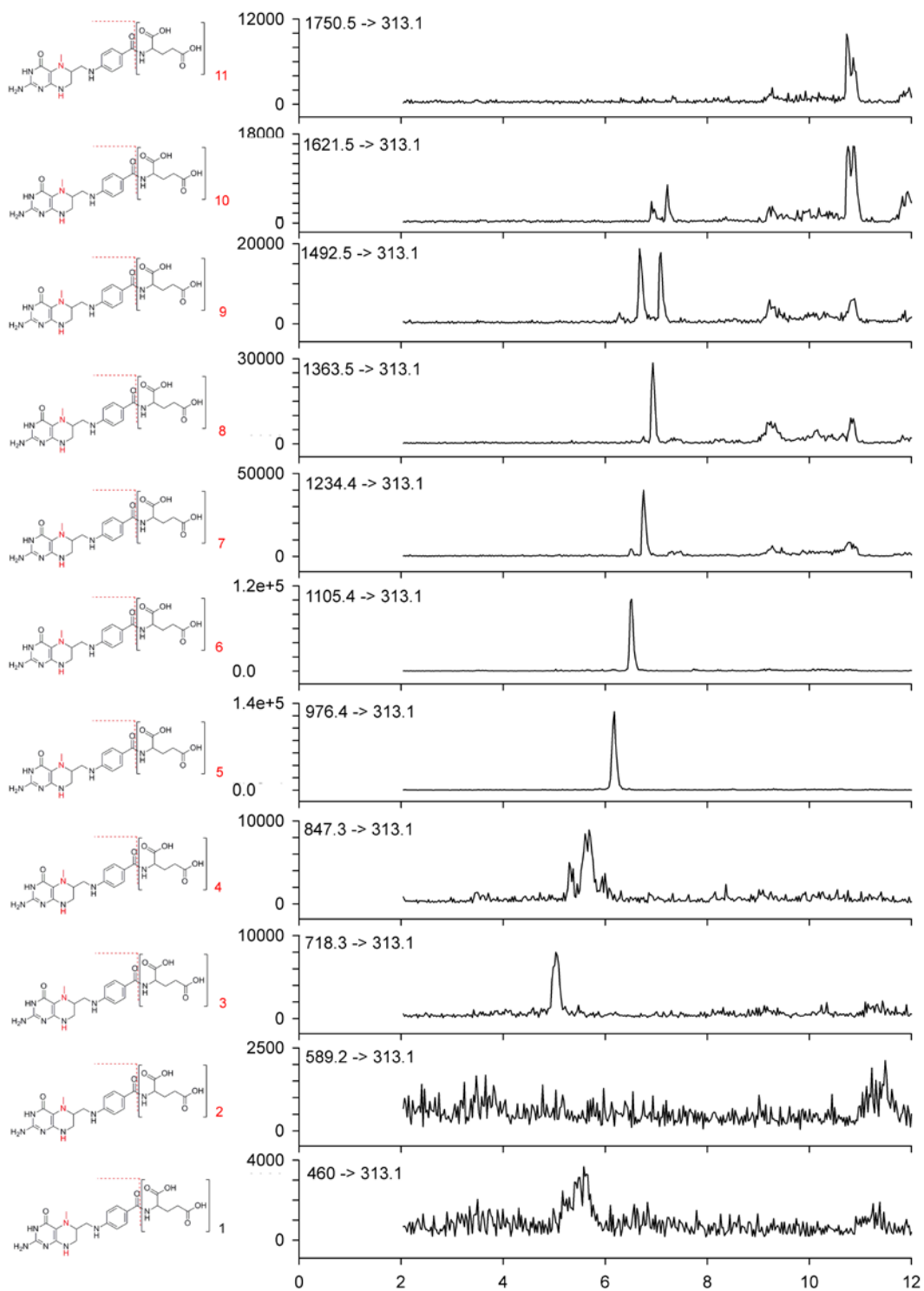
Figure 54. *Individual MRM channels for each 5-MTHFPG.*

230
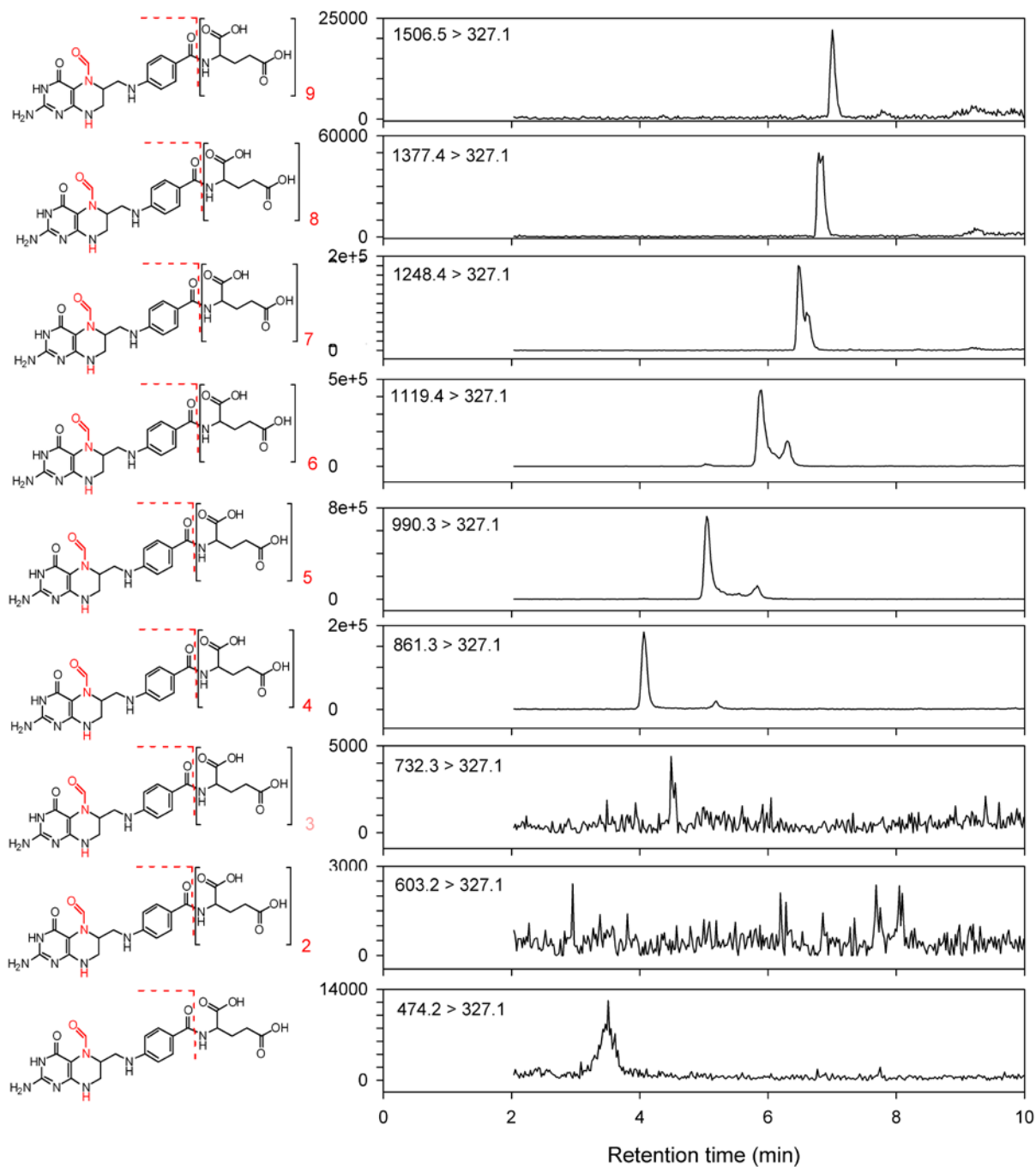
Figure 55. *5-FTHFPGs chromatogram of a RBC extract obtained from patient 46 in the folate control group that was identified as a MTHFR 677 TT homozygote.*
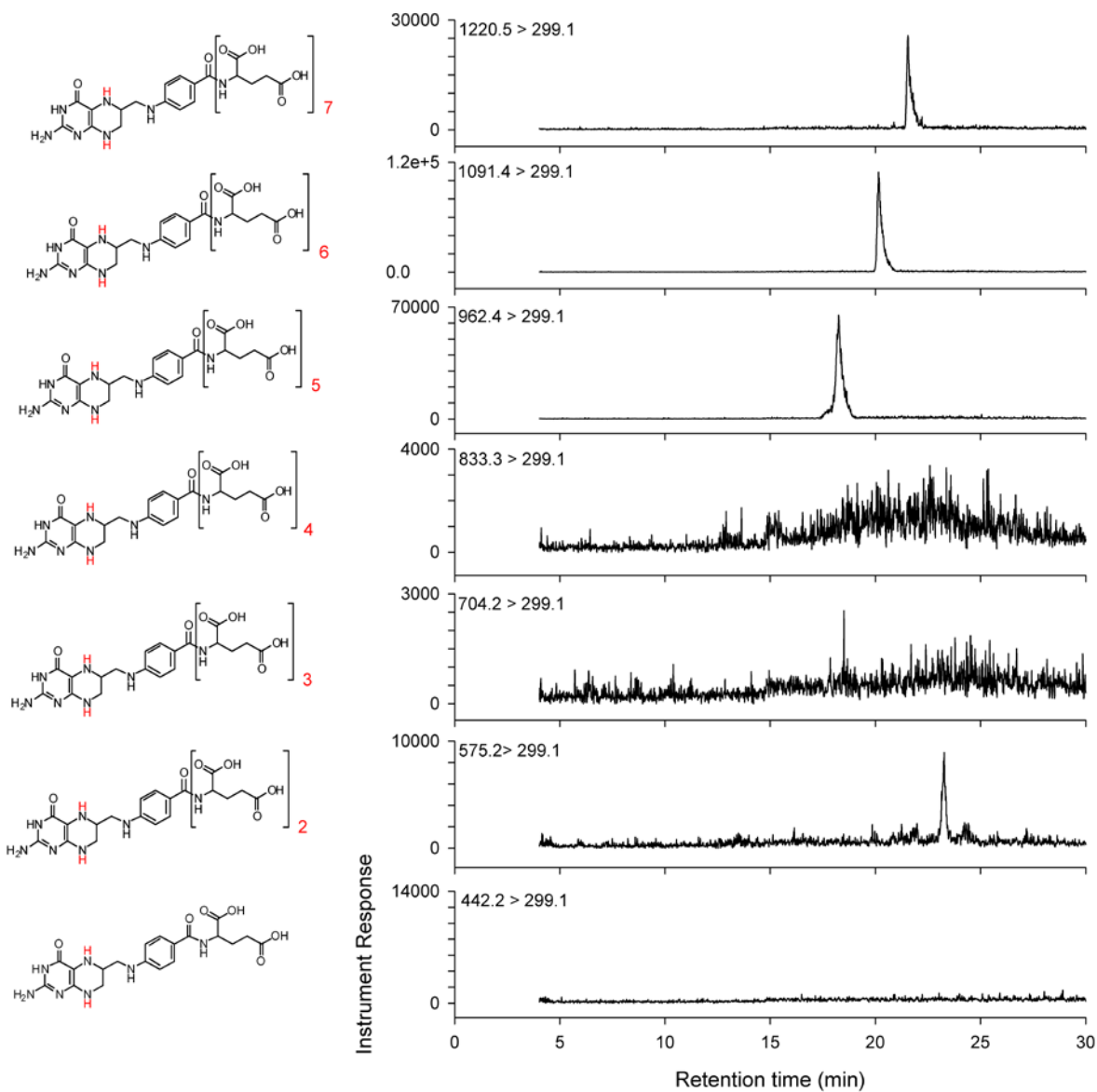
Figure 56. *Chromatogram analyzing the RBC extract from patient 46 for THFPGs.*

232
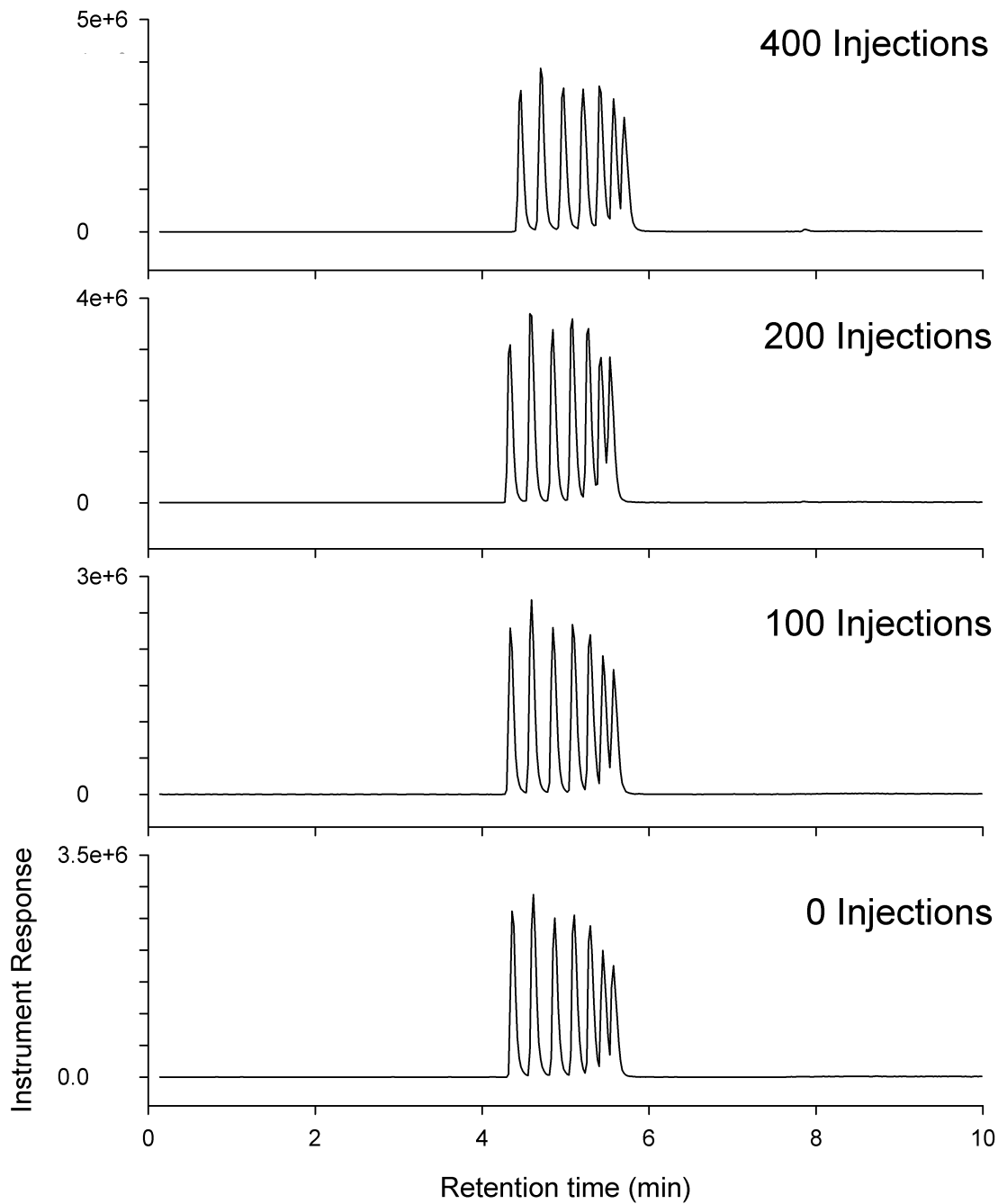
Figure 57. *Analysis of an aqueous 50 nM MTXPG$_{1-7}$ mixture to monitor (mass related) sensitivity drifts of the mass spectrometer during the folate polyglutamation profiling of patient RBCs. The sensitivity was relatively constant over the entire sample set, and therefore correction using response factors was not necessary.*

7.3.3 Whole blood folate analysis

The previous section described method development for the relative measurement of folate polyglutamation status. As presented in section 7.3.1, the quantification of RBC folate has to occur through an alternative indirect route, involving folate analysis in whole blood and plasma, due to absence of standards. The first step, in whole blood analysis is cell lysis and deglutamation of the various folatepolyglutamates to their mono-glutamyl-analogs. Since isotope labeled mono-glutamyl-folate standards are commercially available, folates can be quantified accurately using stable isotope dilution mass spectrometery. The following sections deal with the individual analytical components required for successful whole blood folate analysis.

7.3.3.1 Deglutamation

Folate deglutamation is catalyzed by the pteroylpoly-ɣ-glutamylcarboxypeptidase enzyme. This enzyme has also been called pteroyl-y-glutamate hydrolase, or folate hydrolase, and even the misleading term folate conjugase has been used. For the folate analysis in various food products external sources of pteroylpoly-ɣ-glutamylcarboxypeptidase are used. Commonly used sources of pteroylpoly-ɣ-glutamylcarboxypeptidase are: hog kidney, chicken pancreas or rat plasma. The pH range where optimal enzyme activity is obtained varies with the enzyme source, from 4.5 for hog kidney to 7.5 for chicken pancreas pteroylpoly-ɣ-glutamaylcarboxypeptidase.

Pteroylpoly-ɣ-glutamylcarboxypeptidase is also present in the human plasma, where it plays an important role in the deglutamation of consumed folates, a process

which is essential for folate absoption and bioavalability. Researchers have taken advantage of the presence of pteroyl-ɣ-glutamylcarboxypeptidase in plasma, by using it as an "auto-deconjugase" in human whole blood folate assays, where red blood cell lysis is induced to expose their folate content to the plasma pteroyl-ɣ-glutamylcarboxypeptidase enzyme, resulting in folate deglutamation.

The optimal conditions for folate polylgutamate conversion have been the subject of a number of recent papers discussing methodology for the measurement of RBC folate concentent. As each of the presented analytical methods was geared to folate measurement in the monoglutamated or diglutamated form, reproducible analytical recovery of the deglutamation process was the hall-mark. In 2005 Fazili et al. published a report where the important reaction (i.e. deglutamation) variables, pH, temperature and time required to obtain quantitative deglutamation were investigated. It was concluded optimal deconjugation condition consisted of 3 a hour incubation of the hemolysate, at a pH of 4.7, with the temperature fixed at 37 °C. Furthermore it was demonstrated that by the use of ascorbic acid as anti-oxidant, folate interconversion was avoided through the entire procedure.

Whilst this method of preparing deconjugated folate hemolysates has been generally accepted, the incubation period has often been shorter (in contrast to what Fazili had demonstrated). Smulders et al. used deconjugation times of 90 minutes, Zhang et al. used 4 hours at room temperature. As we have developed a strategy to measure the various individual folate polyglutamates, we studied the deglutamation behavior of 5-MTHPGs in whole blood at pH 4.7, incubated at 37°C (figure 58 A). At 0 minutes of incubation (the pH of the solution was adjusted to 4.7 and titrated back up to approximately pH 7.8 with HEPES/CHES buffer before placing it in boiling water) a

spectrum of 5-MTHF species were observed up to 5-MTHFPG$_9$. After 10 minutes of incubation the observed polyglutamation picture had shifter significantly in towards the short chain mono- and di-glutametes (figure 58B), demonstrating the deglutamation capability of human plasma. After 60 minutes of incubation (figure 58C), the deglutamation was 97.4% complete (i.e. 97.4% was in the 5-MTHF monoglutamate form and 2.6% was in the diglutamate form). After 2 hours the deglutamation procedure was 99.3% complete (figure 58D). 5-MTHF could not be detected after 3 hours of incubation (results not shown), consistent with the statements made by Fazili. Conveniently the 100 µL pH whole blood lysate could be adjusted to 4.7 by the addition of 100 µL of a 10 g/L (1% W/W) solution of ascorbic acid solution, therefore redox stabilization and pH adjustment occurred in a single step.
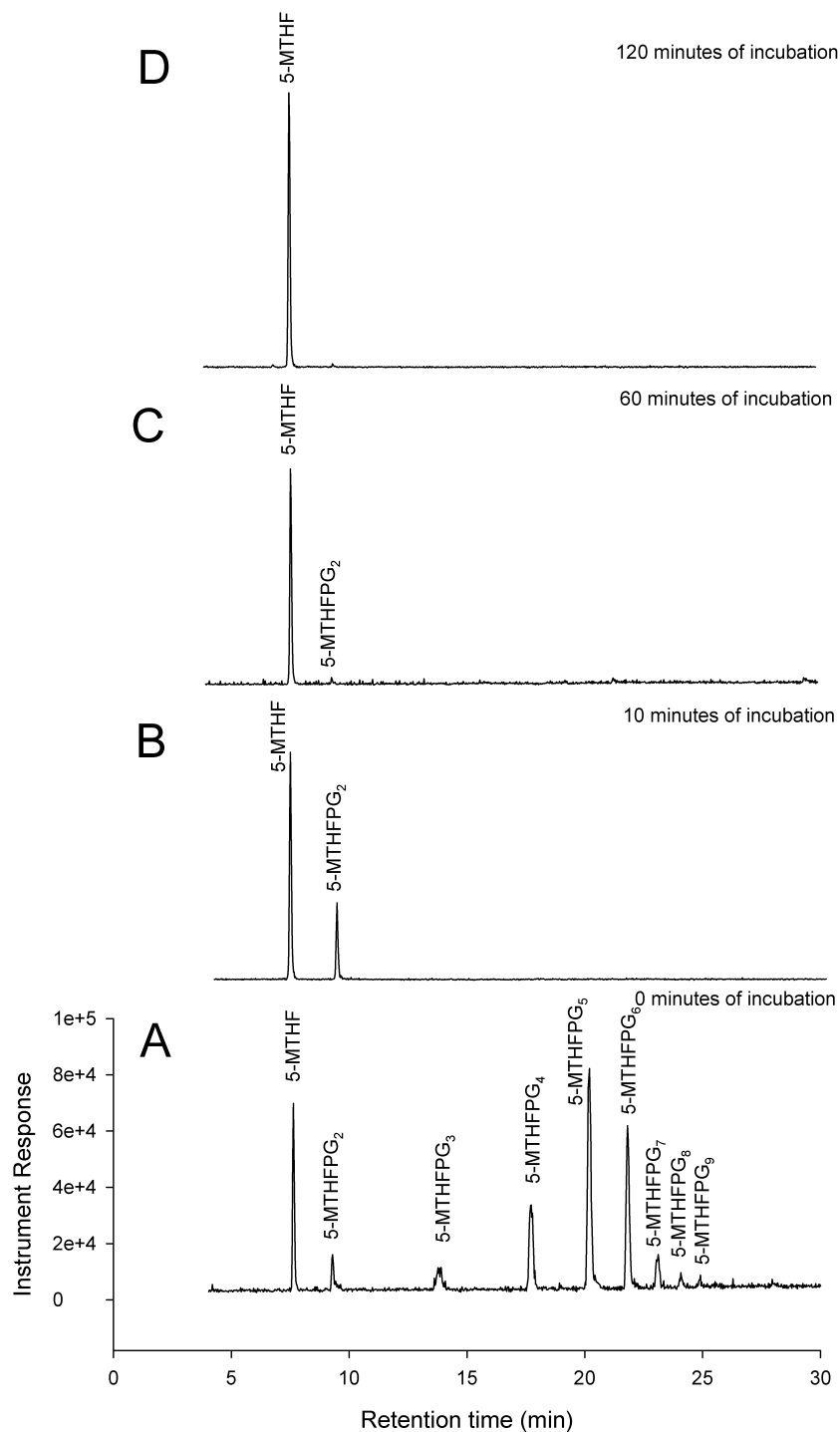
Figure 58. Deglutamation of erythrocyte folates in a whole blood lysate. (A) Instantaneous analysis of the diluted whole blood sample. (B) analysis after 10 minutes of incubation. (C) analysis after 1 hour of incubation. (D) analysis after 2 hours of incubation, revealing almost complete deglutamation

7.3.3.2 Whole blood mono-glutamyl-folate analysis

The previous section demonstrates that folates in their polyglutmated form can be quantitatively converted to their mono-glutamyl analogs, using a tightly controlled deglutamation process. The quantitation of the various mono-glutamyl-folates using stable isotope dilution LC-MS/MS has been described by a select number of recent publications. Analysis parameters described by these publications formed the basis for method development of our clinical whole blood polyglutamation assay, where analysis of a large samples sets is a expected.

7.3.3.3 LC/MS/MS method development

Separation of the various folate forms is commonly performed by reversed phase chromatography. As a consequence, the pH of the mobile phase is kept low (i.e. acidic) to enhance chromatographic retention by avoiding charge formation on the glutamyl residue. J.D.M. Patring et al., investigated ionization efficiency of the various mono-glutamyl folates under different acidic mobile phase conditions[39]. It was demonstrated that the optimal resolution and sensitivity was obtained by using a mobile phase that consisted of an aqueous blend of acetonitrile with an aliquot of methanol, acidified by acetic acid. The consequence of the use of low pH mobile phases is that 5-formyl- and 10-formylTHF dehydrate to 5,10-MTHF, and thus sample preparation and analytical targets have been defined accordingly. Based on previously reported RBC folate compositions, analytes were identified as FA, THF, 5-MTHF, 5,10-MTHF (representative for the 5,10-MTHF, 5-FTHF and 10-FTHF group). Furthermore as these JIA patients are on MTX therapy, MTX quantification was desirable as well. The structures of the target analytes together with their internal standard are presented in figure 59.
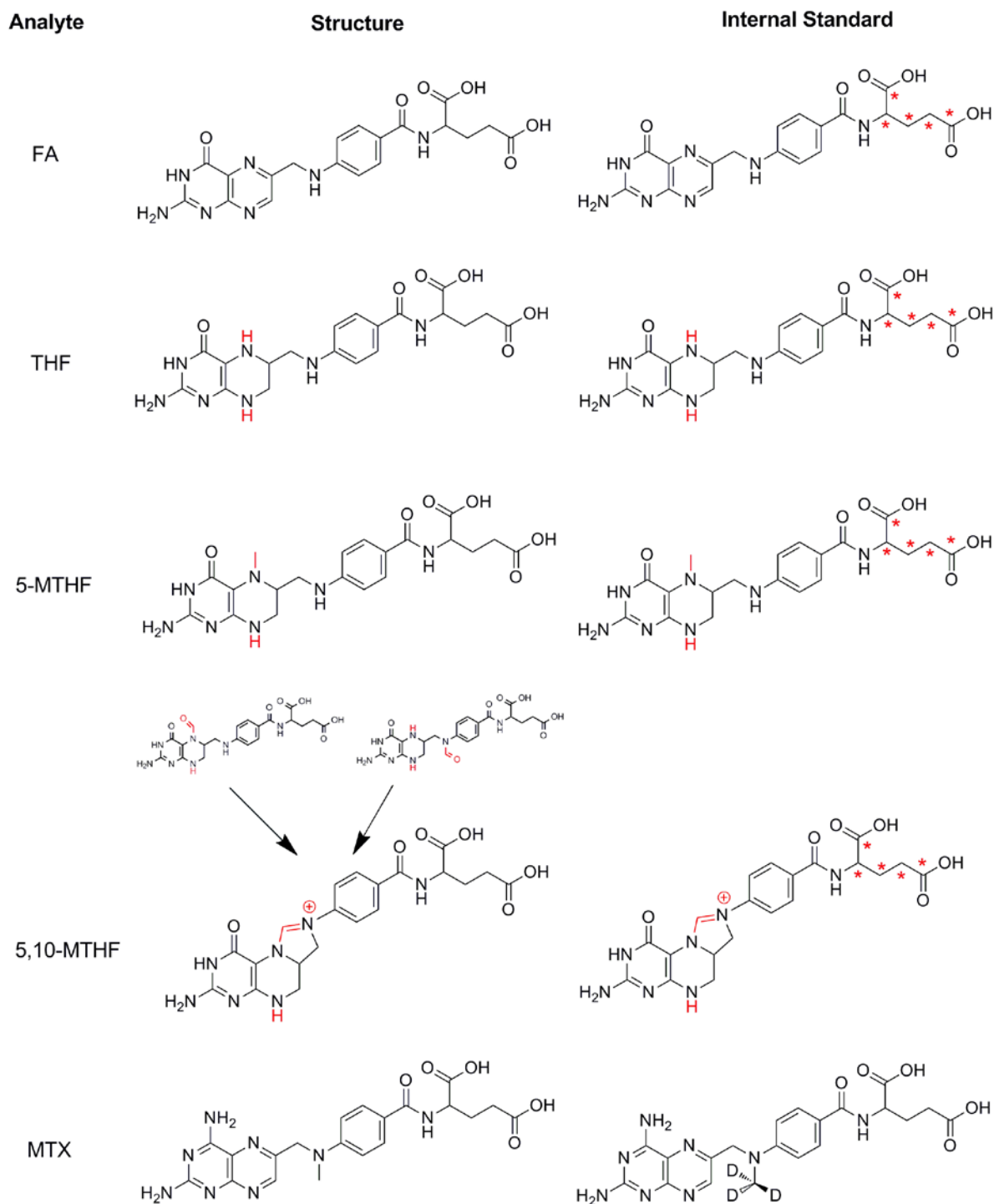
Figure 59. *(mono-glutamyl) Analytes of interest with their corresponding isotope labeled internal standard. All analytes are [$^{13}C_5$]-labeled in the glutamic acid residue, with the exception of MTX that has a D_3 methyl group.*

Prior to LC method development, mass spectrometer settings such as electrospray ionization mode (positive or negative), cone voltage and collision energy required for SIR of the folates of interest were optimized. It was found that the ionization mode had little effect on the absolute ionization efficiency (i.e. MS1 signal) of the folates in their monoglutamate form, with the exception of 5,10 methenylTHF that was only detectable in positive ion-mode due to the fixed positive charge. A comparison between positive and negative electrospray ionization for representative folate is demonstrated in figure 60A and 60C, where a 1 µM solution of 5-methylTHF is infused in the MS (note the signal intensity in the right top of each quadrant).

In contrast to the absolute ionization efficiency, the fragmentation behavior of the various folates was found to be much more favorable in positive ion mode (figure 60B and 60D). The buildup of a positive charge in the molecule together with relatively low collision energies (25 eV) leads to a clean intra molecular fragmentation of the amide bond, linking the glutamic acid to the pteroyl moiety (m/z 313). The efficiency of this gas phase reaction appears to be close to 100% (note signal intensity) in positive mode. Fragmentation in negative ion-mode required elevated collision energies (35 eV) and led to the formation of a wide spectrum of fragment ions. Furthermore, as a result of the various competing fragmentation pathways, signal generated by the most abundant ion was an order of magnitude lower (m/z 329.1), compared to the intensity of the pteroyl fragment obtained in positive ion-mode. Whilst this example discusses the optimal settings for 5-methyltetrahydrofolate, it was found to be representative for all of the folates of interest.

Fragmentation spectra of MTX, 5-MTHF, THF and 5,10-MTHF are presented in figures 61-64, along with the fragmentation spectra of their stable isotope labeled

versions. The spectra of FA, $^{13}C_5$-FA and $^3C_5$-5,10-MTHF are not presented in this dissertaion, however MS parameters were optimized in a similar manner as the other folates.

7.3.3.4 A sample preparation and chromatographic method for the detection of the target folates

The analysis of THF in addition to FA, 5-MTHF, 5,10-MTHF and MTX is complicated by the fact that THF is not stable in acidic samples. Huang and colleagues developed an analysis strategy to address this issue by analyzing an extracted (C18 SPE) whole blood patient sample twice[19]. First the whole blood folate extract was analyzed for FA, 5-MTHF and THF and the remainder of the extract was acidified by the addition of an aliquot of 1M HCl. Three hours after acidification, 5-FTHF and 10-FTHF were quantitatively converted to 5,10-MTHF and the sample was re-analyzed for 5,10-MTHF content. Analysis occurred by chromatographic methodology involving gradient elution and had a cycle time of 25 minutes. Since each whole blood sample has to be analyzed twice, quantitation of whole blood folate would require approximately one hour of instrument time per sample.

Since our study consisted of whole blood samples obtained from 200 participants, the re-analysis of the samples would result in an excess of 400 analysis using LC-MS/MS, requiring over 400 hours of instrument time for whole blood analysis. This excluding the plasma and RBC analysis time that would be required for the determination of erythrocyte folatepolyglutamation. In attempt to reduce analysis time, a faster chromatographic method was developed using a phenomenex kinetex C18

column. The stationary phase for this type of columns consists of fused core C18 silica particles, resulting in short analyte diffusion distances. The chromatographic properties of a fused core particle (3 µM) therefore mimic that of much smaller particle (1.7 µM). Since the column is effectively packed with larger particles, these columns typically do not demonstrate the high back-pressures associated with actual small particle columns, and therefore linear velocities can be increased without reaching excessive back-pressures.

The mobile phase conditions described by J.D.M. Patring and colleagues[39] were used in combination with the Phenomenex Kinetex chromatographic column. A gradient elution program was developed consisting of a 1 minute isocratic hold at 1% B, allowing focusing of the analytes on the head of the chromatographic column (especially necessary since large volume of sample is introduced). After the focusing phase, a gradient was initiated with a steepness of 6% increase in B per minute to 6 minutes (reaching 30% B). The gradient was followed by a step-gradient and re-equilibration for 2 minutes, resulting in a total runtime of 8 minutes. A representative chromatogram is presented in figure 65. Calibrations reports for the various [$^{13}C_5$]-folates are demonstrated in figure 66. Calibrations were linear in the 10 to 1000 range for each folate form, except THF, and correlation coefficients were adequate, except for THF. Using this analysis procedure, analytical throughput was effectively enhanced by a factor of 3.

When the presented whole blood analysis strategy was applied towards whole blood sample analysis of our large patient set, it was discovered that the sample preparation strategy did not yield adequately clean extracts. Repetitive injection of whole blood samples extracts lead to clogging of the chromatographic material in typically 10-

30 injections. Furthermore chromatographic peak shape changed and peak splitting started to occur, indicating an alternative retention mechanism, possibly induced by coating of the chromatographic media by residual proteins in the sample extract. Various guard columns in a number of sizes were explored in an attempt to increase the number of samples that could be analyzed sequentially, but none of these attempts were successful. Next an additional boiling step was incorporated prior to folate extraction by SPE. It was hypothesized that this boiling step would denature the majority of the proteins, allowing removal by centrifugation and avoiding breakthrough of these entities during SPE. Again, analysis of 10 to 30 sample extracts would lead to a clogged guard column in the chromatographic system and prevented further analysis. It was therefore concluded that whilst the presented sample preparation method involving SPE extraction was useful for the analysis of a limited amount of samples, it was not suitable for routine clinical analysis or analysis of larger sample sets.

In an attempt to develop a more robust folate extraction procedure, acid and organic mediated protein precipitations were explored. Organic mediated protein precipitations resulted in low but reproducible recoveries. The recovery for THF and FA was about 10-15% and resulted in detection limits in the order of 50-100 nM for THF and FA. These folates are typically present in lower concentrations in whole blood, and therefore this sample preparation strategy was abandoned. This sample preparation strategy could however be revisited when a more sensitive mass spectrometer is used.

Perchloric acid mediated protein precipitation such as presented in chapter 4 lead to clean whole blood extracts that did not lead to increases in backpressure as observed when using SPE. Perchloric acid protein precipitation is typically performed by two uncomplicated steps. First, an aliquot of 70% perchloric acid was added to the whole

blood lysate to induce protein precipitation. In a second step the precipitated proteins are removed by centrifugation, yielding a chromatographic compatible extract. As a result perchloric acid protein precipitation was found to be a convenient sample preparation technique suitable for the analysis of a large number of sample. The disadvantage of acid mediated protein precipitation is that THF is degraded during the procedure. Attempts were made to stabilize THF, such as direct neutralization following protein precipitation, but none of these attempts resulted in reproducible THF analysis.

THF is the most unstable of the folate forms identified as analytical targets. As mentioned before, THF is so unstable that 20% degradation occurs instantaneously upon dissolving the standard[16]. This instability raises the question as to if THF values could be reproducibly obtained, in order to provide a basis for inter patient pool comparisons. Furthermore, this instability required a complicated sample preparation process (i.e. SPE extraction) and analysis schemes (re-analysis after acidification) that were not suitable for analysis of larger sample sets. Perchloric acid protein precipitation was identified as a simple robust sample preparation procedure that was suitable for the analysis of large sample sets for FA, 5-MTHF and 5,10-MTHF. Based on the arguments presented above, the analysis of THF in whole blood extracts was abandoned. All patients were analyzed by the perchloric acid protein precipitation method. Example chromatograms of perchloric acid precipitated whole blood extracts from a MTHFR 677 CC healthy volunteer, and a JIA patient on MTX therapy identified as a MTHFR 677 TT homozygote, are demonstrated in figure 67 and 68. A typical calibration report for the folates of interest (i.e. 5-MTHF, 5,10-MTHF, MTX and FA) is given in figure 69. Whole blood folate values for all the patients in the study are presented in table 30.
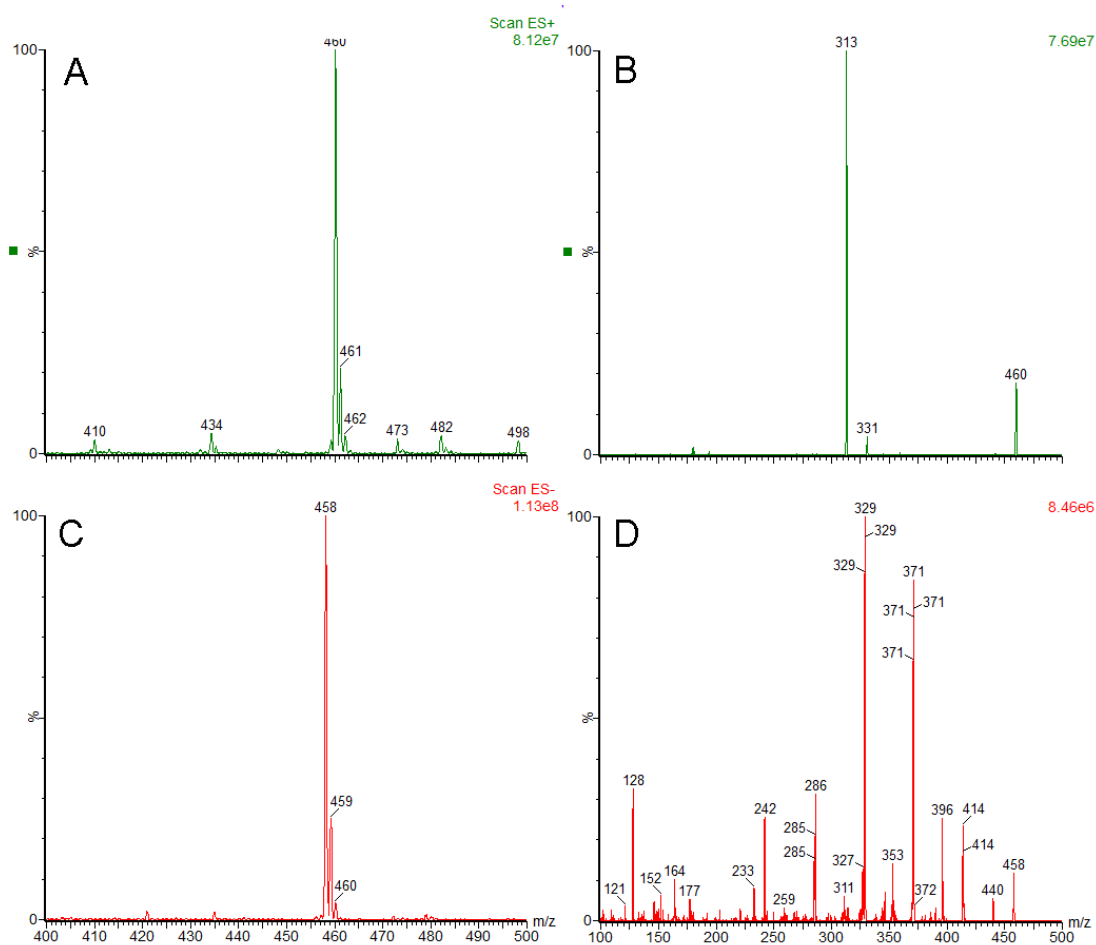
Figure 60. *Ionization and fragmentation behavior of 5-MTHF under positive ionization conditions (A) and (B) and negative ionization conditions (C) and (D). (A) MS1 scan from 400-500 m/z showing the parent at 460m/z. (B) fragmentation for the parent (m/z 460) to form the charged pteroyl residue with a mass of 313. (C) in negative ion-mode the deprotonated form of 5-MTHF was detected by the MS1 scan (m/z 458), sensitivity was about 20% higher when compared to detection in positive mode. (D) fragmentation of the negatively charged parent yielded a wide spectrum of fragment ions.*
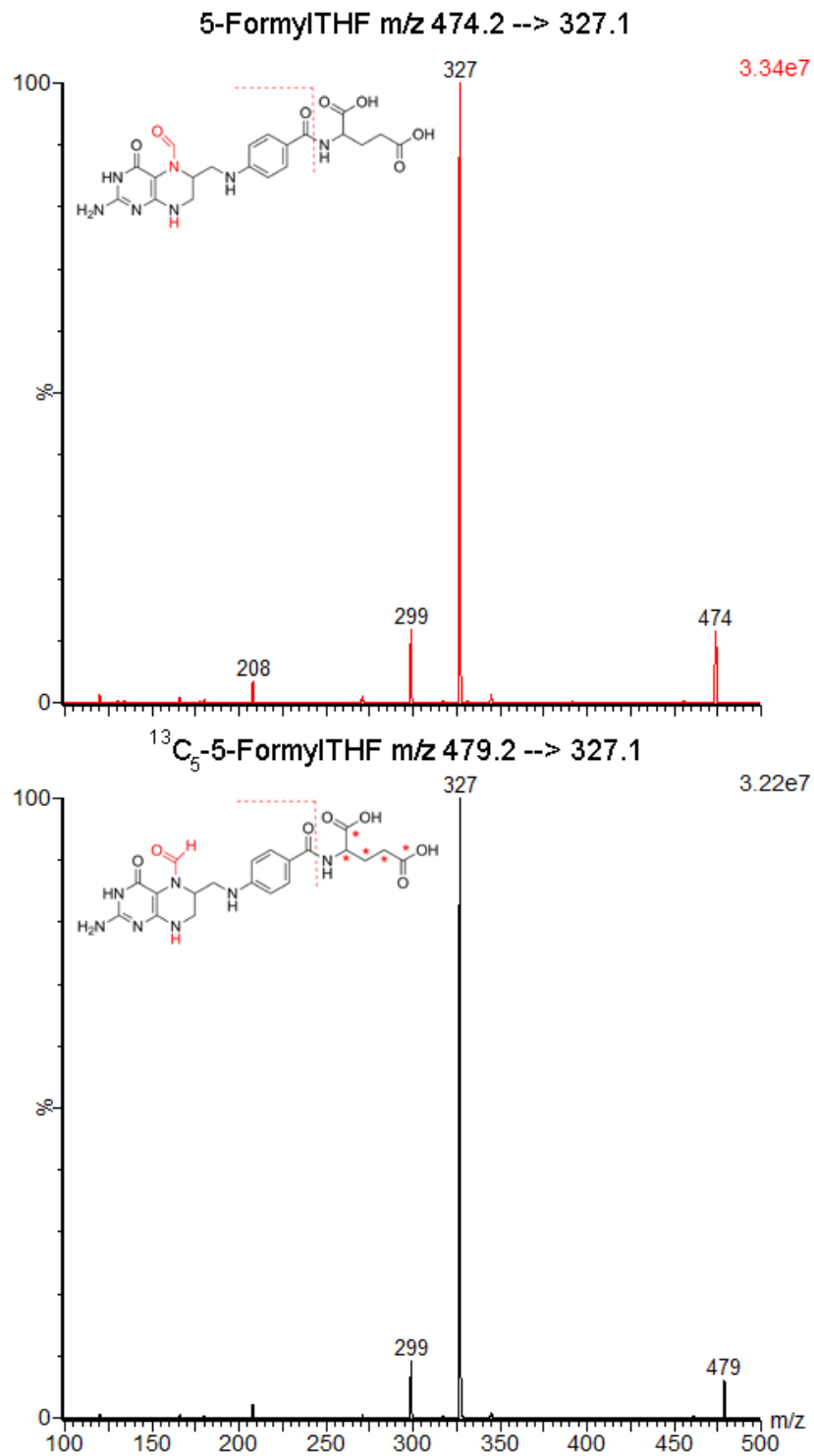
Figure 61. *Fragmentation spectrum of 5-FTHF and its internal standard ([$^{13}C_5$])-5-FTHF in positive ion-mode.*
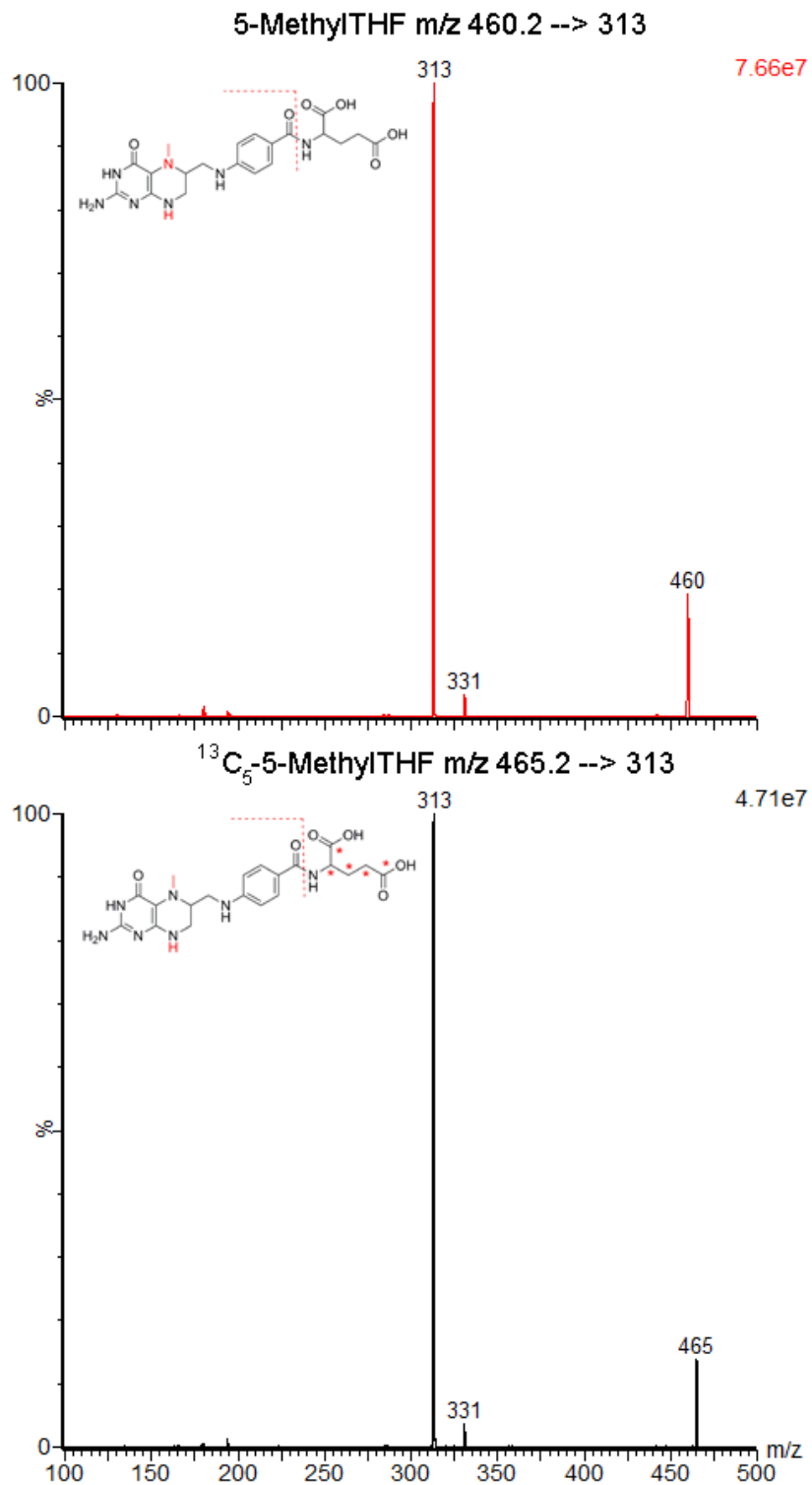
Figure 62. Fragmentation spectrum of 5-MTHF and its internal standard ($[^{13}C_5]$)-5-MTHF in positive ion-mode.
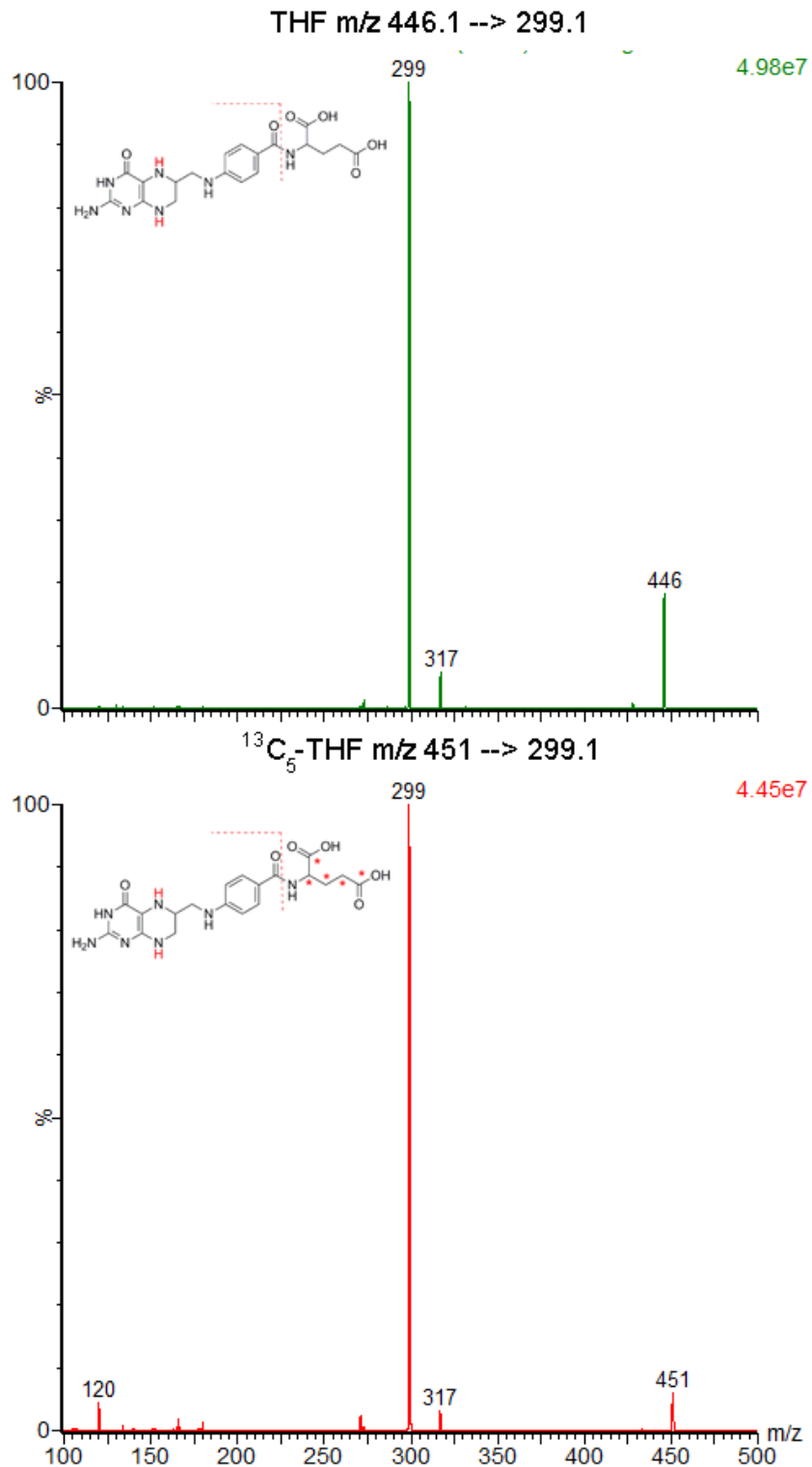
Figure 63. *Fragmentation spectrum of THF and its internal standard ([$^{13}C_5$])THF in positive ion-mode.*
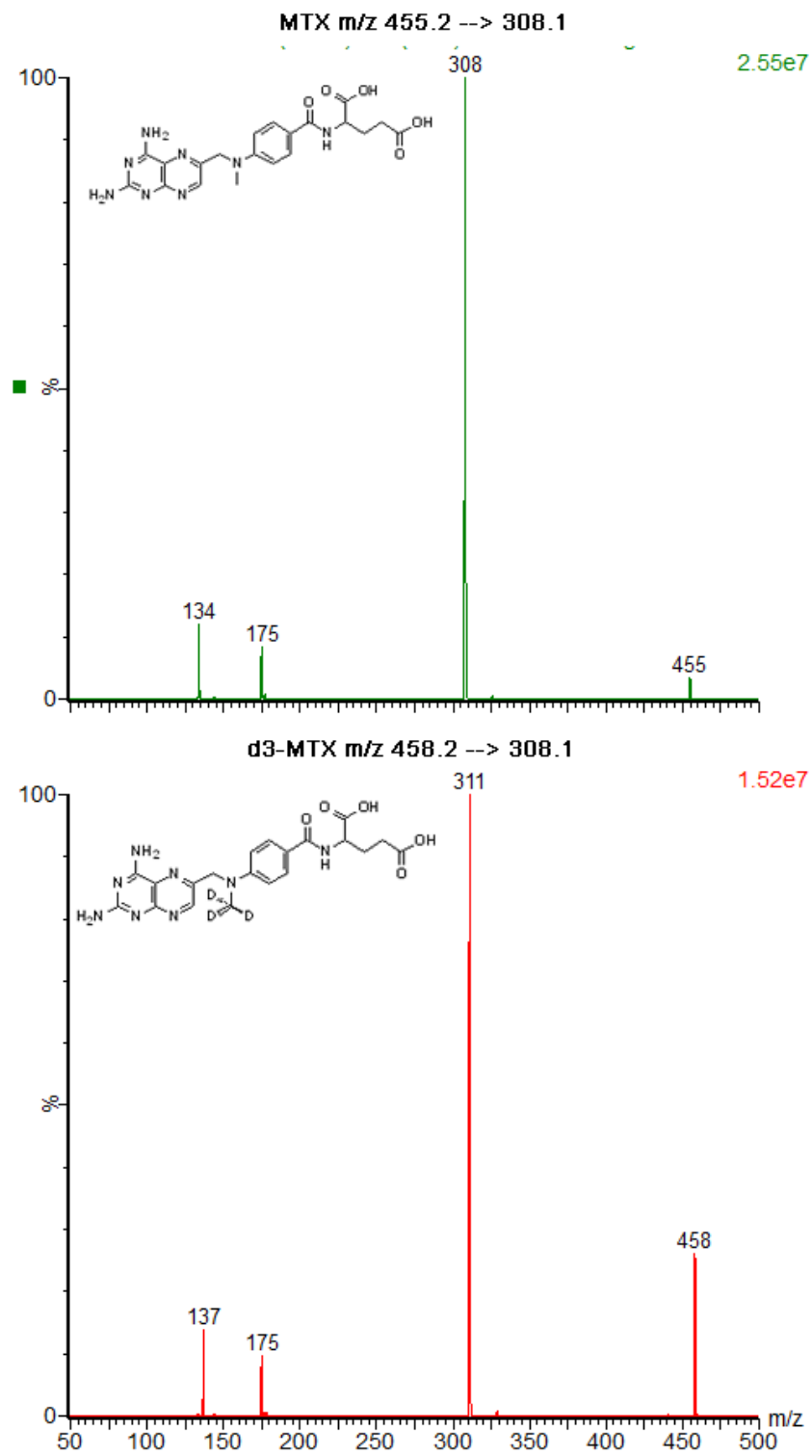
Figure 64. *Fragmentation spectrum of MTX and its internal standard D₃-MTX in positive ion-mode.*
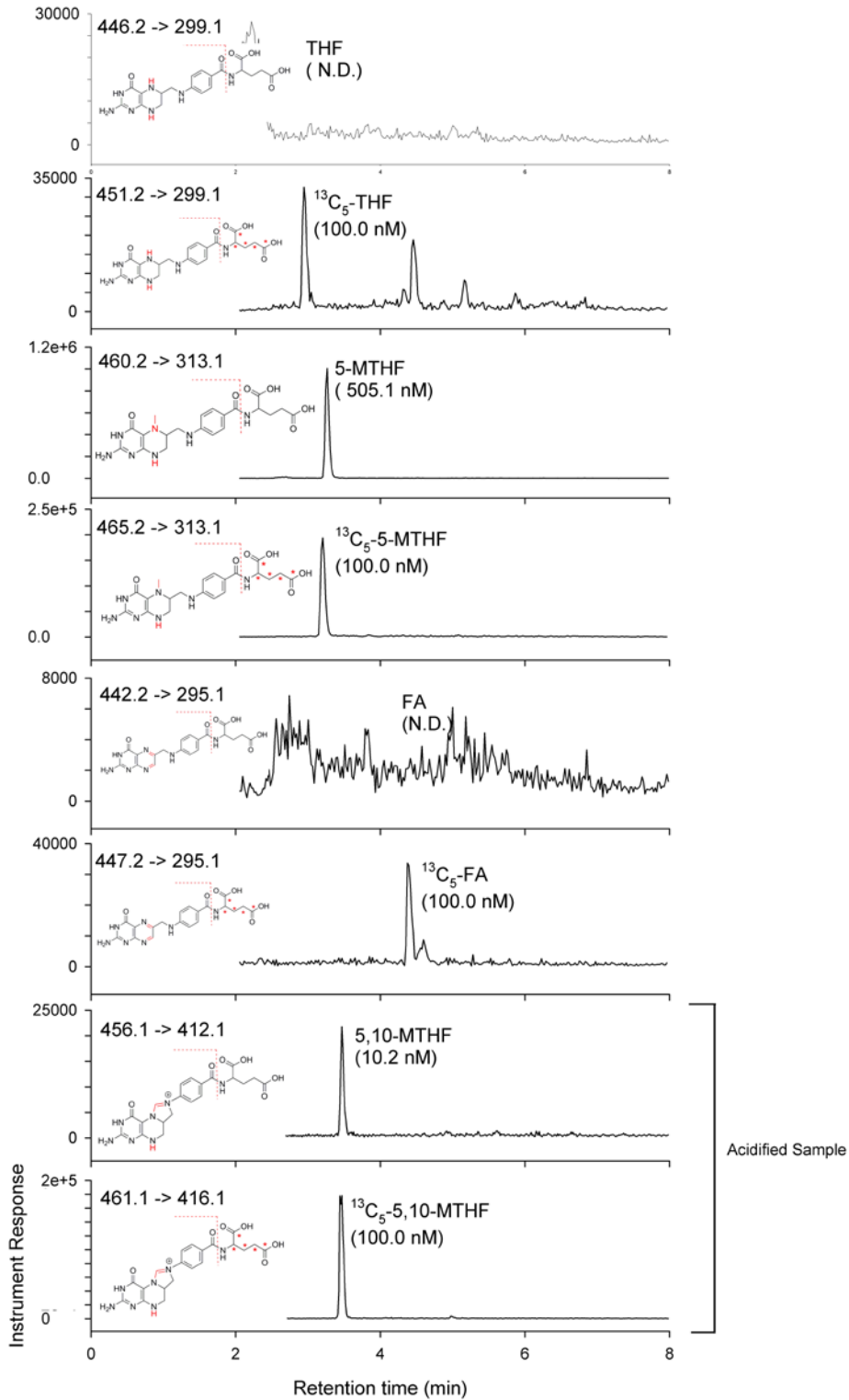
Figure 65. *Whole blood folate chromatogram, folate exctration occurred according to Huang and colleagues.*
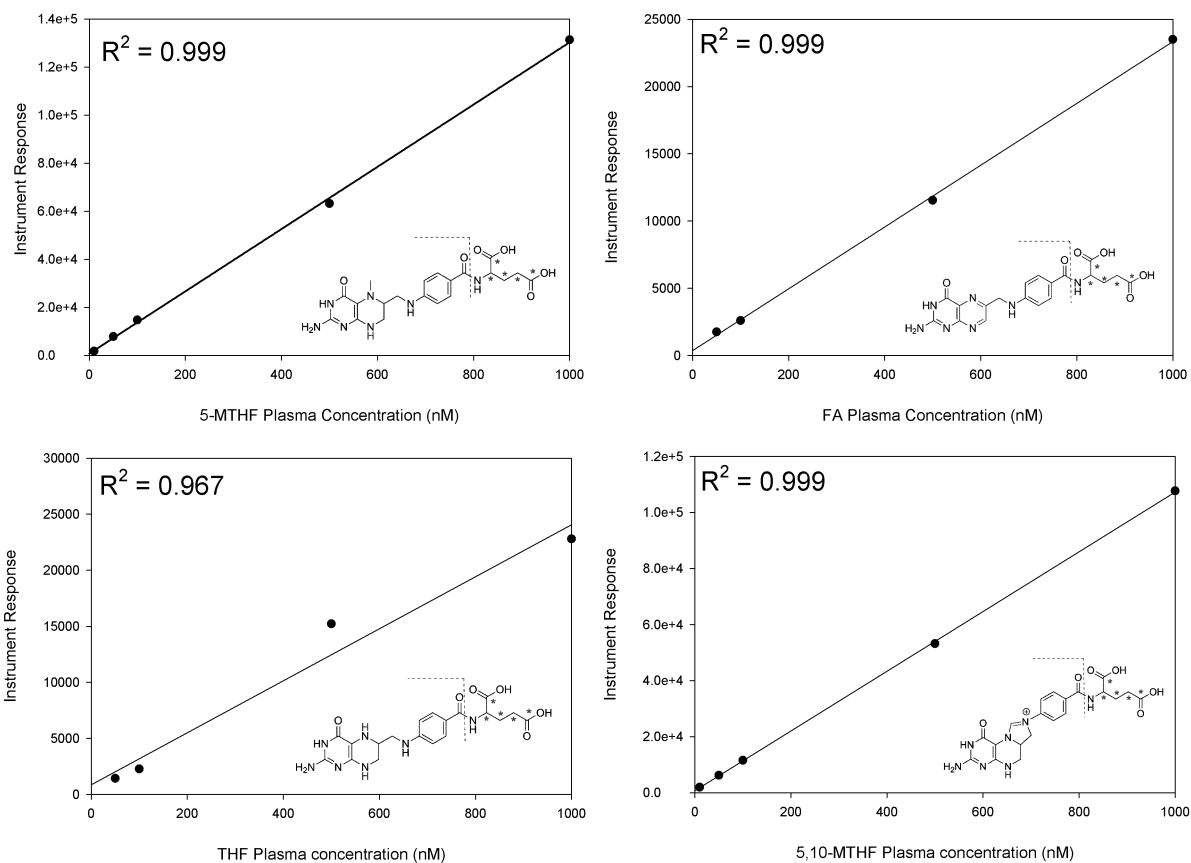
Figure 66. *Calibration plots for [$^{13}C_5$]-5-MTHF, [$^{13}C_5$]-FA, [$^{13}C_5$]-THF and [$^{13}C_5$]-5,10-MTHF out of whole blood. Sample extraction occurred according to Huang and colleagues using SPE extraction*

251
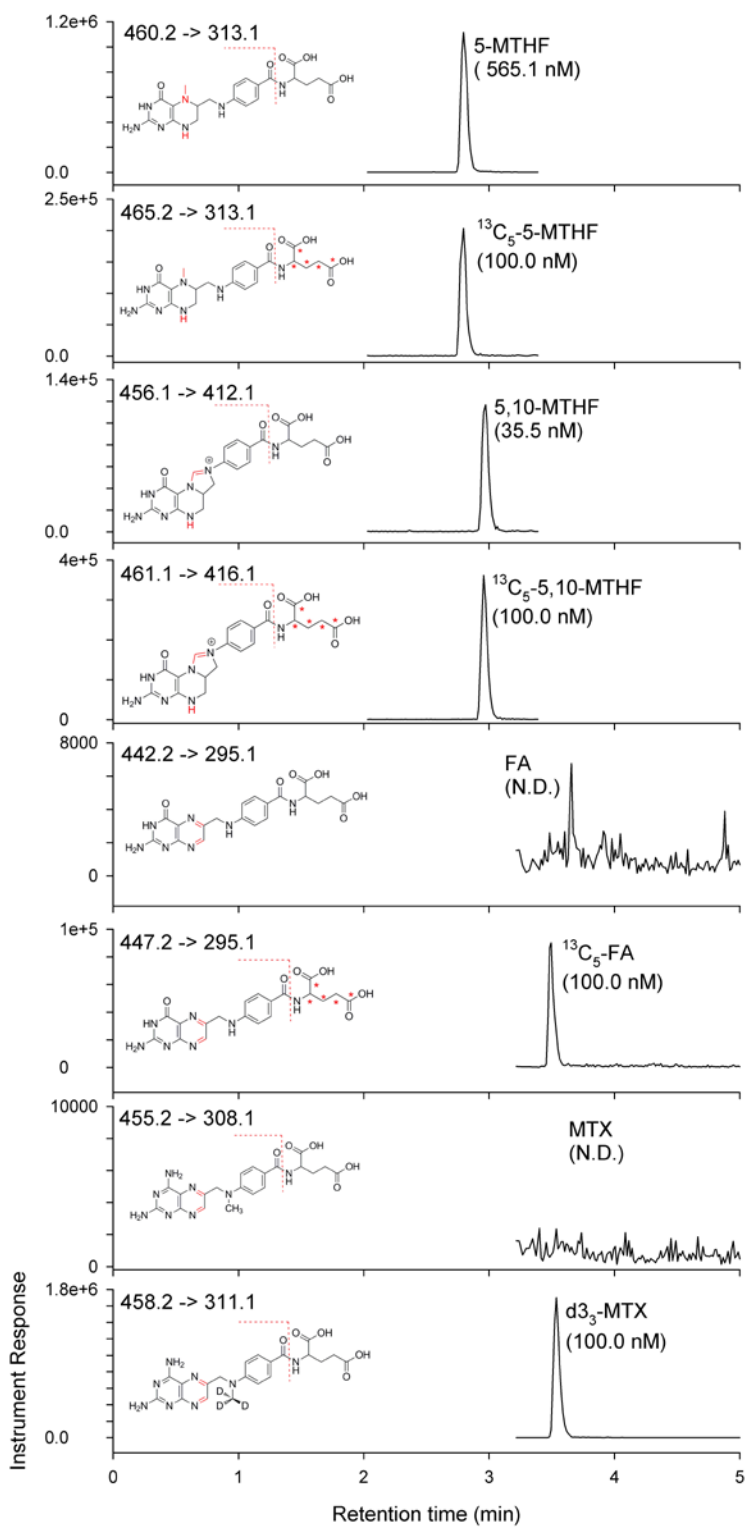
Figure 67. *Whole blood extract chromatogram of MTHFR CC genotype healthy volunteer*
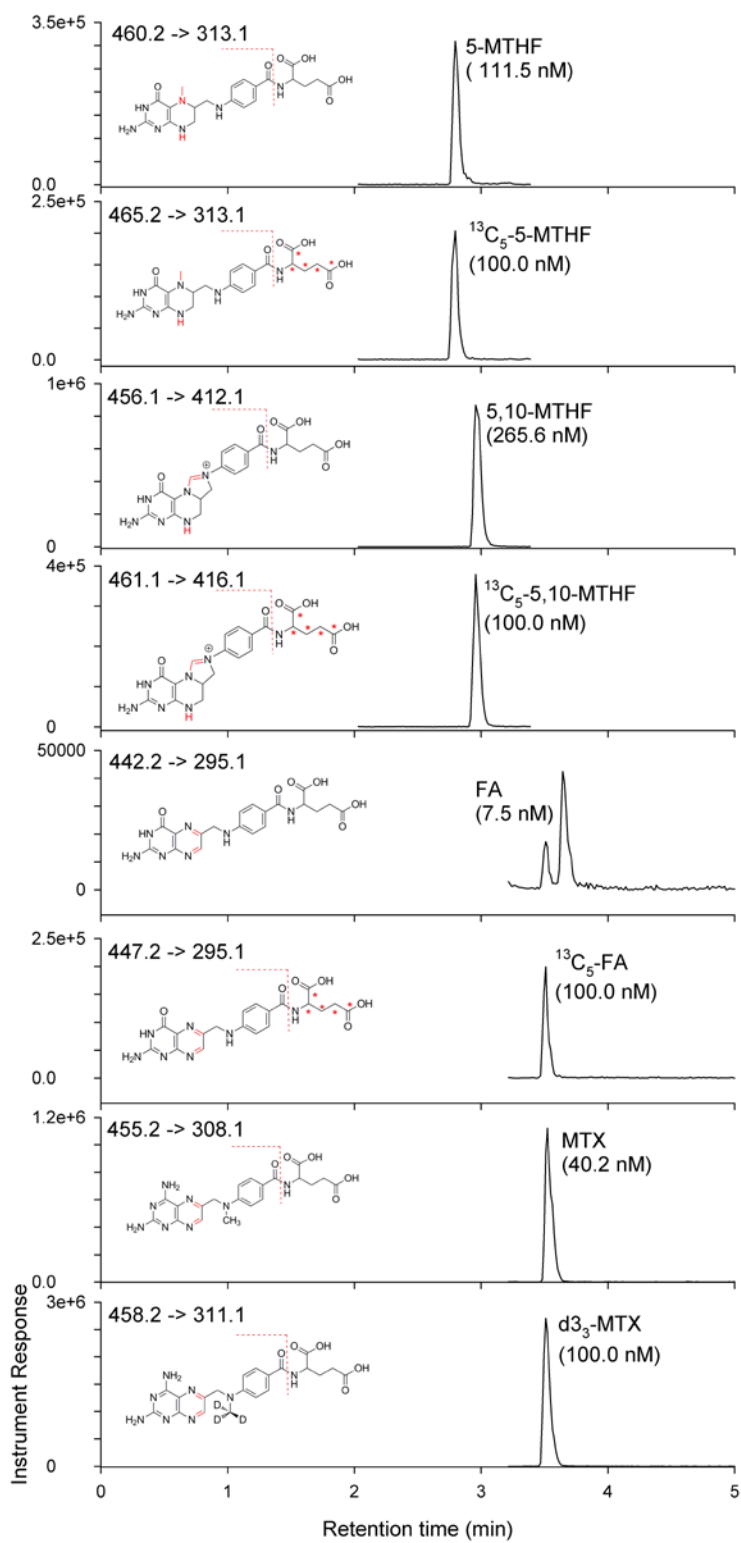
Figure 68. *Whole blood extract chromatogram of JIA patient 22 on MTX therapy*

253
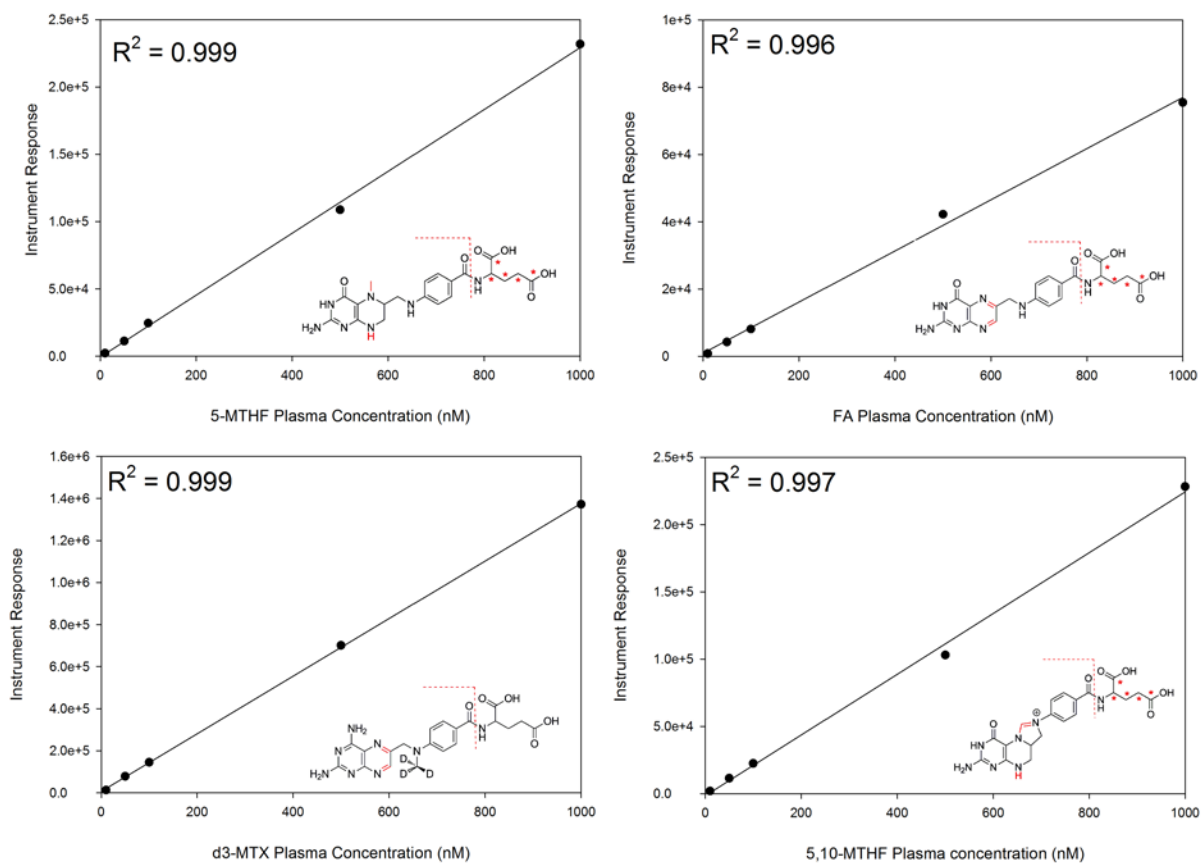
Figure 69. *Calibration plots for $[^{13}C_5]$-5-MTHF, $[^{13}C_5]$-FA, $[^{13}C_5]$-5,10-MTHF, and D_3-MTX extracted from whole blood. Sample extraction occurred by perchloric acid protein protein precipitation.*

7.3.4 Plasma folate analysis

For the calculation of RBC folate content, whole blood folate concentrations need to be corrected for the plasma folate content. In contrast to the earlier reported whole blood and RBC analysis, plasma folate analysis is relatively straight forward as folates reside in the monoglutamyl form within plasma and are not protein or tissue bound. Therefore deglutamation can be circumvented, extraction is uncomplicated, and the appropriate isotopically labeled standards are available through commercial sources, allowing for accurate quantitation using stable isotope dilution LC-MS/MS. Plasma folate analysis occurred by sample preparation according to Huang et al., followed by LC-MS/MS using the chromatographic method presented for whole blood analysis. The analysis of SPE extracted plasma samples did not lead to the increasing backpressures and clogging of analytical guard columns after a limited amount of injections, that occured during whole blood analysis as previously noted. Therefore the folate extraction procedure was not altered and sample extracts were analyzed twice. In the primary injection of the extract FA, 5-MTHF and THF were quantititated. Following the first analysis, samples were acidified and re-analyzed for 5,10-MTHF and MTX. Representative patient plasma chromatograms are presented in figure 70. Typical calibration curves for FA, 5-MTHF, THF, 5,10-MTHF and MTX in plasma are presented in figure 71. Correlation coefficients 0.998 or better, and the intercept of the calibration curves was equal to 0 at the 95% confidence interval. The results of the JIA patients plasma analysis are presented in table 30 folate control group, and for the group on MTX therapy.   Typically   folate plasma folate values were relatively low (30 nM) and predominantly in the 5-MTHF form, conform earlier reports using LC-MS/MS for plasma analysis.
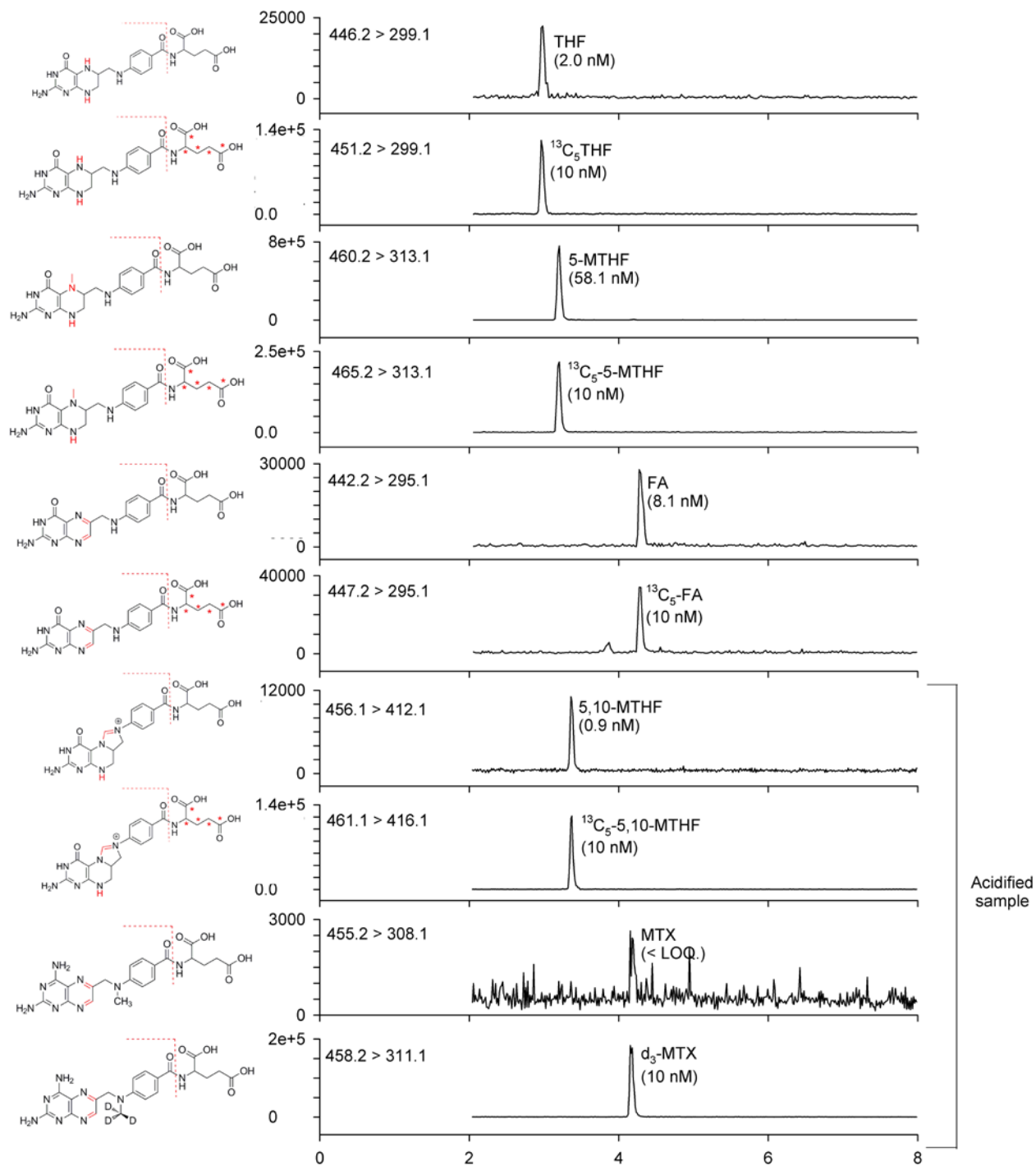
Figure 70. *Plasma folate chromatogram for JIA patient 91 on MTX therapy. MRM channels for THF, [$^{13}C_5$]-THF, 5-MTHF, [$^{13}C_5$]-5-MTHF, FA, [$^{13}C_5$]-FA, 5,10-MTHF, [$^{13}C_5$]- 5,10-MTHF, MTX, and D_3-MTX are displayed individually.*
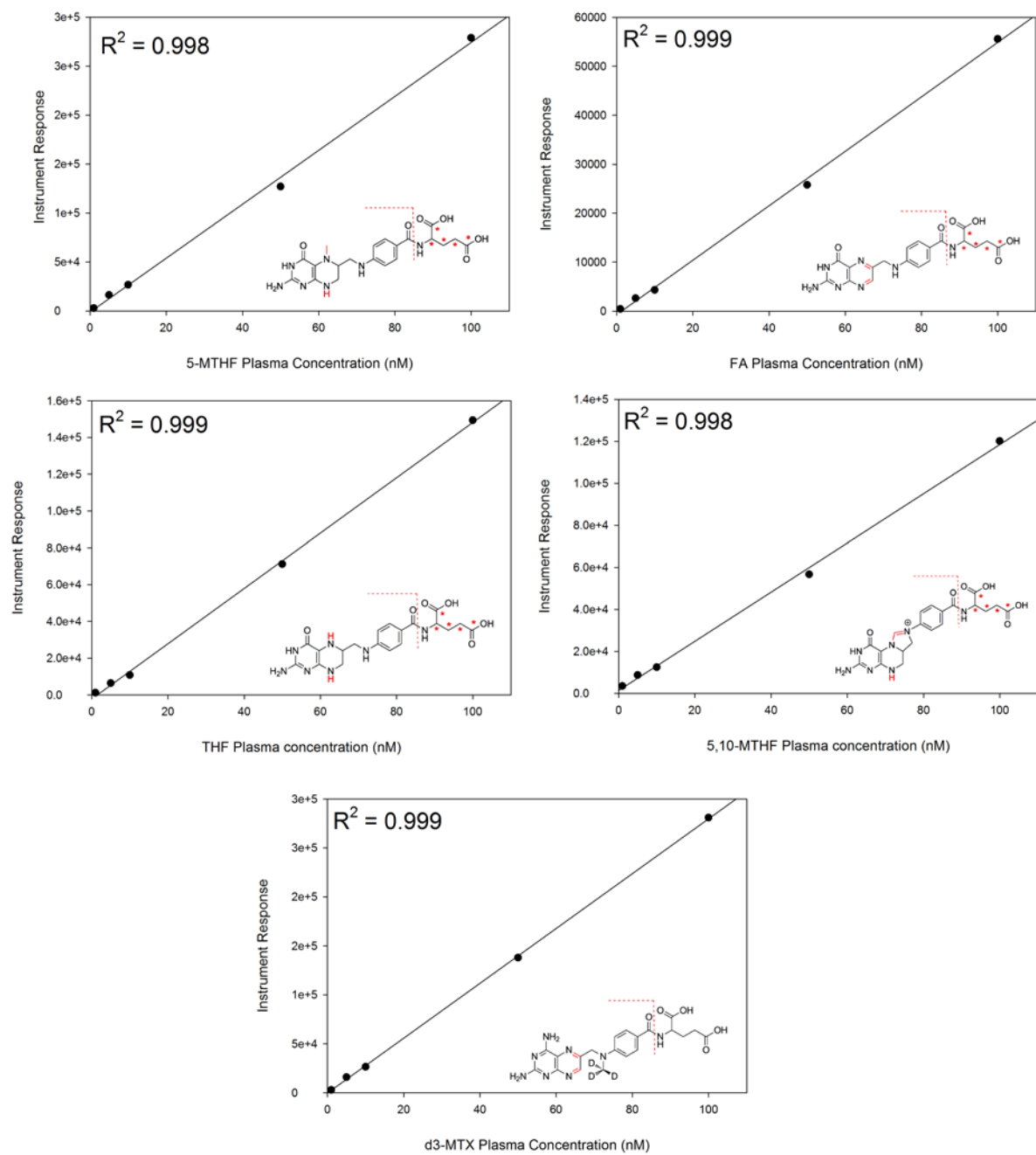
Figure 71. Calibration reports using for the various folate forms and MTX, measured in plasma extracts. Calibrations were linear and correlation coefficients were acceptable.

7.3.5 Patient Results

Table 29				5-MTHF-PG% Distribution: Means (± SD)				
	PG3%	PG4%	PG5%	PG6%	PG7%	PG8%	PG9%	PG10%
No MTX	2.1 (1.6)	6.3 (1.5)	47.7 (5.1)	30.3 (3.6)	8.4 (2.0)	3.5 (0.8)	1.4 (0.4)	0.29 (0.2)
MTX	1.5 (1.4)	7.1 (1.8)	43.9 (3.9)	31.1 (4.0)	9.8 (1.9)	4.2 (2.2)	2.0 (1.6)	0.43 (0.2)
p value	0.0007	0.0006	<0.0001	0.1	<0.0001	<0.0001	<0.0001	<0.0001

RBC samples from JIA patients for the folate control group (n=100) and for the MTX group were analyzed by the presented comprehensive folate measurement strategy (table 30 attached at the end of the chapter). Analysis of the obtained results is being conducted in conjunction with our collaborators at Children's Mercy Hospitals, and was beyond the scope of this dissertation. At the time of dissertation preparation, analysis of the patients data was still in progress, however a brief summary of the obtained preliminary clinical relevant results is provided below.

Subjects on MTX had expectedly lower folate isoform concentrations than those not on MTX including 5-MTHF (678.6 ± 281.2 nmol/L vs. 1022.2 ± 489.3 nmol/L, $p<0.0001$) and 5,10-MTHF (68.4 ± 77.0 nmol/L vs. 91.7 ± 106.3 nmol/L, $p=0.04$). 5-MTHFPG relative distribution analysis revealed higher proportions of long chain polyglutamates in patients receiving MTX over the control group, suggesting an up-regulation of folate polyglutamation status when a cell reaches a folate depleted state (table 29). Increasing folate polyglutamation status upon folate depletion has been observed in various rat tissues before[40].

Of all clinical variables tested (including the use of folate supplementation) only MTX dose (in mg/kg) was inversely related to 5-MTHF concentrations ($p=0.0009$). More importantly, it was also observed that study participants with active arthritis had higher

concentrations of summed RBC folates than those without active arthritis (p=0.01), suggesting a correlation between folate status and disease activity.

7.4   Conclusion

The quantitative measurement of erythrocyte folate isoform in combination with polyglutamation status is an analytical challenge at various levels. The complex nature arises from the fact that standards are largely unavailable, extraction is complicated, folates are unstable, interconversion is dependant of analytical conditions, analytes are present at low levels, and changes in polyglutamation status alters physical chemical properties. This chapter of the dissertation was centered around dealing with each of these variables and the presented analytical method was ultimately a compromise between all of these factors. Erythrocyte polyglutamayl folate isoforms were measured semi-quantitatively using whole blood and its individual components. Pools of folate isoforms were quantitatively measured in whole blood after deglutamation by stable isotope dilution LC-MS/MS strategies. Erythrocyte folate isoforms were quantitatively established after plasma folate determination. Finally, polyglutamation distribution was measured on a relative basis using erythrocyte extracts in combination with IP-LC-MS/MS. The combined method was applied towards the analysis of two JIA patients groups, with and without MTX therapy. A total of over 200 patients were analyzed and data analysis revealed a correlation between a patients folate status and disease activity. Since a patients folate status seems to play a major role in disease activity the comprehensive measurement of folates might provide a quantitative basis for individualization of patient therapy in the future.

7.5 References

[1]   S. L. Morgan, J. E. Baggott, W. H. Vaughn, P. K. Young, J. V. Austin, C. L. Krumdieck, G. S. Alarcon, The effect of folic acid supplementation on the toxicity of low-dose methotrexate in patients with rheumatoid arthritis. *Arthritis Rheum.* **1990**, *33*, 9.

[2]   M. A. Peeters, M. O. Rethore, J. Lejeune, In vivo folic acid supplementation partially corrects in vitro methotrexate toxicity in patients with Down syndrome. *Br J Haematol.* **1995**, *89*, 678.

[3]   A. Ravelli, D. Migliavacca, S. Viola, N. Ruperto, A. Pistorio, A. Martini, Efficacy of folinic acid in reducing methotrexate toxicity in juvenile idiopathic arthritis. *Clin Exp Rheumatol.* **1999**, *17*, 625.

[4]   P. G. Hunt, C. D. Rose, G. McIlvain-Simpson, S. Tejani, The effects of daily intake of folic acid on the efficacy of methotrexate therapy in children with juvenile rheumatoid arthritis. A controlled study. *J Rheumatol.* **1997**, *24*, 2230.

[5]   J. Chladek, M. Simkova, J. Vaneckova, M. Hroch, J. Chladkova, J. Martinkova, J. Vavrova, M. Beranek, The effect of folic acid supplementation on the pharmacokinetics and pharmacodynamics of oral methotrexate during the remission-induction period of treatment for moderate-to-severe plaque psoriasis. *Eur J Clin Pharmacol.* **2008**, *64*, 347.

[6]   L. K. Stamp, J. L. O'Donnell, P. T. Chapman, M. Zhang, J. James, C. Frampton, M. L. Barclay, Methotrexate polyglutamate concentrations are not associated with disease control in rheumatoid arthritis patients receiving long-term methotrexate therapy. *Arthritis & Rheumatism.* **2010**, *62*, 359.

[7]   C. J. Allegra, R. L. Fine, J. C. Drake, B. A. Chabner, The effect of methotrexate on intracellular folate pools in human MCF-7 breast cancer cells. Evidence for direct inhibition of purine synthesis. *J Biol Chem.* **1986**, *261*, 6478.

[8]   J. Baram, C. J. Allegra, R. L. Fine, B. A. Chabner, Effect of methotrexate on intracellular folate pools in purified myeloid precursor cells from normal human bone marrow. *J Clin Invest.* **1987**, *79*, 692.

[9]   V. Kesavan, P. Sur, M. T. Doig, K. J. Scanlon, D. G. Priest, Effects of methotrexate on folates in Krebs ascites and L1210 murine leukemia cells. *Cancer Lett.* **1986**, *30*, 55.

[10]   A. J. Barak, R. J. Kemmy, D. J. Tuma, The effect of methotrexate on homocysteine methylating agents in rat liver. *Drug Nutr Interact.* **1982**, *1*, 303.

[11] Z. Fazili, C. M. Pfeiffer, M. Zhang, R. Jain, Erythrocyte Folate Extraction and Quantitative Determination by Liquid Chromatography-Tandem Mass Spectrometry: Comparison of Results with Microbiologic Assay. *Clin Chem.* **2005**, *51*, 2318.

[12] P. J. Bagley, J. Selhub, A common mutation in the methylenetetrahydrofolate reductase gene is associated with an accumulation of formylated tetrahydrofolates in red blood cells. *Proc Natl Acad Sci U S A.* **1998**, *95*, 13217.

[13] Y. M. Smulders, D. E. Smith, R. M. Kok, T. Teerlink, H. Gellekink, W. H. Vaes, C. D. Stehouwer, C. Jakobs, Red blood cell folate vitamer distribution in healthy subjects is determined by the methylenetetrahydrofolate reductase C677T polymorphism and by the total folate status. *J Nutr Biochem.* **2007**, *18*, 693.

[14] Z. Fazili, C. M. Pfeiffer, Measurement of folates in serum and conventionally prepared whole blood lysates: application of an automated 96-well plate isotope-dilution tandem mass spectrometry method. *Clin Chem.* **2004**, *50*, 2378.

[15] V. De Brouwer, G. F. Zhang, S. Storozhenko, D. V. Straeten, W. E. Lambert, pH stability of individual folates during critical sample preparation steps in prevision of the analysis of plant folates. *Phytochem Anal.* **2007**, *18*, 496.

[16] D. E. Smith, R. M. Kok, T. Teerlink, C. Jakobs, Y. M. Smulders, Quantitative determination of erythrocyte folate vitamer distribution by liquid chromatography-tandem mass spectrometry. *Clin Chem Lab Med.* **2006**, *44*, 450.

[17] S. D. Wilson, D. W. Horne, Evaluation of ascorbic acid in protecting labile folic acid derivatives. *Proc Natl Acad Sci U S A.* **1983**, *80*, 6500.

[18] S. D. Wilson, D. W. Horne, High-performance liquid chromatographic determination of the distribution of naturally occurring folic acid derivatives in rat liver. *Anal Biochem.* **1984**, *142*, 529.

[19] Y. Huang, S. Khartulyari, M. E. Morales, A. Stanislawska-Sachadyn, J. M. Von Feldt, A. S. Whitehead, I. A. Blair, Quantification of key red blood cell folates from subjects with defined MTHFR 677C>T genotypes using stable isotope dilution liquid chromatography/mass spectrometry. *Rapid Commun Mass Spectrom.* **2008**, *22*, 2403.

[20] Z. Fazili, C. M. Pfeiffer, M. Zhang, Comparison of Serum Folate Species Analyzed by LC-MS/MS with Total Folate Measured by Microbiologic Assay and Bio-Rad Radioassay. *Clin Chem.* **2007**, *53*, 781.

[21] P. B. Utz, Y. Serfert, A. F. Garcia, S. Dieterich, R. Lindauer, A. Bognar, B. Tauscher, Influence of High-Pressure Treatment at 25°C and 80°C on Folates in Orange Juice and Model Media. *Journal of Food Science.* **2004**, *69*, SNQ117.

[22]   A. M. Molloy, J. M. Scott, Microbiological assay for serum, plasma, and red cell folate using cryopreserved, microtiter plate method. *Methods Enzymol.* **1997**, *281*, 43.

[23]   E. M. Newman, J. F. Tsai, Microbiological analysis of 5-formyltetrahydrofolic acid and other folates using an automatic 96-well plate reader. *Analytical Biochemistry.* **1986**, *154*, 509.

[24]   E. McGown, C. Lewis, M. Dong, H. Sauberlich, Results with commercial radioassay kits compared with microbiological assay of folate in serum and whole-blood. *Clin Chem.* **1978**, *24*, 2186.

[25]   A. M. Molloy, S. Daly, J. L. Mills, P. N. Kirke, A. S. Whitehead, D. Ramsbottom, M. R. Conley, D. G. Weir, J. M. Scott, Thermolabile variant of 5,10-methylenetetrahydrofolate reductase associated with low red-cell folates: implications for folate intake recommendations. *Lancet.* **1997**, *349,* 1591.

[26]   E. P. Quinlivan, A. D. Hanson, J. F. Gregory, The analysis of folate and its metabolic precursors in biological samples. *Anal Biochem.* **2006**, *348*, 163.

[27]   E. Gunter, B. Bowman, S. Caudill, D. Twite, M. Adams, E. Sampson, Results of an international round robin for serum and whole-blood folate. *Clin Chem.* **1996**, *42*, 1689.

[28]   A. J. Clifford, E. M. Noceti, A. Block-Joy, T. Block, G. Block, Erythrocyte Folate and Its Response to Folic Acid Supplementation Is Assay Dependent in Women. *J. Nutr.* **2005**, *135*, 137.

[29]   J. D. Patring, J. A. Jastrebova, S. B. Hjortmo, T. A. Andlid, I. M. Jagerstad, Development of a simplified method for the determination of folates in baker's yeast by HPLC with ultraviolet and fluorescence detection. *J Agric Food Chem.* **2005**, *53*, 2406.

[30]   P. J. Bagley, J. Selhub, Analysis of folate form distribution by affinity followed by reversed- phase chromatography with electrical detection. *Clin Chem.* **2000**, *46*, 404.

[31]   C. R. Santhosh-Kumar, J. F. Kolhouse, Molar quantitation of folates by gas chromatography-mass spectrometry. *Methods Enzymol.* **1997**, *281*, 26.

[32]   Y. Lin, S. R. Dueker, A. D. Jones, A. J. Clifford, A parallel processing solid phase extraction protocol for the determination of whole blood folate. *Anal Biochem.* **2002**, *301*, 14.

[33]   S. D. Garbis, A. Melse-Boonstra, C. E. West, R. B. van Breemen, Determination of folates in human plasma using hydrophilic interaction chromatography-tandem mass spectrometry. *Anal Chem.* **2001**, *73*, 5358.

[34] C. M. Pfeiffer, Z. Fazili, L. McCoy, M. Zhang, E. W. Gunter, Determination of folate vitamers in human serum by stable-isotope-dilution tandem mass spectrometry and comparison with radioassay and microbiologic assay. *Clin Chem.* **2004**, *50*, 423.

[35] S. Monch, M. Netzel, G. Netzel, M. Rychlik, Quantitation of folates and their catabolites in blood plasma, erythrocytes, and urine by stable isotope dilution assays. *Anal Biochem.* **2010**, *398*, 150.

[36] L. C. Garratt, C. A. Ortori, G. A. Tucker, F. Sablitzky, M. J. Bennett, D. A. Barrett, Comprehensive metabolic profiling of mono- and polyglutamated folates and their precursors in plant and animal tissue using liquid chromatography/negative ion electrospray ionisation tandem mass spectrometry. *Rapid Commun Mass Spectrom.* **2005**, *19*, 2390.

[37] W. Lu, Y. K. Kwon, J. D. Rabinowitz, Isotope ratio-based profiling of microbial folates. *J Am Soc Mass Spectrom.* **2007**, *18*, 898.

[38] Y. Lamers, R. Prinz-Langenohl, S. Bramswig, K. Pietrzik, Red blood cell folate concentrations increase more after supplementation with [6S]-5-methyltetrahydrofolate than with folic acid in women of childbearing age. *Am J Clin Nutr.* **2006**, *84*, 156.

[39] J. D. M. Patring, J. A. Jastrebova, Application of liquid chromatography-electrospray ionisation mass spectrometry for determination of dietary folates: Effects of buffer nature and mobile phase composition on sensitivity and selectivity. *Journal of Chromatography A.* **2007**, *1143*, 72.

[40] G. Varela-Moreiras, J. Selhub, Long-Term Folate Deficiency Alters Folate Content and Distribution Differentially in Rat Tissues. *J. Nutr.* **1992**, *122*, 986.

Table 30. Quantitative folate isoform distribution from the prospective study (JIA patients on MTX)

Group	Patient	Hct (%)	5-MTHF plasma (nM)	5-MTHF WB (nM)	5-MTHF RBC (nM)	5,10-MTHF plasma (nM)	5,10-MTHF WB (nM)	5,10-MTHF RBC (nM)	FA plasma (nM)	FA WB (nM)	FA RBC (nM)
MTX	1	36.8	11.8	117.6	299.3	2.3	13.1	31.6	8.4	7.7	6.4
MTX	2	39	24.1	249.6	602.4	2.2	23.4	56.7	3.5	5.2	7.9
MTX	3	36.3	25.6	131.8	318.3	2.6	12.9	30.9	12.6	13.9	16.2
MTX	4	38.4	24.4	223.4	542.4	2.7	16.1	37.5	1.0	2.5	5.1
MTX	5	39.7	10.2	289.0	712.4	2.7	34.7	83.4	118.7	87.4	39.8
MTX	6	37.6	15.1	186.5	471.0	3.0	26.5	65.5	1.8	2.1	2.7
MTX	7	34.6	15.6	208.9	574.3	3.0	38.8	106.5	21.0	22.1	24.3
MTX	8	35.5	69.8	497.8	1275.5	2.5	26.6	70.4	1.6	2.4	3.8
MTX	9	38.2	28.1	312.9	773.6	2.6	22.6	55.1	0.3	3.0	7.4
MTX	10	40.2	26.4	300.4	708.0	3.1	11.5	24.1	26.7	19.6	9.0
MTX	11	35.4	19.2	218.0	580.9	3.7	20.9	52.5	33.5	25.9	12.0
MTX	12	33	20.7	152.5	419.9	2.3	11.3	29.7	1.7	2.3	3.7
MTX	13	40.8		0.2		2.1		-3.1	244.0		
MTX	14	35.8				1.7		-3.1	1.9		
MTX	15	38.3	29.8	307.5	754.8	2.2	29.0	72.2	11.8	8.2	2.3
MTX	16	39.5	45.1	373.1	875.5	2.2	27.3	65.8	0.6	0.6	0.6
MTX	17	35.5				2.1		-3.8	15.2		
MTX	18	36.6	20.8	272.0	707.0	1.8	24.6	64.0	0.8	1.3	2.2
MTX	19	NA	35.5	360.2		2.2	20.9		1.2	1.0	
MTX	20	38.7	42.5	299.3	705.9	2.3	46.3	116.0	64.5	47.8	21.4
MTX	21	39.7	19.9	126.1	287.4	2.5	14.1	31.8	0.7	1.3	2.1
MTX	22	39.6	34.8	111.5	228.4	2.0	265.6	667.7	0.7	7.5	17.9
MTX	23	38.4	25.2	274.7	674.9	2.5	22.1	53.6	5.3	3.7	1.0
MTX	24	36.4	49.1	384.3	970.1	2.4	25.4	65.7	4.8	2.1	-2.6
MTX	25	38.2	46.6	370.0	893.2	2.4	27.4	67.7	1.1	1.7	2.8

Table 30. Continued (JIA patients on MTX)

Group	Patient	Hct (%)	5-MTHF plasma (nM)	5-MTHF WB (nM)	5-MTHF RBC (nM)	5,10-MTHF plasma (nM)	5,10-MTHF WB (nM)	5,10-MTHF RBC (nM)	FA plasma (nM)	FA WB (nM)	FA RBC (nM)
MTX	27	41.6	26.4	495.4	1153.9	2.7	82.3	194.1	1.5	3.7	6.8
MTX	28	39	20.5	221.6	536.1	2.5	47.6	118.2	0.9	1.8	3.1
MTX	29	37.9	55.6	439.1	1067.4	2.5	17.0	40.8	0.9	4.7	11.0
MTX	30	37.1	20.9	284.1	730.4	2.3	18.7	46.4	1.6	2.1	2.9
MTX	31	35.9				1.7		-3.0	2.1		-3.7
MTX	32	34	25.1	445.4	1261.5	2.4	24.9	68.5	1.1	2.5	5.2
MTX	33	42.2	11.8	264.9	611.6	2.0	34.4	78.7	13.5	10.2	5.5
MTX	34	39.5	30.6	346.4	830.1	2.1	26.4	63.5	0.4	0.9	1.8
MTX	35	39.1	27.7	424.7	1043.2	2.1	31.4	77.2	1.1	1.5	2.1
MTX	36	39.1	32.1	262.1	620.2	1.9	23.0	55.9	4.2	4.0	3.7
MTX	37	39.7	31.5	120.4	255.4	2.1	7.3	15.2	1.0	5.0	11.1
MTX	38	36.3	26.5	168.9	418.7	1.8	7.3	17.0	1.2	6.8	16.6
MTX	39	34.1	15.4	126.1	340.0	1.7	12.0	31.9	6.7	10.3	17.3
MTX	40	45.9	21.7	307.6	644.6	1.7	70.1	150.7	11.7	23.7	38.0
MTX	41	41.3	66.2	245.7	500.9	2.7	17.4	38.3	1.2	6.9	15.1
MTX	42	38.7	30.5	183.6	426.2	2.0	12.0	27.9	47.5	38.0	23.0
MTX	43	33.9	44.1	95.4	195.6	2.2	10.1	25.5	7.6	29.3	71.7
MTX	44	43.1	15.7	207.6	461.0	2.0	14.6	31.3	0.5	8.5	19.0
MTX	45	30.1	11.4	96.8	295.1	1.5	4.8	12.4	2.2	6.2	15.6
MTX	46	34.5				2.1		-3.9	0.5		
MTX	47	36.7	40.0	393.4	1003.0	1.9	42.3	112.1	40.2	29.8	11.8
MTX	48	39	31.0	289.5	693.8	2.1	10.0	22.4	156.4	97.8	6.1
MTX	49	39.6	18.3	189.3	450.1	1.8	5.6	11.5	66.3	55.0	37.7
MTX	50	38.9	16.8	121.5	286.0	1.7	4.8	9.7	7.4	12.7	21.0

Table 30. Continued (JIA patients on MTX)

Group	Patient	Hct (%)	5-MTHF plasma (nM)	5-MTHF WB (nM)	5-MTHF RBC (nM)	5,10-MTHF plasma (nM)	5,10-MTHF WB (nM)	5,10-MTHF RBC (nM)	FA plasma (nM)	FA WB (nM)	FA RBC (nM)
MTX	51	41.6	25.4	260.1	589.7	2.9	6.2	10.8	0.8	4.2	9.0
MTX	52	37.6	49.4	201.9	454.8	2.7	89.8	234.5	1.2	11.5	28.6
MTX	53	34.8	18.7	168.6	449.5	2.9	41.9	115.0	1.0	1.7	3.0
MTX	54	37.3	20.8	184.2	458.8	2.6	7.7	16.2	1.5	2.7	4.8
MTX	55	41.5	16.7	246.6	570.7	2.8	33.1	76.0	0.6	5.9	13.3
MTX	56	36.6	28.6	168.0	409.5	1.8	8.7	20.6	8.2	14.9	26.6
MTX	57	38.5	25.6	237.5	576.0	2.7	16.4	38.3	26.3	29.9	35.7
MTX	58	35.8	66.2	409.0	1023.6	3.2	14.0	33.6	16.7	8.8	-5.3
MTX	59	37.9	33.3	248.5	601.2	2.5	18.0	43.5	0.8	0.4	-0.2
MTX	60	37.9	16.3	275.3	699.5	2.5	41.9	106.6	2.6	0.0	-4.3
MTX	61	35.7	44.0	321.4	821.2	2.7	11.5	27.4	0.9	5.8	14.6
MTX	62		0.0								
MTX	63	40.9	32.0	140.9	298.3	2.7	44.8	105.6	7.4	40.8	89.2
MTX	64	39.3	46.2	280.0	641.1	2.7	23.8	56.0	1.8	4.9	9.7
MTX	65	34.1				2.9			12.3		-23.8
MTX	66	39.9	49.6	281.2	630.1	3.0	11.0	23.1	4.0	6.3	9.7
MTX	67	39.2	44.8	373.3	882.9	3.1	9.9	20.9	1.2	6.1	13.7
MTX	68	39.7	26.9	139.0	309.2	2.8	8.8	17.5	0.5	3.2	7.2
MTX	69	39	21.0	310.7	763.7	3.1	47.8	118.2	5.2	4.9	4.6
MTX	70	36.5	37.8	381.4	979.1	2.8	17.0	45.8	3.6	7.5	14.3
MTX	71	36	29.5	175.7	435.7	0.4	51.6	141.8	4.7	15.2	33.8
MTX	72	41	54.3	539.8	1238.4	0.8	17.1	40.8	1.6	7.7	16.5
MTX	73	42.5	117.2	476.7	963.2	0.7	9.9	21.5	0.8	9.0	20.2
MTX	74	36.1	23.4	245.2	638.0	1.3	35.3	96.6	19.3	20.6	22.7
MTX	75	34.5	30.9	77.7	166.7	0.7	7.2	19.3	0.8	23.7	67.1

266

Table 30. Continued (JIA patients on MTX)

Group	Patient	Hct (%)	5-MTHF plasma (nM)	5-MTHF WB (nM)	5-MTHF RBC (nM)	5,10-MTHF plasma (nM)	5,10-MTHF WB (nM)	5,10-MTHF RBC (nM)	FA plasma (nM)	FA WB (nM)	FA RBC (nM)
MTX	77	37.4				5.1		-1.1	580.9		
MTX	78	37.9	40.4	292.1	704.6	0.6	8.8	22.3	4.6	11.9	24.0
MTX	79	38.6	64.2	181.9	369.2	0.5	6.2	14.6	1.4	10.5	25.0
MTX	80	39.7	25.3	185.5	428.9	0.9	5.6	13.3	8.7	13.5	20.8
MTX	81	36.7	65.0	323.4	769.2	0.5	9.1	23.8		8.2	22.3
MTX	82								1.1		
MTX	83	44.8	52.5	343.4	701.9	0.6	20.1	44.2	1.2	3.5	6.2
MTX	84	25.3	19.1	213.6	787.8	0.4	35.1	137.1	1.0	1.1	1.5
MTX	85	37.9	55.4	414.2	1002.2	0.5	14.2	36.9	3.0	2.9	2.8
MTX	86	34	37.9	80.9	164.5	0.5	8.2	23.7	1.8	2.7	4.4
MTX	87	38	80.8	518.5	1232.7	0.3	24.2	62.9	72.5	47.7	7.1
MTX	88	34.1	28.8	298.7	820.3	0.3	43.9	127.7	2.4	8.2	19.2
MTX	89	40.7	25.1	222.4	510.0	0.5	18.8		0.5	0.4	0.3
MTX	90	43.1	52.7	495.8	1080.9	0.6	29.9		131.5	106.9	74.4
MTX	91	40.3	58.1	618.6	1448.8	0.9	36.6	89.6	8.1	11.5	16.5
MTX	92	38.3	28.8	334.9	828.2	0.5	17.8	45.7	0.3	1.5	3.4
MTX	93	39.5	24.8	406.6	991.3	0.6	16.7	41.4	5.8	4.2	1.8
MTX	94	34.9	41.6	228.9	578.2	0.3	17.8	50.5	1.6	2.6	4.5
MTX	95	42.4	33.7	317.9	704.0	0.8	18.8	43.2	42.8	27.4	6.6
MTX	96	39	15.5	175.7	426.2	0.4	14.0	35.4	7.9	5.0	0.4
MTX	97	39.2	24.7	235.3	562.0	0.3	27.2	68.8	54.2	39.7	17.3
MTX	98	31.6	13.6	222.5	674.6	0.2	32.4	102.1	4.4	6.4	10.6
MTX	99	40	13.4	236.7	571.8	0.3	20.0	49.6	35.8	32.7	28.0
MTX	100	34.8	37.1	265.7	693.8	0.5	91.6	262.2	0.9	2.7	5.9

Table 30. Continued (JIA patients on MTX)

Group	Patient	Hct (%)	5-MTHF plasma (nM)	5-MTHF WB (nM)	5-MTHF RBC (nM)	5,10-MTHF plasma (nM)	5,10-MTHF WB (nM)	5,10-MTHF RBC (nM)	FA plasma (nM)	FA WB (nM)	FA RBC (nM)
MTX	102	38.9	31.5	346.4	841.1	0.8	5.8	13.8	55.1		-86.6
MTX	103	36.3	13.2	303.8	813.7	0.5	4.9	12.7	2.3		-4.0
MTX	104	32.8	42.8	413.1	1171.8	0.5	24.8	74.5	0.9	1.9	4.0
MTX	105	38.6	28.9	268.0	648.5	0.6	33.7	86.3	26.7	22.5	15.8
MTX	106	34.1	24.6	189.6	508.4	1.0	30.5	87.5	38.8	31.1	16.2
MTX	107	38	24.7	357.6	900.8	7.3	63.8	156.0	1.7	1.0	-0.2
MTX	108	34.6	12.9	338.7	954.5	0.3	57.9	166.7	53.9	52.1	48.8
MTX	109	34.6	22.4	479.0	1341.9	0.9	46.4	132.4	10.3	8.4	4.8
MTX	110	39.1	10.4	331.8	832.4	0.8	38.2	96.5	55.1	50.5	43.4

268

Table 30. Quantitative folate isoform distribution from the prospective study (JIA patients off MTX)

Group	Patient	Hct (%)	5-MTHF plasma (nM)	5-MTHF WB (nM)	5-MTHF RBC (nM)	5,10-MTHF plasma (nM)	5,10-MTHF WB (nM)	5,10-MTHF RBC (nM)	FA plasma (nM)	FA WB (nM)	FA RBC (nM)
Folate	2	34.1	63.7	90.5	142.2	0.5	5.4	14.8	1.0	1.9	3.5
Folate	3	31.3	34.7	752.9	2329.2	0.4	17.5	55.1	0.3	0.8	1.9
Folate	4	43	30.6	108.8	212.4	0.4	22.3	51.3	0.0	4.1	9.5
Folate	5	36.8	63.2	88.0	130.5	0.4	11.9	31.5	0.1	1.4	3.8
Folate	6	37.5	36.5	248.2	601.0	0.2	11.9	31.3	0.7	2.1	4.3
Folate	7	40.1	82.3	355.0	762.4	0.3	27.2	67.4	5.9	3.8	0.7
Folate	8	39.6	48.5	469.2	1110.9	0.3	29.2	73.2	27.4	7.2	-23.7
Folate	9	36.1	44.5	260.8	643.8	0.4	6.8	18.2	1.8	1.6	1.4
Folate	10	38.6	30.7	375.6	924.3	0.3	8.7	22.0	0.0	2.1	5.4
Folate	11	40.4	74.7	419.3	927.7	0.4	47.4	116.7	3.2	2.7	1.8
Folate	12	32.2	48.3	199.5	517.8	0.3	8.4	25.5	0.7	1.3	2.7
Folate	13	40	42.7	264.4	597.0	0.4	14.6	35.9	0.0	1.3	3.2
Folate	14	36	43.4	236.9	580.8	0.4	9.7	26.2	0.6	0.6	0.6
Folate	15	42.5	57.2	274.8	569.2	0.4	9.3	21.3	1.5	2.9	4.9
Folate	16	33.5	14.1	206.4	588.0	1.2	8.4	22.6	9.0	3.5	-7.4
Folate	17	46.1	7.1	186.8	396.9	0.3	3.5	7.3	1.7	0.6	-0.6
Folate	18	38	21.3	92.3	208.2	0.6	6.9	17.2	1.5	7.2	16.5
Folate	19	35	49.0	615.4	1667.2	0.3	16.7	47.1	1.8	3.5	6.7
Folate	20	-	20.1	212.5		0.3	5.6		0.2	0.3	
Folate	21	-	72.5	493.1		0.2	34.2		11.0	9.1	
Folate	22	37.6	30.9	258.8	637.0	0.2	23.2	61.5	5.6	6.4	7.7
Folate	23	30.3	55.6	219.7	597.0	0.3	29.7	97.4	1.3	4.9	13.1
Folate	24	41.1	20.9	278.7	648.2	0.4	23.2	55.9	0.2	4.5	10.6
Folate	25	39.1		473.3	1210.4		30.1	76.9		13.7	35.0

Table 30. Continued (JIA patients off MTX)

Group	Patient	Hct (%)	5-MTHF plasma (nM)	5-MTHF WB (nM)	5-MTHF RBC (nM)	5,10-MTHF plasma (nM)	5,10-MTHF WB (nM)	5,10-MTHF RBC (nM)	FA plasma (nM)	FA WB (nM)	FA RBC (nM)
Folate	26	37	45.2	414.8	1044.0	0.3	127.2	343.3	76.7	4.5	-118.4
Folate	27	38	25.0			0.4		-0.7	0.0		0.0
Folate	28	40.4	28.0			0.5		-0.7	1.0		-1.4
Folate	29	34.1	24.5	275.5	760.4	0.5	23.2	66.9	0.0	1.1	3.2
Folate	30	38	46.3	384.9	937.2	0.4	58.0	152.0	9.2	7.5	4.7
Folate	31	35.9	19.9	232.8	612.8	0.1	19.8	55.0	1.0	2.3	4.6
Folate	32	37.5	52.9	298.0	706.4	0.8	16.2	41.8	1.1	7.2	17.4
Folate	33	34.2		389.8	1139.7		60.4	176.6			0.0
Folate	34	39.5	37.9	527.8	1278.3	0.3	35.4	89.2	0.0	4	10.1
Folate	35	39.2	43.1	571.9	1392.1	0.2	46.4	118.2	0.6	12.3	30.4
Folate	36	39.1	66.9	701.6	1690.3	0.4	14.5	36.3	14.9	15.3	15.9
Folate	37	38.7	94.5	482.9	1098.0	0.2	20.4	52.4	0.0	31.4	81.1
Folate	38	39.9	15.7			0.2		-0.3	0.5		-0.7
Folate	39	39.1	33.9	417.9	1015.9	0.3	66.3	169.0	0.0	4	10.2
Folate	40	39.5	80.7	601.4	1398.9	0.2	33.2	83.7	1.4	5.8	12.6
Folate	41	42.7	45.9	349.1	756.1	0.2	28.1	65.7	0.8	18.2	41.5
Folate	42	37.1	16.4	249.5	644.6	0.2	25.5	68.5	0.7	12.5	32.5
Folate	43	41	12.7	87.2	194.4	0.2	11.0	26.6	0.1	1.2	2.8
Folate	44	38.1	60.7	256.5	574.7	0.1	23.9	62.7	0.9	3	6.5
Folate	45	36.2	72.5	375.4	909.2	0.2	33.2	91.4	0.2	7.8	21.1
Folate	46	30.3	80.3	621.2	1865.4	1.6	126.8	414.9	63.6	57.7	44.1
Folate	47	36.7	72.4	481.8	1188.0	0.5	12.0	31.8	0.5	13.8	36.7
Folate	48	41.2	42.0	522.9	1209.1	0.2	12.5	30.1	0.9	14.8	34.6
Folate	49	37.9	75.3	445.3	1051.7	0.4	71.4	187.6	5.0	18.2	39.8
Folate	50	32.8	42.7	367.5	1033.0	0.5	36.9	111.5	2.0	11.5	31.0

Table 30. Continued (JIA patients off MTX)

Group	Patient	Hct (%)	5-MTHF plasma (nM)	5-MTHF WB (nM)	5-MTHF RBC (nM)	5,10-MTHF plasma (nM)	5,10-MTHF WB (nM)	5,10-MTHF RBC (nM)	FA plasma (nM)	FA WB (nM)	FA RBC (nM)
Folate	52	33.3	69.3	403.8	1074.0	0.8	34.7	102.5	0.2	15.3	45.6
Folate	53	39.1	62.3	461.5	1083.2	0.4	10.4	26.0	0.7	9.3	22.6
Folate	54	37.6	29.5	369.6	934.0	0.5	36.2	95.5	2.3	7.1	15.0
Folate	55	39.9	28.4	442.3	1065.8	0.4	14.6	35.9	1.6	10	22.7
Folate	56	36.3	25.8	280.9	728.5	0.3	21.6	59.1	1.2	7.8	19.4
Folate	57	39.4	64.5	644.7	1537.1	0.5	23.6	59.2	1.9	11.4	26.0
Folate	58	41.2	47.2	272.5	594.0	0.5	47.7	115.2	0.8	7	15.8
Folate	59	36.7	42.4	160.1	363.2	0.5	46.9	126.8	0.8	38.2	102.6
Folate	60	38.5	75.7	629.4	1513.9	0.3	26.8	69.0	0.1	7.7	19.9
Folate	61	45.2	23.7	529.5	1142.9	0.6	18.5	40.2	0.3	3.3	6.9
Folate	62	41.5	32.4	441.9	1019.2	0.3	16.1	38.5	7.1	4	-0.4
Folate	63	35.9	11.5	543.9	1494.5	0.3	24.6	67.9	1.6	2.9	5.1
Folate	64	36.8	37.3	216.2	523.3	0.4	6.1	15.8	0.5	1.9	4.3
Folate	65	34.2	32.1	1060.6	3039.3	0.3	35.5	103.1	0.7	5	13.3
Folate	66	42.9		1039.9	2424.1		37.9	88.4		9	21.0
Folate	67	37.6	36.3	351.3	874.1	0.2	11.9	31.2	13.5	9.7	3.4
Folate	68	35.9	25.6	224.0	578.4	0.3	239.0	665.3	0.9	35.8	98.1
Folate	69	36.9	20.5	312.6	812.0	0.3	16.6	44.5	0.8	2.9	6.5
Folate	70	-	40.6	346.4		0.3	121.0		4.6	40.3	
Folate	71	36.8	11.4	246.0	649.0	0.3	12.8	34.3	1.6	1	0.0
Folate	72	33.2	81.3	482.7	1290.4	0.5	22.6	67.0	0.3	5	14.4
Folate	73	40.3	42.5	428.1	999.4	0.4	17.2	42.1	0.0	1.8	4.5
Folate	74	-	20.3	285.0		0.3	17.5		0.4	1	
Folate	75	37.3	66.1	451.2	1098.6	0.5	226.2	605.6	0.8	28.8	75.9

Table 30. Continued (JIA patients off MTX)

Group	Patient	Hct (%)	5-MTHF plasma (nM)	5-MTHF WB (nM)	5-MTHF RBC (nM)	5,10-MTHF plasma (nM)	5,10-MTHF WB (nM)	5,10-MTHF RBC (nM)	FA plasma (nM)	FA WB (nM)	FA RBC (nM)
Folate	77	36.6	40.7	595.9	1557.6	0.4	34.8	94.3	0.9	1.3	1.9
Folate	78	39.3	20.9	570.5	1419.3	0.2	112.7	286.3	0.6	16.5	41.1
Folate	79	33.7	44.3	412.7	1137.6	0.2	21.6	63.7	0.8	0.3	-0.7
Folate	80	38	37.9	511.0	1282.8	0.6	18.8	48.4	0.0	2.7	7.1
Folate	81	38.8	34.5	491.1	1211.3	0.3	19.2	48.9	2.3	4.7	8.6
Folate	82	39.9	52.2	753.8	1810.6	0.4	9.0	22.1	0.9	0.2	-0.9
Folate	83	36.2	91.4	300.3	668.3	0.4	7.3	19.3	0.0	2.5	6.9
Folate	84	39.1	12.9			0.2		-0.4	0.6		-0.9
Folate	85	37.7	47.8	486.7	1212.1	0.5	18.0	47.0	0.7	2.1	4.5
Folate	86	35.4	88.3	619.0	1587.4	0.4	24.6	68.9	0.8	2.9	6.7
Folate	87	33.5	45.1	409.2	1132.0	0.3	48.2	143.4	0.0	11.7	34.9
Folate	88	36.2	28.2	439.9	1165.5	0.3	36.9	101.4	0.7		-1.3
Folate	89	31.6	26.4	338.7	1014.9	0.3	49.4	155.7	2.2	6.7	16.4
Folate	90	30.9	26.4	529.3	1653.9	0.2	39.2	126.5	0.0	3.9	12.6
Folate	91	37.2	35.4	483.1	1238.7	0.3	49.6	133.0	0.5	3.7	9.1
Folate	92	33	89.4	438.7	1147.9	0.5	18.9	56.3	0.0	3.3	10.0
Folate	93	35.7	44.7	480.7	1265.9	0.2	37.3	104.2	0.9	2.9	6.6
Folate	94	35.5	65.8	634.1	1666.7	0.2	26.7	74.7	1.0	6.4	16.1
Folate	95	30.9	21.2	377.1	1173.1	0.5	41.8	134.3	30.7	1.3	-64.5
Folate	96	34.5	24.1	289.9	794.5	0.2	28.7	82.7	1.1	2	3.7
Folate	97	37.6	65.6	380.0	901.7	0.3	26.9	71.1	0.0	4.9	13.0
Folate	98	36	33.3			0.3		-0.6	0.7		-1.3
Folate	99	35.4	87.7			0.4		-0.8	1.0		-1.7
Folate	100	37.9	18.3	497.2	1282.0	0.5	32.6	85.1	0.0	0.1	0.3

Table 31. 5-MTHF relative polyglutamation distribution (JIA patients on MTX)

Group	Patient	5MTHFPG$_3$ (%)	5MTHFPG$_4$ (%)	5MTHFPG$_5$ (%)	5MTHFPG$_6$ (%)	5MTHFPG$_7$ (%)	5MTHFPG$_8$ (%)	5MTHFPG$_9$ (%)	5MTHFPG$_{10}$ (%)	5MTHF$_{11}$ (%)
MTX	1	2.4	6.8	46.2	28.8	8.3	4.2	2.6	0.6	0.0
MTX	2	1.8	5.7	45.4	31.9	8.7	4.1	2.0	0.4	0.0
MTX	3	2.0	6.9	46.3	29.8	8.1	3.9	2.2	0.7	0.0
MTX	4	1.9	5.2	43.2	30.5	10.2	5.4	2.9	0.6	0.0
MTX	5	1.0	6.7	45.1	32.3	8.1	4.0	2.1	0.6	0.0
MTX	6	2.2	5.9	36.8	33.5	12.7	5.6	2.6	0.8	0.0
MTX	7									
MTX	8	1.8	6.9	46.5	31.1	8.3	3.6	1.4	0.5	0.0
MTX	9	1.2	5.6	44.3	33.5	9.6	3.4	1.7	0.6	0.0
MTX	10	0.0	0.0	47.8	7.3	5.4	23.2	16.4	0.0	0.0
MTX	11	3.1	6.6	44.5	28.9	9.6	4.8	2.0	0.5	0.0
MTX	12	3.3	5.3	39.4	32.4	11.6	4.4	2.7	1.0	0.0
MTX	13	0.9	4.4	41.2	35.5	11.0	5.0	1.7	0.3	0.0
MTX	14	4.1	7.2	40.3	29.6	11.4	4.9	2.0	0.4	0.0
MTX	15	9.6	5.2	30.9	34.9	12.2	5.0	1.4	0.8	0.0
MTX	16	1.8	4.9	42.1	33.2	10.5	4.4	2.4	0.6	0.0
MTX	17	3.4	5.2	38.8	29.5	10.4	6.9	4.4	1.4	0.0
MTX	18	2.3	6.7	41.6	32.4	9.6	4.4	2.1	0.8	0.0
MTX	19	2.0	5.0	45.4	32.2	9.0	3.5	2.2	0.7	0.0
MTX	20	2.3	6.8	44.1	33.6	8.3	3.3	1.2	0.4	0.0
MTX	21	1.7	6.7	41.3	31.9	12.5	4.2	1.8	0.0	0.0
MTX	22	2.2	6.8	39.6	36.6	9.5	3.7	1.4	0.2	0.0
MTX	23	1.7	9.8	45.5	27.4	8.9	4.4	1.9	0.4	0.0
MTX	24	1.2	9.3	39.1	34.4	10.4	4.0	1.5	0.1	0.0
MTX	25	1.5	7.7	47.6	29.1	8.5	3.2	1.8	0.5	0.0
MTX	26	1.9	10.8	43.7	27.9	9.3	4.2	1.7	0.4	0.0
MTX	27	0.8	7.1	42.9	34.1	9.9	3.5	1.4	0.3	0.0
MTX	28	1.9	8.4	45.5	28.9	10.0	3.6	1.4	0.3	0.0

273

Table 31. Continued (JIA patients on MTX)

Group	Patient	5MTHFPG$_3$ (%)	5MTHFPG$_4$ (%)	5MTHFPG$_5$ (%)	5MTHFPG$_6$ (%)	5MTHFPG$_7$ (%)	5MTHFPG$_8$ (%)	5MTHFPG$_9$ (%)	5MTHFPG$_{10}$ (%)	5MTHFPG$_{11}$ (%)
MTX	29	0.6	5.1	52.3	31.8	6.5	2.3	1.2	0.2	0.0
MTX	30	1.1	8.4	43.6	29.7	10.2	4.3	2.0	0.6	0.0
MTX	31	3.3	11.4	46.9	24.9	7.2	3.8	2.2	0.2	0.0
MTX	32	0.9	6.2	40.6	36.7	10.5	3.4	1.3	0.4	0.0
MTX	33	1.5	8.6	47.2	29.2	8.0	3.2	1.6	0.6	0.0
MTX	34	0.9	7.3	51.9	28.9	7.0	2.8	1.1	0.1	0.0
MTX	35	1.2	6.5	41.7	37.2	9.7	2.6	1.0	0.0	0.0
MTX	36	2.0	7.7	44.5	30.6	9.0	4.0	1.7	0.4	0.0
MTX	37	2.5	12.7	51.1	24.3	5.3	3.1	0.8	0.0	0.0
MTX	38	3.0	8.4	47.1	28.3	7.4	3.9	1.6	0.2	0.0
MTX	39	2.5	9.0	45.0	28.5	8.7	4.6	1.6	0.0	0.0
MTX	40	1.4	7.1	39.4	36.4	9.6	4.2	1.7	0.2	0.0
MTX	41	1.2	7.3	40.5	34.7	10.5	3.8	1.5	0.4	0.0
MTX	42	1.9	7.9	49.9	27.5	8.1	3.4	1.4	0.0	0.0
MTX	43	2.6	8.0	45.8	27.2	9.7	5.1	1.3	0.2	0.0
MTX	44	2.4	8.7	46.4	29.5	7.5	3.3	1.8	0.4	0.0
MTX	45	2.1	7.8	41.0	30.9	11.9	4.3	2.1	0.0	0.0
MTX	46	1.5	6.8	34.4	33.9	16.4	6.2	0.9	0.0	0.0
MTX	47	5.6	7.7	43.9	28.5	9.5	3.2	1.3	0.3	0.0
MTX	48	1.3	8.2	48.0	28.9	7.7	3.7	1.9	0.2	0.0
MTX	49	3.5	10.3	42.0	28.2	9.0	4.6	2.1	0.5	0.0
MTX	50	3.3	8.3	45.4	30.1	8.1	3.1	1.3	0.5	0.0
MTX	51	0.6	6.4	43.6	32.1	10.4	4.3	2.2	0.5	0.0
MTX	52	1.5	5.4	43.2	32.1	12.0	3.6	1.8	0.4	0.0
MTX	53	0.6	5.5	37.4	35.6	13.2	4.7	2.3	0.8	0.0
MTX	54	0.4	7.6	44.7	29.2	10.0	5.4	2.2	0.3	0.0
MTX	55	0.4	5.3	43.6	33.6	10.9	4.0	1.7	0.6	0.0
MTX	56	0.2	6.3	42.8	33.5	11.2	3.8	1.8	0.6	0.0
MTX	57	0.0	5.9	39.6	38.0	11.0	3.3	1.7	0.4	0.0

Table 31. Continued (JIA patients on MTX)

Group	Patient	5MTHFPG$_3$ (%)	5MTHFPG$_4$ (%)	5MTHFPG$_5$ (%)	5MTHFPG$_6$ (%)	5MTHFPG$_7$ (%)	5MTHFPG$_8$ (%)	5MTHFPG$_9$ (%)	5MTHFPG$_{10}$ (%)	5MTHF$_{11}$ (%)
MTX	58	0.0	4.0	37.8	36.4	13.6	5.4	2.4	0.4	0.0
MTX	59	1.4	9.2	41.4	31.8	9.5	4.0	2.1	0.6	0.0
MTX	60	1.0	5.5	43.4	33.7	10.6	3.9	1.5	0.3	0.0
MTX	61	0.7	6.6	40.9	35.6	10.9	3.3	1.6	0.4	0.0
MTX	62									
MTX	63	1.3	9.4	44.7	29.0	10.8	2.9	1.9	0.0	0.0
MTX	64	1.4	9.3	44.7	29.2	8.1	4.6	2.1	0.6	0.0
MTX	65	0.5	8.6	49.8	25.9	8.7	4.7	1.8	0.0	0.0
MTX	66	0.3	8.6	47.1	30.7	7.3	3.3	1.9	0.7	0.0
MTX	67	0.1	6.9	47.0	31.1	9.5	3.3	1.7	0.4	0.0
MTX	68	0.4	10.9	46.5	27.8	7.9	3.5	2.5	0.5	0.0
MTX	69	4.0	10.7	46.3	27.9	6.8	2.8	1.0	0.5	0.0
MTX	70	1.0	7.4	47.4	30.7	7.9	3.6	1.6	0.4	0.0
MTX	71	0.5	6.6	48.8	28.8	9.0	4.1	1.8	0.4	0.0
MTX	72	0.1	6.1	41.0	36.2	10.6	4.0	1.7	0.3	0.0
MTX	73	0.1	7.0	49.2	30.1	8.3	3.5	1.5	0.3	0.0
MTX	74	0.3	5.6	39.4	32.5	13.6	5.9	2.2	0.6	0.0
MTX	75	0.7	7.1	43.3	31.5	10.4	3.9	2.6	0.6	0.0
MTX	76	0.4	7.7	47.6	29.0	8.6	4.1	2.0	0.5	0.0
MTX	77	0.6	4.8	58.2	27.8	6.3	1.8	0.4	0.0	0.0
MTX	78	0.2	6.0	46.3	33.6	9.0	3.1	1.4	0.3	0.0
MTX	79	1.1	6.9	46.7	29.0	9.7	3.8	2.3	0.5	0.0
MTX	80									
MTX	81	0.0	5.7	38.0	36.2	13.1	5.3	1.7	0.0	0.0
MTX	82									
MTX	83	0.6	9.0	46.2	28.3	10.6	3.3	1.5	0.4	0.0
MTX	84									
MTX	85									
MTX	86									

Table 31. Continued (JIA patients on MTX)

Group	Patient	5MTHFPG$_3$ (%)	5MTHFPG$_4$ (%)	5MTHFPG$_5$ (%)	5MTHFPG$_6$ (%)	5MTHFPG$_7$ (%)	5MTHFPG$_8$ (%)	5MTHFPG$_9$ (%)	5MTHFPG$_{10}$ (%)	5MTHF$_{11}$ (%)
MTX	88	0.5	7.2	42.2	30.9	11.3	5.1	2.3	0.5	0.0
MTX	89	0.9	6.2	42.5	32.0	10.8	4.4	2.5	0.7	0.0
MTX	90	0.7	6.6	41.7	33.8	11.3	3.6	1.8	0.4	0.0
MTX	91	0.2	5.3	49.6	31.5	9.1	2.9	1.1	0.3	0.0
MTX	92	0.4	4.9	42.1	35.3	11.6	3.0	2.0	0.6	0.0
MTX	93	0.6	7.7	46.8	29.5	10.6	3.5	1.4	0.0	0.0
MTX	94	0.1	5.1	39.8	33.5	13.2	4.8	2.6	0.9	0.0
MTX	95	0.1	6.2	45.2	32.6	9.5	3.9	1.9	0.6	0.0
MTX	96	0.6	6.1	38.1	34.8	13.0	4.7	2.0	0.7	0.0
MTX	97	0.3	4.1	35.5	37.4	15.0	4.9	2.3	0.6	0.0
MTX	98	1.0	7.5	46.2	28.8	9.8	3.9	2.3	0.6	0.0
MTX	99	1.0	6.4	44.2	29.3	10.5	5.1	2.7	0.8	0.0
MTX	100	0.7	6.1	44.4	30.2	10.7	4.7	2.5	0.8	0.0
MTX	101	1.7	7.0	39.5	30.8	11.9	5.9	2.5	0.6	0.0
MTX	102	2.3	11.3	54.5	21.6	6.0	3.1	1.1	0.0	0.0
MTX	103	4.7	8.5	45.6	25.1	10.2	3.7	1.7	0.5	0.0
MTX	104									
MTX	105	2.5	8.8	42.3	31.9	10.2	3.3	1.0	0.0	0.0

Table 31. 5-MTHF relative polyglutamation distribution (JIA patients off MTX)

Group	Patient	5MTHFPG$_3$ (%)	5MTHFPG$_4$ (%)	5MTHFPG$_5$ (%)	5MTHFPG$_6$ (%)	5MTHFPG$_7$ (%)	5MTHFPG$_8$ (%)	5MTHFPG$_9$ (%)	5MTHFPG$_{10}$ (%)	5MTHF$_{11}$ (%)
Folate	1	3.0	5.4	49.1	31.3	7.0	2.7	1.2	0.3	0.0
Folate	2	2.9	7.6	57.6	25.1	4.3	1.8	0.7	0.0	0.0
Folate	3									
Folate	4	1.5	5.8	56.7	27.2	5.9	2.2	0.7	0.0	0.0
Folate	5	2.4	8.0	52.4	28.1	5.5	2.2	1.1	0.3	0.0
Folate	6	4.0	5.0	45.6	30.8	9.3	3.7	1.5	0.0	0.0
Folate	7	2.7	6.2	56.2	26.3	5.7	2.0	0.9	0.0	0.0
Folate	8	4.7	6.1	50.3	29.2	6.3	2.4	1.0	0.0	0.0
Folate	9	3.4	7.6	50.6	26.8	6.5	3.4	1.4	0.4	0.0
Folate	10	3.9	5.1	42.8	34.6	8.9	2.9	1.3	0.4	0.0
Folate	11	0.7	5.1	58.2	26.6	5.3	2.6	1.2	0.3	0.0
Folate	12	1.3	3.9	48.0	33.2	8.8	3.4	1.3	0.1	0.0
Folate	13	0.9	5.3	48.3	30.6	8.6	3.8	1.9	0.5	0.0
Folate	14	0.8	5.3	42.8	35.1	10.4	3.6	1.5	0.4	0.0
Folate	15	3.2	7.6	55.0	24.3	5.5	2.8	1.2	0.4	0.0
Folate	16	3.1	9.1	45.2	30.3	9.2	3.1	0.0	0.0	0.0
Folate	17	6.1	2.6	32.6	35.8	14.8	5.4	2.3	0.4	0.0
Folate	18	5.3	6.4	45.4	30.0	7.7	3.2	1.7	0.2	0.0
Folate	19	2.0	3.6	39.5	39.7	10.9	3.4	0.8	0.0	0.0
Folate	20	2.4	6.2	43.5	30.5	11.5	4.5	1.3	0.1	0.0
Folate	21	3.7	4.6	39.2	32.4	12.7	5.5	2.0	0.0	0.0
Folate	22	1.5	5.4	42.7	34.4	10.3	4.4	1.3	0.0	0.0
Folate	23	4.1	5.4	45.7	30.1	8.9	3.8	1.9	0.1	0.0
Folate	24	3.0	6.6	42.4	29.1	10.7	6.2	1.9	0.0	0.0
Folate	25	4.0	4.7	49.2	32.1	6.4	3.2	0.0	0.4	0.0
Folate	26	3.3	6.6	48.2	28.5	7.8	4.0	1.7	0.0	0.0
Folate	27	11.2	4.5	43.2	26.9	10.5	3.7	0.0	0.0	0.0
Folate	28	6.5	4.7	41.7	33.7	9.6	2.9	0.8	0.2	0.0
Folate	29	4.1	6.4	43.6	30.7	10.5	3.3	1.3	0.0	0.0

Table 31. Continued (JIA patients off MTX)

Group	Patient	5MTHFPG$_3$ (%)	5MTHFPG$_4$ (%)	5MTHFPG$_5$ (%)	5MTHFPG$_6$ (%)	5MTHFPG$_7$ (%)	5MTHFPG$_8$ (%)	5MTHFPG$_9$ (%)	5MTHFPG$_{10}$ (%)	5MTHF$_{11}$ (%)
Folate	30	7.8	8.3	47.0	25.9	6.9	3.1	0.9	0.0	0.0
Folate	31	1.5	8.0	50.0	25.9	8.7	3.7	1.7	0.5	0.0
Folate	32	0.6	4.3	49.5	33.6	7.5	3.1	1.2	0.1	0.0
Folate	33	1.5	5.9	45.6	30.9	9.8	4.1	1.7	0.5	0.0
Folate	34	0.9	4.2	46.6	33.4	9.3	3.9	1.4	0.2	0.0
Folate	35	0.6	4.3	48.4	34.2	8.6	2.7	1.1	0.2	0.0
Folate	36	1.1	6.5	54.3	28.3	5.8	2.7	1.1	0.2	0.0
Folate	37	1.4	5.8	56.1	26.5	5.8	2.9	1.2	0.2	0.0
Folate	38	1.9	6.1	41.9	32.1	11.3	4.8	1.6	0.3	0.0
Folate	39	0.8	6.4	46.7	32.8	9.2	2.7	1.2	0.3	0.0
Folate	40	1.3	5.6	42.6	35.1	10.5	3.5	1.3	0.2	0.0
Folate	41	2.9	6.4	46.8	31.0	7.8	3.2	1.5	0.4	0.0
Folate	42	1.5	5.5	44.1	32.9	9.9	4.0	1.7	0.4	0.0
Folate	43	1.7	5.1	40.9	33.9	11.6	4.6	1.3	0.9	0.0
Folate	44	1.1	7.4	50.2	29.3	7.2	3.0	1.3	0.5	0.0
Folate	45									
Folate	46	1.4	5.4	45.1	35.3	9.3	2.5	1.0	0.0	0.0
Folate	47	2.0	4.5	41.6	36.0	10.2	4.0	1.4	0.3	0.0
Folate	48	2.3	6.3	47.9	29.5	8.8	3.4	1.3	0.5	0.0
Folate	49	1.6	8.4	55.0	26.2	5.7	2.2	0.9	0.0	0.0
Folate	50	1.9	7.1	52.2	28.0	6.5	2.8	1.5	0.0	0.0
Folate	51	0.6	3.8	40.1	36.1	12.1	4.9	2.0	0.4	0.0
Folate	52	1.5	6.5	52.8	27.6	6.4	3.2	1.5	0.4	0.0
Folate	53	1.4	6.9	49.7	29.2	7.9	3.6	1.2	0.2	0.0
Folate	54	1.8	7.1	49.9	29.0	7.3	3.3	1.3	0.3	0.0
Folate	55	1.9	6.1	48.0	30.1	8.4	3.5	1.6	0.4	0.0
Folate	56	1.5	7.7	49.7	26.2	7.9	4.8	1.9	0.4	0.0
Folate	57	1.5	6.2	49.9	29.5	7.7	3.3	1.5	0.4	0.0
Folate	58	2.4	9.7	56.6	20.2	5.6	3.6	1.8	0.0	0.0

Table 31. Continued (JIA patients off MTX)

Group	Patient	5MTHFPG2 (%)	5MTHFPG3 (%)	5MTHFPG4 (%)	5MTHFPG5 (%)	5MTHFPG6 (%)	5MTHFPG7 (%)	5MTHFPG8 (%)	5MTHFPG9 (%)	5MTHFPG10 (%)	5MTHF11 (%)
Folate	59		3.9	7.5	44.8	30.1	7.3	4.4	2.1	0.0	0.0
Folate	60		1.7	5.2	51.7	30.8	6.8	2.3	1.2	0.2	0.0
Folate	61		3.2	6.4	44.4	31.1	10.1	3.4	1.0	0.4	0.0
Folate	62		1.0	7.6	43.8	30.5	10.5	4.3	1.8	0.5	0.0
Folate	63		1.6	8.7	58.0	22.9	5.3	2.6	1.0	0.0	0.0
Folate	64		0.9	6.1	39.9	33.7	11.9	4.9	2.0	0.6	0.0
Folate	65		1.3	6.9	51.6	30.2	6.8	2.2	0.9	0.2	0.0
Folate	66		1.3	4.6	43.1	35.6	9.8	3.8	1.5	0.2	0.0
Folate	67		3.7	5.3	43.2	30.2	9.4	4.5	2.8	0.8	0.0
Folate	68										
Folate	69										
Folate	70		7.4	5.1	44.3	31.3	7.1	3.3	1.0	0.5	0.0
Folate	71		3.5	6.1	41.0	32.4	10.8	3.9	1.8	0.6	0.0
Folate	72		4.0	7.0	44.3	31.3	8.9	3.1	1.1	0.3	0.0
Folate	73		1.9	7.3	53.1	25.7	6.6	3.4	1.5	0.6	0.0
Folate	74		8.0	4.1	41.6	32.5	9.0	3.1	1.6	0.0	0.0
Folate	75		1.6	4.8	43.1	34.1	10.4	4.1	1.6	0.3	0.0
Folate	76		1.1	11.2	48.1	24.1	8.3	4.5	2.2	0.5	0.0
Folate	77		0.7	5.5	47.7	32.0	8.3	3.7	1.7	0.4	0.0
Folate	78		0.9	6.4	37.6	36.4	11.7	4.7	1.9	0.5	0.0
Folate	79		1.1	6.6	45.4	32.0	8.8	4.0	1.5	0.5	0.0
Folate	80		0.8	5.8	48.1	33.4	8.1	2.5	0.9	0.2	0.0
Folate	81		1.1	6.0	48.1	32.0	7.9	3.2	1.4	0.4	0.0
Folate	82		0.9	6.2	49.6	30.9	7.3	3.3	1.5	0.4	0.0
Folate	83		0.9	7.5	50.9	27.7	7.6	3.5	1.5	0.4	0.0
Folate	84		1.1	6.3	44.7	32.6	9.0	4.0	1.9	0.5	0.0
Folate	85		1.4	9.5	57.3	20.0	5.9	3.5	1.9	0.5	0.0
Folate	86		0.8	6.6	52.0	29.7	6.2	2.9	1.4	0.4	0.0
Folate	87		1.1	5.0	47.1	32.6	8.4	3.4	1.8	0.5	0.0

Table 31. Continued (JIA patients off MTX)

Group	Patient	5MTHFPG$_3$ (%)	5MTHFPG$_4$ (%)	5MTHFPG$_5$ (%)	5MTHFPG$_6$ (%)	5MTHFPG$_7$ (%)	5MTHFPG$_8$ (%)	5MTHFPG$_9$ (%)	5MTHFPG$_{10}$ (%)	5MTHF$_{11}$ (%)
Folate	88	1.3	8.2	52.0	26.1	6.8	3.4	1.8	0.4	0.0
Folate	89	0.5	4.1	40.9	36.8	11.5	4.2	1.6	0.4	0.0
Folate	90	1.0	7.0	50.8	27.4	8.0	3.7	1.7	0.4	0.0
Folate	91	0.8	5.4	45.0	33.4	10.1	3.5	1.5	0.3	0.0
Folate	92	1.3	7.0	49.0	28.2	8.3	4.0	1.8	0.4	0.0
Folate	93	1.1	7.1	51.6	27.6	7.2	3.3	1.6	0.4	0.0
Folate	94	0.8	5.2	46.9	33.2	8.7	3.4	1.5	0.3	0.0
Folate	95	1.1	7.2	52.0	26.7	7.8	3.4	1.4	0.3	0.0
Folate	96	1.5	6.6	45.0	29.4	10.2	4.5	2.2	0.5	0.0
Folate	97	1.5	8.7	47.1	28.7	7.9	4.0	1.8	0.4	0.0
Folate	98	0.8	6.6	49.0	31.7	7.6	2.8	1.3	0.3	0.0
Folate	99	0.7	6.8	54.9	26.8	6.0	2.8	1.4	0.4	0.0
Folate	100	0.9	7.1	52.1	27.6	7.3	3.3	1.4	0.3	0.0

Chapter eight: General summary and conclusions

Chapter eight: General summary and conclusions

Table of contents

8.1   General conclusions

This dissertation focused on development of analytical detection strategies for pharmaceutically relevant compounds including: the antifolate MTX, its (in)active metabolites, its conjugates, and endogenous folates in biological systems. All of the target analytes share a common structural feature, the pteroyl ring system, analyte identity is resulting from limited variations in ring redox state, minor structural substitutions of the pteridine ring, and changes in conjugation status (i.e. polyglutamated or nanoparticle conjugated). Specific and sensitive detection of the individual species is of high interest as they may constitute biomarkers for individualizing low dose MTX therapy in autoimmune diseases such as JIA, but is also required for the (pre)clinical studies of novel MTX drug delivery entities. In this dissertation various assays are presented for the specific determination of these analytes in the presence of each other. Each of these strategies has their own strengths and weaknesses, and the appropriate analysis strategy is dependent on the nature of the analyte, its biological environment, stability and the clinical question to be answered.

Chapter 2 and 3 of this dissertation focused on bioanalytical method development for a G5-MTX-FA nanoparticle. The effectiveness of this experimental therapeutic for the treatment of neoplastic diseases has been demonstrated in various *in vitro* [1] and *in vivo* [2] studies. Continued development requires the establishment of bioanalytical methodology in order to appropriately study the *in vivo* behavior (i.e. MTX release profile etc), pharmacokinetics and dosing regimen of the entity. Since the nanoparticle was designed as a delivery system for MTX, analytical targets were identified as nanoparticle conjugated MTX, nanoparticle released (free) MTX and (free) 7OH-MTX, a product

resulting from MTX metabolism. The specific measurement of these diverse entities was accomplished by an innovative cascade of complementary assays. First total MTX content (i.e. the sum of free and G5-MTX-FA related MTX) was determined in the sample by initiating a non-selective reductive cleavage of the C(9)-N(10) bridge in MTX. The resulting fluorescent pteridine derivative could subsequently be determined by reversed phase separation and fluorescence detection. A second assay involving HPLC separation followed by online postcolumn photochemical degradation of the same C(9)-N(10) bond was then used to reveal the MTX origin (i.e. free or dendrimer conjugated).

The newly developed methodology was validated in plasma and urine obtained from rats and dogs. The validated method was applied to determine the *in vivo* pharmacokinetics of G5-MTX-FA in animals, dosed at various different concentrations by either a bolus IV injection or through the subcutaneous tissue. The nanoparticle did not demonstrate significant release of MTX in the systemic circulation, indicating that the conjugate linkage is esterase stable and observed therapeutic effects cannot be attributed to free MTX generated by rapid release from the MTX-nanoparticle conjugate.

Chapter 4 and 5 address bioanalytical method development for MTX polyglutamyl conjugates, which are bioactive metabolites of MTX, and present in human erythrocytes of JIA patients on MTX therapy. Erythrocyte MTXPGs content is currently of high interest , as it may provide a biomarker for therapeutical guidance of MTX treatment in RA[3]. However such strategy was conceived to the present investigation and had not previously been applied to JIA patients. The present work was conducted in collaboration with Childrens Mercy Hospital (KC, MO). The Initial plan were to implement a previously described HPLC postcolumn reactor method for the measurement of

MTXPG in a cohort involving JIA patients (n=99). Trial experiments revealed the approach to be inadequate, thus necessitating the development of methodology of improved sensitivity and selectivity. The approach ultimately employed was a ion-pair based HPLC separation, coupled with tandem mass spectrometric detection for MTXPGs present in human erythrocytes.

This methodology was applied towards the analysis of erythrocyte samples obtained from 99 JIA patients on MTX therapy. Analysis of the intracellular MTXPG distribution revealed the route of administration (oral vs subcutaneous) as a primary determinant of intracellular MTX glutamate chain elongation (appendix 1)[4]. Furthermore JIA patients that were encountering liver toxicity (defined as an elevated liver function test) had a tendency to form longer intracellular MTXPGs (appendix 2)[5]. Attempts to correlate intracellular MTXPG levels to MTXs efficacy in JIA were unsuccessful, and recently similar observations are being reported in adulthood arthritis[6].

Due to the discrepancies in findings between different research groups, the utility of erythrocyte MTXPG determination is still an unresolved clinical issue[3]. Larger standardized studies are required in order to fully understand the clinical impact of these measurements, supported by more specific and sensitive bioanalytical assays, as presented in chapter 4 and 5. The observation that MTXPG population distribution is related to drug induced toxicity and is dependent of route of administration, advocates for the routine measurement of erythrocyte MTXPGs in JIA, especially in an attempt to reduced drug induced toxicity, which is the primary cause of MTX discontinuation.

Chapter 7 of the dissertation focuses on the comprehensive measurement of folate isoform and polyglutamation distribution in human erythrocytes. The assay was developed with the intent to measure the influence of low-dose MTX therapy upon folate homeostasis, as it was hypothesized that the antagonist (MTX)/agonist (folate) ratio within the cell is important for MTX efficacy and toxicity. Semi-quantitative comprehensive folate measurement was accomplished by the development of a cascade of highly specific and sensitive LC tandem mass spectrometric assays. First, the various folate isoforms were quantitated individually utilizing a deglutamated whole blood sample and stable isotope dilution techniques. A second assay determined the plasma folate contribution in a similar manner. Erythrocyte folate content was calculated by the method of Lamers[7] utilizing plasma and whole blood folate concentrations. As folates were quantitated in the monoglutamyl form, the folate polyglutamation fingerprint was lost. The folate polyglutamation fingerprint was determined by performing a third assay where intact folates were extracted from erythrocytes, with relative quantitation accomplished by ion-pair LC separation followed by tandem mass spectrometry, in the absence of an isotopic standard.

The method was utilized to determine the impact of MTX therapy on the folate status of a JIA pediatric population by analyzing blood samples obtained from approximately 100 JIA patients not on MTX, and 100 JIA patients on MTX therapy (in a collaborative effort with Childrens Mercy Hospitals KC, MO). It was found that patients on MTX had on average a statistically significant lower folate status. Furthermore patient folate status correlated with the effectiveness of MTX therapy, indicated by the fact that individuals with low(er) erythrocyte folate status were more likely to be responders to

MTX therapy and disease more adequately controlled. Although not yet confirmed this might be indicative of an important balance between agonist and antagonist within the biological system.

It is acknowledged that this study has limitations. It is a cross-sectional analysis of patients suffering from JIA supplied by a single center, which is a design that does not allow us to dynamically follow up trends over time or related to disease activity. However, this is the largest cohort of JIA patients reported to date, and data has been obtained by the most advanced bioanalytical methods in the field to date, providing a detailed description of intracellular red blood cell folate isoform, polyglutamation and antifolate (MTX) polyglutamation status. At the time of dissertation preparation, it is unclear and impossible to predict what the exact impact will be of the presented bio-analytical methodology in the field of JIA. Larger more controlled patient studies are necessary to prove its usefulness in guiding JIA therapy in the future. However the potential of simultaneous MTXPG and comprehensive folate measurement to differentiate various patient phenotypes has been demonstrated in this dissertation by a single center study. With the bioanalytical methods in place, the next step is up to collaborative research between the bioanalyst and physician to gain an understanding in how to utilize the presented methodology, and translate raw bioanalytical measurements ultimately in the optimization of MTX treatment in the pediatric population.

8.2   Future directions of pteroyl analysis

Overall, the presented bioanalytical methods are validated and their robustness has been demonstrated extensively. An exception is the folate methodology, where the limited availability of (isotope) labeled standards complicated method development, validation and quantitation. As suggested in the previous section, larger patient studies are required to validate our initial observations and further investigate the importance of folate measurement during MTX therapy. However such studies do need to be backed up by stable and standardized bioanalytical methods to avoid assay induced bias. Ideally the quantitation of folatePG species in human erythrocytes requires the synthesis of stable isotope labeled standards of each folate polyglutamyl form of interest. This dissertation suggests that these biological relevant folate species include the isoforms of 5-MTHF, 5-FTHF, 10-FTHF, 5,10-MTHF and THF. Furthermore the ɣ-glutamyl chain length of these standards needs to span from 3-10 residues minimally. Although the synthesis of many of these entities has not been reported to date, it appears that synthesis could be accomplished by the use of biological or chemical (solid phase or solution) procedures, utilizing specialized building blocks.

The presented bioanalytical methodology may also have potential application in other clinical areas where MTX is commonly used, or where folate metabolism is critical such as oncology[8], dermatology[9], gastroenterology[10-12], neurology[13], genetics[14], and maternal fetal medicine[15]. Gastrointestinal toxicity and hepatotoxicity from the drug limit its use in all conditions and there are no predictors to help clinicians identify patients at risk for these effects, nor the full understanding of how to optimize therapy to a specific patient. Additionally, alterations in maternal folate have been linked to congenital heart

disease[16], neural tube defects[16], and Down syndrome[14], therefore the bioanalytical measurement of folates, and if relevant antifolates, has the potential to impact diverse patient populations in several fields in medicine

8.3   References

[1]   T. P. Thomas, I. J. Majoros, A. Kotlyar, J. F. Kukowska-Latallo, A. Bielinska, A. Myc, J. R. Baker, Targeting and Inhibition of Cell Growth by an Engineered Dendritic Nanodevice. *Journal of Medicinal Chemistry.* **2005**, *48*, 3729.

[2]   J. F. Kukowska-Latallo, K. A. Candido, Z. Cao, S. S. Nigavekar, I. J. Majoros, T. P. Thomas, L. P. Balogh, M. K. Khan, J. R. Baker, Jr., Nanoparticle Targeting of Anticancer Drug Improves Therapeutic Response in Animal Model of Human Epithelial Cancer. *Cancer Res.* **2005**, *65*, 5317.

[3]   M. Danila, L. Hughes, E. Brown, S. Morgan, J. Baggott, D. Arnett, S. Bridges, Measurement of Erythrocyte Methotrexate Polyglutamate Levels: Ready for Clinical Use in Rheumatoid Arthritis? , *Current Rheumatology Reports.* **2010**, *12*, 342.

[4]   M. L. Becker, L. van Haandel, R. Gaedigk, A. Lasky, M. Hoeltzel, J. Stobaugh, J. S. Leeder, Analysis of intracellular methotrexate polyglutamates in patients with juvenile idiopathic arthritis: Effect of route of administration on variability in intracellular methotrexate polyglutamate concentrations. *Arthritis & Rheumatism.* **2010**, *62*, 1803.

[5]   M. L. Becker, R. Gaedigk, L. van Haandel, B. Thomas, A. Lasky, M. Hoeltzel, H. Dai, J. Stobaugh, J. S. Leeder, The effect of genotype on methotrexate polyglutamate variability in juvenile idiopathic arthritis and association with drug response. *Arthritis & Rheumatism.* **2010**, n/a.

[6]   L. K. Stamp, J. L. O'Donnell, P. T. Chapman, M. Zhang, J. James, C. Frampton, M. L. Barclay, Methotrexate polyglutamate concentrations are not associated with disease control in rheumatoid arthritis patients receiving long-term methotrexate therapy. *Arthritis & Rheumatism.* **2010**, *62*, 359.

[7]   Y. Lamers, R. Prinz-Langenohl, S. Bramswig, K. Pietrzik, Red blood cell folate concentrations increase more after supplementation with [6S]-5-methyltetrahydrofolate than with folic acid in women of childbearing age. *Am J Clin Nutr.* **2006**, *84*, 156.

[8]   M. C. Hum, B. A. Kamen, Folate, antifolates, and folate analogs in pediatric oncology. *Invest New Drugs.* **1996**, *14*, 101.

[9]   C. A. Bangert, M. I. Costner, Methotrexate in dermatology. *Dermatol Ther.* **2007**, *20*, 216.

[10]   M. Yakut, Y. Ustun, G. Kabacam, I. Soykan, Serum vitamin B(12) and folate status in patients with inflammatory bowel diseases. *Eur J Intern Med.* **2010**, *21*, 320.

[11] V. Giljaca, G. Poropat, D. Stimac, C. Gluud, Methotrexate for primary biliary cirrhosis. *Cochrane Database Syst Rev.* **2010**, CD004385.

[12] G. Rogler, Gastrointestinal and liver adverse effects of drugs used for treating IBD. *Best Pract Res Clin Gastroenterol.* **2010**, *24*, 157.

[13] J. L. Fuh, Homocysteine, cognition and brain white matter hyperintensities. *Acta Neurol Taiwan.* **2010**, *19*, 150.

[14] F. Coppede, E. Grossi, F. Migheli, L. Migliore, Polymorphisms in folate-metabolizing genes, chromosome damage, and risk of Down syndrome in Italian women: identification of key factors using artificial neural networks. *BMC Med Genomics.* **2010**, *3*, 42.

[15] S. H. Zeisel, Importance of methyl donors during reproduction. *Am J Clin Nutr.* **2009**, *89*, 673S.

[16] H. J. Blom, Y. Smulders, Overview of homocysteine and folate metabolism. With special references to cardiovascular disease and neural tube defects. *J Inherit Metab Dis.* **2010**.

Appendices

Appendix 1: Analysis of Intracellular Methotrexate Polyglutamates in Patients with Juvenile Idiopathic Arthritis.

Abstract

Objective. Intracellular methotrexate (MTX) polyglutamates (MTXGlu) have been shown to be potentially useful biomarkers of clinical response in adult patients with rheumatoid arthritis. The present study was undertaken to measure intracellular MTXGlu concentrations in a cohort of patients with juvenile idiopathic arthritis (JIA) to determine the predictors of MTXGlu variability in these patients.

Methods. Blood samples were obtained from patients with JIA who were being treated with a stable dose of MTX for >3 months. Clinical data were collected by chart review. Concentrations of $MTXGlu_{1-7}$ in red blood cell lysates were quantitated using an innovative ionpairing chromatography procedure, with detection by mass spectrometry.

Results. Patients with JIA from a single center (n = 99; mean ± SD age 117.8 ± 56.5 months, 69 female) were included in the analysis. The mean ± SD dose of MTX was 0.51 ± 0.25 mg/kg per week, with a median treatment duration of 18 months (interquartile range 3–156 months). MTX was administered subcutaneously in 66 patients (67%). Fifty-six patients (57%) had active arthritis at the time of the clinic visit. Totalintracellular MTXGlu ($MTXGlu_{TOT}$) concentrations varied 40-fold, with a mean ± SD total concentration of 85.8 ± 48.4 nmoles/liter. Concentrations of each MTXGlusubtype ($MTXGlu_{1-7}$) were measured individually and as a percentage of $MTXGlu_{TOT}$ in each patient.

$MTXGlu_3$ was the most prominent subtype identified, comprising 42% of $MTXGlu_{TOT}$, and the interindividual variability in the concentration of $MTXGlu_3$ was the most highly correlated with that of $MTXGlu_{TOT}$ (r = 0.96). The route of MTX administration was significantly associated with MTXGlu1–5 subtypes; higher concentrations of $MTXGlu_{1-2}$

were observed in patients receiving oral doses of MTX, whereas higher concentrations of $MTXGlu_{3-5}$ were observed in patients receiving subcutaneous doses of MTX ($P <$ 0.0001).

Conclusion*.* In this cohort of patients with JIA, the MTXGluTOT concentration varied 40-fold. Individual MTXGlu metabolites ($MTXGlu_{1-7}$), which have, until now, not been previously reported in patients with JIA, were detected. The route of MTX administration contributed to the variability in concentrations of $MTXGlu_{1-5}$.

For complete publication see:

M. L. Becker, L. van Haandel, R. Gaedigk, A. Lasky, M. Hoeltzel, J. Stobaugh, J. S. Leeder, Analysis of intracellular methotrexate polyglutamates in patients with juvenile idiopathic arthritis: Effect of route of administration on variability in intracellular methotrexate polyglutamate concentrations. *Arthritis & Rheumatism.* **2010**, *62*, 1803.

Appendix 2: The Effect of Genotype on Methotrexate Polyglutamate Variability in Juvenile Idiopathic Arthritis and Association with Drug Response

Abstract

Objective: Response and toxicity to methotrexate (MTX) are unpredictable in Juvenile Idiopathic Arthritis (JIA). Intracellular MTX polyglutamates (MTXGlu) have shown promise as a predictor of drug response. We investigated genetic predictors of MTXGlu variability and associations between MTXGlu and drug response in JIA.

Methods: This is a single center cross-sectional study evaluating JIA patients on stabledoses of MTX at a tertiary care children's hospital. After obtaining informed consent, blood was drawn from 104 JIA patients during routine MTX screening labs. Clinical data was collected by chart review. Genotyping for 34 SNPs in 18 genes within the MTX metabolic pathway was performed. An ion-pairing chromatographic procedure with mass spectrometric detection measured $MTXGlu_{1-7}$.

Results: MTXGlu analysis and genotyping was completed in 104 patients. K-means clustering resulted in 3 distinct patterns of MTX polyglutamation. Cluster 1 had low RBC MTXGlu concentrations, cluster 2 had moderately high RBC $MTXGlu_{1+2}$ concentrations, and cluster 3 had high concentrations of MTXGlu, specifically $MTXglu_{3-5}$. SNPs in the purine and pyrimidine synthesis pathway, as well as the adenosine pathway were significantly associated with cluster subtype. The cluster with high concentrations of $MTXGlu_{3-5}$ was associated with elevated liver function studies (LFTs), and there were higher concentrations of $MTXGlu_{3-5}$ in children who reported GI side effects and LFT elevation. No association was noted between MTXGlu and active arthritis.

Conclusions: MTXGlu remains a potentially useful tool for determining outcomes of JIA patients on MTX. The genetic predictors of MTXGlu variability may also contribute to the better understanding of MTX intracellular biotransformation.

For complete publication see:

M. L. Becker, R. Gaedigk, L. van Haandel, B. Thomas, A. Lasky, M. Hoeltzel, H. Dai, J. Stobaugh, J. S. Leeder, The effect of genotype on methotrexate polyglutamate variability in juvenile idiopathic arthritis and association with drug response. *Arthritis & Rheumatism.* **2010**, online first.

Appendix 3: LC-MS/MS Method for the Determination of

Carbamathione in Human Plasma

Abstract

Liquid chromatography-tandem mass spectrometry methodology is described for the determination of S-(N,N-diethylcarbamoyl)glutathione (carbamathione) in human plasma samples. Sample preparation consisted of a straightforward perchloric acid medicated protein precipitation, with the resulting supernatant containing the carbamathione (recovery ~98%). For optimized chromatography/mass spec detection a carbamathione analog, S-(N,N-di-*i*-propylcarbamoyl)glutathione, was synthesized and used as the internal standard. Carbamathione was found to be stable over the pH 1-8 region over the timeframe necessary for the various operations of the analytical method. Separation was accomplished via reversed-phase gradient elution chromatography with analyte elution and re-equilibration accomplished within 8 minutes. Calibration was established and validated over the concentration range of 0.5-50 nM, which is adequate to support clinical investigations. Intra- and inter-day accuracy and precision determined and found to be < 4% and < 10%, respectively. The methodology was utilized to demonstrate the carbamathione plasma-time profile of a human volunteer dosed with disulfiram (250 mg/d). Interestingly, an unknown but apparently related metabolite was observed with each human plasma sample analyzed.

Appendix 4: Phenylisothiocyanate as a Multiple Chemical Dimension Reagent for the Relative Quantitation of Protein Nitrotyrosine

Abstract

A highly selective sequential derivatization sequence has been developed for the transformation of 3-nitrotyrosine to a 2-anilino-benzoxazole derivative. This sequence can be applied to any ortho-nitrophenol, such as 3-nitrotyrosine or 3-nitrotyrosine residues present in proteins and/or peptides as a result of oxidative stress. The sequence involves a standard

reduction of the nitro functional group to the corresponding amine using aqueous dithionite, followed by aqueous solution coupling with phenylisothiocyanate (PITC) and then eventual product formation by a photochemical mediated intramolecular cyclization of the intermediate thiourea. While this cyclization step has been effected numerous times by various reagents commonly used in synthetic organic chemistry, many requiring non-aqueous reaction media, the present transformation appears to the be first description this reaction using 350 nm light in aqueous media. The resulting overall transformation provides a specific mass shift signature of 116 amu when conducted with $^1H_5$-PITC and 121 amu with $^2H_5$-PITC, thus forming the basis of relative quantitation by MS detection. In preliminary experiments, relative quantitation was accomplished for the decapeptide angiotensin I that had been subjected to nitration.